

REPORT DOCUMENTATION PAGE

1. Recipient's Reference	2. Originator's Reference	3. Further Reference	4. Security Classification of Document
	AGARD-LS-120	ISBN 92-835-1419-X	UNCLASSIFIED
5. Originator	Advisory Group for Aerospace Research and Development North Atlantic Treaty Organization 7 rue Ancelle, 92200 Neuilly sur Seine, France		
6. Title	ELECTROMAGNETIC PROPAGATION PROBLEMS IN THE TACTICAL ENVIRONMENT		
7. Presented at	a Lecture Series under the sponsorship of the Electromagnetic Wave Propagation Panel and the Consultant and Exchange Programme of AGARD on 3–4 May 1982 in Munich, Germany and on 6–7 May 1982 in Paris, France.		
8. Author(s)/Editor(s)	Various		9. Date April 1982
10. Author's/Editor's Address	Various		11. Pages 160
12. Distribution Statement	This document is distributed in accordance with AGARD policies and regulations, which are outlined on the Outside Back Covers of all AGARD publications.		
13. Keywords/Descriptors	Electromagnetic wave transmission Tactical command and control Combat zones		
14. Abstract	<p>Modern battlefield activities require an increasing employment of electronic equipment. The large variety of applications extends from communications to surveillance, from reconnaissance to command and control. With regard to efficiency and limitations, many systems depend on the characteristics of the propagation medium and on operational adaptation to the propagation environment.</p> <p>In order to optimize system performance, operational personnel should possess adequate knowledge of system-relevant propagation criteria, and in addition, a training level which permits an efficient reaction under changeable battlefield conditions. This Lecture Series on Electromagnetic Propagation Problems in the Tactical Environment should be of interest to qualified technical officers and teaching staff, as well as to other personnel qualified in engineering science or natural sciences and connected with tactical electronics of any kind.</p>		

AGARD

ADVISORY GROUP FOR AEROSPACE RESEARCH & DEVELOPMENT

7 RUE ANCELLE 92200 NEUILLY SUR SEINE FRANCE

AGARD LECTURE SERIES No. 120

Electromagnetic Propagation Problems in the Tactical Environment

NORTH ATLANTIC TREATY ORGANIZATION



DISTRIBUTION AND AVAILABILITY
ON BACK COVER

NORTH ATLANTIC TREATY ORGANIZATION
ADVISORY GROUP FOR AEROSPACE RESEARCH AND DEVELOPMENT
(ORGANISATION DU TRAITE DE L'ATLANTIQUE NORD)

AGARD Lecture Series No.120
ELECTROMAGNETIC PROPAGATION PROBLEMS
IN THE TACTICAL ENVIRONMENT

The material in this publication was assembled to support a Lecture Series under the sponsorship of the Electromagnetic Wave Propagation Panel and the Consultant and Exchange Programme of AGARD presented on 3–4 May 1982 in Munich, Germany and on 6–7 May 1982 in Paris, France.

THE MISSION OF AGARD

The mission of AGARD is to bring together the leading personalities of the NATO nations in the fields of science and technology relating to aerospace for the following purposes:

- Exchanging of scientific and technical information;
- Continuously stimulating advances in the aerospace sciences relevant to strengthening the common defence posture;
- Improving the co-operation among member nations in aerospace research and development;
- Providing scientific and technical advice and assistance to the North Atlantic Military Committee in the field of aerospace research and development;
- Rendering scientific and technical assistance, as requested, to other NATO bodies and to member nations in connection with research and development problems in the aerospace field;
- Providing assistance to member nations for the purpose of increasing their scientific and technical potential;
- Recommending effective ways for the member nations to use their research and development capabilities for the common benefit of the NATO community.

The highest authority within AGARD is the National Delegates Board consisting of officially appointed senior representatives from each member nation. The mission of AGARD is carried out through the Panels which are composed of experts appointed by the National Delegates, the Consultant and Exchange Programme and the Aerospace Applications Studies Programme. The results of AGARD work are reported to the member nations and the NATO Authorities through the AGARD series of publications of which this is one.

Participation in AGARD activities is by invitation only and is normally limited to citizens of the NATO nations.

The content of this publication has been reproduced directly from material supplied by AGARD or the authors.

Published April 1982

Copyright © AGARD 1982
All Rights Reserved

ISBN 92-835-1419-X



*Printed by Technical Editing and Reproduction Ltd
Harford House, 7-9 Charlotte St, London, W1P 1HD*

PREFACE

Modern battlefield activities require an increasing employment of electronic equipment. The large variety of applications extends from communications to surveillance, from reconnaissance to command and control. With regard to efficiency and limitations, many systems depend on the characteristics of the propagation medium and on operational adaptation to the propagation environment.

In order to optimize system performance, operational personnel should possess adequate knowledge of system-relevant propagation criteria, and in addition, a training level which permits an efficient reaction under changeable battlefield conditions. This Lecture Series on Electromagnetic Propagation Problems in the Tactical Environment should be of interest to qualified technical officers and teaching staff, as well as to other personnel qualified in engineering science or natural sciences and connected with tactical electronics of any kind.

As tutorial lectures, papers No.1 to No.5 cover all relevant aspects of the present state of the art and likely future development. In subsequent system-oriented lectures, papers No.6 to No.10, electromagnetic propagation problems in the tactical environment are addressed with respect to typical systems. The Lecture Series is concluded by a round-table discussion on the topics dealt with.

Appreciation is expressed to all who assisted in the organization of this Lecture Series as well as in the compilation of this volume, to lecturers, AGARD-staff and other collaborators.

H.J.ALBRECHT
Lecture Series Director

LIST OF SPEAKERS

Lecture Series Director: Dr H.J.Albrecht
Forschungsgesellschaft für
Angewandte Naturwissenschaften e.V.
(F.G.A.N.)
5307 Wachtberg-Werthoven
Germany

SPEAKERS

Dr J.Aarons
Boston University
Department of Astronomy
725 Commonwealth Avenue
Boston, Massachusetts 02215
USA

Dr B.Burgess
Radio and Navigation Department
Royal Aircraft Establishment
Farnborough, Hampshire
UK

Dr T.Fitzsimons
Allied Radio Frequency Agency (ARFA)
CCCS Division IMS
NATO Headquarters
1110 Evere
Belgium

Dr E.Lampert
Siemens A.G.
Postfach 700074
8000 Munich 70
Germany

Dr F.H.Palmer
Directorate of Scientific Planning
Research & Development Branch
National Defence Headquarters
Ottawa, Ontario
Canada

Dr B.A.Prew
Royal Signals and Radar
Establishment (LI Division)
St.Andrews Road
Great Malvern, Worcestershire
UK

Dr C.M.Rush
Propagation Predictions and
Model Development
Institute for Telecommunication Sciences
US Department of Commerce
Boulder, Colorado 80803
USA

CONTENTS

	Page
PREFACE by H.J.Albrecht	iii
LIST OF SPEAKERS	iv
	Reference
GENERAL REVIEW OF EM SPECTRUM CHARACTERISTICS IN TACTICAL APPLICATIONS by H.J.Albrecht	1
GROUND-WAVE PROPAGATION CHARACTERISTICS OF INTEREST TO THE TACTICAL COMMUNICATOR by F.H.Palmer	2
PROPAGATION ASPECTS OF IONOSPHERIC LINKS OVER SHORT AND MEDIUM DISTANCES by C.M.Rush	3
PROPAGATION CHARACTERISTICS OF SATELLITE LINKS by J.Aarons	4
LIMITATIONS IN SCATTER PROPAGATION by E.Lampert	5
INTRODUCTION TO PROPAGATION EFFECTS ON TYPICAL SYSTEMS by H.J.Albrecht	6
E.M. PROPAGATION PROBLEMS FOR TACTICAL RADIO RELAY SYSTEMS by T.K.Fitzsimons	7
PROPAGATION PROBLEMS ASSOCIATED WITH AIRCRAFT COMMUNICATIONS SYSTEMS by B.Burgess	8
SYSTEMS OF MULTIFUNCTION INFORMATION DISTRIBUTION AND FOR COMMAND, CONTROL, AND COMMUNICATIONS – C ³ by E.Lampert	9
PROPAGATION EFFECTS IN TACTICAL RADARS by B.A.Prew	10
BIBLIOGRAPHY	B

General Review of EM Spectrum Characteristics in Tactical Applications

by
H.J. Albrecht

Summary.

Characteristics of propagation media may have a more or less decisive influence upon the performance of systems used in any environment, and thus also in tactical applications. Following a general introduction to the subject of atmospheric propagation media and their effects, this review summarizes those typically encountered in a tactical environment.

In order to lead to and to supplement a more detailed treatment of particularly representative propagation conditions, the review mentions features and limitations governed by medium characteristics in various portions of the electromagnetic wave spectrum.

In addition to the discussion of the present state of the art, possible and feasible future development is addressed.

1. INTRODUCTION

Electromagnetic waves experience propagation through the environmental medium whenever they are utilized to carry information from one point to another, to detect and monitor a distant object by an evaluation of a wave reflected by it, or to determine one's own location through a precise measurement of the time taken by a wave to travel from a reference point. The quality of their service is governed and may be limited by the features of the media concerned. In other words, the typical areas of military applications mentioned above, viz., communications, radar, and navigation and/or location determination, may be severely hampered by regular and less regular variations of medium characteristics.

Fundamentally, tactical applications may use any type of propagation paths, so-called ground-wave links along the terrain (fig. 1a) as well as those transmitted and received at an elevation angle with respect to ground level (fig. 1b). Typical distances are of the order of up to several 100 km. Depending upon frequencies used within the electromagnetic wave spectrum, as well as on the distance to be covered by the radiated signal, the behaviour of the medium may be more or less influential. Turning to the field of tactical applications, "solid propagation lines", such as cables, can only be used within certain operational categories, due to the requirements of mobility and flexibility. Thus the propagation of electromagnetic waves through the far more variable atmospheric media is of primary importance. It is for this reason that this Lecture Series commences with, and thus this review concentrates on, a general treatment of medium characteristics with respect to propagation.

2. Propagation Media

In general terms, a propagation medium may obviously be defined as a solid, gaseous, or liquid material in which an electromagnetic wave propagates. Depending upon the state of the art, our knowledge of medium characteristics is yet being augmented with some configurations of waves of certain frequency ranges in certain media, or may even have reached some saturation level prior to new advances in measurement technology and methods of analysis. Media of primary interest for our review are generally those in the atmosphere of our planet, mainly the ionosphere and troposphere and adjacent regions.

The frequency spectrum of interest extends from about 10 kHz to 1000 THz; table I shows the nomenclature generally considered valid, as well as typical tactical features.

As a summary of propagation effects in all paths other than those depending on ground characteristics, fig. 2 illustrates the atmospheric environment and its effect on all frequencies within the spectrum 10 KHz to 100 GHz (Albrecht, 1978). Altitude above ground and frequency are drawn to logarithmic scales. On the left-hand side, generally adopted designations are used for regions of the atmosphere. Within the troposphere, a distinction has been made for typical altitude ranges of clouds in lower, medium, and upper heights. The difference in average altitude of the tropopause between equator and polar regions is also shown. The change in electron density between D, E, F₁ and F₂ layer regions is responsible for different reflection characteristics; reference is made to relevant basic literature (e.g. Davies, 1965).

The logarithmic altitude scale in the figure permits us to find, within the illustration, the altitude for geostationary satellites as well as that of the moon. Looking at the atmospheric behaviour within the entire frequency spectrum and commencing at low frequencies, ionospheric reflections are the governing factor up to frequencies of about 30 MHz, with some partial transparency in the lower frequency range, depending upon the relationship of operating frequency to gyro-frequency and upon the direction of propagation with respect to the magnetic field lines. The range of ionospheric scatter propagation and meteor back-scatter is shown up to 100 MHz.

The so-called "radio-window" for propagation between satellites and other spacecraft on the one hand, and ground terminals on the other hand, extends from about 100 MHz to frequencies of the order of 10 GHz and higher. Although here the average atmospheric attenuation is low, basic literature refers to sporadic disturbance by severe ionospheric scintillations (e.g. Aarons, 1973). It should be emphasized that most terrestrial propagation links also use frequencies within this radio-window. Its lower limit is given by reflection features of the ionosphere while its upper one is caused by high signal attenuation due to precipitation and to absorption by tropospheric constituents, e.g. by O_2 around 60 GHz. Turning momentarily to a special application of this feature, attention can be drawn to the militarily attractive use of this highly absorptive frequency range for terrestrial links displaying a low probability of intercept.

Characteristics of the troposphere in the so-called planetary boundary layer, or up to approximately 1000 m above ground, are particularly important for a large number of services in tactical environment. Mainly three meteorological features may be utilized to describe the behaviour in this portion of a tropospheric propagation medium: temperature, humidity, and barometric pressure. They have been employed to define the refractive index. It normally decreases as a function of height and thus causes a bending of the path of electromagnetic waves. Deviations from such a gradient occur with meteorological disturbances and for certain altitude regions, as is sketched in fig. 3. Under certain conditions, a reversal of refractive-index gradient may lead to a super-refraction or "reflection" of waves in the height region concerned. An opposite characteristics, or "sub-refraction", may cause waves to be bent away from the Earth's surface.

In system planning and similar work, a straight-line path may be handled more easily. Assuming propagation in the planetary boundary layer, such a condition may be satisfied by increasing, fictitiously, the Earth's radius by a factor k given by the gradient of refractive index, as follows:

$$k = \frac{1}{1 + R \frac{dn}{dh}} \quad \dots\dots\dots (1)$$

where R = Earth's radius
 n = refractive index
 h = height

This factor k is frequently used as parameter to describe propagation behaviour in the troposphere as a function of altitude and geographical locations. For a standard atmosphere, the value of k amounts to 1.33. As another supplement to fig. 2, the attenuation behaviour may be shown in somewhat more detail for the range from 20 to 260 GHz, as is illustrated in fig. 4. Curves refer to undisturbed tropospheric conditions, as well as to the situation with a heavy rainfall of 16 mm/h over the entire path length considered.

In a recent AGARD Symposium, the present state of the art and special military applications in the optical wave range have been discussed in detail (Halley, 1981). For the purposes of the present Lecture Series, it may suffice to state that, up to 1000 THz, a number of absorption lines determine bands of optimum transmission characteristics on terrestrial as well as space/earth links. Using the latter application as a typical example, fig. 5 illustrates the relative atmospheric transparency in the entire spectrum from 10 kHz to 1000 THz.

The Earth's surface is an important propagation medium which may become effective in several ways. These refer to action upon antenna characteristics in the so-called near-field of the antenna, to attenuation in ground-wave propagation along the surface, to the effects of vegetation and of ground parameters on the reflection properties with respect to wave polarization, intensity, and phase, and, with sub-surface propagation, to the attenuation experienced by a wave travelling through a layer. The two characteristic parameters, ground conductivity and dielectric constant, are functions of humidity and temperature, and of frequency; they may be considered variable with appropriately detrimental effects upon wave propagation. The geographical distribution of ground characteristics is of importance when considering world-wide communication or navigation using reference signals radiated on very low frequencies, e.g. 10 kHz such as are used by the OMEGA System of navigation. Connected with the Earth's surface as a propagation medium is water in its various configurations, with salinity and other parameters being responsible for changes in the electromagnetic characteristics. Fig. 6 illustrates a world-map of ground conductivity expressed in

in appropriate units, i.e. Siemens/m ($=\text{mho/m}$) as an example of the geographical distribution (Albrecht, 1967), with an average validity for frequencies up to the HF-range; again for average estimates, the distribution of dielectric constant may be derived from ground conductivity by the use of established relationships. More recently, additional attention has been directed at terrain profiles and contours (Biggs, 1979).

Data on noise in its various configurations are other parameters of considerable interest in applications concerning electromagnetic wave propagation within the spectrum here under discussion. In general, one distinguishes atmospheric, anthropogenic (man-made) and galactic (cosmic) noise. The noise conditions at any location are a function of frequency, season of the year and time of the day and local electromagnetic environment. Details may be found in an appropriate CCIR-document (CCIR-Report, 322); fig. 7 depicts general characteristics of noise level with respect to frequency (Hagn, 1974).

For completeness' sake, reference should be made to the possibilities of modifying propagation media artificially. Methods known for about four decades use solid material, such as chaff, i.e. metallic or, more recently, metallized elements tuned to the frequency range to be affected and released in the troposphere to cause wave scattering; it may be used to establish intended scatter links, and also for shielding purposes. In the process of research is medium modification by "ionospheric heating" using intensive HF radiation and producing ionospheric irregularities, which may again be employed for scattering purposes. Somewhat further away yet may be a system implementation of methods of weather modification to change tropospheric propagation characteristics.

3. Areas of Application

Fundamentally, application areas of electromagnetic wave propagation may be subdivided into communication, surveillance including radar, and navigation. Typical propagation paths may be identified for any one of these categories, yet the field of communications includes all possible kinds and thus allows to discuss larger variety of these. Fig. 8 depicts typical paths in terms of frequency ranges and features, such as predominant medium parameters, bandwidths possible, and distances, followed by types of terminals and limitations due to propagation characteristics; the illustration also includes a reference to terrestrial cable for comparison. Three categories of terminals have been utilized to differentiate between the wide scale of possible combinations. Fixed terminals of constant location are designated as stationary ones, whereas mobile terminals are those in operation while in motion. The intermediate type, comprising terminals which are transportable but not in operation while in motion, has been called "transportable". Limiting characteristics due to propagation behaviour have been listed in the figure; they are described in very general terms.

3.1 Line-of-sight and Diffraction Paths

In the second column from the left-hand side of the illustration, line-of-sight paths and those based on diffraction around obstacles are shown. Links in these categories may employ any frequency, but mainly those above 30 MHz are used as such. In addition to a geometric limitation by line-of-sight conditions, the type of terrain below the path and the environment may cause severe multipath effects, which may lead to appropriate bandwidth limitations. On the other hand, abnormal tropospheric conditions, such as refraction layers in the troposphere, may give rise to reflections and to multipath occurrence of temporary as well as variable nature. Proper attention to problems due to propagation characteristics permits to optimize such paths for links connecting stationary, transportable, and mobile terminals.

The use of the diffraction mechanism is theoretically possible and represents an imperfect but nevertheless existing form of propagation paths in the fringe zones of line-of-sight conditions. Signal fluctuations are common; their dependence upon propagation media is similar to that mentioned under line-of-sight conditions. A comparable level of reliability is indicated for propagation by super-refraction due to refraction layers in the troposphere; so-called duct propagation may render possible communication links beyond the horizon, yet can also cause path distortion detrimental for radar applications. Above a sea surface, an "evaporation duct", due to layer formation caused by evaporation from the surface, may occur with a somewhat higher predictability. The following lecture in this series will deal with ground wave propagation in detail, special attention being given to characteristics of interest to the tactical communicator (Palmer, 1982).

3.2 Reflections at Ionospheric Layers

Another column in fig. 8 deals with reflections at ionospheric layers. These form in different regions of our planet's atmosphere, on the basis of ionization caused

by various processes. A dependence on solar radiation and solar activity has been verified. The action of the ionosphere upon propagation is very complex. Although largest distances on the Earth's surface may be covered by such links, and even with a minimum of radiated electromagnetic energy, the proper use of special features of this propagation mechanism requires expertise and continuous research.

For large distances, the wave is reflected once or several times at an appropriate height within the ionosphere, and, not necessarily but possibly, at one or more intermediate points on the Earth's surface. With reflection heights varying between 100 and 400 km (see fig. 2) surface distances amount to a maximum of the order of 4000 km if the horizontal layer structure is parallel to the ground; far larger distances may be covered if the layer is inclined with respect to the ground beneath it, with the excitation of a chordal hop path inside and along the layer, or by a sequence of single reflections. The complexity of propagation via ionospheric reflections leads to different path components with the consequence of a reduction in the bandwidth of such links.

The maximum propagation frequency depends upon the state of ionization which is governed by the time required for a neutralization or recombination of ions and electrons and by the strength of the ionizing radiation. Whereas the former parameter is a function of atmospheric density or, largely, of the height above the Earth's surface, the latter is determined by solar radiation and thus by a variety of components, as time of the day, season, and solar activity. A measure of the last-mentioned variable is the number of sunspots.

Of particular interest for tactical applications is the coverage of short and medium distances by ionospheric reflections. Such paths involve distances of up to about 1000 km, thus usually only one reflection. On the other hand, an optimization of such links with respect to the requirements in battlefield environment require particular attention to special characteristics such as the disturbing effect of multiple paths, the variability of propagation conditions, etc.. Within this Lecture Series, paper no. 3 will deal with all relevant details (Rush, 1982). Although a large number of variables in ionospheric propagation has been investigated successfully during the last fifty years and although results are useful for reasonably reliable average predictions, a continuing augmentation of relevant knowledge, for instance on irregular and abnormal characteristics, allows an increasing implementation of modern technologies.

3.3 Propagation on Satellite Links

Communication or navigation links using artificial satellites in space have been known for about two decades. The transparency of the atmosphere in certain frequency regions, in so-called "radio-windows" (see fig. 2), enables such space links to be established. The right-hand column of fig. 8 illustrates some of their features. They are also applicable to guidance and surveillance use.

In principle, propagation paths between satellites and ground terminals resemble line-of-sight ones with a relay or reference terminal in space. Earlier experiments in space communications used passive satellites, such as "Echo", which reflected energy arriving from a ground terminal back towards the Earth, thus enabling reception by another terminal on the Earth's surface. With the advancement in aerospace technology, active repeaters in space took their place. Initially, these satellites displayed only elliptical, non-stationary orbits, "Telestar" being an early example. As time went on, the precision attainable in launching satellites increased, and, today, highly accurate positioning of satellites in geostationary or any other suitable orbits belongs to the state of the art. The altitude required for a satellite being "stationary" with respect to its fixed "sub-satellite" point on the equator has already been referred to in fig. 2; it amounts to 36000 km. Geostationary or quasi-geostationary orbits are normally circular at low inclination angles with respect to the equator. They are useful for most requirements in geographical areas up to a certain high altitude. For special purposes, elliptical orbits are employed.

The concept of using a global positioning system involving a sufficient number of satellites, and a continuous knowledge of their actual positions in space has led to the very modern satellite navigation system NAVSTAR for world-wide and highly accurate determination of location of the Earth's surface. Its use for tactical purposes is indicated.

As far as path characteristics of space links are concerned, they can obviously be considered similar to line-of-sight conditions if frequencies in the ranges of transparencies are utilized. Depending upon frequency and geographical location of surface terminals, severe limitation may occur in various applications. Of particular importance is the fading produced by irregularities in the ionosphere and in the troposphere, as well as time delay errors and attenuation. Details on such and related propagation characteristics encountered with satellite links will be covered in Paper No. 4 of this Lecture Series (Aarons, 1982).

3.4 Scatter Propagation

Turning to scatter paths as another typical application area, it may be remembered that appropriate research was initiated about three decades ago in order to increase the overall reliability of terrestrial communication. Features are illustrated in the appropriate column of fig. 8. With this type of propagation, a volume in the atmosphere, a so-called scatter volume, is illuminated by a transmitter, and the energy scattered towards the receiving terminal is being used for communication links. Obviously, energy requirements of such systems are much larger than those of line-of-sight links; however, the overall reliability of scatter links may be better under certain conditions. Distances larger than those of line-of-sight links and systems requiring moderate bandwidth are representative applications. Two types of scatter propagation have become known: ionospheric scatter using volumes at the altitude of the D-layer and tropospheric scatter using scatter volumes below the tropopause. Stratospheric scatter links have also been tested. Any scatter mechanism usually leads to a limitation in the bandwidth which may be transmitted.

Irregularities or variations of electron density in the height region of the D-Layer, between 70 and 90 km, are one basis of the ionospheric scatter mechanism. These variations can be considered to be due to turbulent mixing; they provide regular but weak scattering. In addition, the passage of meteors through the atmosphere causes a short-lived existence of ionized trails which lead to intermittent reflections, useful for burst communications. Furthermore, diffuse reflections may be due to patches of a layer in the E-region of the ionosphere, the so-called sporadic E-layer, or due to irregularities in the higher regions of the ionosphere, approximately in the upper F₂-layer. The typical frequency range for ionospheric scatter propagation commences above the highest yet regularly reflected frequency in the short-wave range, around 30 MHz, and is generally limited to frequencies of the order of 100 MHz. On account of path geometry, maximum possible distances amount to the order of 2000 km.

With tropospheric scatter propagation, the scatter mechanism may be based on turbulence, using scatter elements formed by random fluctuations of the dielectric constant, or on diffuse and partial reflections from layer-like structures in the troposphere. The mechanism is similar to the ionospheric one but higher frequencies are usually employed; the typical range extends from about 1 to 15 GHz. Depending again upon geometric limitations given by the altitude range of the scatter volume, distances of 100 to 600 km may be covered.

Within the tactical arena, scatter propagation represents an important feature. Its characteristics and limitations deserve appropriate attention for communication purposes as well as for a recognition of intentional and unintentional interference hazards to other systems. Relevant aspects will be discussed in detail by Paper No.5 of this Lecture Series (Lampert, 1982).

4. Natural and Technological Limitations

As has already been indicated, limitations in using propagation paths for any purpose vary in different frequency ranges on account of conditions of environment, noise, and changes in parameters which affect the path, either by reflection, scatter, or absorption.

In fig. 9, an attempt has been made to illustrate the more important propagation-path characteristics as a function of frequency, effective atmospheric altitude ranges, and typical distances. These three parameters are represented by mutually perpendicular axes using logarithmic scales throughout. This graphical synopsis is now to be commented upon in somewhat more detail.

Commencing with very low frequencies (VLF) shown at the top of the figure, a world-wide coverage is possible by means of waveguide-like propagation in the belt formed by the Earth's surface and the lowest ionospheric layer, the D-layer, whose relatively low electron density is adequate for a reflection of these frequencies. Obviously, changes in the characteristics of both boundary zones influence the quality of such paths and may represent inherent limitations to their use. Assuming a path between two points to follow a great-circle on the Earth's surface, electrical characteristics of this surface region, as well as the diurnally and seasonally variable state of D-layer ionization, affect the amplitude of a signal and its phase, which may, for instance, cause deviations in measurements of times of arrival and thus influence essential navigation data.

With regard to somewhat higher frequencies and, e.g., long-distance paths in this HF range, the state of ionization in the here relevant layers - F₂ and perhaps F₁ and E - is an essential source of variability, again in addition to earth-surface characteristics in possible reflection areas. On the other hand, the latter feature is of no effect with chordal paths which, by definition, do not touch the surface between the end points of a link; as has been mentioned in a previous section of this paper, such conditions prevail for certain distance ranges with regularly existing inclined horizontal structures in ionospheric layers.

The following, rather large portion of the spectrum from about 30 MHz to frequencies of the order of about 100 GHz accommodates a number of applications for propagation paths. Fig. 9 illustrates the information given in previous sections.

Irregularities in the ionosphere may limit the usefulness of satellites in certain geographic regions and up to about 10 GHz; on higher frequencies, rain and other precipitation may severely affect communication and other paths between Earth and space. In any portion of the spectrum, abnormal tropospheric conditions may cause changes in path geometry, such as refraction layers or other types of unusual gradients of the refractive index as a function of altitude. Additional sources of path unreliability towards the higher frequencies of the total spectrum may be represented by attenuation due to fog, and signal fluctuations or scintillations due to turbulence characteristics.

In the interest of clarity, fig. 9 does not include scatter links using irregularities in the ionosphere. Those in the tropospheric region are indicated with typical distance and useful frequency ranges. The reliability of such scatter links depends on the turbulence structure in the tropospheric scatter volume, or on conditions prevailing for another scatter mechanism, such as partial reflections at layer-like structures. Disturbances in the weather can thus cause significant changes in limitations with respect to required power and obtainable bandwidth. Some time ago, studies aiming at better reliability under average conditions resulted in the use of so-called diversity paths, i.e. a simultaneous transmission of the signal by means of several path components differing slightly in spatial antenna position, frequency, angle of transmission or portion of scatter volume used, provided that both, frequency of operation and antenna beam-width, permit an adequate distinction between such path components.

The bottom portion of fig. 9 shows line-of-sight links which are representative of typical use in most parts of the entire spectrum, up to the optical range above frequencies of the order of 10 THz. Depending upon the frequencies utilized, electrical characteristics of the ground, abnormal gradients of refractive index, attenuation due to precipitation and fog may all influence the reliability and may thus represent limitations.

With regard to limitations in tactical applications, below about 10 GHz these may be of technological kind when miniaturized equipment is to be considered for mobile and portable systems. With increasing frequency, a technological limitation may more and more concern the feasibility of implementing systems of one or the other configuration, depending upon power levels and operational stability achievable.

5. Trends in Research and Development

Objectives of research and development in electromagnetic wave propagation comprise an optimization of links used for communication, radar, and navigation by identifying, predicting, and, where possible, mastering difficulties indicated in previous sections of this paper. For applications of electromagnetic propagation in tactical fields, such work continues with respect to both regions of our planet's atmosphere, ionosphere and troposphere.

5.1 Ionospheric Radio Wave Propagation

Activities in the field of ionospheric propagation refer to the extension of the useful spectrum by means of artificially modifying the medium such that the maximum usable frequency for high-frequency long-distance applications (so-called MUF) is increased and the lowest usable frequency (LUF) is lowered. A promising method of extending the MUF may be represented by "ionospheric heating", or the use of extremely high radio energy to heat a certain portion in the ionosphere which in turn assists in forming a satisfactory propagation mechanism for frequencies above the natural maximum usable one. The reduction of the lowest usable frequency may perhaps be achieved by the release of chemical substances in certain ionospheric volumes. During recent years, two AGARD symposia dealt with recent research work in this area (Coyne, 1979; Schmerling, 1980).

5.2 Tropospheric Radio Wave Propagation

A steadily progressing technological development has enabled the use of increasingly higher frequencies; this process can be expected to continue with the result of reliable equipment becoming available in ranges of millimetre, submillimetre and optical waves. As far as research and development in the propagation area are concerned, this progress leads to an increasing importance of work directed at identifying, analyzing, and predicting areas, occurrence, and intensity of natural limitations discussed in previous sections. Up to the present, an enormous amount of data has been collected on the behaviour of propagation in all relevant frequency ranges

up to the optical range, and under many representative geographic conditions. To mention only a few examples, investigations during recent years have concentrated somewhat on attenuation and phase effects of rain and other precipitation in SHF and EHF ranges, and of natural and anthropogenic fog and dust on EHF and higher frequencies, including the optical range.

Similar to its application in ionospheric propagation, the artificial modification of tropospheric propagation media may, some time in the future, yield a higher reliability in tropospheric propagation. Special fields in the area of tropospheric wave propagation were topics of three recent AGARD symposia (Spitz, 1978; Albrecht, 1980; Halley, 1981).

5.3 Radio Wave Propagation Involving Spacecraft

Considerable advances have been registered in radio wave propagation involving links between terminals in space and on the Earth's surface, as well as inter-satellite and interplanetary links.

The impact of satellite technology about fifteen years ago caused a change with regard to the application of ionospheric research results to problems connected with this then new type of path requiring an optimum atmospheric transparency. Research activities on ionospheric irregularities commenced in those days; in the meantime, a wealth of material has been gathered and evaluated on world-wide basis. Continuous investigations will permit existing models to be optimized.

Likewise, the area of attenuation and phase characteristics contributed by the tropospheric portion of an earth/space path has experienced an enormous accumulation of relevant material. Appropriate evaluation will ensure the establishment of models required for future planning. AGARD symposia mentioned in section 5.2 also contain the recent research results in space/earth propagation.

5.4 Radio Wave Propagation Involving Ground Parameters

During the past decade, research in this field has concerned a completion of data on ground conductivity and dielectric properties and has initiated considerable activities with regard to terrain profiles and contours. In this respect, the establishment and employment of topographical databanks is a major topic, for the purpose of automatic computerized link design and adaptation. A recent AGARD-symposium reported on state of the art and trend (Biggs, 1979).

6. Conclusions

With the view upon the special field of communications, surveillance, and navigation in tactical applications, a huge amount of possible propagation paths continues to exist, and new possibilities are being investigated in many countries of the world in order to account for steadily increasing requirements of modern systems. On the other hand, an adequate level of knowledge on matters concerning propagation becomes more and more important for system planners, equipment designers, as well as for the military user, to ensure optimum performance of both, man and equipment.

References

- Aarons, J. (1973) (ed.) Total electron content and scintillation studies of the ionosphere, AGARDograph No. 166, 1973
- Aarons, J. (1982) Propagation characteristics of satellite links, Paper No. 4 in AGARD Lecture Series No. 120, May 1982
- Albrecht, H.J. (1967) Geographical distribution of electrical ground parameters and effects on navigational systems, Paper No. 25 in K. Davies (ed.), Phase and Frequency Instabilities in Electromagnetic Wave Propagation, Proceedings AGARD-CP-33, AGARD Symposium, October 1967, Ankara, Turkey
- Albrecht, H.J. (1978) Introductory notes on propagation effects and related aspects, Paper No. 17 in H. Lueg (ed.), Digital Communications in Avionics, Proceedings AGARD-CP-239, AGARD-AVP-Symposium, June 1978, Munich, Federal Republic of Germany
- Albrecht, H.J. (1980) (ed.) Propagation effects in space/earth paths, Proceedings AGARD-CP-284, AGARD-EPP-Symposium, May 1980, London, United Kingdom

- Biggs, A.W. (1979) (ed.) Terrain profiles and contours in electromagnetic wave propagation, Proceedings AGARD-CP-269, AGARD-EPP-Symposium, September 1979, Spatind, Norway
- Coyne, V.J. (1979) (ed.) Special topics in HF propagation, Proceedings AGARD-CP-263, AGARD-EPP-Symposium, May/June 1979, Lisbon, Portugal
- Davies, K. (1965) Ionospheric radio propagation, NBS Monograph 80, April 1965
- Hagn, G.H. (1974) Definitions and fundamentals of electromagnetic noise, interference, and compatibility, Paper No. 1 in Electromagnetic Noise, Interference, and Compatibility, Proceedings AGARD-CP-159, AGARD-AVP/EPP-Symposium, October 1974, Paris, France
- Halley, P. (1981) (ed.) Special topics in optical propagation, Proceedings AGARD-CP-300, AGARD-EPP-Symposium, April 1981, Monterey, U.S.A.
- Lampert, E. (1982) Limitations in scatter propagation, Paper No. 5 in AGARD Lecture Series No. 120, May 1982
- Palmer, F.H. (1982) Ground-wave propagation characteristics of interest to the tactical communicator, Paper No. 2 in AGARD Lecture Series No. 120, May 1982
- Rush, C.M. (1982) Propagation aspects of ionospheric links over short and medium distances, Paper No. 3 in AGARD Lecture Series No. 120, May 1982
- Schmerling, E. (1981) (ed.) The physical basis of the ionosphere in the solar-terrestrial system, Proceedings AGARD-CP-295, AGARD-EPP-Symposium, October 1980, Naples, Italy
- Spitz, E. (1979) (ed.) Millimeter and submillimeter wave propagation, Proceedings AGARD-CP-245, AGARD-EPP-Symposium, September 1978, Munich, Federal Republic of Germany
- CCIR-Report No. 322, World distribution and characteristics of atmospheric radio noise, International Radio Consultative Committee of the International Telecommunications Union, Geneva

Table I Frequency Ranges

Frequency	Band		Typical Tactical Use	Typical Message Bandwidth
3 - 30 kHz	Very Low	VLF	Navigation	50 Hz
30 - 300 kHz	Low	LF	Navigation	1 kHz
0.3 - 3 MHz	Medium	MF	Navigation	5 kHz
3 - 30 MHz	High	HF	Communication, Radar (OTH)	10 kHz
30 - 300 MHz	Very High	VHF	Communication, Radar	10 kHz, 6 MHz
0.3 - 3 GHz	Ultra High	UHF	Communication, Radar, Navigation	10 kHz, 10-50 MHz
3 - 30 GHz	Super High	SHF	Communication, Radar	50 MHz
30 - 300 GHz	Extremely High	EHF	R & D (Communication, Radar)	R & D
1 - 400 THz	Infrared	IR	R & D (Communication, Radar)	R & D
400 - 800 THz	Optical		R & D (Communication, Radar)	R & D

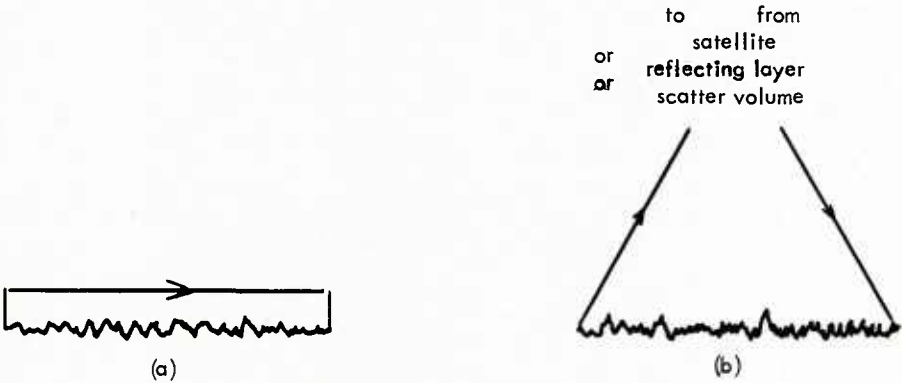
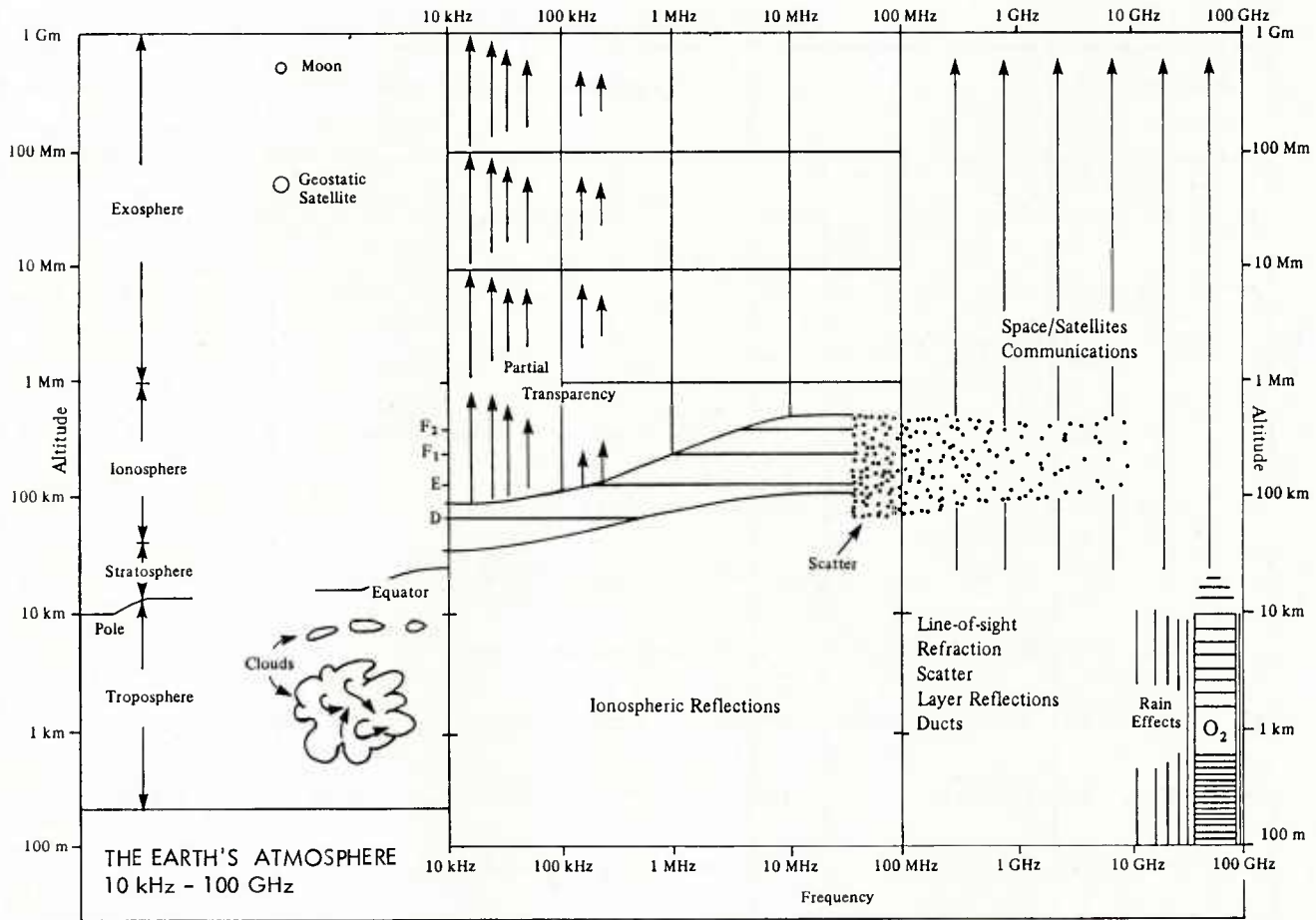


Fig. 1 Typical Propagation Paths in Tactical Environment
(a) Along the ground (b) At elevation angles



(H.J. Albrecht 1968/76)

Fig. 2 EM Wave Propagation 10 kHz - 100 GHz

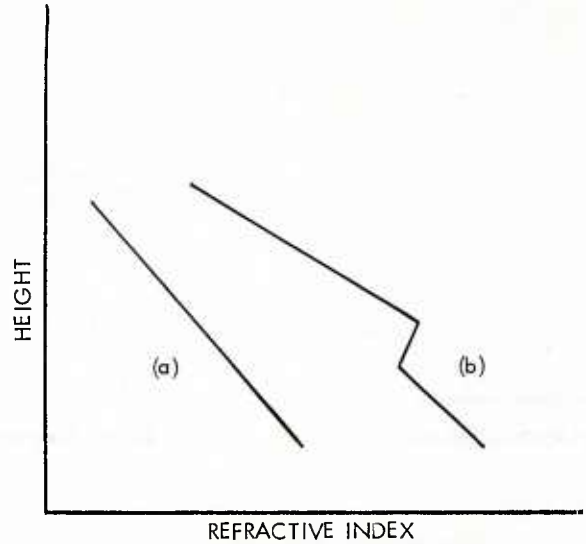


Fig. 3 Typical Gradients of Refractive Index
(a) Normal tropospheric conditions
(b) Disturbed conditions

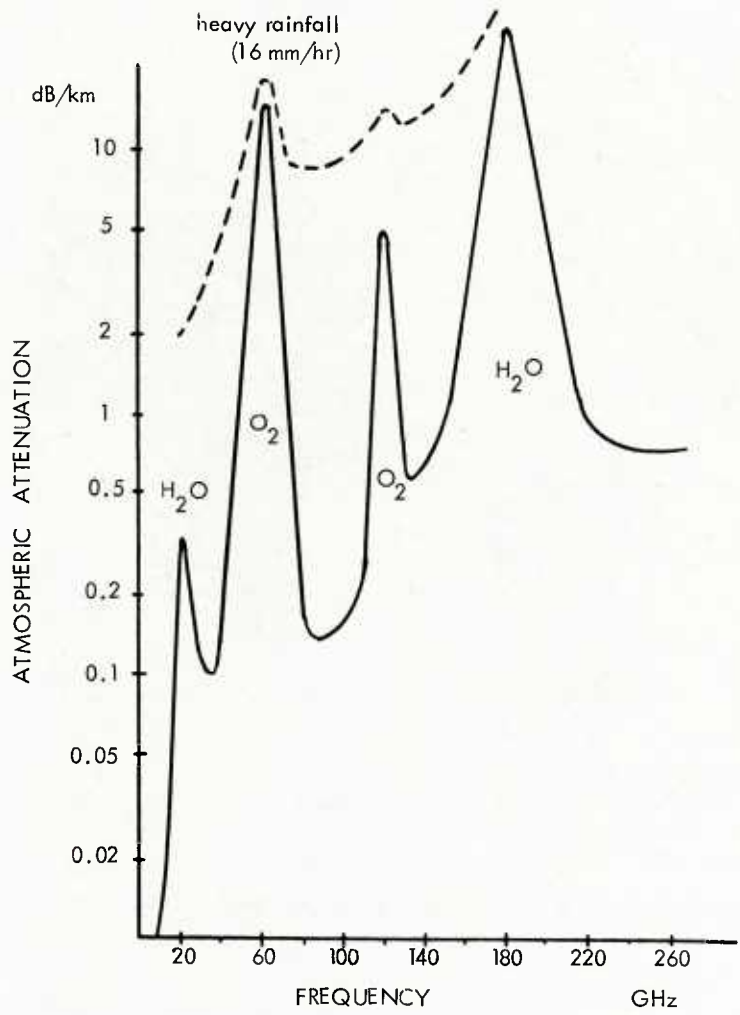


Fig. 4 Attenuation 20 - 260 GHz

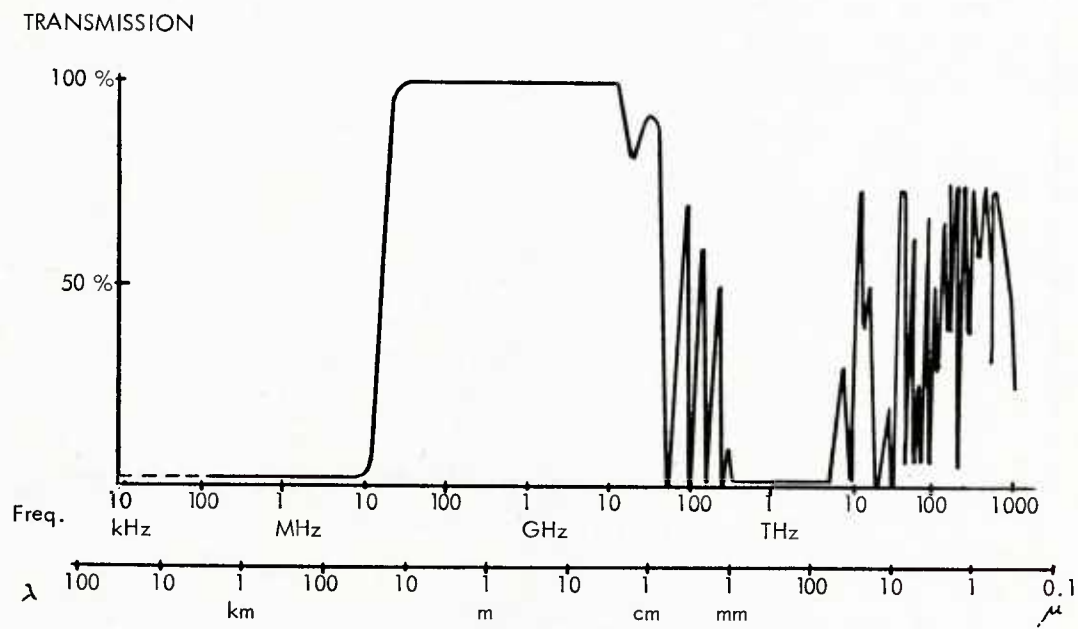


Fig. 5 Relative Space/Earth Transparency

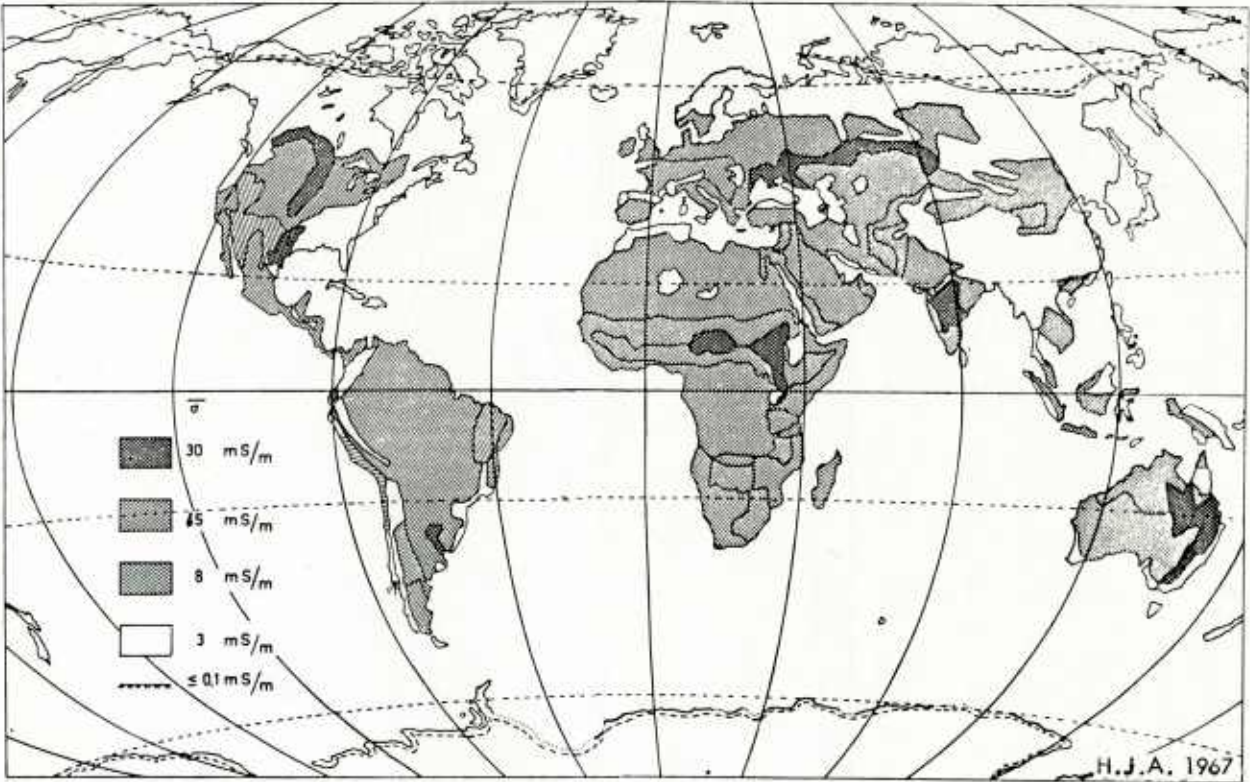


Fig. 6 World Map of Ground Conductivities

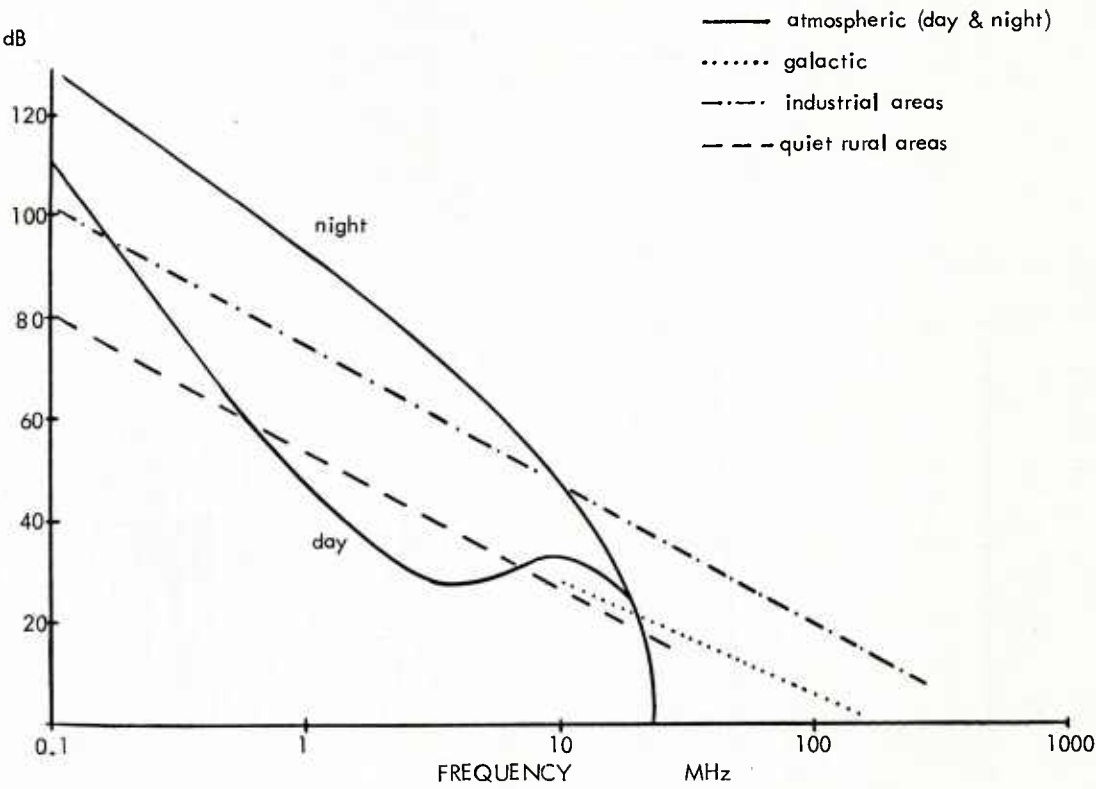


Fig. 7 Relative Noise Levels

LINK	TERRESTRIAL CABLE		LINE-OF-SIGHT & DIFFRACTION PATHS	SCATTER PATHS TROPOSCATTER IONOSCATTER	HF-GROUND WAVE & REFLECTIONS AT IONOSPHERE	SATELLITE LINKS LINE-OF-SIGHT SPACEBORNE RELAY
	WIRE	FIBRE OPTICS				
OPERATING FREQUENCY	AUDIO	>100 THZ	ABOVE 30 MHZ VHF UHF SHF EHF/ OPTICS	100 MHZ - 15 GHZ VHF UHF SHF	3 - 30 MHZ HF	ABOVE 100 MHZ VHF UHF SHF
TYPICAL SYSTEM APPLICATIONS	PTT AND PTT-RELATED		CNR MIDS (R&D)	(R&D) ACE HIGH		SEVERAL SATCOM SYSTEMS
PATH CRITERIA	CONSTRUCTIONAL CONDITIONS		LINE-OF-SIGHT AND/OR DIFFRACTION	IONO-SCATTER TROPO-SCATTER DEPENDENT ON MEDIUM	IONOSPHERIC CONDITIONS & THEIR VARIATIONS REQUIRE ADAPTATION	LINE-OF-SIGHT CONDITIONS, BUT ATMOSPHERIC EFFECTS
BANDWIDTHS	~ 4.0 KHZ	>100 MHZ	WIDE BANDWIDTHS POSSIBLE (UP TO 10% OF OPERATING FREQUENCY)	WIDE BANDWIDTHS, PRECAUTIONS WITH DATA TRANSMISSION	SMALL BANDWIDTHS, SMALL NO. OF CHANNELS	WIDE BANDWIDTHS POSSIBLE
DISTANCES	NET-DEPENDENT		SHORT DISTANCES	MEDIUM DISTANCES	LARGE DISTANCES	LARGE DISTANCES
MOBILITY	STATIONARY, BUT GENERAL NET ACCESS		STATIONARY, MOBILE OR TRANSPORTABLE	STATIONARY OR TRANSPORTABLE ONLY	STATIONARY, MOBILE OR TRANSPORTABLE	STATIONARY, MOBILE OR TRANSPORTABLE
PHYSICAL LIMITATIONS	CONSTRUCTIONAL FEASIBILITY		MULTIPATH ENVIRONMENT, TROPOSPHERIC CONDITIONS	EFFECTS OF SCATTER MEDIUM	IONOSPHERIC CONDITIONS	CONSTANCY OF ATMOSPHERIC TRANSPARENCY
EW HAZARDS	EMP	(EMP IF ABOVE SURFACE)	EMP; INTERCEPT & ECM; SIDELOBES, DECREASING WITH FREQUENCY	EMP; INTERCEPT AND ECM; SIDELOBES AND SIDE SCATTER	EMP; INTERCEPT AND ECM, EVEN GLOBAL	EMP; INTERCEPT AND ECM WITHIN GROUND COVERAGE

Fig. 8 General Criteria of Typical Paths

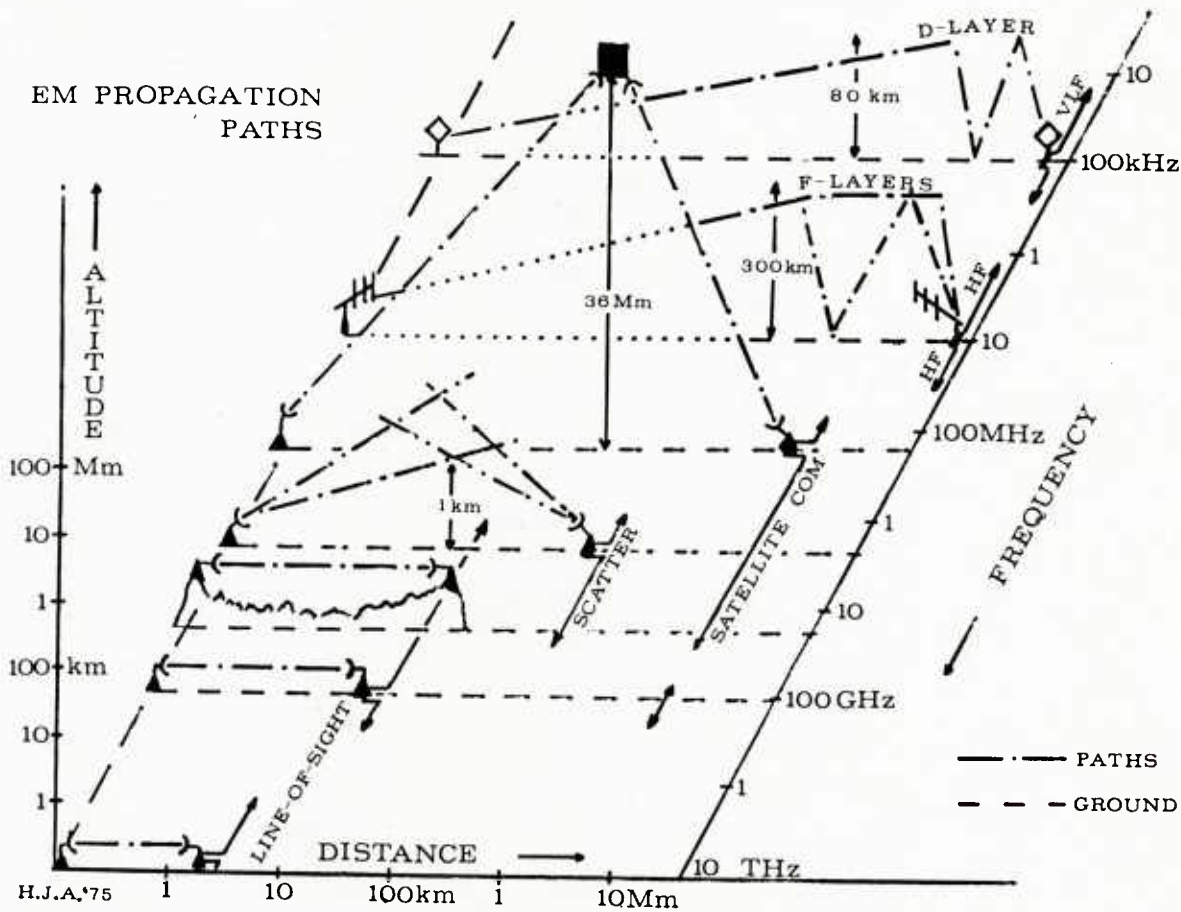


Fig. 9 EM Propagation Paths

GROUND-WAVE PROPAGATION CHARACTERISTICS OF INTEREST TO THE TACTICAL COMMUNICATOR

F.H. Palmer
CRAD/DSP-4
National Defence Headquarters
Ottawa, Ontario, K1A 0K2
CANADA

SUMMARY

This lecture presents a broad review of the effects of terrain and terrain cover on ground-wave propagation at frequencies of interest to the tactical communicator. Starting with the simplest case, that of free-space propagation, complexities are subsequently added until most of the factors which relate to path-loss, path-loss variability, and multipath effects have been addressed. It is hoped that the discussion will show that propagation prediction, and the choice of appropriate models, is as much an art as a science.

OUTLINE

1. INTRODUCTION
2. NOMENCLATURE
3. POINT-TO-POINT PATHS
 - 3.1 Free-space paths
 - 3.2 Free-space plus ground reflections
 - 3.3 Smooth earth: diffraction and surface waves
 - 3.4 Hills and mountains
 - 3.5 Terrain surface cover
 - 3.6 Signal variability
 - 3.7 Computer models
4. MOBILE COMMUNICATIONS
 - 4.1 Urban areas
 - 4.2 Rural areas
 - 4.3 Computer models
5. MULTIPATH EFFECTS
 - 5.1 Delay spread
 - 5.2 Doppler spread
6. SUMMARY

1. INTRODUCTION

This paper will discuss the effects of terrain and terrain cover on the propagation of radiowaves at frequencies and distances of interest to the tactical communicator. Both the MF/HF and VHF/UHF bands will be considered. Ranges of system parameters are as follows: for land scenarios, antenna heights range from essentially zero up to about 20 metres; for air, from about 20 to 15,000 metres; and for sea, from a few metres up to about 50 metres. Path lengths relevant to most operational scenarios are shown in Table 1.

Land:	MF/HF	up to 300 Km
	VHF/UHF	up to 80 Km
Air:	VHF/UHF	up to 200 Km
Maritime:	MF/HF	up to 500 Km
	VHF/UHF	up to 30 Km

Table 1.

It should be noted that the system parameters cited above are intended only to be representative of broad classes of systems. Since propagation characteristics change relatively slowly with frequency and path-length, the following discussion will also be useful as a guide for systems having operating parameters somewhat outside those given above.

In the following discussion, emphasis will be placed on the characterization of propagation parameters having the most immediate practical interest: path-loss, path-loss variability, and multipath delay spread.

2. NOMENCLATURE

Let us first define what we mean by the term 'path-loss'. Path-loss, also called 'basic transmission loss', is defined as

$$L = 10 \log(P'_t / P'_r) \quad \text{dB}$$

where P'_t and P'_r are measured in watts. Equivalently,

$$L = P'_t - P'_r \quad \text{dB}$$

where P'_t and P'_r are measured in dB relative to some power level such as 1 Watt or 1 Kw. P'_t is the power that would be radiated from a fictitious loss-free isotropic antenna at the same location as the actual transmitting antenna. P'_r is related to the power, P_t , input to the actual antenna terminals by the expression

$$P'_t = P_t \cdot G_t \quad \text{Watts}$$

where G_t is the numerical gain of the transmitting antenna. Equivalently,

$$P'_t = P_t + G_t \quad \text{dBW}$$

where P_t is measured in dBW and G_t in dB.

P'_r is the RF power which would be available from a similar fictitious loss-free, isotropic antenna at the same location as the actual receiving antenna. P'_r is related to the power available at the actual receiving antenna terminals by the expression

$$P'_r = G_r \cdot P_r \quad \text{Watts}$$

where G_r is the numerical gain of the receiving antenna, or

$$P'_r = G_r + P_r \quad \text{dBW}$$

where G_r is measured in dB.

The above expressions may be combined to give:

$$P_r(\text{dBW}) = P_t(\text{dBW}) - G_t(\text{dB}) - G_r(\text{dB}) - L(\text{dB})$$

which gives received signal power in terms of the system parameters P_t , G_t , and G_r and the path-loss L . The concept of path-loss enables the separation of the effects of the transmitting and receiving antenna gains and circuit losses from the effects of propagation.

What is meant by the term 'ground-wave'? In general, radio waves may be propagated by any of a number of modes. The modes of interest here are shown in Figure 1.

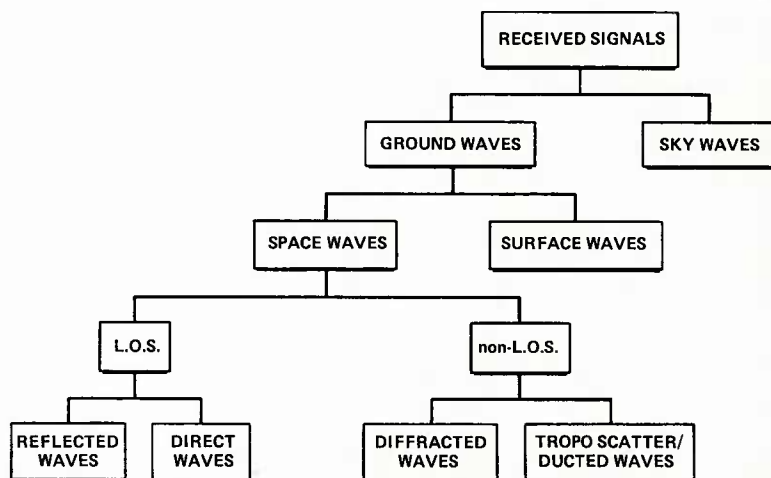


Figure 1 - Signal Propagation Modes

'Sky-waves' (the sky-wave mode) comprise those signals which arrive at a receiver after reflection or scattering by the ionosphere or by meteor trails. 'Ground-waves' can then be defined as the totality of all signals, other than sky-waves, which arrive at a receiver. The received ground-waves have characteristics which depend on the nature and geometry of the propagation path. These characteristics can, in principle, be determined by solving the electromagnetic wave propagation equations together with the appropriate boundary conditions. In some cases, such as propagation over a smooth sphere, this procedure can be carried out, by computer, to obtain estimates of path-loss over very smooth ground or calm sea. Results, usually presented graphically, will be discussed shortly. In general, such analytic mathematical procedures are too complex to be useful, particularly when dealing with rough terrain or rapidly changing tactical environments, and approximations must be made. The usual assumption is that various ground-wave propagation (sub) modes can be identified, treated independently, and vectorially summed at the receiving antenna location.

Reference to Figure 1 shows the subdivision of ground-waves into 'surface' waves and 'space' waves. Surface waves are excited by currents induced in the earth's surface by the transmitting antenna and are subsequently constrained to propagate along the interface between the earth's surface and the troposphere. The efficiency of a transmitter in generating surface waves depends upon the conductivity and permittivity of the ground. Efficiency decreases with increasing frequency and with increasing antenna height. Vertically polarized antennas are more efficient in exciting surface waves than are horizontally polarized antennas.

Space waves may be defined as all components of the received ground-wave other than the surface wave. For space waves, the effects of induced earth currents are negligible (except in the case of reflections) and the conductivity and permittivity of the earth's surface are relatively unimportant.

In general, a transmitting antenna generates both surface waves and space waves. At VHF/UHF frequencies however, transmitting and receiving antenna heights are usually sufficiently great, even for manpack or vehicle mounted systems, that the amplitude of the surface wave is very small compared to that of the space wave. For example, at 300 MHz and with vertically polarized antennas 2 metres off the ground, the space wave is typically 30 dB stronger than the surface wave. With horizontal polarization, the ratio is nearer 70 dB. An exceptional case is that of vertically polarized antennas over sea-water, where VHF transmitting antennas at heights up to about 10 metres can excite significant surface wave amplitudes. At MF/HF frequencies, the surface wave is dominant for almost all antenna heights of interest in ground-based tactical scenarios. Calculation of received field-strength in any given situation is considerably simplified if it can be assumed that either the surface wave or the space wave is dominant, and that the other mode may be ignored.

For convenience, space waves may be further subdivided into line-of-sight (LOS) modes and non-LOS modes. LOS signals may be received directly (free-space propagation), by reflection from the earth's surface or from structures upon it, or by a combination of direct and reflected modes. Non-LOS signals arrive at a receiver by diffraction around the earth's surface or over hills and mountains, or by scattering or ducting by the troposphere.

Each of the above propagation modes will be discussed in turn, starting with the simplest conceptual case: that of free-space LOS propagation. Complexities will be subsequently added until each of the factors relevant to ground-wave propagation in the tactical environment has been addressed.

3. POINT-TO-POINT PATHS

3.1 Free-space paths

This case obtains when airborne or land-based terminals are sufficiently high or close together that the line of sight between them is not close to the earth's surface at any point, where the path geometry is such that signals reflected from the earth's surface cannot be received or are highly attenuated by the transmitting or receiving antenna patterns, and where the transmitting antennas are sufficiently elevated that surface waves may be ignored. 'Not close' implies here that no part of the earth's surface lies within about 0.6 of the first Fresnel zone of the propagation path. The radius of the first Fresnel zone at a point distant d_t from the transmitter and d_r from the receiver is given by the expression

$$R = (\lambda d_t d_r / (d_t + d_r))^{1/2}$$

where λ is the operating wavelength.

VHF/UHF air/ground or hilltop to hilltop links often, but by no means always, satisfy the requirements for free-space propagation. It is difficult, on the other hand, to achieve free-space conditions in Maritime VHF/UHF applications because of reflections from the sea surface, or at MF/HF under any circumstances because the large Fresnel zone radii almost always include part of the earth's surface.

Free-space propagation represents one of the few cases in which a simple, exact analytic expression is available for the calculation of path-loss. This expression, as in more complex cases to be discussed later, may be presented in a number of formats, each leading to essentially the same result, but each having its own appeal in terms of convenience and accuracy. For example, communicators having access to a calculator or computer may prefer to work with the analytic expressions themselves; in this case:

$$L = 32.5 + 20 \log d + 20 \log f \quad (\text{dB})$$

In this and all subsequent expressions, d represents distance in Km, f the system frequency in MHz, and, where applicable, h_t and h_r the transmitting and receiving antenna heights in metres.

Others may prefer to work with the equivalent nomogram shown in Figure 2.

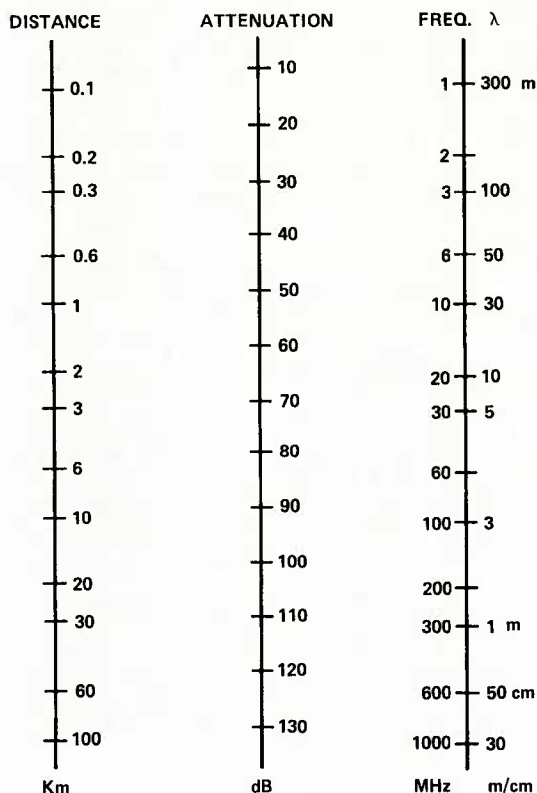


Figure 2 - Nomogram for Determining Free-space Path-Loss

Path-loss under free-space conditions may also be determined from the knowledge that the loss is 22 dB for the first wavelength of antenna separation, plus 6 dB every time this distance is doubled.

Choice of the method of calculation is usually dictated by the amount of computing power on hand, the precision to which results are to be calculated, and the time available in which to provide the results.

3.2 Free-space plus ground reflections

For path lengths up to a few kilometres, prairie or sea surfaces may often be treated as planes which, if smooth on a scale of wavelengths, may support strong reflections. For antennas which are at least a significant fraction of a wavelength in height, but whose heights are nonetheless very small compared to the path length, simple geometry may be used to add the direct and reflected signals. The result may be expressed as:

$$L = 120.0 + 40 \log d - 20 \log h_t - 20 \log h_r \quad (\text{dB}) \quad - 1$$

In this case, path-loss varies smoothly with antenna height and is independent of frequency. Note that as either the transmitting or receiving antenna heights become very low the above expression loses validity and predicts very high values of path-loss. This

is not observed in practice where path-loss is found to be relatively constant for antenna heights below about:

$$h^{(v)} = \lambda((\epsilon + 1)^2 + (60\sigma\lambda)^2)^{\frac{1}{4}} / 2\pi \quad (\text{vertical polarization})$$

$$h^{(h)} = \lambda((\epsilon - 1)^2 + (60\sigma\lambda)^2)^{-\frac{1}{4}} / 2\pi \quad (\text{horizontal polarization})$$

Because of this, the use of this expression is restricted to the VHF/UHF bands.

As the elevations of the terminals increase, the approximations implicit in the above are no longer valid. The vectorial addition of the direct and reflected signals at the receiving antenna results in interference lobes and path-loss varies in a 'sine-squared' manner with both antenna height and path-length. These interference effects diminish in magnitude as the land or sea surface becomes rough and the specular component of the reflected wave decreases in amplitude.

Figure 3 shows plots of received VHF signal strength over an ideally smooth earth. For very short paths, off the left in the figure, free-space values of path-loss and signal strength obtain. As expected, interference effects are visible at the higher frequencies and for intermediate path lengths where the antenna heights are still an appreciable fraction of the path-length. As path length increases, for fixed antenna heights, the assumptions in (1) gain validity, and a smooth variation of signal strength (or, correspondingly, of path-loss) is observed as a function of distance. At distances beyond about 20 kilometres, the assumption of a plane earth breaks down, but this produces no qualitative changes in path-loss or signal-strength behaviour. As the receiver approaches the horizon of the transmitter however, simple methods of computing path-loss break down as diffraction effects over the earth's surface assume increasing importance. These effects will be discussed later.

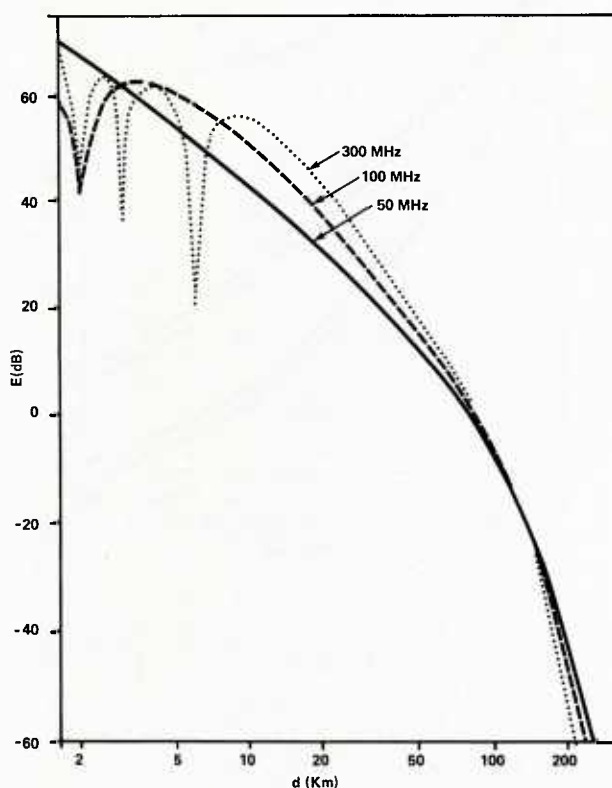


Figure 3 - Variation of VHF signal strength over an ideal smooth earth. P_t : 1 kW, h_t : 300 m, h_r : 10m.

In the interference region, fading occurs if either transmitter or receiver move in height or in range. If the land or sea surface is sufficiently smooth, nulls in excess of 30 dB may be encountered. Digital systems may encounter intersymbol interference problems due to the difference in arrival times of the direct and reflected signals. These problems may be alleviated by utilizing highly directive antennas to discriminate against the reflected wave.

3.3 Smooth Earth: diffraction and surface waves

In this section, we will discuss two essentially different phenomena. The first, diffraction of VHF/UHF waves over a smooth earth, represents an extension of the previous discussion to longer paths. The second, surface wave propagation, represents the dominant mode of propagation of MF/HF signals over the earth's surface.

VHF/UHF

As path length increases and the earth's surface blocks a significant fraction of the first Fresnel zone of the propagation path, diffraction effects assume increasing importance. It should be noted that these effects can be large, even at UHF, and even when an unobstructed optical path exists between transmitter and receiver. The exact calculation of diffraction effects over the smooth earth requires sophisticated mathematical techniques and is outside the scope of this paper. An approximate method, also valid for diffraction over obstacles such as hills and mountains, is discussed in the next section. Since most methods require the use of a computer, results are usually precalculated and presented in the form of tables or 'atlases' (1, 2). Nomograms, having limited accuracy, but having the advantage of speed, have been presented by, for example, Bullington (3).

Sample curves showing UHF signal strength as a function of distance are shown in Figure 4.

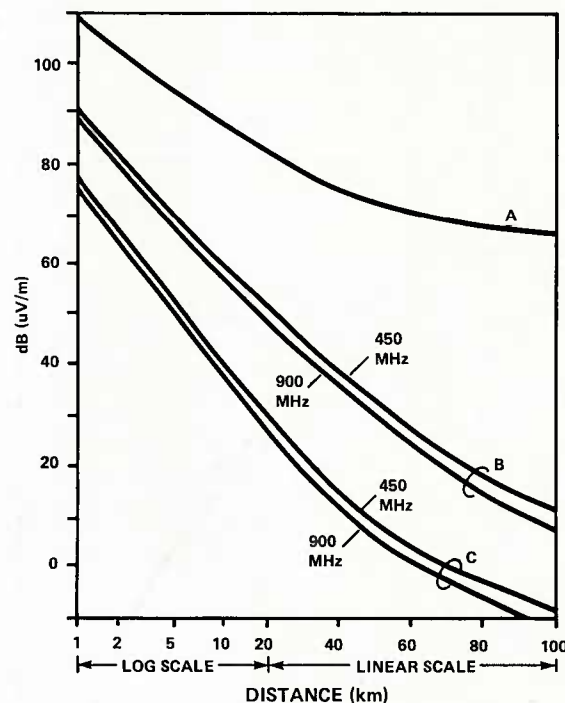


Figure 4 - UHF path loss as a function of distance over a smooth earth. P_t : 1 kW; h_t = 30m in all cases.
 'A' - free-space reference curve
 'B' - h_r = 3m
 'C' - h_t = 1.5m

In this example, receiving antenna heights are sufficiently low that no interference effects between direct and reflected paths are observable at any distance. At these frequencies, considerable fading of the received signal with respect to both time and location (for moving terminals) can be observed, particularly for paths longer than about 50 Km. For this reason, the curves shown in Figure 4 pertain to median values of path-loss, denoted by $L(50,50)$. The first '50' refers to the median value of path-loss with respect to location at a given time. Values of path-loss exceeded for other percentages of time or locations will be discussed later. At VHF/UHF frequencies, path-loss is strongly dependent on antenna height, but almost completely independent of ground constants. As will be seen, this is almost the reverse of the MF/HF case.

It is important to note that, at any frequency, the horizon of a smooth earth does not cause any abrupt changes in path-loss. Reference to Figure 4 shows that, in fact, the horizon cannot even be identified on the signal strength curves. This fact must be kept in mind when designing systems to be used at low elevation angles within the horizon and where smooth-earth diffraction losses can easily reach 20 dB.

On over-the-horizon paths, path-losses are usually not as high as predicted on the basis of smooth-earth diffraction theory. Small irregularities in refractive index cause the troposphere to scatter a small amount of signal around the curvature of the earth at all times (tropo-scatter). Path-losses for such paths must be computed using both diffraction and tropo-scatter models (1, 9). The smaller of the two losses is taken as representing probable observed losses. Tropospheric effects are further discussed in Section 3.6.

MF/HF

Because of the longer wavelengths at these frequencies, antennas in almost all terrestrial applications may be assumed to be sited on the surface of the earth. Under these circumstances, the dominant propagation mode is that of the surface wave. As for VHF/UHF diffraction over the smooth earth, sophisticated mathematical techniques* are required to calculate exact results, although various approximate techniques are available (4, 5, 6, 7). In this case also, results are usually precomputed and presented in the form of atlases. See again (1, 2).

Figure 5 shows the variation of signal strength with distance at a frequency of 3 MHz. In this case, losses and corresponding signal strengths depend upon the ground conductivity and permittivity. In general, the higher the conductivity of the earth's surface, the lower the losses because of lower attenuation of induced currents in the earth's surface. For this reason, and as is quite evident in Figure 5, losses on over-sea paths are lower than on equivalent land paths.

As at VHF/UHF, there is no abrupt change in signal strength as the receiver crosses the horizon of the transmitter.

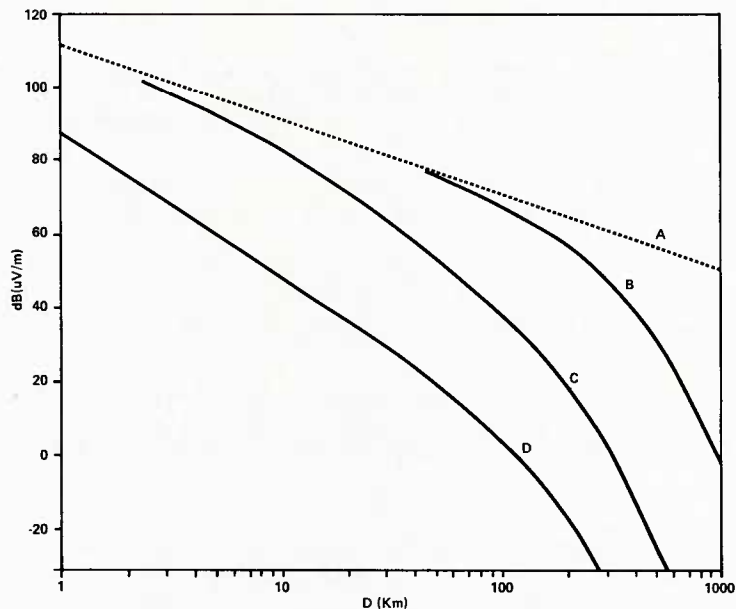


Figure 5 - MF signal strength as a function of distance over a smooth earth. P_t : 1 kW. Antennas on ground surface.

'A' - free-space reference curve

'B' - Sea: $\sigma = 4 \text{ S/m}$; $\epsilon = 80$

'C' - Land: $\sigma = 3 \times 10^{-2} \text{ S/m}$; $\epsilon = 4$

'D' - Land: $\sigma = 3 \times 10^{-4} \text{ S/m}$; $\epsilon = 4$

*In fact, the same basic mathematical expressions cover smooth-earth propagation phenomena at all frequencies.

3.4 Hills and Mountains

The preceding discussions of idealized propagation paths are applicable, with corrections for such things as fading (see Section 3.6), or for excess attenuation due to high seas, to propagation over water or relatively smooth land. Land paths are seldom smooth. In this section we deal with the effects on point-to-point links of hills or mountains lying along the propagation path. Later, we shall discuss the effects of rough terrain on mobile systems.

In the simplest instance, transmitting or receiving VHF/UHF antennas placed on hills or mountains, and having an unobstructed view toward the other terminal, may be treated as having heights equal to that of the actual antenna plus the height of the hill or mountain above the average height of the surrounding terrain: the 'effective height of the antenna above average terrain', usually denoted by the term 'EHAAT'. The situation is more complex at MF/HF, where we are dealing primarily with the surface wave. Currently, the best techniques for dealing with irregular terrain at MF/HF frequencies are embodied in a computer program developed by Ott (8), and discussed further in Section 3.7. The remainder of the present discussion relates primarily to VHF/UHF frequencies.

Examination of propagation curves for various antenna heights will show the advantage of utilizing the 'high ground'. On the other hand, interception, radiolocation, and hostile jamming activities are more easily carried out, for precisely the same reasons, against systems in such locations.

What of the effect of hills or mountains along the propagation path? As in the case of signals propagating over the horizon of a smooth earth, signal-strength does not fall immediately to zero in the shadow region. As we shall see, a considerable amount of signal may be diffracted around obstacles at low VHF frequencies. As the frequency increases however, the situation more and more closely approximates optical conditions until at high UHF or microwave frequencies, obstacles do in fact cast relatively sharp 'radio shadows'.

Obstacles having sharp (in terms of wavelengths) or 'knife-edge' crests may be treated by classical optical diffraction techniques. Rice et al. (9) have presented equivalent results in a form suitable for machine calculation. They first defined a parameter

$$v = \pm 2 \theta (f d_t d_r / (d_t + d_r))^{1/2}$$

where d_t and d_r are the distances from the obstacle to the transmitter and receiver respectively, and θ is the angle through which the signal is diffracted in passing over the obstacle. v is positive for non-LOS paths and negative otherwise. Diffraction loss may then be computed from

$$\begin{array}{ll} L_d = 2.78^2 + 9.95v + 6.2 & \text{dB} \quad \text{if } -1 \leq v \leq 0 \\ L_d = 6.1 - .005v^4 + .16v^3 - 1.7v^2 + 9.3 & \text{dB} \quad \text{if } 0 < v \leq 3 \\ L_d = 12.9 + 20 \log v & \text{dB} \quad \text{if } v > 3 \end{array}$$

The total path-loss is given by $L = L_{fs} + L_d$ where L_{fs} is the free-space path-loss over the same path in the absence of the obstacle. Nomograms are also available which give effectively the same results (3).

The case of obstacles having rounded crests is more difficult to treat. The following procedure (10, 11) is probably one of the simplest that can be used to obtain estimates of diffraction loss under these conditions. First define the parameters

$$\alpha = \lambda^{2/3} r^{1/3} / R \quad \text{and} \quad \beta = H / R$$

where r is the radius of the obstacle crest, λ is the operating wavelength, R is the Fresnel zone radius of the propagation path at the location of the obstacle, and H is the height of the obstacle above or below a straight line drawn between transmitter and receiver. H is positive for non-LOS paths and negative for LOS paths. Figure 6 may be used to estimate diffraction loss for given values of α and β .

It is quickly seen, on using these techniques, that they are more suited to machine than to hand calculation.

For fixed system parameters, diffraction losses increase as the radius of curvature of the obstacle crest increases. As the frequency decreases, α remains relatively constant (it varies as $\lambda^{1/6}$), but β decreases and we move to the left on Figure 6. This results in lower diffraction losses in agreement with the practical observation that lower frequency signals are easier to receive in the shadows of hills than are those at higher frequencies.

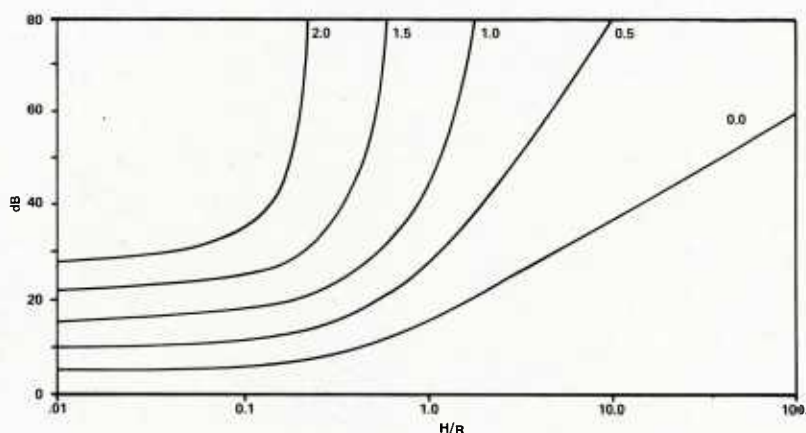


Figure 6 - Curves showing diffraction loss over obstacles with rounded crests as a function of the parameters $\beta = H/R$ and $\alpha = \lambda^{2/3}/R$. The curve $\alpha = 0$ represents the sharp 'knife-edge' case.

Propagation over more than one hill (multiple edges) is primarily a problem encountered in dealing with paths longer than those of interest in the present context. It must be noted however, that longer paths become relevant when dealing with the interception range of a communication system. This case will not be further discussed. Approximate techniques which may be applied in such cases may be found in (10, 12). All require the use of computers.

3.5 Terrain surface cover

Thus far, we have progressed part way along the road from looking at the effects of idealized terrain to looking at the effects of actual terrain. To complete the journey, insofar as it is practical, we must now account for the effects of terrain cover. The following discussion will centre on the losses associated with the presence of trees and buildings. These represent about the only cases where any estimate of propagation loss may be made.

Losses due to these features are usually only important when they are in relatively close proximity to the transmitting or receiving antennas. Losses thus incurred may be directly added to the losses due to the terrain itself.

Trees:

Numerous measurements of 'excess' path-loss in or near treed areas have been carried out (13, 14, 15, 16, 17), but few models have been developed to permit predictions to be made in the general case. The situation is obviously very complex since path-losses depend upon tree type, size, density, whether or not the trees are in leaf, and whether they are wet or dry. However, the following discussion is indicative of the effects expected of all tree types.

Upon entering a wooded area from the transmitter (receiver) side in the case of clutter around the receiver (transmitter) the path loss increases (13) at the rate of:

$$L_v = 1637\sigma + 0.33 (\exp(-90/f) \cdot \log(1 + f/100)) \quad \text{dB/metre}$$

$$L_h = 1637\sigma + 0.43 (\exp(-210/f) \cdot \log(1 + f/200)) \quad \text{dB/metre}$$

where v and h stand for vertical and horizontal polarization respectively, and σ is the average conductivity which depends on the characteristics of the trees. Figure 7 shows typical values of the attenuation rate as a function of frequency for typical mid-latitude deciduous forests. Note that the attenuation is higher when using vertical polarization than when using horizontal, and that the VHF/UHF attenuation rates are an order of magnitude higher than (extrapolated) at MF/HF.

Inside a wooded area, and after the initial increase in attenuation described above, the path-loss relative to free-space reaches a more-or-less constant value independent of distance within the wooded area. This results from the fact that some radiation is always being scattered downward by the treetops. 30 dB is a typical value for this limiting attenuation in the UHF band, for antennas which are short with respect to the trees (14). Corresponding values for the MF/HF band are not available in the literature, but are expected to be only a few dB.

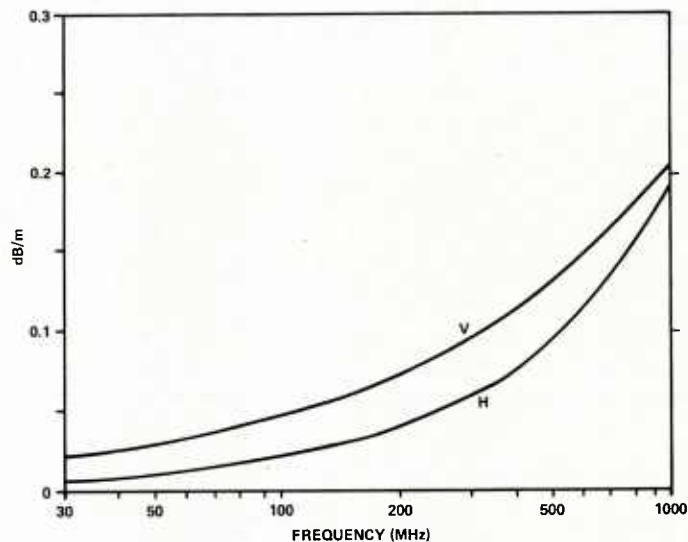


Figure 7 - Attenuation rates, as a function of frequency, of mid-latitude deciduous forest. Curves are shown for both vertical and horizontal polarization

At distances behind a wooded area greater than about five times the mean height of the trees, the treetops may be taken as defining a knife-edge, and the resultant excess path-loss is that expected as a result of diffraction over this edge.

Buildings:

The effects of buildings, particularly those of metal construction, or nearby communication links can be extremely difficult to predict. The greatest difficulties are caused by the presence of reflections, having unknown amplitudes and phases, from various parts of the structures. The only situation for which much guidance can be given is for the case of a terminal situated within, or immediately behind, a single isolated structure.

Two loss factors need to be computed for terminals situated immediately behind an isolated building. The first is to compute the diffraction loss for signals propagating over or around the building. For tractability, the edges of the building are usually assumed to be sharp knife-edges. The second is the determination of the attenuation of signals passing directly through the structure. This is extremely difficult in practice because of the wide diversity of building types and construction materials and because of the paucity of experimental data. One attempt (11) for VHF/UHF frequencies, has been to compute an empirical loss factor $L = M \cdot d / 15$ (dB), where d is the extent of the building along the line-of-sight, and M is a loss factor dependent upon the building construction type, e.g., $M = 15$ for wood, 30 for concrete, and so forth.

It is also difficult to present guidelines for determining excess losses for terminals located within buildings. Present evidence (18) suggests that, at VHF/UHF at least, path-losses fluctuate widely as a function of position within buildings and that losses increase with distance from windows.

3.6 Signal Variability

Time variability:

If the troposphere were perfectly homogeneous and unchanging, path losses for fixed terminals would be independent of time. In practice, the troposphere is subject to fluctuations in temperature, density, and humidity, all of which are reflected in fluctuations of tropospheric refractive index n (or refractivity, defined as $N = 10^6 \times (n-1)$). The results of these fluctuations can range from negligible to the radio frequency equivalent of mirages. In some cases, sufficiently intense stratification of the troposphere results in partial reflection of VHF/UHF signals. This has the effect of 'trapping' the wave between the stratified part of the troposphere and the earth's surface. Such 'trapped' or 'ducted' waves can propagate for large distances with relatively low losses. Generally, fading due to tropospheric effects is predictable only in a statistical sense. Figure 8 shows the percentage of time, at a given location, that VHF/UHF path-loss has any given value above or below its long-term $L(50, 50)$ value. Corrections are seen to be strongly dependent upon path length. Path loss exceeded for a specified percentage of time, as measured at a fixed location, is given by

$$L(t, 50) = L(50, 50) + \Delta L(t)$$

where $\Delta L(t)$ is determined from Figure 8. As expected, short paths show little time variability while, for example, a 200 Km path is expected to experience path-losses 10 dB below the long-term median for 10% of the time, and 25 dB below it for 1% of the time. These curves are important for determining the probability of intercept of communications as well as for determining the fading margins required to ensure reliable communications over longer paths. Separate sets of curves are available for each type of climate (9). At MF/HF frequencies, the effects of tropospheric refractivity fluctuations are far smaller than at VHF/UHF, partly because of the longer wavelength in relation to the scale size of the tropospheric fluctuations.

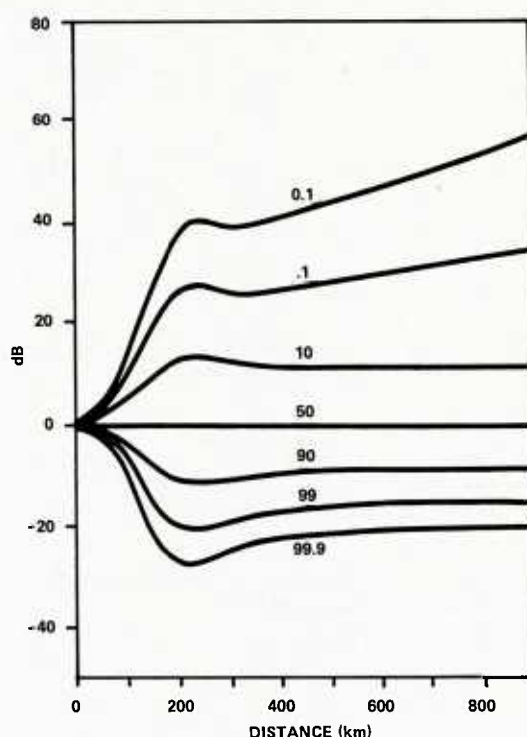


Figure 8 - Variation of path-loss with distance for the indicated percentages of time. (VHF/UHF)

In the maritime situation, it is observed that high sea-states result in path-losses additional to those expected for propagation over a smooth sea surface (19). Again, this effect is more pronounced at the higher frequencies. Typically, such excess loss at 50 MHz and over a 30 Km path is about 1 dB for sea-state 1 and near 10 dB for sea-state 6.

Space variability:

As a receiver is moved about over distances of a few wavelengths, fluctuations in path-loss are usually observed. These 'small scale' fluctuations are usually Rayleigh distributed. If one now tabulates the median values of path-loss over many of these small areas (spread over perhaps a square kilometre), and determines their resultant 'large-scale' distribution, it is usually found that it is log-normal. For a complete description of spatial path-loss variability the two types of fading distributions should be combined. This can be done using computer techniques, but is of limited interest in the tactical scenario. Figure 9 shows an example of the log-normal distribution of path-loss about the large scale median. The standard deviation of this distribution depends upon the nature of the immediate environment of the receiving antenna. The path-loss exceeded at a specified percentage of locations, as measured at a fixed time, is given by

$$L(50, x) = L(50, 50) + \Delta L(x)$$

where $\Delta L(x)$ is determined from Figure 9.

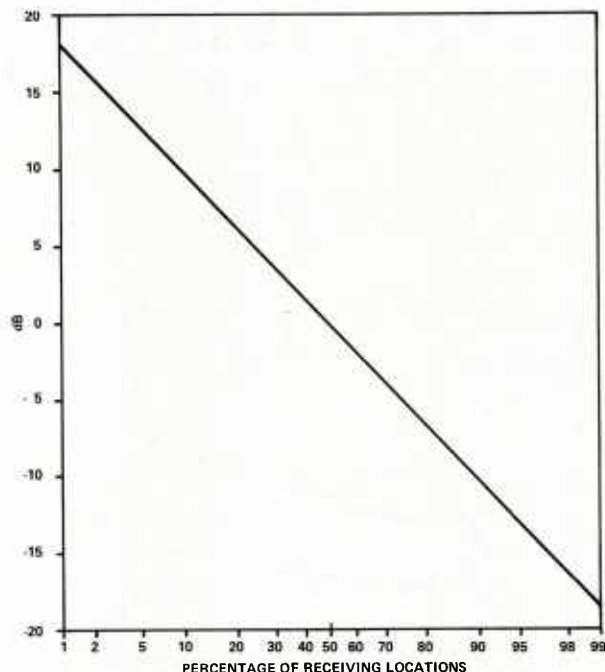


Figure 9 - Ratio (dB) of the path-loss for a given percentage of locations to the path-loss for 50% of the receiving locations.

For any given system, the value of path-loss exceeded for any given percentages of locations or times may be found from the expression:

$$L(t, x) = L(50, 50) + \Delta L(t) + \Delta L(x)$$

3.7 Computer models

Estimates of path-loss and its variability over point-to-point paths may be obtained through the use of nomograms and empirical or approximate expressions such as those presented in the foregoing sections. Computational complexity precludes, however, the taking into account in such a simple way of many factors necessary for the accurate determination of path-loss. Such factors include the radii of curvature of obstacles, and location of multiple obstacles, along the propagation path. Similarly, the vectorial addition of numerous reflected or diffracted waves is not possible in any simple manner. Manual techniques are too time-intensive. For this reason, computer-based techniques have become widely used within the last ten or fifteen years: for example, (8) at MF/HF and (9, 20, 21, 22) at VHF/UHF. The program of Ott(8) is unique in the MF/HF frequency bands in that, given a path profile and associated ground constants, it enables prediction of detailed path-loss profiles as a function of distance from the transmitter.

In order that detailed terrain profiles do not have to be constructed by hand for each path of interest, the use of digital topographic data bases has also become widespread. These data bases usually have a horizontal resolution of between a few tens and a few hundreds of metres, and usually contain information pertaining to the ground surface cover at each point in the data base. They are usually accessed automatically by the propagation prediction programs. Because the programs and data bases are at present only available on large computer systems, they are of limited utility in ever-changing real-time tactical scenarios. The advent of high density and high speed integrated circuits may remove this difficulty in the relatively near future.

4. MOBILE COMMUNICATIONS

4.1 Urban areas

In mobile situations, it is often impractical to determine path-loss at every point to be traversed by the mobile terminal. It is more realistic to determine the median path-loss expected between a fixed and a mobile terminal in a given area, and to then estimate the variability of path-loss as the mobile moves from one point to another in that area. This is particularly true in urban areas where the complexity of the terrain precludes most attempts at detailed point-to-point modelling. An empirical model developed by Egli (23), using data from large U.S. cities, is commonly used to estimate path-loss and its variability on roads within urban areas. Path-loss may be determined from:

$$L = 85.9 + 20 \log f + 40 \log d - 20 \log h_t - 20 \log h_r \quad (\text{dB}) \text{ if } h_r > 10 \text{ m.}$$

$$L = 76.3 + 20 \log f + 40 \log d - 20 \log h_t - 10 \log h_r \quad (\text{dB}) \text{ if } h_r \leq 10 \text{ m.}$$

The predicted large-scale standard deviation of path-loss encountered by a moving terminal is estimated to be:

$$\sigma = 5.5 \log f - 3.2 \quad (\text{dB})$$

Variability is only 1 dB or so at frequencies near the top of the HF band, rising to 10 - 15 dB at UHF.

Additional losses and variability are incurred when one or both terminals are within buildings. These effects were discussed earlier in the section dealing with the effects of terrain cover.

4.2 Rural areas

A variety of models exist for predicting median path-losses over various types of non-urban irregular terrain where the dominant cause of path-loss variability is variable shadowing by natural terrain features. Among these are the U.S. Electromagnetic Compatibility Analysis Centre (ECAC) models (24):

LOS paths:

$$L = 95.6 + 2.5 \log f + (31.5 + 0.5 \log f)(\log d - .21) \quad (\text{dB})$$

Non-LOS paths:

$$L = 92.6 + 11.0 \log f + (26.0 + 4 \log f)(\log d - .21) \quad (\text{dB})$$

'Mountainous' paths:

$$L = 107.6 - 3.5 \log f + (22.0 \log f - 9)(\log d - .21) \quad (\text{dB})$$

It is assumed that the paths are not over water, that path lengths are less than 50 Km, and that antenna heights are less than 6 metres.

Other empirical expressions have been presented by Murphy (25):

'Level' terrain:

$$L = 99.2 + .016 \log f + 40 \log d - 20 \log h_t - 18.5 \log h_r \quad (\text{dB})$$

'Mountainous' terrain:

$$L = 21.4 + 39.4 \log f + 40 \log d - 20 \log h_t - 5.3 \log h_r \quad (\text{dB})$$

Standard deviations of path-loss are given as:

$$\sigma = 13.7 - 0.11 h_r + .002 f \quad (\text{dB})$$

$$\text{and } \sigma = 17.3 - 0.019 h_r + .0012 f \quad (\text{dB}) \text{ respectively.}$$

It is clear from substitution of a fixed set of parameters into each of the preceding expressions that variations between models of up to about 10 dB can be expected for prediction of path-loss over similar types of terrain. This is indicative of the problems encountered in the practical applications of empirical path-loss expressions based on limited sets of data.

4.3 Computer models

Computer-based propagation models exist which provide better estimates of median path-loss over statistically irregular terrain than do the relatively simple expressions detailed above. Probably the best known of these is the 'Irregular Terrain' model of Longley and Rice (26). It is applicable to propagation over irregular terrain in sub-urban and rural areas. Calculations are based on analytic techniques and approximations similar to those discussed in the first part of this paper. However, the values of parameters such as horizon distance, obstacle height, etc., that are used in these calculations are statistical medians based on a median terrain irregularity height Δh which is chosen to be typical of the propagation path.

Models such as this are suited to path-loss calculations over 'statistically-uniform' types of terrain where there are no large isolated obstacles. If such obstacles exist, all models of this type will seriously underestimate path-loss within the obstacle shadows.

As with the 'detailed' point-to-point models described earlier, the Longley and Rice program is presently restricted to use with relatively large computer systems.

5. MULTIPATH EFFECTS

5.1 Delay spread

High data rate VHF/UHF digital communications systems are susceptible to errors due to intersymbol interference resulting from the simultaneous reception of various reflected signals, each having a different absolute time delay (delay spread). Systems operating in areas remote from buildings, and in relatively flat terrain, usually do not suffer greatly. In built-up areas however, the flat, vertical sides of buildings can be very efficient reflectors of radio waves. Over open water, the water surface can likewise be an efficient reflector. In the latter case, which can be especially troublesome in airborne scenarios, system geometries are usually quite simple, and the delay spread of the direct and reflected waves can easily be calculated. If the problem is severe, directive antennas can often be used at UHF to discriminate against the reflected signals and to thus reduce or eliminate the problem. In urban areas, directive antennas may also be used to reduce the severity of the problem. It is not usually possible to eliminate the problem under these circumstances, however, because of the wide range of delays often encountered within small angles of arrival of the signals.

Numerous measurements of UHF delay spread have been carried out in suburban and urban areas of the U.S. (27, 28, 29). These measurements, made using relatively non-directive antennas, indicate that for suburban residential and commercial areas on relatively flat terrain, the delay spread is generally less than $\frac{1}{4}$ microsecond with a corresponding correlation bandwidth (0.9 correlation) greater than 250 kHz. In more dense urban areas delay spreads greater than 2 microseconds are observed, with associated correlation bandwidths as low as 40 kHz. In some cases, discrete multipath components with excess delays of 5 to 7 microseconds were observed. Sophisticated error detection and correction codes are often required to provide acceptably low bit-error rates in these environments.

In cases where the transmitter-receiver line-of-sight is blocked by local buildings, reflected signal components can be stronger than the direct component. Moving terminals may thus have synchronization problems as they move from shadowed to non-shadowed areas and the dominant signal component shifts abruptly in arrival time.

UHF multipath measurements have also been carried out in rural areas of Sweden (30, 31) over paths ranging from about 8 to 40 Km in length. Measurements at 445 and 900 Mhz showed that multipath effects are more serious at the higher frequency than at the lower, and that the use of lower antennas and vertical polarization provides poorer results than do higher antennas and horizontal polarization. As in the urban situation, directional antennas discriminate against multipath signals and reduce the amplitude of delayed signal components. Even so, and using horizontal polarization at the lower frequency, multipath components within 8 dB of the direct signal amplitude were observed with delays of up to about 1 microsecond.

5.2 Doppler spread

Few measurements of doppler spread have been made, although see (27 and 29). Doppler spread of received signals arises because the angles-of-arrival of the various reflected waves can be widely spread in azimuth as seen from the receiver. Motion of the receiver then results in a different doppler shift for each multipath component. The total spread is:

$$f = 2 v f / c$$

where v is the vehicle speed and c the speed of light. The total doppler spread width can reach 20 Hz at 300 MHz for a vehicle speed of 10 m/second.

6. SUMMARY

Ideally, a single set of E-M wave propagation equations could be solved, using appropriate boundary conditions, to solve any problem at hand. Unfortunately, even high speed computers do not allow this except in certain simplified situations. As is evident from the preceding text, we are forced to make approximations suitable for each situation, to assume that various propagation phenomena can be subdivided into separate, manageable parts, evaluated independently, and then summed to provide the required answer. We are also forced to assume that certain phenomena may be neglected without unduly compromising the final results. In other situations, theory is foregone altogether, and empirical expressions are constructed from experimental data. It is then assumed that these expressions are generally valid. In view of this, it may be wondered how useful predictions of radio system performance can be made at all. Perhaps it is because radiowave prediction is as much an art as a science that progress is possible.

It is the task of the communicator to become proficient at the art as well as at the science.

REFERENCES

1. "Propagation in non-ionized media", CCIR, XIIIth Plenary Assembly, Vol. 5, Geneva, (1974).
2. "Atlas of ground-wave propagation curves for frequencies between 30 and 300 MHz", CCIR, Geneva, (1955).
3. "Radio propagation fundamentals", K. Bullington, BSTJ 3, 593-626, (1957).
4. "Calculation of the ground-wave field intensity over a finitely conducting spherical earth", K.A. Norton, Proc. IRE, 29, 623-639, (1941).
5. "The calculation of field-strengths over a spherical earth", C. Domb and M.H. Pryce, J. of the IEE, 94, 325-339, (1947).
6. "Calculation of groundwave attenuation in the far diffraction region", L.E. Vogler, J. Res. NBS, 68D, 819-826, (1964).
7. "The propagation of radio waves over the surface of the earth and in the upper atmosphere", K.A. Norton, Proc. IRE, 25, 1203-1236, (1937).
8. "An alternative integral equation for propagation over irregular terrain", R.H. Ott, Radio Science, 6, 429-435, (1971).
9. "Transmission loss predictions for tropospheric communication circuits", P.L. Rice et al., NBS Tech. Note 101 (2 vols.), (1966).
10. "A simplified solution to the problem of multiple diffraction over rounded obstacles", M.S. d'Assis, IEEE Trans. Ant. and Prop., AP-19, 292-295, (1971).
11. "VHF/UHF path-loss calculations using terrain profiles deduced from a digital topographic data base", F.H. Palmer, AGARD Conf. Proc. 269 (1979).
12. "Multiple knife-edge diffraction of microwaves", J. Deygout, IEEE Trans. Ant. and Prop., AP-14, 480-489, (1966).
13. "Some effects of buildings and vegetation on VHF/UHF propagation", P.L. Rice, IEEE Mountain-West EMC Symposium, pp 1-10, (1971).
14. "The influence of trees on television field strength at ultra-high frequencies", H.T. Head, Proc. IRE, 48, 1016-1020, (1960).
15. "Height gain measurements at VHF and UHF behind a grove of trees", A.H. LaGrone, P.E. Martin, and C.W. Chapman, IRE Trans. on Broadcasting, BC-9, 37-54, (1953).
16. "VHF and UHF reception - effects of trees and other obstacles", J.A. Saxton and J.A. Lane, Wireless World, 61, 229-232, (1955).
17. "Field strength and its variability in VHF and UHF land mobile radio service", Y. Okumura et al., Review of the Electrical Communications Laboratory (Japan), 16, 825-873, (1968).
18. "Building attenuation and product susceptibility", S. Mir and D.J. White, IEEE EMC Symposium Record, 76-84, (1974).
19. "Theory of HF and VHF propagation across the rough sea; application to HF and VHF propagation above the sea", D.E. Barrick, Radio Science, 6, 527-533, (1971).
20. "The CRC VHF/UHF propagation prediction program: description and comparison with field measurements", F.H. Palmer, AGARD Conf. Proc. 238, (1978).
21. "Computer prediction of UHF broadcast service areas", J.H. Causebrook, BBC Engineering Research Report: BBC RD 1974/4, (1974).
22. "Computer prediction of service areas for VHF mobile radio networks", R. Edwards and J. Durkin, Proc. IEEE, 116, 1493-1500, (1969).
23. "Radio propagation above 40 Mc/s over irregular terrain", J.J. Egli, Proc. IRE, 45, 1383-1391, (1957).
24. "Empirical ground wave propagation model", ECAC Tech. Note TN-003-259, (1966).
25. "Statistical propagation model for irregular terrain paths between transportable and mobile antennas", J.P. Murphy, AGARD Conf. Proc. CP-70-71, (1971).

26. "Prediction of tropospheric radio transmission over irregular terrain - a computer method", A.G. Longley and P.O. Rice, ESSA Tech. Rept. ERL 79 - ITS 67, (1968).
27. "Delay doppler characteristics of multipath propagation at 910 MHz in a suburban mobile radio environment", D.C. Cox, IEEE Trans. Ant. and Prop., AP-20, 625-635, (1972).
28. "Distributions of multipath delay spread and average excess delay for 910 MHz urban mobile radio paths", D.C. Cox, IEEE Trans. Ant. and Prop., 206-213, (1975).
29. "Time and frequency domain characterizations of multipath propagation at 910 MHz in a suburban mobile radio environment", Radio Science, 7, 1069-1077, (1972).
30. "Multipath characteristics at UHF in rural irregular terrain", L. Ladell, FOA (Sweden) Report C 30125-E2, (1977).
31. "Multipath propagation over irregular terrain at UHF", L. Ladell, FOA (Sweden) Report C 30100-E2, (1977).

Propagation Aspects of Ionospheric Links Over Short and Medium Distances

by

Charles M. Rush

Acting Chief, Applied Electromagnetic Science Division
Institute for Telecommunication Sciences
National Telecommunications and Information Administration
U.S. Department of Commerce
Boulder, Colorado 80303
United States of America

SUMMARY

Radio communications under tactical battlefield conditions involve a number of complex and often competing effects: portability of equipment and stability of signal; secure communications and general surveillance capability; and optimum circuit performance and simplified operating procedures. In addition, the medium within which radio signals are transmitted will impact upon the performance of the radio circuit. The impact of the propagation medium upon the performance of a radio circuit is perhaps greatest for those circuits that depend upon reflection (or scatter) of radio waves from the ionosphere.

The purpose of this paper is to describe those aspects of ionospheric propagation that are pertinent to understanding, assessing, and predicting the performance of ionospheric-dependent radio links under tactical scenarios. Emphasis will be given to those aspects of ionospheric propagation that compete for control of overall circuit performance: path geometry, signal loss, ionospheric structure and its variation with location and time, ionospheric parameters, and their relationship to circuit performance. Discussion will include the problems associated with predicting the performance of ionospheric links for long-term planning purposes as well as for satisfying short-term operational requirements.

1.0 INTRODUCTION

In attempting to assess the likely circuit performance of ionospheric-dependent radio links at short and medium distances, it is necessary to consider those aspects of ionospheric propagation that determine overall system performance: path geometry, signal loss, ionospheric structure, and variations in the ionospheric medium. Many applications involving short and medium distance propagation are predictive in nature, permitting predictions to be made of expected circuit performance. Such predicted performance must be based not only on realistic logistical considerations (availability of proper equipment, acceptable terrain features) but also on realistic expectations of the structure of the propagation medium at the time for which the predictions are being made.

In this paper, we discuss the major aspects of ionospheric propagation at distances of 3000 km or less. In the next section, we discuss the appropriate path geometries that are assumed for the propagation of radio waves via the ionosphere to distances of 3000 km. Such paths generally are assumed to be controlled by normal reflection of radio waves that are incident on the ionosphere from the ground. In Section 3, we discuss the processes that contribute to the loss of the radio signal strength as it propagates from the transmitter to the receiver. The discussion will highlight the important processes rather than provide a detailed explanation of radio signal loss. In Section 4, the pertinent aspects of the structure of the ionosphere and its variability will be provided. Emphasis will be placed upon relating the structure to the performance characteristics of short to medium distance ionospheric links. In Section 5, selected aspects of predicting the behavior of short to medium distance links will be addressed. Particular discussion will be given to the short-term (time period of a day or less) prediction of ionospheric parameters pertinent to overall ionospheric propagation system performance.

2.0 GEOMETRY OF IONOSPHERIC RADIO PATHS

2.1 Equivalence Relationships - Plane Ionosphere

A radio wave that is incident upon the ionosphere from the ground is slowed down and refracted by the electron density in the ionosphere. If it is assumed that the ionosphere is horizontally uniform, that collisions between particle constituents in the ionosphere can be ignored, and that the effects of the earth's magnetic field are minimal, then the refractive index, μ , of a radio wave with frequency, f , is given by

$$\mu^2 = 1 - \left(\frac{f_p}{f} \right)^2 \quad (1)$$

where f_p is the plasma frequency and is related to the electron density, N_e , through the relationship

$$N_e (\text{cm}^{-3}) = 1.24 \times 10^4 \times f_p^2 \quad (f_p \text{ in MHz}) . \quad (2)$$

Applying Snell's Law to the level of reflection, it can be shown (Davies¹) that

$$f = f_v \sec \phi_0 \quad (3)$$

where f_v is the equivalent vertical-incidence frequency corresponding to f and ϕ_0 is the angle of incidence on the ionosphere. Eq. (3) is the so-called Secant Law. It is obvious from Eq. (3) that the ionosphere can reflect oblique incident radio waves at much higher frequencies than with normal incidence.

Because a radio wave incident on the ionosphere is slowed down compared to its travel in free space, it will appear to be reflected from a height in the ionosphere that is higher than in actuality. This height is designated as the virtual height. It can be shown (Davies¹, for example) that if f and f_v are equivalent frequencies of waves reflected obliquely and vertically from the same real height, then the virtual height of reflection is equal to the height of the equivalent triangular path for the oblique signal. Martyn's equivalent path theorem² expresses this important relationship.

2.2 Equivalence Relationships - Curved Ionosphere

Figure 1 shows the geometry that is appropriate for the reflection of HF radio waves by the ionosphere. The angle of elevation or take-off angle at the surface of the earth is designated as Δ , the angle measured from the true path to the earth's normal is designated as θ , and ϕ is the angle of incidence on the ionosphere. The true height of reflection is designated as h , and the virtual height or equivalent height is designated as h' . The angle ϕ' is the angle of incidence corresponding to the virtual height of reflection.

It can be shown (Davies¹) that

$$a \cos \Delta = (a + h) \sin \phi' \quad (4)$$

and

$$f_v = f \cos \phi' \quad (5)$$

where a is the earth's radius (6370 km). For a curved ionosphere, the equivalent frequency depends on both the take-off angle, Δ , and on the height of reflection.

2.3 Propagation Path Distance

The relationship between oblique and equivalent vertical frequencies for a plane reflector at a virtual height of h' for transmissions over a distance D is given by

$$f_{ob} = f_v \sec \phi = f_v \sqrt{1 + \left(\frac{D}{2h'}\right)^2} \quad (6)$$

In the case of a curved earth and a plane ionosphere, ϕ_0 is given by

$$\tan \phi_0 = \frac{\sin 1/2 \theta}{1 + \frac{h'}{a} - \cos \frac{\theta}{2}} \quad (7)$$

To obtain f_{ob} for a given value of f_v , it is necessary to know h' as a function of f_v and the relationship between $\sec \phi_0$ and h' .

The equivalence theorems break down in the case of a curved ionosphere. However the relationships derived from the theorems are generally modified in a simple fashion such as (Davies¹)

$$f_{ob} = k f_v \sec \phi_0 \quad (8)$$

where k is a correction factor depending upon distance and real height of reflection. Because it depends upon the real height of reflection, k therefore depends upon the electron density along the radio path. In order to solve for k , it is necessary to assume a model ionosphere. Many such models now exist, made possible largely through the use of high-speed digital computers. Methods for determining the distance that a given radio wave will travel can be obtained from material reported by the International Radio Consultative Committee³.

For a given ionosphere, there is some limiting upper frequency which is reflected vertically. The reflection occurs at the height of maximum electron concentration. The frequency is known as the critical frequency. At frequencies above the critical frequency, there is a ground distance out from the transmitter at points along which illumination is not possible by waves reflected from the ionosphere. This distance is known as the skip distance. The skip distance increases as the wave frequency increases and, in the limit for a very high frequency, can extend to the maximum ground range possible for rays launched at grazing incidence. For a fixed point of reception, there is some maximum frequency at which the waves can be reflected to it. This is the frequency making the distance from the transmitter to the point equal to the skip distance. The frequency is known as the maximum usable frequency (MUF). The MUF increases with ground distance and depends on the amount of ionization present - if the critical frequency is doubled, so will be the MUF for all distances. It depends also on the height of the ionosphere since the determining factor as to whether reflection occurs is the angle of

incidence at the layer. The same incidence angle yields different ground ranges for different layer heights. The greater the layer height, the steeper the angle of incidence to achieve propagation to a fixed range, and therefore the lower the MUF.

2.4 Practical Considerations

The ionosphere is a complex medium permeated by a magnetic field. Because of the presence of the earth's magnetic field, the ionosphere is a doubly refracting medium. Magnetoionic theory shows that there are two separate waves with differing but related polarizations that once excited can propagate within it. The polarizations change as these waves progress and are dependent on frequency and ray direction, the electron concentration and collision frequency, and the strength and direction of the magnetic field. In general, the polarizations are elliptical with the so-called ordinary (O) wave having an anticlockwise sense of vector rotation viewed in the direction of propagation for an angle of less than $\pi/2$ between the ray and field directions. For these conditions, the other wave, the extraordinary (X) wave, has a clockwise vector rotation. The O and X wave vector rotation reverses for greater angles between the ray and field directions. The O and X waves experience different amounts of refraction so that once excited at the base of the ionosphere they travel independently along somewhat displaced raypaths. Fortunately for prediction purposes, the O-wave, which at HF suffers less absorption and so is usually the stronger and hence the more important, tends to follow a path which is nearly that which would arise if there were no magnetic field.

In addition to the complexity due to the earth's magnetic field, radio circuits are made complicated because the ionosphere is not spatially uniform. Changes in the ionization distribution influence the radio path. Variations in ionization along the radio path produce differences in the elevation angle on the upgoing and downgoing legs of an ionospheric radio path. They can also give rise to changes in propagation modes. Changes in ionization perpendicular to the radio path can give rise to lateral deviations and departure of the signal from the great circle path.

In addition to propagation modes resulting from ionospheric reflections, there are modes associated with ionospheric scattering and ducting. Various mechanisms are involved. Signals are scattered by irregularities in the electron density distribution in the ionosphere. The scattering of signals can be such that energy is propagated forward (forward scattering), is deviated out of the great circle path (sidescatter), or is returned along the same path (backscatter). Scatter signals tend to be weaker than signals reflected from the ionosphere in the conventional manner, and they tend to fade more⁴. The geographical and temporal occurrence of scatter is associated with the incidence of ionosphere irregularities. The occurrence of ducting, i.e., signals traversing large distances in the ionosphere without coming to the earth's surface, generally are not of importance in short and medium distance ionospheric propagation systems.

Despite the complexities mentioned above, certain features of radio circuits can be generalized:

- i. waves incident more obliquely on the ionosphere tend to travel to greater distances along the earth,
- ii. waves suffer more refraction at higher heights in the ionosphere,
- iii. waves of higher frequency are reflected from higher ionospheric heights, and
- iv. waves incident more obliquely on the ionosphere are reflected from a lower height in the ionosphere.

3.0 FACTORS CONTRIBUTING TO SIGNAL LOSS

Radio signals will, in general, experience an amplitude gain due to transmitter antenna gain (G_T) and the receiving antenna gain (G_R) and will suffer a loss due to such phenomena as spatial attenuation, ionospheric absorption, polarization coupling loss, and ground-reflection loss if multiple hops are involved.

The gain of the transmitting and receiving antennas is dependent upon the antenna configuration and frequency. Theoretical values of the gains of numerous antennas have been given by Ma⁵ and by the International Radio Consultative Committee (CCIR)⁶. The performance of antennas under operational conditions can depart significantly from theoretical expectation because of buildings, trees, nearby hills, uneven ground, and ground with varying electrical properties. The antenna gains most commonly used in HF circuit performance predictions are those given by Barghausen et al.⁷

The loss of signal amplitude has been a subject of major study throughout the years. The losses due to spatial attenuation arise from the spreading of power flux over an increasing area during signal propagation. In free space, the power flux density is inversely proportional to the square of the path length. The ionosphere, because of its refractive properties, modifies this and can lead to focusing of radio waves, particularly for those waves with low elevation angles⁸. Polarization coupling loss results from the fact that two waves of differing polarizations (ordinary and extraordinary) are excited when a radio wave enters the ionosphere. Each of these waves propagates independently in the ionosphere and is subject to different amounts of absorption.

The loss of signal strength due to ionospheric absorption is of paramount interest in this paper. The absorption that an HF radio wave suffers as it propagates through the ionosphere is dependent upon the electron density, the frequency of collisions between the electrons and the ambient atmospheric constituents, and the (electron) gyrofrequency along the entire path traversed by the radio energy. Further, the absorption is a function of the frequency of the radio wave, f , and the relative magnitudes of f and the ionospheric plasma frequency f_p . If the ratio f_p/f approaches zero, the refractive index does not differ significantly from unity, and the absorption is approximately proportional to the product of the electron density and the electron collision frequency. If, on the other hand, f_p/f is near unity, the radio wave is significantly retarded, and it can be shown (for instance, Alpert⁹), that the absorption is dependent upon the collision frequency and the group and phase paths of the radio wave. This latter case has been termed "deviative" absorption, while the former is referred to as a "non-deviative" absorption.

Because of the need for accurate predictions of the field strength of ionospherically propagated HF radio waves, there has evolved, over the years, a number of techniques to specify the absorption, the most notable of which are those reported by Lucas and Haydon¹⁰ and Barghausen et al.⁷ These methods attempt to estimate the amount of absorption of radio waves reflected from the F-region on their passage through the D- and E-region assuming only non-deviative absorption. George¹¹ and George and Bradley¹² have developed a technique to estimate non-deviative and deviative absorption for HF waves in the D- and E-region. Rush and Elkins¹³ have shown that the amount of F-region absorption is usually less than 1 dB.

It is to be noted that enhanced ionospheric absorption is associated with auroral activity and is referred to as auroral absorption. While there is still substantial work to be performed before an operationally useful model of auroral absorption emerges, the work of Foppiano¹⁴ is a significant first step. The physics of radio wave absorption has recently been reviewed in detail by Thrane¹⁵.

4.0 STRUCTURE OF THE IONOSPHERE AND ITS VARIABILITY

All radio wave systems that rely upon the ionosphere as a medium for propagation are subjected to the manifestations of ionospheric changes and variability. The description of the ionospheric structure given below follows very closely that provided by Rush¹⁶.

4.1 Vertical Structure of the Ionosphere

The vertical structure of the ionosphere extends from about 50 km to roughly 2000 km above the surface of the earth. The ionosphere is divided into three vertical regions: D, E, and F, which increase in altitude and in electron density. The D region spans the altitude range 50 to 90 km. The electron density exhibits large diurnal variations with maximum density shortly after local noon and small values at night. The variation of electron density generally follows a direct solar zenith angle dependence with the highest electron density values during the summer and, as stated above, during the daylight hours. The D region provides the upper boundary of the waveguide for VLF propagation and at times can reflect radio waves in the VLF, LF, and MF spectrum. For radio waves in the HF portion of the spectrum and above, the D region acts principally as an attenuator of radio signals that are propagated through it.

The E region spans the height range 90 to 130 km. The electron density in the E region encompasses the so-called "normal" and "sporadic E" layers. The normal region conforms closely to a Chapman layer with a strong solar zenith angle dependence with maximum electron density near noon and a seasonal maximum in summer. The sporadic-E layer is characterized as an anomalous-ionization layer that has little direct relationship to solar ionizing radiation. Sporadic E can assume various forms, sometimes irregular and patchy, sometimes smooth and disc-like. The diurnal variation of the occurrence of sporadic E varies with location over the globe. The normal E region acts principally as a reflector of HF waves, particularly during the daylight hours. The electron density associated with sporadic-E ionization can reflect or scatter HF waves.

The F region extends upward from 130 km. The lower part of the region displays a different variation than the upper part. This has resulted in a subdivision into F1 and F2 layers. The F1 layer, like the normal E layer, follows an approximate Chapman model but with a different solar zenith angle dependence. The F1 layer electron density reaches its maximum near local noon and during the summer. At night and during the winter, there is essentially no distinction between the F1 and F2 layers. The F2 layer is the highest ionospheric layer and usually displays the greatest electron density. The electron density in the F2 layer is strongly influenced by neutral-air winds, electrodynamic drifts, and diffusion processes. The result of these influences is that the electron density in the F2 layer departs significantly from a simple solar zenith angle dependence. The maximum electron density tends to occur well after local noon, and the density at noon during the winter months exceeds the corresponding summer value. There are also significant differences in the structure of the ionosphere that depend upon geomagnetic latitude. The latitudinal dependence of F2-region features is not confined to just the normal electron density distribution, but also pertains to a family of electron irregularities that are part of the overall F-region morphology.

4.2 Ionospheric Temporal Variability

The ionosphere displays variations in electron density on many temporal scales. The 11-year solar cycle is manifested in electron density and critical frequency changes with higher values generally occurring during periods of higher solar activity. In addition to the solar cycle dependency, the ionospheric electron density displays seasonal and monthly changes. These changes vary over the solar cycle. There are models of the critical frequency of the E, F1, and F2 regions (foE, foF1, and foF2) that provide hourly median values of the parameters as a function of solar cycle and month for each hour of the day. The models of the ionospheric critical frequencies that are used for propagation purposes tend to be statistical in nature. The E-region models of Muggleton¹⁷ and Leftin¹⁸, the F1-region models of DuCharme et al.¹⁹ and Rosich and Jones²⁰, and the F2-region models of Jones et al.²¹ and Jones and Obitts²² are the models that are primarily used in HF propagation prediction methods. There are, however, ionospheric models that are theoretical in nature that are based upon a numerical solution of the time-dependent continuity equation for electrons in the ionosphere. These models generally provide average values of electron density at a given height in the ionosphere for specific levels of solar activity and solar zenith angle.

The ionospheric temporal variability that is perhaps the most difficult to model, and hence the one leading to the largest uncertainties in ionospheric propagation prediction programs, is the day-to-day variability. Studies reported by Rush and Gibbs²³, for example, show that the variability of daily hourly values of foE and foF1 about the monthly median hourly values expressed in terms of the standard deviation is on the order of 5 to 10 percent. The same study provides evidence that the daily variability of foF2 is between 10 and 20 percent.

Observations of the daily variability of foF2 are shown in Figure 2 for stations located at Slough, England, and Lindau, Federal Republic of Germany. The results indicate a tendency for the nighttime variability to exceed the daytime by about a factor of 2. Average values of the nighttime variability are on the order of 20 percent; average values for the daytime are on the order of 10 percent.

The magnitude of the daily variability in foF2 displays a marked dependence upon geomagnetic latitude. The daily variability of the F2 region in the equatorial and polar regions of the globe substantially exceeds that illustrated in Figure 2 for midlatitude locations. The cause of the enhanced variability at equatorial and polar geomagnetic latitudes is attributed to the daily variability observed in processes such as electrodynamic drift, diffusion, neutral-air winds, and particle precipitation that compete for control of the ionization distribution in the low and high latitude F region. This is further discussed in the context of the spatial variability of the ionosphere addressed in the next section.

There are other parameters that characterize the electron density distribution that also display variations with time. The height of the maximum electron density in the different ionospheric regions varies with time and location. The F2 region maximum height, hmF2, tends to show the most significant changes of all the ionospheric maximum heights. At middle latitudes, hmF2 is on the order of 300 to 400 km during nighttime hours and between 250 and 350 km during daytime hours. At equatorial latitudes, on the other hand, the daytime values of hmF2 are higher than the nighttime values by some 100 to 150 km. The height of the maximum density in the polar region displays a more complicated time history reflecting the strong magnetospheric control of polar ionospheric processes. The values of hmF2 at all locations on the globe vary on a monthly and seasonal basis. Changes in hmF2 lead to changes in propagation conditions that are comparable to those resulting from changes in the F2 region critical frequency.

4.3 Ionospheric Spatial Variability

The electron density in the D, E, and F1 regions follows a solar zenith angle dependence. The latitudinal distribution of electron density in the D, E, and F1 regions as well as the temporal distribution maximizes near the sub-solar point. In the F2 region, the normal electron density displays a complicated latitudinal behavior. In addition, irregularities in the F region and in the E region (sporadic E) also display a significant latitudinal dependence.

The normal F2-region electron densities and the ionospheric irregularities are aligned in accord with magnetic coordinates. There are several forms of magnetic latitude in use: geomagnetic latitude, corrected geomagnetic latitude, and invariant latitude. For the purposes of this discussion, geomagnetic latitude, which is based on an approximation to a centered-dipole magnetic field, is sufficient. Adopting geomagnetic latitude as a frame of reference, the F2-region electron densities and the ionospheric irregularities can be discussed in terms of features associated with low, middle, and high latitudes. It is generally convenient to view the low latitude ionosphere as extending from between $\pm 30^\circ$ geomagnetic latitude, the high latitude ionosphere as being those latitudes greater than 60° geomagnetic latitude, and the geomagnetic latitudes between 30° and 60° comprising the middle latitude ionosphere, subject to the fact that the boundaries are not strictly fixed. Figure 3 provides an indication of the low, middle, and high geomagnetic latitudes with respect to the geographic latitudes. Because the geomagnetic and geographic poles do not coincide, there are substantial differences between the geographic and geomagnetic latitudes, particularly in the Americas and throughout Asia.

4.3.1 F2 Region Latitudinal Dependence

4.3.1.1 Low Latitude Behavior

In low geomagnetic latitudes, the F2 region is dominated by the equatorial anomaly²⁴, and significant latitudinal gradients in the F-region ionization vary markedly with local time. Around sunrise, generally, there is a single maximum of ionization existing near the geomagnetic equator. Shortly after that time, the latitudinal distribution changes with the appearance of two ionization maxima separated by a trough that is centered more or less on the magnetic equator. The ionization maxima or crests continue to increase in ionization density and continue to become more separated as time progresses. The time at which the crests are farthest from the magnetic equator varies with solar activity, occurring in the early afternoon during solar minimum and in the early evening during solar maximum. Later the crests move equatorward, finally merging together to form a maximum of ionization above the equator. When the crests are farthest from the equator and most intense, the highest values of the electron density anywhere in the ionosphere are observed. The formation of the equatorial anomaly is attributed to the combined influence of an eastward-directed electric field associated with the equatorial electrojet and the horizontal geomagnetic field at low latitudes. Ionization in the F region drifts upward due to electrodynamic drifts until gravitation processes begin to dominate. At this point, the ionization, which is confined to motion along magnetic field lines, diffuses downward along the field lines, being deposited at higher geomagnetic latitudes. Work by Anderson and Roble²⁵, drawing on the results of numerous other investigators, shows the high degree of sophistication in combining electrodynamic drifts, neutral-air winds, and ambipolar diffusion effects necessary to accurately reproduce the structure of the low latitude F region.

Considerable day-to-day variability is seen in the time of onset, decay, and maximum development of the anomaly²⁶. Marked differences can occur between the latitudinal distributions of foF2 observed on a particular day at the same local time, but separated in longitude by only 30 degrees. These differences are associated with differences in the relative importance of the processes--drift, winds, diffusion--that compete for control of the ionization distribution at low latitudes. However by accounting for temporal and spatial changes in electrodynamic drift and neutral-air winds, the day-to-day and longitudinal differences in the structure of the low latitude ionosphere can be realistically modeled²⁷.

4.3.1.2 Middle Latitude Behavior

The F2 region at middle geomagnetic latitudes does not display the large gradients in the latitudinal distribution of the electron density that are observed at the lower latitudes. The midlatitude F2 region is much more quiescent than either the low or high latitude F2 region. The F2 region at middle latitudes does however display certain characteristics that result from the influence of neutral-air winds and diffusion on the ionization distribution. The observed diurnal maximum occurring well after local noon and the winter noon electron density values exceeding those in the summer are indicative of the effects of other than solar radiation processes on the ionosphere. The values of the F2 region critical frequency, foF2, tend to decrease with increasing latitude as do the values of the height of the F2 region maximum density, hmF2. Figure 4 shows the latitude and longitude variation of foF2 and hmF2 above Western Europe at a time near local noon during March 1966. The values of foF2 and hmF2 display the latitudinal behavior typical of the middle latitude F2 region.

4.3.1.3 High Latitude Behavior

Perhaps the most complex and variable region of the ionosphere is the high latitude F2 region. It is convenient to view high latitude F-region phenomena in terms of shapes or ovals, particularly the auroral oval. The auroral oval is the region, originally defined by Feldstein and Starkov²⁸, in which there is a high probability of occurrence of visible aurora. The oval varies with time, season, and magnetic activity. The auroral oval is the location of numerous discrete ionospheric phenomena, such as Spread F, electron density enhancements and lower altitude auroral absorption effects. In addition to the auroral oval, the high latitude ionosphere displays features that tend to be aligned with constant geomagnetic latitudes. Hartz and Brice²⁹ have defined this region as a zone of diffuse auroral events that are attributable to a drizzle of hard particle precipitation.

South of the auroral oval in the high latitude ionosphere is the ionospheric trough, which is a region of strongly depressed electron density, occurring primarily on the night side of the earth. The trough is aligned approximately along constant geomagnetic latitudes. The equatorial edge of the trough coincides approximately with the locus of the plasmapause, and the electron density increases gradually from the center of the trough to the midlatitude ionosphere. The electron density at the polar edge of the trough changes with latitude much more rapidly than at the equatorial edge, and the polar edge of the trough coincides with the equatorial diffuse boundary of the auroral oval. Poleward of the trough, enhanced electron density (almost an order of magnitude greater than in the trough) can sometimes be observed. This enhancement is associated with the dayside magnetosphere.

An example of how the trough is manifested in foF2 can be seen in Figure 5. This figure shows values of the F2 region critical frequency between the latitudes of 10° and

70° north geographic and the longitudes of 0° and 120° west geographic valid for January 20, 1981 at a time of 2300 hours universal time (UT). The low values of foF2 near 60° to 65° north and 0° to 30° west are readily apparent. Although not illustrated here, the depressed values of foF2 are accompanied by enhanced values of the height of the F2 region peak electron density, hmF2, in the vicinity of the trough. This can lead to large depressions in the MUF for HF circuits operating in high latitudes.

4.4 Ionospheric Irregularities

In addition to the large-scale distribution of electrons in the ionosphere, HF radio systems are impacted by irregular electron density structures in the ionosphere. A report of the International Radio Consultative Committee³⁰ provides details of these irregularities insofar as they are of importance to radio propagation. Only a brief summary is provided here.

4.4.1 F-Region Irregularities

4.4.1.1 Low Latitude F-Region Irregularities

Irregularities in the low latitude F region electron density tend to occur in the evening hours and continue throughout the night hours. Generally, the irregularities are more widespread in the equinoxes but may be different in different longitudes. The occurrence of irregularities at low latitudes tends to decrease during times of geomagnetic disturbances. The low latitude F-region irregularities display significant longitudinal variability as well as latitudinal and temporal dependencies. The source of low latitude F-region irregularities is generally attributed to the influence of strong electric fields near the geomagnetic equator that give rise to instabilities in the ionospheric electron density. Low latitude irregularities have been observed to cause fading on HF circuits.

4.4.1.2 Middle Latitude F-Region Irregularities

Irregular structures in the middle latitude electron density have been observed. These structures, for the most part, are associated with the phenomenon called "Spread F." The magnitude, duration, and effect on telecommunications system performance of middle latitude F-region irregularities are generally much smaller than on irregularities in the low and high latitudes.

4.4.1.3 High Latitude F-Region Irregularities

Irregularities in the structure of the high latitude ionosphere appear more or less routinely. The irregularities are most intense during hours of darkness and are associated with auroral activity, magnetospheric phenomena, and solar activity. The occurrence and intensity of F-region irregularities at high geomagnetic latitudes are at times greater than those observed at the low geomagnetic latitudes. In addition to causing fading on HF circuits, irregularities at high latitudes can lead to large-scale signal attenuation, off-great-circle propagation, and clutter on backscatter signals.

4.4.2 E-Region Irregularities

4.4.2.1 Low Latitude E-Region Irregularities

Irregularities in the low latitude E region generally are characterized as "sporadic E." Sporadic-E layers are present during a high percentage of the daytime, but the latitude of maximum occurrence varies with longitude. A special type of sporadic E appears regularly during daylight hours. This sporadic-E layer is highly transparent and reaches top penetration-frequency values of about 10 MHz. The structure of the sporadic E irregularities are magnetically field aligned.

4.4.2.2 Middle Latitude E-Region Irregularities

Irregularities in the middle latitude E region are also characterized as "sporadic E." Middle latitude sporadic E occurs most frequently in summer daytime. The diurnal variation exhibits maxima in the mid-morning hours and near sunset, lagging growth and decay of the regular E region. The seasonal variation is complex and possibly related to the upper atmosphere winds; the seasonal minimum is usually near midwinter or the spring equinox.

4.4.2.3 High Latitude E-Region Irregularities

E-region irregular electron density structures are quite common at high geomagnetic latitudes. For the most part, all the irregularities in the high latitude E region are attributable to an influx of charged particles due to magnetospheric or solar activity. Irregularities in the high latitude E region have been observed in conjunction with auroral activity. The occurrence of these irregularities are principally a nighttime phenomenon. They can occur in thick layers giving rise to substantial radio wave retardation. At latitudes that are higher than those at which visible aurora generally occur, E-region irregularities display characteristics like sporadic E. The irregularities in this case extend in bands or ribbons across the entire area.

4.5 Ionospheric Impact on the Performance of Short and Medium Distance Radio Circuits

Radio circuits operating over short and medium distances (i.e., up to 3000 km) that utilize the ionosphere as a propagation medium, are, for the most part, confined to the HF (3 to 30 MHz) portion of the electromagnetic spectrum. Frequencies in the VHF (30 to 300 MHz) portion of the spectrum however have been used to effect communication over distances of hundreds of kilometers by relying upon scattering of radio waves from ionospheric irregularities. Most notable is the scatter from patches of sporadic-E ionization. Methods for calculating the signal strength due to sporadic E occurrence have been described in Report 259-4 of the International Radio Consultative Committee³¹.

The performance of HF circuits that rely upon the skywave mode of propagation must be considered in terms of ionospheric impact. In fact it is useful to view the ionosphere as being an integral part of such systems, no matter what the length of the circuit. The structure of the ionosphere and its variability are directly related to the overall performance of these circuits. As mentioned in Section 4.2, techniques have been developed to assess the performance of HF radio circuits that use specifications of various ionospheric parameters. By varying the ionospheric parameters, it is possible to estimate how the performance of a radio circuit will vary at different times, and geographic locations. Prediction methods such as given by Barghausen et al.⁷ and the International Radio Consultative Committee³ provide a convenient means to assess the performance of HF circuits under numerous scenarios.

In order to gain an appreciation of how the ionosphere impacts on the performance of HF circuits, it is perhaps more edifying to employ ray tracing techniques³² in conjunction with a model of the ionospheric electron density. Figure 6 shows the results obtained by ray tracing with a model ionosphere described by Rush and Elkins¹³ and derived from the values of foF2 and hmF2 given in Figure 4. Shown in Figure 6 are curves of ground range as a function of take-off angle for frequencies of 5, 10, 15, and 20 MHz. The curves were deduced from results obtained assuming that a fictitious transmitter was located at 45° north geographic latitude and 10° east geographic longitude. The ionospheric region (E, F1, or F2) from which the frequencies were reflected are indicated as either 1E, 1F1, or 1F2. In this simulation, only one reflection from the ionosphere was considered. Differences in ground range as a function of take-off angle for eastward and northward transmission illustrate the effects of gradients in the ionization distribution along the circuit path.

Another illustration of how the ionosphere impacts on HF circuits can be seen in Figure 7. In this figure, only results for radio waves reflected from the F2 region are shown. In this particular example, ray tracing was performed using the same form of the ionospheric model as given by Rush and Elkins¹³, but the values of foF2 and hmF2 were decreased from the median values of the parameters by 10 percent. It can be seen, for example, that the reception distance for a 20 MHz signal can vary from about 1700 km to over 2500 km due to a 10 percent change in foF2 or hmF2. A 10 percent change in foF2 and hmF2 is typical of the day-to-day variations observed in these parameters at middle latitudes during the daytime. The results show how the variability in foF2 and hmF2 changes the distance to which a given frequency will propagate compared to the median specification. This illustrates the need for predictions of the ionosphere and its structure for those operations where secure communications are desired.

In addition to changes in ground range, the ionosphere can give rise to changes in other parameters such as the amount of absorption a radio wave suffers and the MUF for a given circuit. Changes in absorption and MUF can be quite severe for HF circuits depending upon the application and have been described in detail by Rush and Elkins¹³ and Rush et al.³³

5.0 PREDICTIONS OF THE PERFORMANCE OF IONOSPHERIC-DEPENDENT CIRCUITS

Short to medium distance ionospheric circuits are used for a number of purposes: fixed-service operation, surveillance and point-to-point communication. Different systems have different requirements for performance predictions. It is not practical to discuss these requirements in specific terms, but rather it is more useful to attempt to isolate some general requirements that apply to propagation systems. A detailed description of ionospheric predictions for HF radio systems has recently been provided by Bradley and Lockwood³⁴ and need not be addressed here.

One obvious requirement pertains to the need to effect long-term planning of the radio frequency spectrum. Systems designers and managers require information regarding how a particular radio system will operate over its projected lifetime. The quality of service that can be expected and the percentage of time a system is likely to be inoperable due to ionospheric-induced causes needs to be provided. Likewise, individuals concerned with effective frequency management of the HF spectrum require knowledge of optimum frequencies for use in specific applications, the probability that multipath phenomena will occur, and an estimate of the likelihood of signals from one system interfering with those of another. Certain users require that errors in system performance induced by ionospheric phenomenon be quantified³⁵. The Doppler-induced spreading of an HF signal and the error rates in digital communication systems due to ionospheric irregularities need to be provided. Methods for accomplishing the necessary calculations have in fact been undertaken³⁶.

In order to satisfy these requirements, a knowledge of the ionospheric structure and its variability on time and space scales commensurate with those of the requirements is needed. Such knowledge is not always readily available in a form that is readily useful. There exists a comprehensive knowledge of how the ionosphere is formed, how it varies, what causes the variation, and of its gross morphological features. Further, there exists a very good understanding of the predominant physical processes that are responsible for the control and variations observed in the ionospheric plasma. The ability to predict the ionosphere on a long-term basis and to assess its general impact on HF propagation systems in general terms is well within present capabilities³⁷.

The diurnal variation, month-to-month changes, and solar cycle dependence in monthly median HF propagation conditions can be readily obtained from existing techniques. Changes in propagation conditions associated with day-to-day, hour-to-hour, and minute-to-minute variations in the ionosphere are more difficult to quantify. This is particularly the case when the ionosphere is undergoing changes induced by solar flares and geomagnetic storms. It may be necessary to implement specific short-term ionospheric prediction methods to quantify these short-term changes. Short-term prediction techniques such as described by Rose³⁸ may provide the type of prediction support to insure a specified level of circuit performance.

Not all of the requirements pertaining to improving the prediction and assessment of HF radio systems can be met by addressing ionospheric propagation effects alone. Specific systems require that other parameters be identified in order to optimize overall performance. Maximum transmitter power necessary, type of modulation, bandwidth, and antenna design need to be determined and effects other than those related only to propagation phenomena must be considered. In order to effectively plan the use of the HF spectrum, the radio noise environment in which systems operate must be known. The CCIR has provided a number of documents^{39, 40} that contain estimates of average man-made and atmospheric noise. The time scales for which the information is given may be too coarse for certain applications however. In many instances, the limitation to system performance is not due to external noise but is due rather to interference from other systems. There exists a need to describe and develop models of the interference environment as a function of time, frequency, and receiving location.

6.0 CONCLUSION

Short to medium distance ionospheric radio links are the primary means to effect telecommunication objectives under many operational scenarios. The performance of such links is tied directly to the structure of the ionosphere. In order to insure proper system performance, it is necessary that the impact of the ionospheric structure and its variability on the overall system performance be understood by the user. The effects of the ionosphere on radio propagation systems must be assessable, quantifiable, and predictable, and the predictions must be verifiable.

7.0 REFERENCES

1. Davies, K., Ionospheric Radio Propagation, Washington, D.C., Superintendent of Documents, U.S. Government Printing Office, 1965, 160-173.
2. Martyn, D. F., The propagation of medium waves in the ionosphere, *Proc. Phys. Soc.*, 47, 1935, 323.
3. International Radio Consultative Committee, Supplement to Report 252-2, Second CCIR computer-based interim method for estimating sky-wave field strength and transmission loss at frequencies between 2 and 30 MHz, Documents of the XIVth Plenary Assembly, International Telecommunication Union, Geneva, 1978.
4. Bradley, P. A., AGARD Lecture Series No. 99, Propagation at medium and high frequencies: Practical radio systems and modelling needs, 1979, AGARD-LS-99, 3-1 to 3-21.
5. Ma, M. T., Theory and Application of Antenna Arrays, New York, John Wiley and Sons, 1974.
6. International Radio Consultative Committee, Antenna Diagrams, International Telecommunication Union, Geneva, 1978.
7. Barghausen, A. F., J. W. Finney, L. L. Proctor, and L. D. Schultz, Predicting long-term operational parameters of high-frequency sky-wave telecommunication systems, ESSA Technical Report ERL 110-ITS 78, 1969.
8. Bradley, P. A., Focusing of radio waves reflected from the ionosphere at low angles of elevation, *Electronics Letters*, 6, 1970, 457-458.
9. Alpert, Y. L., Radio Wave Propagation and the Ionosphere, New York, Consultants Bureau, Enterprises, Incorporated, 1963, 159-163.

10. Lucas, D. L., and G. W. Haydon, Predicting statistical performance indexes for high frequency ionospheric telecommunication systems, ESSA Technical Report IER1 ITSA-1, 1966, NTIS Access No. AD644-827.
11. George, P. L., The global morphology of the quantity $\int N_v dh$ in the D- and E-region of the ionosphere, J. Atmos. Terrest. Phys., 33, 1971, 1893-1906.
12. George, P. L., and P. A. Bradley, Relationship between HF absorption at vertical and oblique incidence, Proc. Institution Electrical Engineers, 120, 1973, 173-180.
13. Rush, C. M., and T. J. Elkins, An assessment of the magnitude of the F-region absorption on HF radio waves using realistic electron density and collision frequency models, ITU Telecommunication Journal, 42, 1975, 476-488.
14. Foppiano, A. J., A new method for predicting the auroral absorption of HF sky waves, International Radio Consultative Committee, Interim Working Party 6/1 Documents 3 and 10, International Telecommunication Union, Geneva, 1976.
15. Thrane, E. V., AGARD Conference Proceedings No. 295, The physics of radio wave absorption, 1980, AGARD-CP-295, 10-1 to 10-15.
16. Rush, C. M., Antennas and Propagation, Part 2: Propagation, HF Propagation: What we know and what we need to know, Institution of Electrical Engineers, London, 1981, Conference Publication Number 195.
17. Muggleton, L. M., A method for predicting foE at any time and place, ITU Telecommunication Journal, 42, 1975, 413-418.
18. Leftin, M., Numerical representation of monthly median critical frequencies of the regular E region (foE), OT Report 76-88, 1976, NTIS Access. No. PB255-484/AS.
19. DuCharme, E. D., L. E. Petrie, and R. Eyfrig, A method for predicting the F1 layer critical frequency, Radio Sci., 6, 1971, 369-377.
20. Rosich, R. K., and W. B. Jones, The numerical representation of the critical frequency of the F1 region of the ionosphere, OT Report 73-22, 1973, NTIS Access. No. COM75-10813/AS.
21. Jones, W. B., R. P. Graham, and M. Leftin, Advances in ionospheric mapping by numerical methods, ESSA Technical Report ERL 107-ITS 75, 1969.
22. Jones, W. B., and D. L. Obitts, Global representation of annual and solar cycle variation of foF2 monthly median 1954-1958, OT Report ITSRR 3, 1970, NTIS Access. No. COM75-11143/AS.
23. Rush, C. M., and J. Gibbs, Air Force Cambridge Research Laboratories, Predicting the day-to-day variability of the midlatitude ionosphere for application to HF propagation predictions, 1973, AFCRL-TR-73-0335.
24. Appleton, E. V., Two anomalies in the ionosphere, Nature, 157, 1946, 691.
25. Anderson, D. N., and R. G. Roble, The effect of vertical ExB ionospheric drifts on F region neutral winds in the low-latitude thermosphere, J. Geophys. Res., 79, 1974, 5231-5236.
26. Rush, C. M., and D. Miller, Some aspects of the day-to-day variability of the equatorial anomaly: American and Japanese sectors, Radio Sci., 7, 1972, 1085-1094.
27. Anderson, D. N., A theoretical study of the ionosphere F region equatorial anomaly - I. Theory, Plan. Space Sci., 21, 1973, 409-419.
28. Feldstein, Y. I., and G. V. Starkov, Dynamics of auroral belt and polar geomagnetic substorms, Plan. Space Sci., 15, 1967, 209-229.
29. Hartz, T. R., and N. M. Brice, The general pattern of auroral particle precipitations, Plan. Space Sci., 15, 1967, 301-329.
30. International Radio Consultative Committee, Report 725, Ionospheric properties, Documents of the XIVth Plenary Assembly, International Telecommunication Union, Geneva, 1978.
31. International Radio Consultative Committee, Report 259-4, VHF propagation by regular layers, Sporadic-E or other anomalous ionization, Documents of the XIVth Plenary Assembly, International Telecommunication Union, Geneva, 1978.
32. Haselgrove, J., Ray Theory and new method for ray tracing, in The Physics of the Ionosphere, London, The Physical Society, 1954, 355-364.
33. Rush, C. M., D. Miller, and J. Gibbs, The relative daily variability of foF2 and hmF2 and their implications for HF radio propagation, Radio Sci., 9, 1974, 749-756.

34. Bradley, P. A., and M. Lockwood, AGARD Conference Proceedings No. 295, Ionospheric predictions for HF radio systems: the future, 1980, AGARD-CP-295, 32-1 to 32-13.
35. Heaps, M. G., Accounting for ionospheric variability and irregularity in high frequency direction finding, in Preprints of Proceedings of the 1981 Symposium on the Effects of the Ionosphere on Radiowave Systems, sponsored by the Naval Research Laboratory, the Office of Naval Research, and the Air Force Geophysics Laboratory, 1981, paper 3B-6.
36. Malaga, A., A global model for wideband HF skywave propagation, in Preprints of Proceedings of the 1981 Symposium on the Effects of the Ionosphere on Radiowave Systems, sponsored by the Naval Research Laboratory, the Office of Naval Research, and the Air Force Geophysics Laboratory, 1981, paper 5-3.
37. Davies, K., Review of recent progress in ionospheric predictions, Radio Sci., 16, 1981, 1407-1430.
38. Rose, R. B., Prophet - an emerging HF prediction technology, in Preprints of Proceedings of the 1981 Symposium on the Effects of the Ionosphere on Radiowave Systems, sponsored by the Naval Research Laboratory, the Office of Naval Research, and the Air Force Geophysics Laboratory, 1981, paper 5-1.
39. International Radio Consultative Committee, Report 258-3, Man-made radio noise, Documents of the XIVth Plenary Assembly, International Telecommunication Union, Geneva, 1978.
40. International Radio Consultative Committee, Report 322-1, World distribution and characteristics of atmospheric radio noise, Documents of the XIVth Plenary Assembly, International Telecommunication Union, Geneva, 1978.

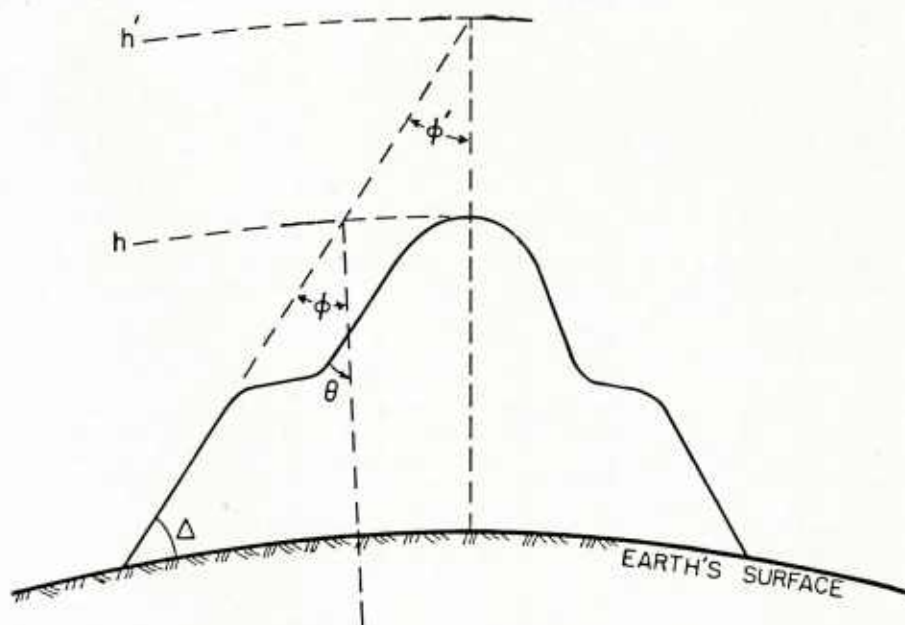


Figure 1. Oblique path geometry.

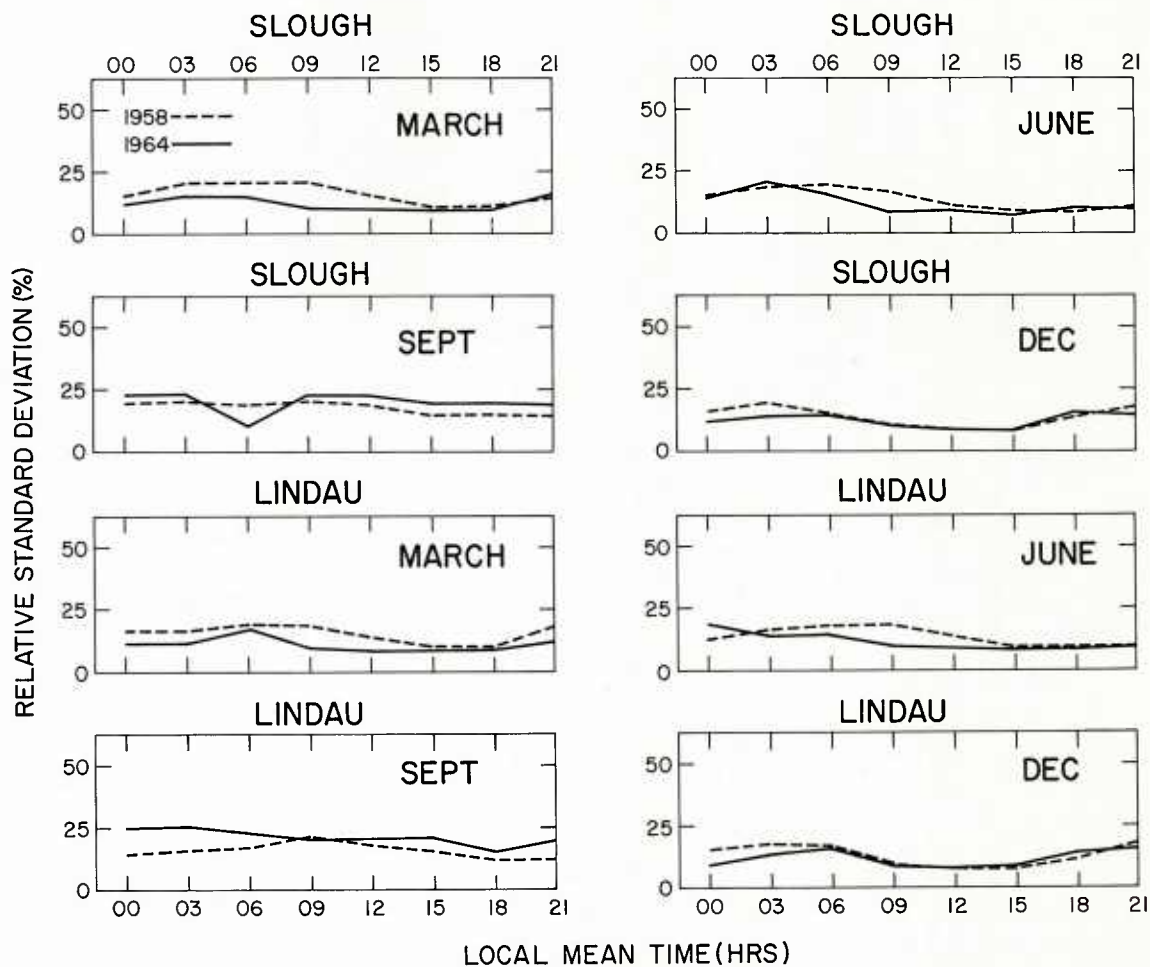


Figure 2. Daily variability of foF2 observed at Slough and Lindau expressed in terms of relative standard deviation.

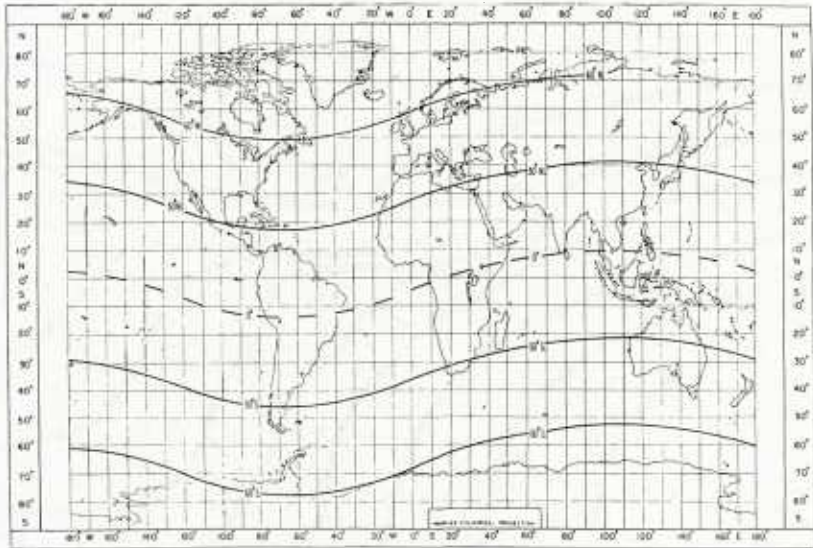


Figure 3. Contours of constant geomagnetic latitudes for 60°S, 30°S, 0°, 30°N, and 60°N.

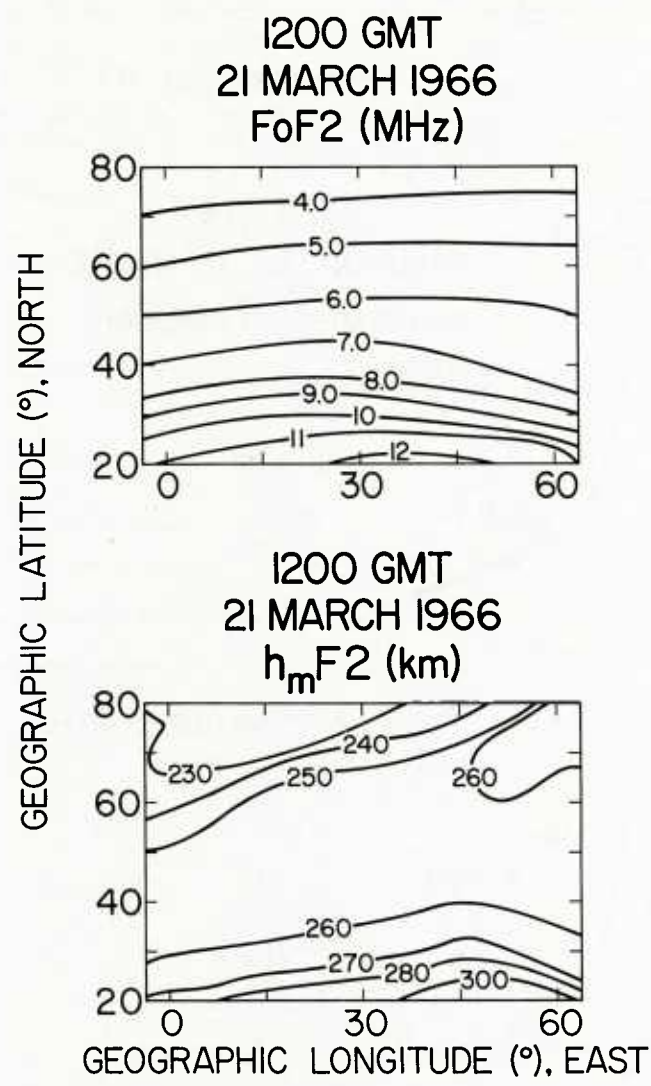


Figure 4. Contours of foF2 and hmF2 above Western Europe for 1200 hours GMT on March 21, 1966.

Date: 1981/01/20 Time - 23:00:00

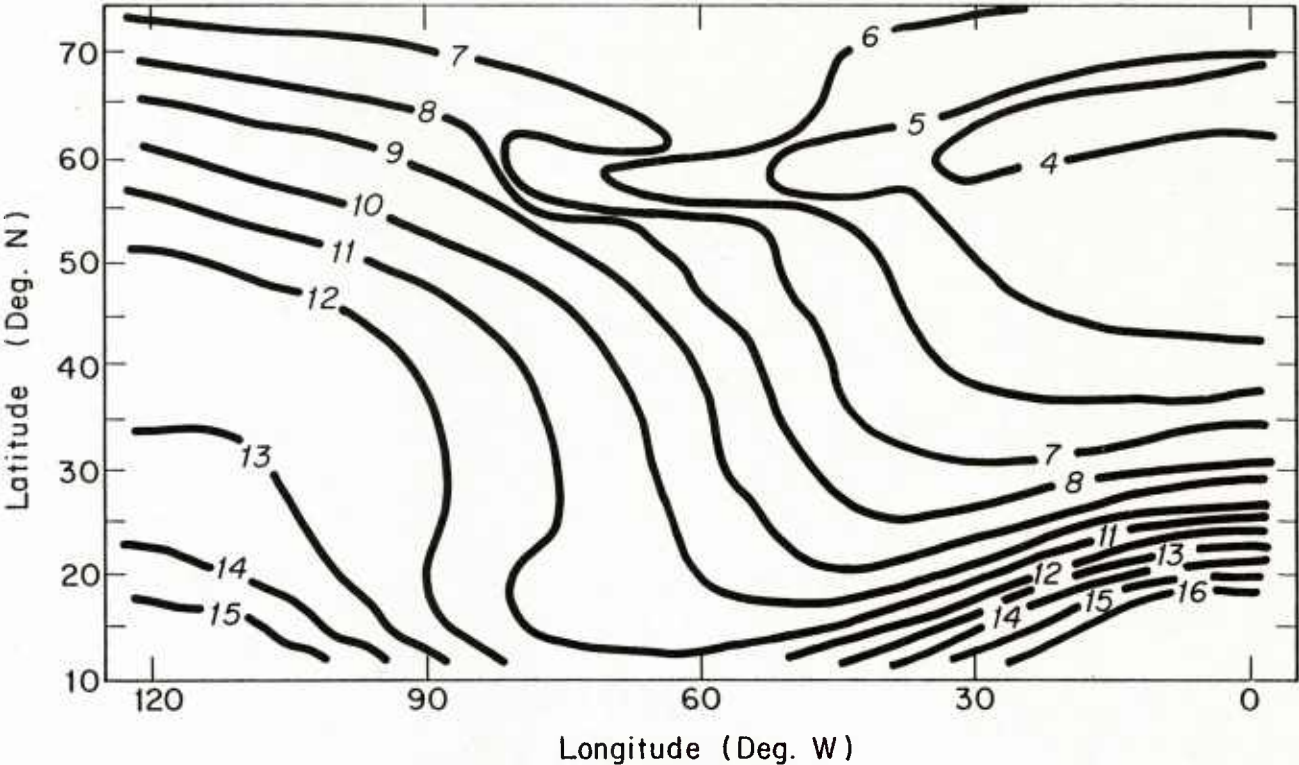


Figure 5. Contours of foF2 for 2300 hours GMT on January 20, 1981 illustrating the ionization trough occurring between 60° to 70° north latitude and 0° to about 60° west longitude.

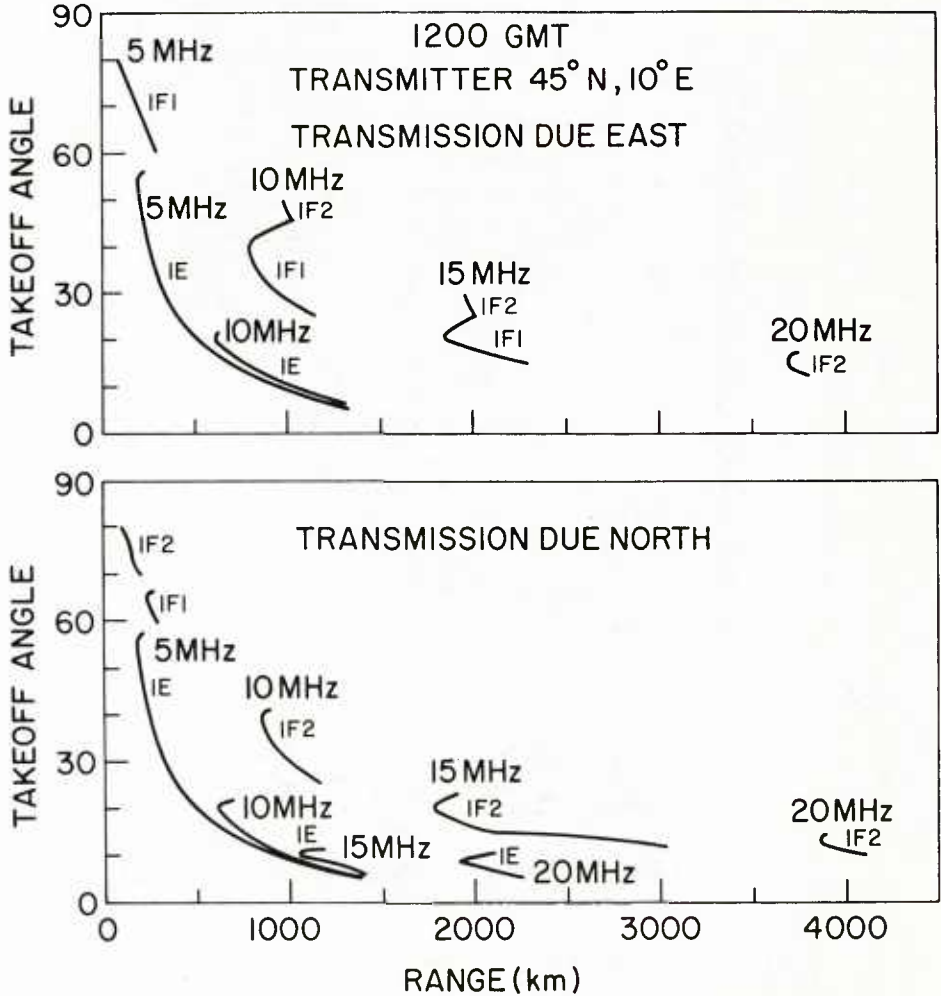


Figure 6. Ground range as a function of take-off angle for different frequencies for transmissions due east and due north from a fictitious transmitter located at 45° north and 10° east.

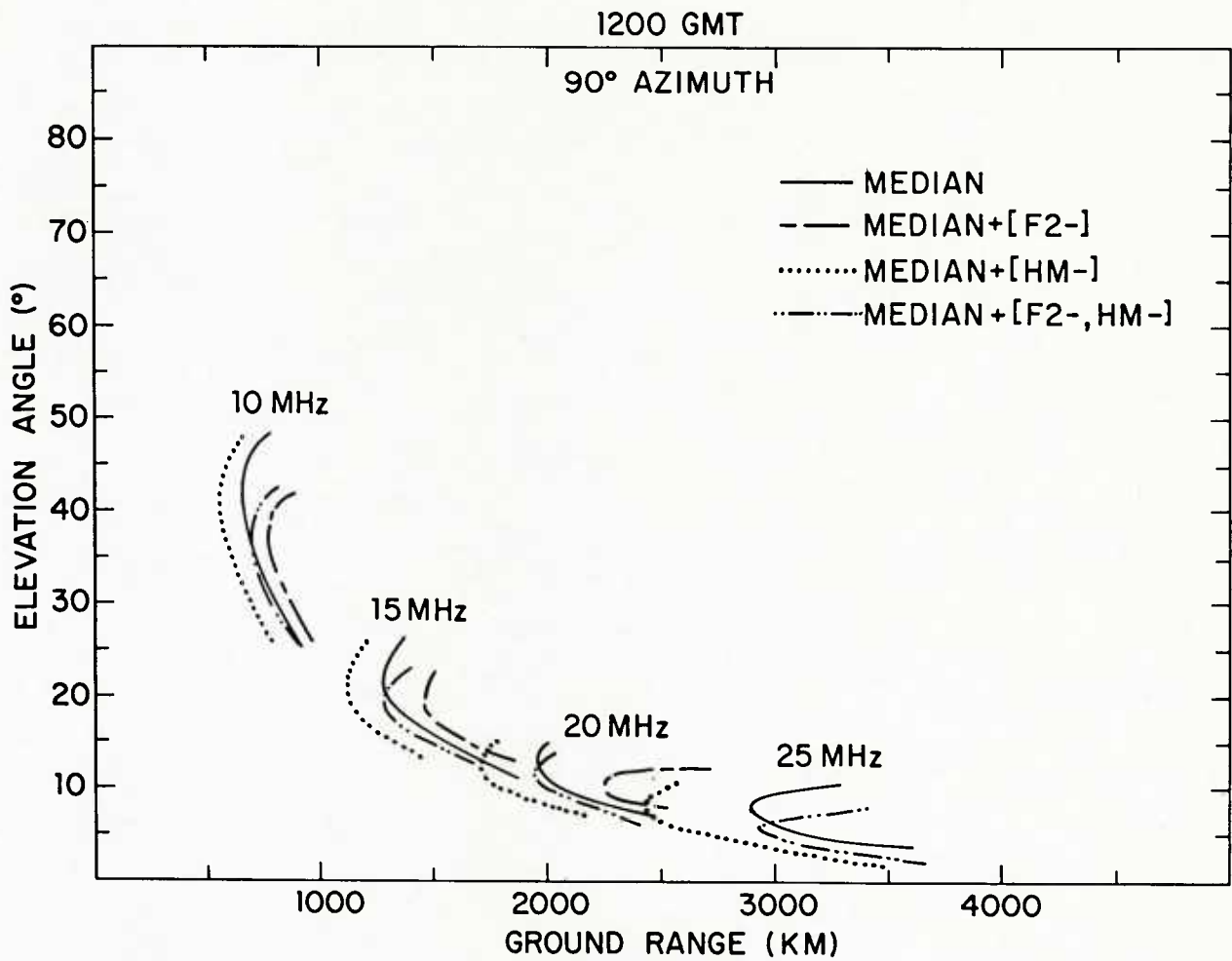


Figure 7. Ground range as a function of elevation angle for different frequencies showing the effect of changes in foF2 and hmF2 on propagation characteristics.

PROPAGATION CHARACTERISTICS OF SATELLITE LINKS

Jules Aarons*
 Boston University
 Dept. of Astronomy
 Boston, MA 02215

SUMMARY

Lower and upper atmospheric effects on signal characteristics of satellite transmissions are reviewed. The effects of importance produced by the ionosphere are the fading, caused by irregularities in the equatorial and high latitude ionospheres, the time delay errors produced by the passage of radiowaves through the ionospheric electrons, and absorption of the lower ionosphere at auroral and polar cap latitudes. The tropospheric effects include absorption by constituents and the problem of scattering of energy into unwanted polarizations. In some applications low angle effects of refraction and scintillation are also of importance.

1.0 INTRODUCTION

The negative effects of the lower and upper atmosphere on earth-space transmissions are absorption, refraction, and scattering. For transmissions lower than 2 GHz, the ionosphere, the region effectively from 60 to 500 km is the seat of most of the problems. For transmissions greater than 6 GHz, the primary region producing unwanted effects is the lower atmosphere from a few kilometers to 15 kilometers. For very low angle transmissions, 0-5° of elevation, the lower atmosphere can deteriorate transmissions from all frequencies and the ionosphere can have a serious effect on signals to 7 GHz.

2.0 SATELLITE SYSTEMS

Simple low-powered equipment can be used in the frequency range to a few hundred megahertz. This is the principal reason why some equipment for both military communications and position finding is in the 200-400 MHz region. In the L-band portion of the spectrum from 1200-1600 MHz, the Global Positioning System and the commercial Maritime Satellite program are occupants. Civilian and military communications utilize the band from 4-7 GHz. Future systems both commercial and military will most certainly utilize the 10-50 GHz portion of the spectrum. It is therefore necessary to review the effects of both the lower and upper atmospheres.

3.0 IONOSPHERIC EFFECTS

The lecturer would like to note that large portions of the ionospheric sections were taken from Goodman (1981), Klobuchar (1978) and works of Millman.

3.1 Absorption

Normal ionospheric absorption principally at the D layer (60-80 km) and the F layer (250-350 km) is not an important effect even at 100 MHz. At the horizon, absorption of a 100 MHz signal is approximately .5 dB for a synchronous satellite. At 30° of elevation the absorption is only about .2 dB.

Polar cap absorption occurs at high latitudes when solar protons of energy 1-100 MeV are channeled into the polar regions after a large solar event. At 30 MHz polar cap absorption of cosmic radio background has produced decreases of over 20 dB at vertical incidence. Since absorption decreases inversely as the square of the frequency approximately 10 dB loss could be suffered by a signal at 100 MHz; this could be increased by the long path length through the ionosphere, the secant factor for a flat earth model. The occurrence of 20 dB absorption in a polar cap event is relatively rare with 2-10 dB absorption at 30 MHz representing the large proportion of major polar cap events. In this case absorption at frequencies over 100 MHz would be unimportant relative to other factors (such as scintillation fading). In observations at 136 MHz from Thule, at the elevation angle of 3° for ATS-3, signals remained several dB above noise during major polar cap events in 1968 and 1969 even with normal quiet S/N ratios of 10 dB.

3.2 Polarization Rotation

The ionosphere rotates the plane of polarization of a beacon signal radiated by a satellite transmitter. Linear polarization can be broken up into right handed and left handed circularly polarized waves. Each wave travels with a different phase velocity since the refractive index of the ordinary (μ_o) and extraordinary wave (μ_x) differ.

*The lecturer would like to note that the ionospheric scintillation studies were completed while the author was at Air Force Geophysics Laboratory.

$$\mu^2 = 1 - \frac{f_o^2}{f(f \pm f_H \cos \theta)} \quad (1)$$

where f_o is the plasma frequency, f_H is the gyro frequency which is proportional to the magnetic field at a fixed point in space, f is the probing frequency, and θ is the angle between the wave normal and the direction of the earth's magnetic field. The + and - signs are used for the two circularly polarized components.

The rotation of the plane of polarization reduces in most practical examples to:

$$\Omega = (k/f^2) \int N_e H \cos \theta ds \quad (2)$$

where N_e is the electron density, ds is the path length, and $H \cos \theta$ is the longitudinal component of magnetic field strength.

Due to the inverse f^2 dependence of Ω , the amount of Faraday rotation diminishes rapidly as the probe frequency is raised. At 7 GHz, for example, the plane of polarization of the transmitted signal would rotate only 1.4 degrees in transit through the entire ionosphere assuming a value for $fN_e dH$ of 10^{18} electrons/m² and $H \cos \theta \sec \times = 40$ amperes turns/meter (Goodman, 1980). Below 1 GHz the amount of rotation begins to become significant and circularly polarized antennas are employed to obviate the effect. However this mitigation scheme disallows the use of polarization as a means for frequency re-use.

3.3 Propagation Delay in Earth-Space Propagation Paths

The total excess delay ΔT for a signal traversing an earth-space path has two additive components, tropospheric and ionospheric. Thus:

$$\Delta T = \Delta T_t + \Delta T_i = \frac{10^{-6}}{c} \int_0^s N_t(s) ds + \frac{40.3}{cf^2} \int_0^s N_e ds \quad (3)$$

where c is the free space velocity of light, N_t is the tropospheric refractivity $(n-1) \times 10^6$, s is the distance along the ray trajectory, and the integral $\int_0^s N_e ds$ is the total electron content (TEC) of the ionosphere.

The first term ΔT_t is approximated by $N_s H \sec \times$ where N_s is the surface refractivity, H is the atmospheric scale height and \times is the ray zenith angle. Taking $N_s = 300$ and $H = 7 \times 10^3$ meters, we see that ΔT_t is the order of 7 nanoseconds. This term may be easily modelled to leave a residual of less than 1.5 nanoseconds. The second term ΔT_i is dependent upon frequency.

3.3.1 The First Order Effect

The additional time delay over the free space transit time between a signal transmitted from above the ionosphere and a user on or near the earth's surface is given by ΔT (seconds) = $40.3/cf^2$. The TEC is generally expressed as the number of electrons in a unit cross section column of one square meter area along this path. Extreme values of this TEC parameter vary from 10^{16} el/m² to 10^{19} el/m². At a system operating frequency of 1 GHz, for example, a TEC of 10^{18} el/m², a value frequently exceeded in low and mid-latitude parts of the world, a time delay of 134 nanoseconds or 132 feet (40.2 meters) of range error will be encountered by the radio wave. At 100 MHz this same TEC value would produce a range error of over 13,000 feet or 4 kilometers! Obviously, the TEC parameter is of potentially great importance to precision satellite navigation systems.

3.3.2 Examples of Typical TEC Values

Fortunately, sufficient ionospheric TEC data is now available from various locations throughout the world to be able to describe the diurnal, seasonal, geographic, solar cycle and magnetic activity dependence of this parameter so that systems design engineers are able to determine the potential effects on any new satellite navigation system. In fact, analytic models of the TEC parameter exist which could be used to estimate the time delay due to the ionosphere. The accuracy and limitations of the typical types of models will be described in a later section of this report, but they are useful now in giving an overall, world-wide view of ionospheric time delay. Figure 1 shows the result of the Bent et al. (1975) model when calculated on a global basis for March 1968, a solar maximum year of an average solar cycle. This figure illustrates the world-wide time delay for a system operating frequency of 1.6 GHz at a universal time of 00 hours. Note from the figure that the regions of maximum time delay occur near the equator at plus and minus 15 to 20 degrees of latitude. These TEC contours move along approximate lines of constant magnetic latitude from east to west as the earth rotates.

3.3.3 Variability of Ionospheric Time Delay

While a model can give a representation of approximate world-wide TEC behavior, actual continuous TEC data recorded at various stations has been recorded to give monthly average and statistical values. An example of a year's TEC data taken at Hamilton, Massachusetts, with the daily values for each month over-plotted, is given in Figure 2. Note the large day-to-day variability within each month and the seasonal changes, with the lowest TEC values occurring during the summer months and the largest values during the equinoxes. Some, but by no means all, of the daily variability of TEC about the monthly mean curve is

due to magnetic storms which have been extensively studied for the behavior of the TEC parameter (Mendillo and Klobuchar, 1974). Other departures from monthly median behavior occur with no clear reason, such as a magnetic disturbance or enhanced solar activity.

Of particular interest is a model described by Klobuchar (1977) which predicts the time delay for single frequency users of the NAVSTAR/GPS system. It is written as

$$\Delta T_1 = DC + A \cos \frac{(t-\phi)2}{P} \quad (4)$$

where DC, A, ϕ , and P are parameters which are modelled.

In general the ionospheric contribution of time delay is compensated for through use of a two-frequency correction technique intrinsic to the GPS system. Thus only single frequency users need to be concerned with the ionospheric contributions to path delay. It will be seen shortly that by far the most important propagation effect as far as GPS is concerned is not propagation delay but scintillation.

In addition to a delay in the mean arrival time ΔT and the well-known pulse distortion effect T_1 (Wong et al., 1978), inhomogeneities in the ionospheric plasma give rise to a time delay spread of the radio-wave signal (denoted by T_2). The time delay spread is directly related to angular scattering. In general the time required for a signal to traverse a distance s is given by:

$$T = \frac{1}{c} \int_0^s ds + \Delta T_t + \Delta T_i + T_1 + T_2 \quad (5)$$

where ΔT_t and ΔT_i are the delays due to propagation through the troposphere and ionosphere respectively, T_1 is due to pulse distortion arising from finite signal bandwidth, T_2 is due to scattering, and $c^{-1} \int ds$ is the free space transit time.

The term ΔT_i has been described previously; it is obviously first order. The term T_1 arises due to the different speeds in which the various Fourier components of the signal travel. The term T_2 is due to scattering from ionospheric turbulence. Millman (1980) has plotted the range error and the ionospheric time delay for a one way path as a function of frequency and electron content (Figure 3).

3.4 Refraction in Earth-Space Propagation

Figure 4a depicts both the tropospheric and ionospheric components of bending introduced over an earth-space path. This is due, of course, to the non-vanishing refractivity in the earth-space medium. The earth-space refractivity may be written

$$N(s) = (n-1) \times 10^6 = N_t + N_i = \frac{77.6}{T(s)} p(s) + \frac{4810 \epsilon(s)}{T(s)} - \frac{40.28 \times 10^{-6}}{f^2} N_e(s) \quad (6)$$

where $N(s)$ is the refractivity, n is the refractive index, N_t is the tropospheric component of refractivity, N_i is the ionospheric component of refractivity, $T(s)$ is the air temperature ($^{\circ}\text{K}$), $p(s)$ is the atmospheric pressure (mb), $\epsilon(s)$ is the partial vapor pressure (mb), f is the radiofrequency (MHz), N_e is the electron density (M^{-3}), and s is the distance parameter. Figure 4b shows radio refractivity versus altitude for both the ionosphere and troposphere.

The index of refraction in the troposphere is greater than unity and since dN/dh is negative in that region, non-zenithal rays are bent away from the normal. As a result, the apparent elevation to the space object is higher than its actual value and the radio range to the object is larger than the geometrical distance. The index of refraction in the ionosphere is less than unity. Nevertheless, the net effect of the ionospheric component of refraction is to combine with the tropospheric contribution such that the total refraction is essentially the sum of the two components. Figure 5 (Millman, 1965) shows the total refraction error introduced at radio frequencies of 100 and 200 MHz as a function of altitude. Limiting tropospheric and ionospheric range errors due to refraction and signal delay are given in Figure 6 as a function of elevation angle. It is noteworthy that the time delay component of range error dominates for elevation angles above 3° . The diurnal variation of the ionospheric component of elevation error at 400 MHz is given in Figure 7 (Evans and Wand, 1975). The ratio of refractive error to range error is not fixed as a function of local time. Of course the range error results from both a time delay due to an increase in path length (caused by bending) and to a reduction in the radiowave signal velocity, so such behavior is not unanticipated.

In summary we may state that the ionospheric component of refractivity remains quite important in comparison to the tropospheric component in the UHF band provided the elevation angle exceeds a critical value, say 5° . Below this elevation the tropospheric component begins to dominate and other effects such as ducting, atmospheric multi-path, and atmospheric scintillation become increasingly important.

There is presently an increased interest in utilizing the earth-space path to transmit increasingly higher data rates and as mentioned above, scintillation conditions in some instances may not support such a requirement. Furthermore the need for greater accuracy and availability of precise navigation only emphasizes the constraint placed on systems by ionospheric inhomogeneities. Techniques for synthesizing large antennas in space by coherent processing and for improving the detection range of space surveillance radars by coherent detection rely heavily on ionospheric smoothness at the frequency involved. Thus the temporal and spatial personality of inhomogeneities in the ionosphere (and the phase

and amplitude scintillation which results) is of utmost relevance. The ionospheric limitation to coherent integration in transionospheric radars has been discussed by Rino et al. (1978). These authors find that the time variation of signal phase is given by

$$\phi(t) = \phi_0 + w(t-t_0) + \dot{w}(t-t_0)^2 + \delta\phi(t-t_0) \quad (7)$$

which is defined over a short interval ($t_0 \leq t \leq t_0+T$) and $\delta\phi$ is a random component of phase defined by a power law probability density function.

The ϕ_0 term is a phase bias due to TEC, the linear term $w(t-t_0)$ is the doppler shift (which causes no problem for target coherent detection), and $\dot{w}(t-t_0)^2$ gives rise to spectral broadening and may reduce processing gain as will the term $\delta\phi(t-t_0)$. For midnight periods both \dot{w} and $\delta\phi$ are quite large over the equator limiting integration at VHF to much less than 10 seconds. More striking is that omnipresent non-vanishing \dot{w} values during the day will limit integration to less than a minute (see Figure 8).

3.5 Doppler Frequency and the Earth-Space Path

The well known expression for ionospheric excess doppler (Hz) is:

$$\Delta f = - \frac{40 \times 10^6}{cf} \frac{d}{dt} \int N_e ds \quad (8)$$

where f is the transmission radio frequency, c is the speed of light, and N_e is the electron density. This number is typically negligible in comparison with the free-space Doppler introduced by satellite or target motion.

For geosynchronous satellites, the Δf correction to the transmission frequency is only academic (being only a fraction of a Hertz) and even for orbiting satellites Δf is relatively unimportant at typical space frequencies. Maximum value of the time derivative occurs near the horizon. Even in this extreme case and for $\int N_e ds = 10^{18}$ electrons/m², Δf will be less than 5 Hz at 1.6 GHz. Typically well-designed ϕ lock tracking loops will encounter no difficulty. Even though the dispersive doppler introduced by the ionosphere is not significant as a system effect in earth-space propagation, it has been quite useful in ionospheric studies.

4.0 SCINTILLATIONS

A radio wave traversing the upper and lower atmosphere of the earth suffers a distortion of phase and amplitude. When it traverses ionospheric irregularities, the radio wave experiences fading, phase deviations and angle of arrival variations, known collectively as scintillations. The irregularities producing scintillations are predominantly in the F layer at altitudes primarily between 250 and 400 km. There are times when E layer irregularities in the 90 to 100 km region produce scintillation, particularly sporadic E and auroral E.

4.1 Scintillation Examples

The intensity fading and its characterization can best be characterized by the idealized example such as in Figure 9. The mean signal level is modulated by the passage thru the irregularities so that the signal level instantaneously both increases and decreases. In Figure 9 the mean signal level at times fades below the 3 dB level and below the 6 dB level. The number of fades and the fade duration for a typical 15 minute length of signal from a synchronous satellite is shown in Figure 9 along with the cumulative probability density function. In this example 91.7 percent of the time the signal was above the 6 dB fade level.

4.1.1 Signal Characteristics

The intensity of the scintillation is characterized by the variance in received power with the S_4 index defined as the square root of the variance of received power divided by the mean value of the received power (Briggs and Parkin, 1963). An alternative measure of scintillation index has been adopted by many workers in the field where

$$SI = \frac{P_{\max} - P_{\min}}{P_{\max} + P_{\min}}$$

where P_{\max} is the power level of the 3rd peak down from the maximum excursion of the scintillations and P_{\min} is the level of the 3rd peak up from the minimum excursion, measured in dB (Whitney et al., 1969). The phase variations are characterized by the standard deviation of phase, σ_ϕ .

Whitney et al. (1972) and Crane (1977) have constructed model probability distribution functions based upon the use of the Nakagami-m distribution ($m = (S_4)^{-2}$) and have shown that the empirical models provide a reasonable approximation to the calculated distribution functions. In addition, the Rayleigh pdf provided a good fit to the data under conditions of very strong scintillation ($S_4 \gg 0.9$).

4.2 Frequency Dependence

Observations (Fremouw et al., 1978) employing ten frequencies between 138 MHz and 2.9 GHz transmitted

from the same satellite, show a consistent $\lambda^{1.5}$ behavior of S_4 for S_4 less than about 0.6. The frequency dependence becomes less steep for stronger scintillation, as S_4 approaches a maximum value near unity with a few rare exceptions. The observations (Fremouw et al., 1978) also show that the phase scintillation index, σ_ϕ , varies as λ under most conditions. Phase fluctuations do not experience a variation in frequency dependence in the strong scattering region.

4.3 Fading Spectra

Radio waves from satellites encountering the ionospheric irregularities undergo spatial phase fluctuations. Intensity fluctuations develop as the wave emerges from the irregularity reaching their maximum intensity in the far field. The amplitude scintillations undergo Fresnel filtering which generate maximum intensity at a spatial wavelength of the Fresnel scale. For weak scattering the spatial spectrum of intensity fluctuations is in effect a convolution of the phase spectrum with the Fresnel filter function. The spectra of very high scintillation indices [$S_4 = .94$ (close to Rayleigh fading)] at equatorial latitudes is shown in Figure 10 (Basu and Whitney, 1980).

The intensity spectrum changes as a function of drift speed, irregularity spectrum, and strength of scattering. Thus the morphology of spectra is in reality the interplay of these factors. In each of the geophysical areas where intense activity occurs, the three factors must be utilized to estimate the spectra of the scintillation intensity.

4.4 Geometrical Considerations

The intensity at which scintillations are observed depends upon the position of the observer relative to the irregularities in the ionosphere that cause the scintillation. Keeping both the thickness of the irregularity region and ΔN , the electron density deviation of the irregularity, constant, geometrical factors have to be considered to predict scintillation effects at a particular location. Among these are:

- a. Zenith distance of the irregularity at the ionospheric layer. The intensity of scintillation is related approximately to the zenith path values by the secant of the zenith distances to 70° ; below that an elevation angle dependence ranging between $1/2$ and the first power of the zenith angles should be used.
- b. Propagation angle relative to the earth's magnetic field. Sheet-like irregularities with forms of 8:8:1 and 5:2:1 have also been found in recent auroral studies. For equatorial latitudes, this elongation along the lines of force may be of the order of 50 to 100 (Koster, 1963).
- c. The distance from the irregularity region to the source and to the observer (near the irregularities, only phase fluctuations are developed).

Mikkelsen et al. (1978) has attempted to determine the theoretical scintillation index, S_4 , when the irregularities are described by a power-law power spectrum. Mikkelsen assumed the approximate dividing line between weak and strong scintillation is ~ 9 dB, with $SI < 9$ dB denoting the weak case. The geometric variation of S_4 is provided in Mikkelsen et al. (1978).

4.5 Spread F and Scintillation

The evidence from the correlation of scintillation occurrence and spread F (Rastogi, 1980) is that at equatorial and middle latitudes range spread is associated with scintillation activity and frequency spread is not. Thus the available spread F maps cannot be used for scintillation observations in these regions; they are dramatically misleading in many cases. In the high latitude region no statistical study has been made to correlate types of spread F with scintillation activity. It might be noted that even range spread occurrence and scintillation have important differences.

4.6 Global Morphology

From the global point of view there are three major sectors of scintillation activity (Figure 11). The equatorial region comprises an area with $\pm 20^\circ$ of the magnetic equator. The high latitude region comprises the area from the high latitude edge of the trapped charged particle boundary into the polar region.

In all sectors there is a pronounced nighttime maximum. At the equator, activity begins only after sunset. Even in the polar region, there appears to be greater scintillation occurrence during the dark months than during the months of continuous solar visibility.

4.6.1 Equatorial Scintillations

a) Patch Characteristics

It has been established that nighttime ionospheric equatorial irregularity regions emerging after sunset develop from bottomside instabilities, probably of the Rayleigh-Taylor type. The depleted density bubble rises into the region above the peak of the F2 layer. Steep gradients on the edges of the hole help to generate the smaller-scale irregularities within the patch which produces intense scintillation effects (Basu and Kelley, 1979).

b) Patch Development, Motion and Decay

A plume-like irregularity region develops after sunset, finally forming a patch of irregularities which has been likened to a banana or an orange segment. A cut through the center of the "banana" is shown in Figure 12. It appears to have a minimum E-W size of ~ 100 km. It is composed of field-aligned elongated rod or sheet irregularities. The vertical thickness of the patch is 50 to several hundred kilometers. Its north-south dimensions are of the order of 2000 km or greater. Once formed, the patch drifts eastward with velocities ranging from 100 to 200 m/s.

c) Polarization Fluctuations

Patches show both depletions and polarization fluctuations, the latter effect is noted by a variation in total electron content as seen on Faraday rotation records (Yeh et al., 1979)

d) Longitudinal Comparison

Comparison was made of scintillation activity at 250 MHz at a variety of observatories with data taken over the same time period (Aarons, 1982). One set of data was taken at Huancayo, Peru, Natal, Brazil, and Accra, Ghana with all observations made at elevation angles greater than 20° and with distance between the most separated stations about 70° of longitude; a map of both geographical and magnetic co-ordinates is shown on the right side of Figure 13.

A second comparison of data at 250 MHz was made between observations from Huancayo and from Guam. The data are shown in Figure 14; activity minima occur from May-July in Huancayo and from November-January in Guam. The conclusion is that the occurrence patterns are longitudinally controlled.

e) Sunspot Cycle Dependence

Recent observations of L Band and 4 GHz scintillations (1979-1981) (DasGupta et al., 1981) have revealed that scintillation intensities maximize in the Appleton anomaly region (at $\pm 15^\circ$ - 20° of dip latitude) rather than near the magnetic equator particularly during years of high solar flux when they reach >30 dB levels at L band and 9 dB at S Band. Scintillations are lower (< 9 dB at L Band) within $\pm 5^\circ$ of the magnetic equator.

4.6.2 Middle Latitude Scintillation

The middle latitude scintillation activity is not as intense as that encountered at equatorial, auroral or polar latitudes. For the engineer, however, activity may reach levels, primarily at VHF and UHF, which will increase error rates of systems with low fade margins. The reader is referred to Aarons (1982) and Bramley (1974).

4.6.3 The High Latitude Region

Figure 15 depicts the intensity of scintillation at high latitudes in a very broad manner for the period of time around midnight. The present evidence is that there is a boundary at the high latitudes where weak irregularities commence. It is probably a few degrees equatorwards of the plasmapause, between 45° - 55° Corrected Geomagnetic Latitude, the system used at high latitudes in this review.

At night a trough or region of low electron density and total electron content exists between the end of normal ionospheric plasma behavior and the auroral region where energetic precipitation and current systems are dominant factors in producing both the normal ionospheric layers and the irregularities.

All observers of irregularities see a dramatic change in irregularities in the auroral oval, at the poleward edge of the trough. In the auroral oval, the intensity of scintillations is a function of local magnetic activity and is well correlated with auroral images as shown by the optical sensors of the Defense Meteorological Satellite Program satellites. Poleward of the aurora there may again be a lowering of scintillation activity until the observing path transits the polar region (Aarons et al., 1981).

a) Morphology in Two Longitudinal Sectors

Perhaps the most consistent studies of long term behavior of scintillations have been in the auroral zone, at Alaskan longitudes and along the 70° W meridian. Both the diurnal pattern of scintillation activity and the seasonal behavior as observed from Narssarsuaq, Greenland can be noted in Figures 16 and 17. The data used for this long term study (Basu and Aarons, 1980) were taken over a period of 6 years by observing 137 MHz scintillations of the ATS-3 beacon; the propagation path traversed the ionosphere at $\sim 63^\circ$ CGL.

b) Geometry and Enhancement

For two sites in Alaska, Rino and Owen constructed the geometrical enhancement factor for rms phase fluctuations for an 8:8:1 irregularity (Figure 18). Data for one year (Rino and Matthews, 1980) is seen in Figure 19 for the Poker Flat station. The amplitude enhancement, less dramatic but present, is also shown in Figure 19. Daytime scintillation does not show the sheet-like structure — at least as observed from Alaska.

4.6.4 Polar Scintillations

There is a scarcity of direct scintillation data at polar latitudes. The auroral oval maximum is quite clear in its behavior, principally its expansion and intensification with magnetic activity. Polewards of the oval, however, sparse data shows a shallow minimum with a second peak located near the corrected geomagnetic pole (Nielsen and Aarons, 1974).

A long term consistent series of measurements has been taken at Thule, Greenland with observations at 250 MHz (Aarons et al., 1981). The scintillations for this study ranged from very low values of 3-6 dB peak to peak on occasion during a period of low sunspot number to saturation fading of 28 dB peak to peak for hours during winter months of years of high sunspot number.

One set of measurements was taken between April and October 1975. During this period of low solar activity, there was an absence of strong scintillation activity to such an extent that only the occurrence of scintillation greater than 6 dB could be plotted. Figure 20 shows the contrast between the 1975 period when solar flux was low (10.7 cm flux was ~ 75) and the same months in 1979 when the solar flux was high

(~ 150 – 225). A contour plot of the percent occurrence of scintillation index > 10 dB is shown in Figure 21.

Auroral arcs in the polar cap are approximately aligned with the noon-midnight magnetic meridian. These arcs generally drift in the dawn to dusk direction, however, reversals have been noted. Recently, Weber and Buchau (1981) described the orientation and motion of subvisual F-layer ($\lambda = 6300$ Å OI) polar cap arcs. Kilometer-size irregularities within the arcs produced intense (saturated) amplitude scintillation at 250 MHz as the arcs drifted through a satellite to ground ray path. Outside the arcs, scintillation frequently persisted at a lower level ($SI \sim 6$ dB).

A picturization of both the small scale anti-sunward irregularity drift and the patch motion (predominantly dawn to dusk) is shown in Figure 22 (E. Weber, private communication). Results point to two irregularity components in the polar cap; antisunward drifting irregularities which produce a background level of weak to moderate scintillation and intense irregularities within F layer polar cap arcs which produce more discrete (~ 1 hr duration) intense scintillation events as the arcs drift through the ray path.

4.7 Empirical Model of Global Scintillation Behavior

Over a period of years, starting from available data and from weak scintillation theory, a model of scintillation termed WBMOD has been developed (Fremouw and Lansinger, 1981). The program provides for phase and amplitude information. Input user parameters include frequency, location, local time, sunspot number and planetary magnetic index, Kp. The user also must specify the longest time the system needs phase stability. Scintillation indices are the output. A model of the irregularity drift velocity is contained in the program.

Program WBMOD permits a user to specify his operating scenario. The code returns the spectral index, p , for power-law phase scintillation, the spectral strength parameter, T , the standard deviation, σ_ϕ , of phase and the intensity scintillation index, S_4 , as functions of a changing independent variable chosen by the user.

5.0 THE LOWER ATMOSPHERE*

The lower atmosphere propagation parameters that are important to the radio system designer and the user have been summarized by Watson (1980). They are:

- (i) The ability to predict the attenuation experienced on earth-space radio links for any satellite-earth station configuration in terms of the percentage time given attenuation thresholds are exceeded on average, and in terms of statistics of fade durations.
- (ii) Prediction of the on-average occurrence of cross-polarization and, if possible, the relationship of this to the occurrence of attenuation.
- (iii) Prediction of the magnitude of incoherent emissions (thermal and forward scatter) causing an enhanced noise background on coherent radio systems.
- (iv) Characterization of off-axis scattering from atmospheric structures, causing interferences between systems.
- (v) Characterization of any other channel impairments, for example dispersion, which may place limits on broadband systems operation.

The data base for prediction even after extended studies with ATS-5, ATS-6, SIRIO and other satellites is limited but because of the proliferation of satellites using the bands from 2–50 GHz the information gleaned from this data base must be used for evaluating deterioration in particular areas under field conditions.

5.1 Tropospheric Scintillations

Fluctuations in signal amplitude are frequently seen during the rise and set of satellites. The scintillations are frequency independent and are very strongly dependent on local real time atmospheric conditions. The rise of one satellite is noted in the tracing of Figure 23. It should be noted however that even with several dB fluctuation the useful signals from satellites can extend to close to the horizon. Similar fluctuations have been noted in the GHz regions.

In addition to low angle tropospheric scintillations, there are high angle amplitude fluctuations of several decibels noted from 4 to 30 GHz range with only weak dependence on frequency. The few dB fluctuation can affect the performance of low margin systems. Cox et al. (1981) show records at 41.5° of elevation (Figures 24a and 24b) from turbulent clouds. These high angle scintillations do not necessarily produce attenuation in the mean level.

5.2 Attenuation

Except for elevations less than 5° , the most important attenuation mechanism in the 2–50 GHz range is due to the occurrence of intense rainfall in the radio path. At higher frequencies, particularly above 30 GHz we also must consider the effects of clouds, fogs and gaseous absorption. The background loss in the various atmospheric windows occurring above 70 GHz appears to be higher than expected and is currently attributed to anomalous water vapor absorption. The general picture of absorption by oxygen and water vapor is given in Figure 25a with peaks at 61, 119 and 183 GHz. Figure 25b contrasts two atmospheric conditions.

Goodman (1980) has reviewed the attenuation characteristics of the lower atmosphere. Absorption and scattering are typically unimportant for frequencies less than 3 GHz. Since the resonance absorption peaks of H_2O and O_2 are well known and can be solved, the most significant future problem for systems which will use the earth-space propagation path at frequencies between 10 and 100 GHz is likely to be

*The lecture on the lower atmosphere is taken from papers of Watson (1980), Moore (1980), Goodman (1980) and Goldhirsch (1980).

rainfall attenuation. Two types of rain are considered: stratiform and convective. Stratiform rain generally develops in stable masses of air, along frontal surfaces typically, and is characterized by steady and uniform rain over wide areas for hours to days; low rain rates are typical. Convective rainstorms, on the other hand, develop in highly unstable air masses, are limited in extent and duration, and are characterized by high rain rates. If rainfall statistics are unavailable for a typical area, it is possible to estimate the rainfall distribution (Bean and Dutton, 1976). Attenuation by hydrometers is given by

$$\alpha \text{ (dB/km)} = 4.343 \int_0^{\infty} Q_T(a) \eta(a, R) da \quad (9)$$

where Q_T is the attenuation cross section/drop, η is the drop size distribution, a is the drop radius, and R is the rain rate.

The attenuation function Q_T is determined from classical Mie and/or Rayleigh scattering theory and for computing α several drop size distributions are available. An empirical relationship between rain rate R and α is shown in Goodman (1980),

$$\alpha \text{ (dB/km)} = a R^b \quad (10)$$

where a , b are frequency dependent constants. Uniform rain attenuation is proportional to the cosecant of the ray elevation angle since the total attenuation is proportional to the product of the specific attenuation α and the path length L . The frequency scaling law for rainfall attenuation is approximately

$$\frac{A(f_2)}{A(f_1)} = \left(\frac{f_2}{f_1} \right)^{1.72} \quad (11)$$

which for uniform rain becomes approximately a_2/a_1 . It may be shown that water cloud attenuation is equivalent to light rain (≤ 5 mm/Hr) attenuation below 100 GHz. Ice cloud attenuation is at least 2 orders of magnitude less than water cloud attenuation and thus is of little relative practical significance.

Characterization of world climatic zones of rainfall intensity is a most important intermediate step being studied at the present. We look towards the synthesis of rainfall intensity maps for short duration rainfalls (1-5 mins) from which the system designer should be able to make viable predictions. Until now the classification of rainfall climates used by system designers has been on the basis of total annual rainfall, a figure which barely relates to the occurrence of extreme intensities. Recently, Dutton and Dougherty (1978) have used the maximum monthly rainfall and the number of thunderstorm days as indicators of intense rainfall climates. However, their classification of climatic zones is still based on broad climatological criteria and do not represent climatic zones of rainfall intensity.

In some countries with long traditions of meteorological research, adequate data for the preparation of short duration rainfall maps are probably already available. In the U.K., for example, the Meteorological Office has published contour maps for short duration rainfalls covering any part of the country. It is possible to use these maps with suitable rainstorm models to produce satisfactory rainfall-attenuation tables.

5.3 Tropospheric Refraction

The complexity of range measurements when a duct is present has been pointed out by Moore (1981). For propagation from a satellite the effect of a duct is to reduce the range for any particular ray, but to increase the total range. Figure 26 shows how this can happen. Ray B would go to the horizon in the absence of a duct. It is shown straight from the satellite to the top of the troposphere (the ionosphere may be treated separately), from there it follows a curved path to point 2 on the earth, at which it is tangent to the surface. If a duct is present, the additional refractivity lapse rate in the duct causes additional curvature from the top of the duct to the ground, and the ray strikes the ground at point 1. Not only is this closer to the sub-satellite point, but the angle of incidence is steeper as shown. If this horizon ray for the normal atmosphere were the shallowest ray leaving the satellite that could reach the ground in the presence of a duct, the net ground area within "sight" would be reduced. Ray A, however, reaches the ground in the duct, even though it would normally be tangent to the sphere whose surface is the top of the duct, and would then pass on out of the atmosphere as shown. With the duct, the ray that is tangent at its top is bent on into the duct and strikes the earth at point 3. Since this is beyond point 2, the actual coverage is extended by the presence of the duct. This ray strikes the ground at an incidence angle greater than zero; no tangent ray exists for the duct situation. A ground station at point 2 would see the satellite on the horizon (zero elevation angle) in the absence of the duct, but in the presence of the duct the satellite will appear at a significant elevation angle.

This picture cannot properly describe Ray A because a ray tangent to the top of the duct does not satisfy the conditions for use of geometric optics. Wave theory (physical optics) should be used to determine the amplitude of waves arriving at the top of the duct at this angle and detected at point 3, but this is beyond the scope of the treatment here. As the wave strikes the duct at steeper angles, the use of rays (geometric optics) becomes increasingly valid.

5.4 Depolarization

In an attempt to double the information capabilities of individual satellites it was thought that two linear polarizations or two oppositely sensed circularly polarized signals could be transmitted along the same path simultaneously. They can be sent but depolarization or scattering into the unwanted polarization is affected by lower atmospheric constituents. Watson has summarized the problem and recent results.

Two distinct particle populations are known to contribute to cross-polarization on earth-space paths, namely raindrops and ice particles. The melting zone, a third region, appears from existing rather limited evidence to be fairly isotropic, though two polarization radar results show an interesting region of high differential reflectivity immediately below the bright band.

(a) Rain

The model for cross-polarization in rainfall involves raindrops approximated by oblate spheroids each with a preferred alignment of their axis of rotational symmetry to the local vertical. The cross-polarization produced for a given attenuation on earth-space or terrestrial paths can be described accurately by a model with a distribution of raindrop tilt (or canting) angles around the local vertical. A gaussian distribution with near zero mean ($<4^\circ$) and 20 to 25° standard deviation can be used. Figure 27 shows one measurement comparing depolarization and signal attenuation.

(b) Ice Particles

It is now well established that on earth-space paths an additional source of cross-polarization is evident to that from distorted raindrops, namely cross-polarization from ice-particles. This form of cross-polarization occurs with little or no attenuation, as would be expected in a medium exhibiting pure differential phase. Radar evidence suggests that the major contribution to this form of attenuation comes from populations of large numbers of small particles, and this observation is consistent with the low attenuations observed, at 20 and 30 GHz. In modelling the medium it is useful to distinguish two particle types which will exhibit different properties, namely needle-like and plate-like particles. The greatest uncertainty in modelling arises at present from an incomplete knowledge of the role played by orientation effects, in particular with needle-like particles. The most simplistic model involves a population of ice plates showing a preferred orientation in the horizontal plane.

A recent workshop (Radio Science, 1981) in lower atmosphere studies concluded the following for frequencies up to at least 30 GHz and for elevation angles in the range of at least 10° to 50° .

1. Depolarization is usually strongest for fixed linear polarizations oriented 45° from vertical and horizontal and for circular polarization. Depolarization is usually minimized for 'vertical' and 'horizontal' polarization. (Horizontal polarization is perpendicular to the propagation direction and tangent to the surface of the earth at the earth terminal. Vertical polarization is perpendicular to the propagation direction and is rotated 90° from horizontal polarization.) These maxima and minima occur for linear polarizations because the axes of minimum depolarization for raindrops and ice crystals are usually oriented vertically and horizontally.

2. For a given XPD the frequency of occurrence of ice depolarization relative to rain depolarization varies with climate and geography. However, rain dominates XPD statistics in regions that experience the severe rain attenuations associated with thunderstorms. Nevertheless, a high level of depolarization (not XPD) may occur more frequently in ice than in rain. This may be important in certain systems.

3. Although there is statistical variation in the relationship between XPD and attenuation at any location and there appears to be a climatic and geographic variation in this relationship, one relationship between XPD and attenuation is similar for all experimental locations.

4. XPD statistics can be estimated for different frequencies, elevation angles, and polarizations by scaling measurements for a particular location. For a particular rain or ice medium the ice or rain XPD amplitude ratio is approximately proportional to frequency f_1 and to $\cos^2 \theta / \sin \theta$, where θ is the path elevation angle. If measurements are not available, rain XPD can be estimated by using rain XPD models.

5.5 Space Diversity

To minimize the effect of rain it is possible to use space diversity. Goldhirsh (1980) has summarized some of the experimental results and the extrapolation from these results. Because of the variability of rain intensity, especially in the lateral directions in convective storms, it may be useful to employ a space diversity configuration. This involves the utilization of two ground stations spaced a given distance apart. When the fades reach levels in excess of a predefined threshold along one earth-satellite path, transmissions are switched to the alternate ground station where because of the variability of rain intensity, the simultaneous fade levels are likely to be less along this second earth-satellite path. A useful concept for characterizing space diversity is the "diversity gain" which was originally introduced by Hodge (1973). This is defined as the dB difference between the single terminal fade distribution curve (labeled $d = 0$ in Figure 28) and the joint probability curve for a given space, d , at a fixed probability level or fixed single terminal attenuation. This characteristic gives a measure of fade margin reduction for a space diversity configuration compared to the single terminal case at any fixed probability levels.

Goldhirsh (1975) and more recently Hodge (1978) analyzed the diversity gain dependence on terminal spacing with radar data. Goldhirsh's results (Wallops Island, VA) were restricted to the case in which the diversity paths were in the same vertical plane as the satellite and the baseline connecting the paths, whereas Hodge's results (McGill radar, Que.) considered various baseline orientations and path directions. In Figure 29 is an example of radar derived diversity-gain variations as a function of terminal separation for different single-terminal fades at $f=30$ GHz (Goldhirsh, 1975). The horizontal lines represent the diversity gains between the single-terminal curve and the conditionally decorrelated case. We note that all the curves appear to asymptotically reach the decorrelated case levels. Dividing the diversity gain levels of Figure 29 by their respective optima, and multiplying by 100, we arrive at a

family of curves referred to as "percentage of diversity gain relative to optimum" versus separation distance. These curves are, in general, within 5 percent of one another for any given separation at the various fade levels, and hence may be represented by a single curve by taking their average at fixed separation distances. The resultant curves are plotted in Figure 30 for frequencies ranging from 13 to 100 GHz. We note that all the curves lie within a ± 2.5 -percent band which demonstrates the frequency independence of these relative diversity gains. The curves also show that at 20 km and beyond, more than 90 percent of the conditionally decorrelated level is achieved making questionable the desirability of increased separation distances beyond this limit.

5.6 Low Angle Effects

5.6.1 Fading

Measurements of low-angle fading using the ATS-6 satellite have shown that fading decreases with increasing elevation angle. Severe fading at 4 and 30 GHz is confined to elevation angles below 3.5° and 6° , respectively. The frequency dependence of low-angle fading is not inconsistent with the hypothesis that the probability of a given fade depth is proportional to frequency.

An extensive series of measurements made in Canada at 4 and 6 GHz at a fixed elevation angle near 1° has shown that severe low-angle fading is principally confined to the summer months and is closely associated with the presence of a sharp temperature inversion at heights of a few hundred meters. The variations in signal strength are uncorrelated for a vertical path separation of 180 m. A model has been proposed in which a sharp refractive index discontinuity exists across a corrugated interface several meters above the surface. Ray tracing has shown that there are regions in which the satellite signal cannot penetrate. Using reasonable values for the various parameters, results have been derived which are consistent with the observed phenomena.

5.6.2 Refraction

Since the refraction of a ray is affected by the lower atmosphere the variation of horizon distance has been observed under different atmospheric conditions. Moore (1980) showed examples with variations in horizon distance ranging from 22 km closer than for a vacuum under extreme conditions of subrefraction to 340 km beyond the free space horizon for an extreme duct condition. Horizon variations due to variations in surface refractivity with normal refraction amount to 109 km. Grazing angle variations between minimum and maximum surface refractivity amount to only about 5 mr, but in a duct they may become as great as 32 mr.

5.6.3 Noise Levels

Watson (1980) has reviewed the problems of other transmissions and of dispersion. He notes the following:

a) Incoherent emissions

Received incoherent energy will raise the noise background for coherent radio systems. Below approximately 30 GHz the thermal emissions from rain appear to be adequately described by the radiometer equation within the uncertainty connected with the choice of medium temperature. Above 30 GHz multiple scattering should be included. With highly directive antennas incoherent forward scattered radiation from rainfall should not be significant until at least 100 GHz. However, with broad-beam antennas it may be necessary to consider this effect at lower frequencies and also to consider the correlation properties of incoherent signals associated with far from axis returns.

b) Off-axis scattering

Off-axis or bistatic scattering from rainfall might be evident in circumstances where a common scattering volume is viewed by satellite and terrestrial radio relay links. Although the total scattering cross-section for a rain volume will increase with increasing frequency in the range 2-50 GHz, whenever significant common volume scattering occurs, there is invariably rain also present on the rest of the radio path, giving rise to attenuation of the scattered signal. Making the simplifying assumption that rain is uniform along the path, it can be shown that the interference-to-signal ratio is given by $\beta A/4.34G$ where A is the rain fade margin, β is the ratio of the scattering to extinction coefficients for the rain volume and G is the receive antenna gain. However, from a practical point of view, other trans-horizon propagation mechanisms are likely to be much more significant than rain scatter in causing interference between systems. In a recent series of measurements at 11 GHz on a number of over-land and over-sea trans-horizon radio paths, no evidence of rain scatter above a measurement threshold of -53 dB on the free space value was detected, whereas super-refractive and ducting effects were observed for significant percentages of time ($\sim 0.01\%$) giving interference -10 dB to -20 dB relative to the free space value.

c) Dispersion

For elevations $< 5^\circ$ there should be little or no mean phase-frequency distortion on earth-space radio links using 2-50 GHz, as confirmed by recent measurements at 20 and 30 MHz. Amplitude-frequency distortion from coherent returns should only be detectable on extremely broadband systems (GHz bandwidth) and can be predicted from published rain attenuation data. Amplitude and phase scintillations due to incoherent returns should also be negligible up to at least 50 GHz for most practical systems, however measurements using broadband data streams have not yet been reported. A more serious dispersion mechanisms may come into play at low elevations ($< 5^\circ$) where deep fading is observed from stable anomalous refractive index gradients. Recently Strickland (1974) has reported that such fading is not frequency selective over bandwidths of several MHz.

5.7 Effects on Digital Transmission

The negative effect of tropospheric multipath propagation on high data rate digital line-of-sight links has been particularly noted. Multipath propagation contributes to intersymbol interference. The impact on the system depends on the format of the digital signal, such as the bandwidth, the number of levels, and the modulation method. There is experimental evidence that amplitude and/or phase variations within the signal bandwidth give rise to the major system impairments during multipath propagation. In many digital systems an amplitude variation of 5-6 dB across the band gives unacceptably high bit error rates. Such in-band distortions may occur at relatively small fade depths, e.g., 10-15 dB. Application of a

method for evaluating system outage probability due to multipath fading has been described. This method assumes a simple echo transfer function for the propagation channel, the amplitude and the delay of the interfering ray being exponentially distributed. Some experimental results concerning the group delay response of the propagation channel showed that in some cases, two random rays added to the direct ray may exist.

Summarizing the studies of lower atmospheric effects of a recent AGARD Symposium, Viddeleer (1980) numbered among his conclusions the following:

- the influence of rain on systems operating above about 10 GHz will be of paramount importance, in particular with respect to attenuation. Even in moderate climates attenuations of 12 dB at 20 GHz and 20 dB at 30 GHz can be expected for 0.01% of a year. The spread in these values from year to year is high.
- the influence of rain on depolarization depends on the type of polarization used (linear vs. circular) and in the case of linear polarization also on the tilt angle. In the optimum case (linear polarization, vertical or horizontal) the depolarization is about 10 dB less severe than for circular polarization.
- strong depolarization can occur without significant attenuation and is likely to be caused by ice crystals. These crystals are likely to be subject to orientation along the field lines in the strong electrostatic fields of thunderstorms.
- systems with frequency reuse by means of polarization diversity will show degraded performance due to extra attenuation as well as to depolarization effects. To describe the system performance the joint probability of these two parameters is required. Some papers give data on this joint probability. The conclusion is, that in most systems the attenuation will be the governing factor in the quality criteria of the system.

ACKNOWLEDGMENT

The author would like to acknowledge the assistance of the Physics Research Division of Emmanuel College with the organization of this material.

REFERENCES

- Aarons, J. (1982) The global morphology of ionospheric scintillations, Proc. IEEE (to be published).
- Aarons, J., J.P. Mullen, H. Whitney, A. Johnson and E. Weber (1981) VHF scintillation activity over polar latitudes, Geophys. Res. Lett., **8**, 277-280.
- Basu, Sunanda and M.C. Kelley (1979) A review of recent observations of equatorial scintillations and their relationship to current theories of F-region irregularity generation, Radio Sci., **14**, 471.
- Basu, S. and J. Aarons (1980) The morphology of high-latitude VHF scintillation near 70°W, Radio Sci., **15**, 59-70.
- Basu, S. and H.E. Whitney (1980) A study of multifrequency intensity scintillation spectra near the magnetic equator, Proc. ISEA, Aguadilla, Puerto Rico.
- Bean, B.R. and E.J. Dutton (1976) Radio meteorological parameters and climatology, Telecomm. J., **43**, 427-435.
- Bent, R.B., S.K. Llewellyn, G. Nesterczuk and P.E. Schmid (1975) The development of a highly-successful worldwide empirical ionospheric model and its use in certain aspects of space communications and worldwide Total Electron Content investigations, in Effects of the Ionosphere on Space Systems and Communications, J.M. Goodman, Ed., Naval Research Laboratory, Washington, D.C. 20375, U.S. Govt. Printing Office Stock No. 008-051-00064-0.
- Briggs, B.H. and I.A. Parkin (1963) On the variation of radio star and satellite scintillation with zenith angle, J. Atmos. Terr. Phys., **25**, 339-365.
- Crane, R.K. (1977) Ionospheric scintillation, Proc. IEEE, **65**, 180.
- Cox, D.C., H.W. Arnold and H.H. Hoffman (1981) Observations of cloud-produced amplitude scintillation on 19- and 28-GHz earth-space paths, Radio Sci., **16**, 885-907.
- DasGupta, A., A. Maitra and S. Basu (1981) Occurrence of nighttime VHF scintillations near the equatorial anomaly crest in the Indian sector, Radio Sci., in press.
- Dutton, E.J. and H.T. Dougherty (1978) Estimating year-to-year variability of rainfall for microwave propagation, IEEE Trans. Comm-26, **8**, 1321-1324.
- Evans, J.V. and R.H. Wand (1975) Ionospheric limitations on the angular accuracy of satellite tracking at UHF or VHF, in Radio Systems and the Ionosphere, ed., W.T. Blackband, NATO-AGARD-CP-173.
- Fremouw, E.J., R.L. Leadabrand, R.C. Livingston, M.D. Cousins, C.L. Rino, B.C. Fair and R.A. Long (1978) Early results from the DNA Wideband satellite experiment - complex-signal scintillation, Radio Sci., **13**, 167-187.
- Goldhirsch, J. (1975) Prediction methods for rain attenuation statistics at variable path angles and carrier frequencies between 13 and 100 GHz, IEEE Trans. on Antennas and Propagation, AP-23, 786-791.

- Goldhirsch, J. (1980) Radar estimation of slant path rain attenuation at frequencies above 10 GHz and comparisons with measured multi-season results, AGARD - CP-284 on Propagation Effects in Space/Earth Paths.
- Goodman, J.M. (1980) Environmental constraints in earth-space propagation, Naval Research Laboratory Memorandum Report 4339, Washington, D.C.
- Hodge, D.B. (1973) Space diversity for reception of satellite signals, Dept. of Electrical Engineering, Ohio State Univ., Columbus, Ohio, Technical Rpt. 2374-16.
- Hodge, D.B. (1978) Path diversity for earth-space communication links, Radio Sci., **13**, 481-487.
- Klobuchar, J.A. (1977) Ionosphere time delay corrections for advanced satellite ranging systems, in Propagation Limitations of Navigation and Positioning Systems, AGARD-CP-209.
- Klobuchar, J.A. (1978) Ionospheric effects on satellite navigation and air traffic control systems, AGARD Lecture Series No. 93, Recent Advances in Radio and Optical Propagation for Modern Communications, Navigation and Detection Systems.
- Koster, J.R. (1963) Some measurements of the irregularities giving rise to radio-star scintillations at the equator, J. Geophys. Res., **68**, 2579-2590.
- Mendillo, M. and J.A. Klobuchar (1974) An atlas of the midlatitude F-region response to geomagnetic storms, AFCRL-TR-74-0065.
- Mikkelsen, I.S., J. Aarons and E. Martin (1978) Geometrical considerations of 136 MHz amplitude scintillation in the auroral oval, J. Atmos. Terr. Phys., **40**, 479-483.
- Millman, G.H. (1965) Atmospheric effects on radio wave propagation, in Modern Radar Analysis, Evaluation, and System Design, R.S. Berkowitz, ed., John Wiley & Sons, Inc., N.Y.
- Millman, G.H. (1980) Ionospheric electron content effects on earth-space radio propagation - a review, R80EMH11, presented at COSPAR Beacon Satellite Group Symposium on Scientific and Engineering Uses of Satellite Radio Beacons, Warsaw, Poland.
- Moore, R.K. (1980) Tropospheric propagation effects on earth-space low elevation angle paths, AGARD-CP-284 on Propagation Effects in Space/Earth Paths.
- Nielsen, E. and J. Aarons (1974) Satellite scintillation observations over the northern high latitude regions, J. Atmos. Terr. Phys., **36**, 159-165.
- Rastogi, R.G. (1980) Seasonal and solar cycle variations of equatorial spread-F in the American zone, J. Atmos. Terr. Phys., **42**, 593-597.
- Rino, C.L., C.H. Hawson, R.G. Livingston and J. Petriceks (1978) The ionospheric limitation to coherent integration in transionospheric radars, in Effect of the Ionosphere on Space and Terrestrial Systems, ed. J.M. Goodman, GPO, Washington, D.C.
- Rino, C.L. and S.J. Matthews (1980) On the morphology of auroral zone radio wave scintillation, J. Geophys. Res., **85**, 4139.
- Strickland, J. (1974) Radar measurements of site-diversity improvement during precipitation, Jour de Recherches Atmosphériques, **8**, 451-464.
- Viddeleer, R. (1980) Summary of Session and Experimental data of SHF/EHF paths, AFARD-CP-284 on Propagation Effects in Space/Earth Paths.
- Watson, P.A. (1980) Characterization of the effects of the lower atmosphere, AGARD-CP-284 on Propagation Effects in Space/Earth Paths.
- Weber, E.J. and J. Buchau (1981) Polar cap F-layer auroras, Geophys. Res. Lett., **8**, 125.
- Whitney, H.E., C. Malik and J. Aarons (1969) A proposed index for measuring ionospheric scintillation, Planet. Space Sci., **17**, 1069-1073.
- Whitney, H.E., J. Aarons, R.S. Allen and D.R. Seemann (1972) Estimation of the cumulative amplitude probability distribution function of ionospheric scintillations, Radio Sci., **7**, 1095-1104.
- Wong, Y.K., K.C. Yeh and C.H. Liu (1978) Mean arrival time and mean pulse width of signals propagating through an inhomogeneous ionosphere with random irregularities, in Effect of the Ionosphere on Space and Terrestrial Systems, ed., J.M. Goodman, GPO, Washington, D.C.
- Yeh, K.C., H. Soicher and C.H. Liu (1979) Observations of equatorial ionospheric bubbles by the radio propagation method, J. Geophys. Res., **84**, 6589.

IONOSPHERIC TIME DELAY (BENT MODEL)
(NANOSECONDS AT 1.6 GHz)

00 h UT, MARCH 1968

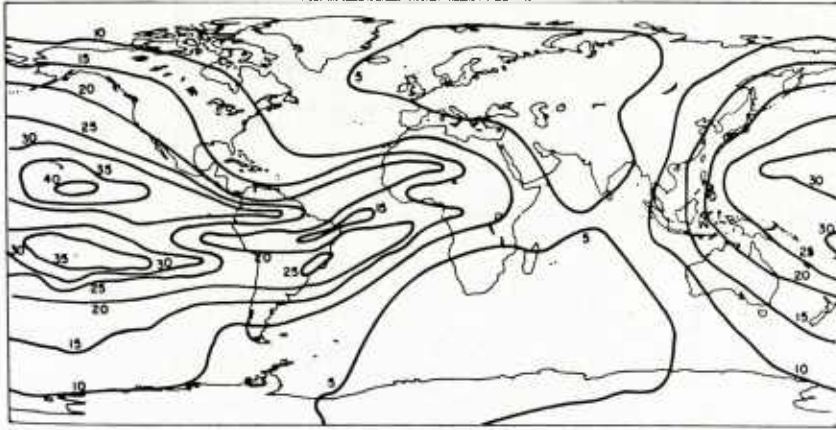


Figure 1. Worldwide average vertical ionospheric time delay at 1.6 GHz for 00 hours U.T., March 1968, an average solar maximum year.

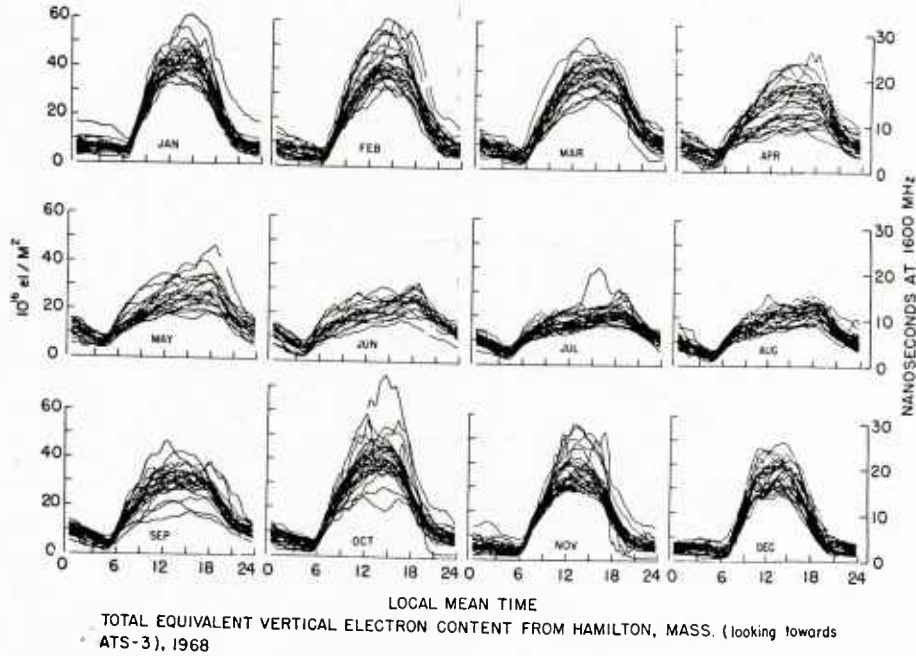


Figure 2. Monthly overplots of equivalent vertical TEC from Hamilton, Massachusetts for the year 1968, a solar maximum year.

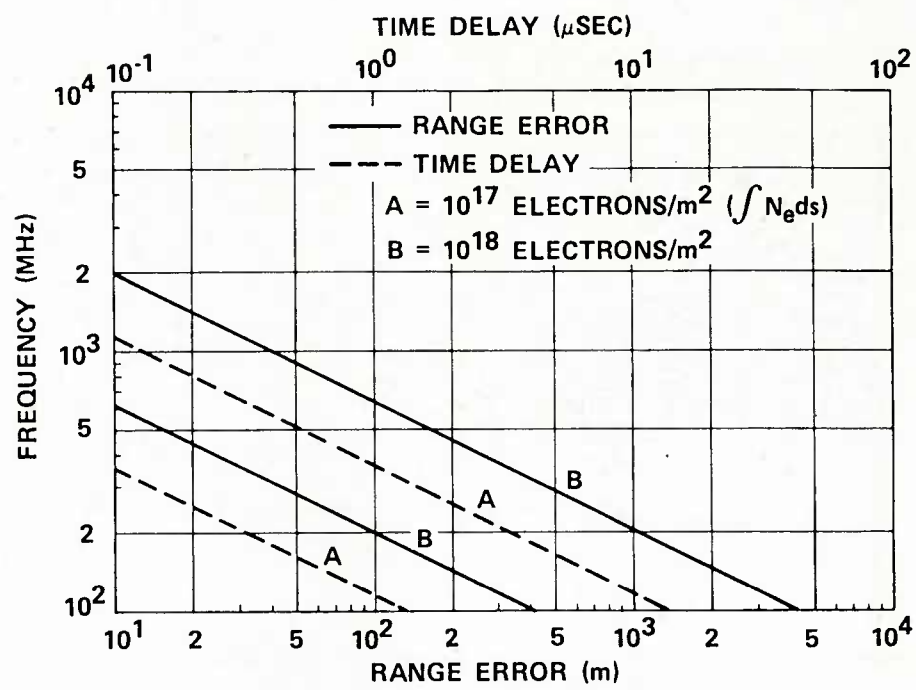


Figure 3. Ionospheric range error and time delay for a one-way path

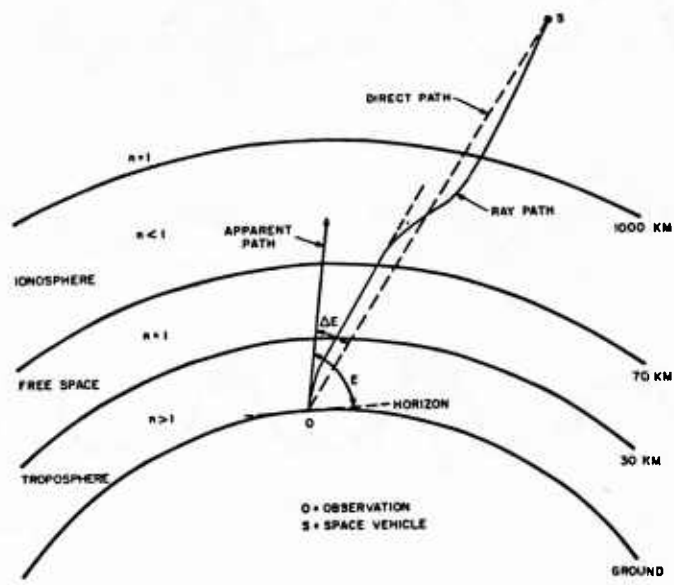


Figure 4a. Radiowave trajectory through the troposphere and ionosphere (after Millman, 1965)

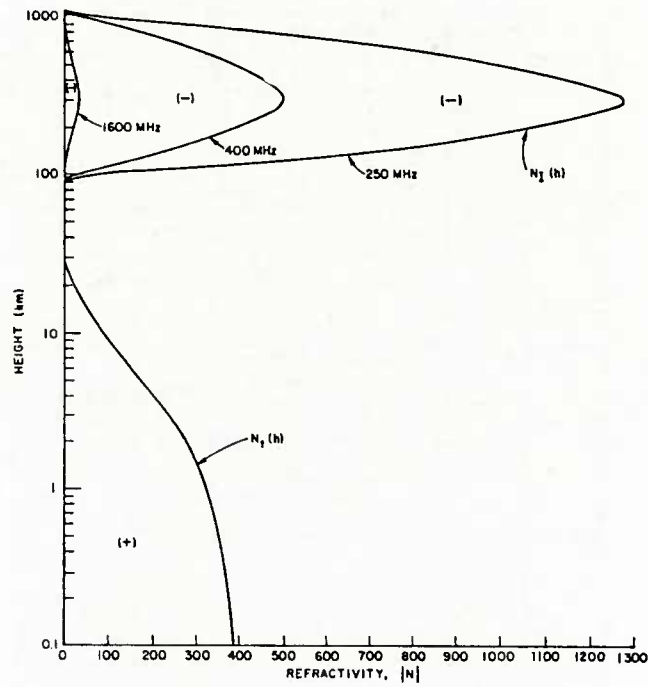


Figure 4b. Radio refractivity versus altitude. Representative ionosphere profiles are shown for 250, 400 and 1600 MHz. The tropospheric refractivity profile is based on data from Bean et al. (1971).

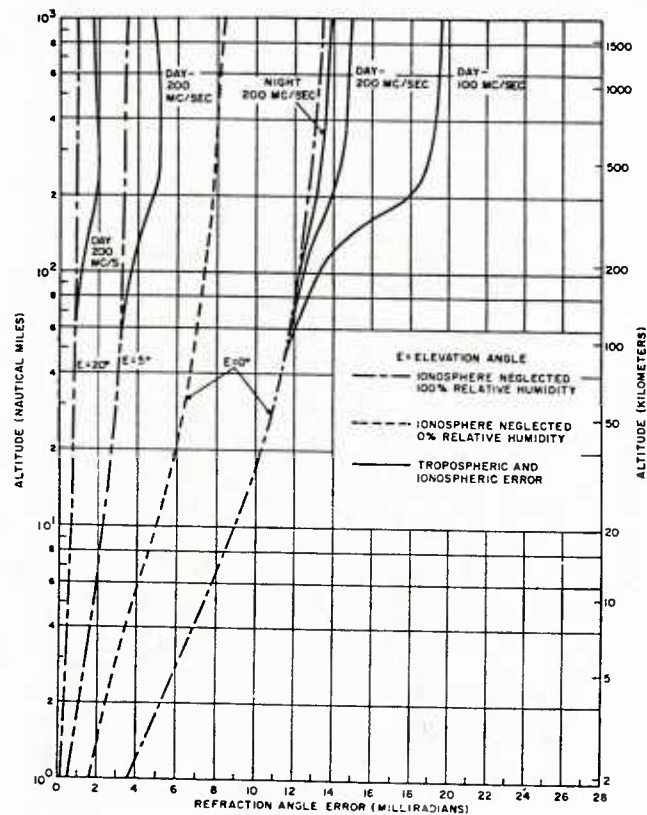


Figure 5. Total refraction error at 100 and 200 MHz as a function of altitude (From Millman, 1966).

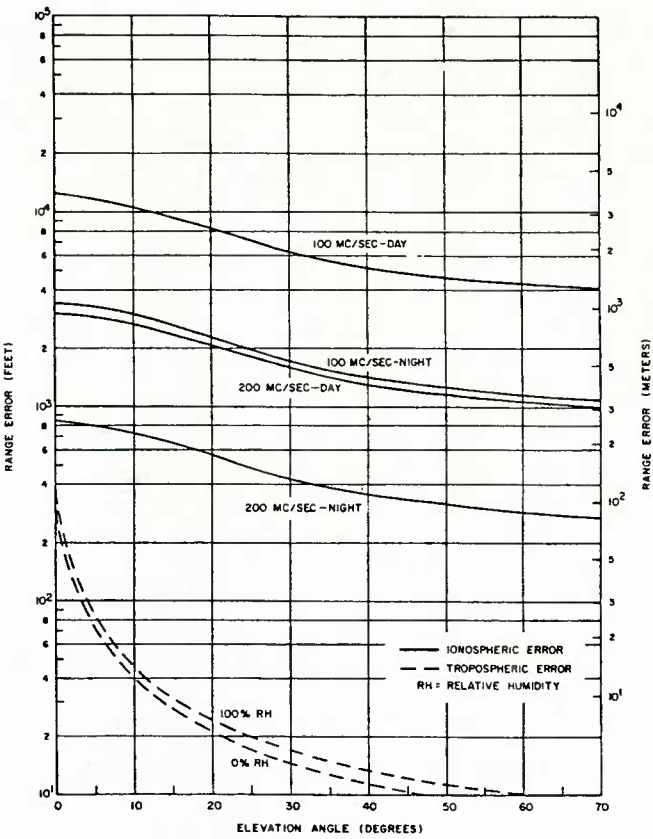


Figure 6. Limiting tropospheric and ionospheric range error as a function of elevation angle. (From Millman, 1965).

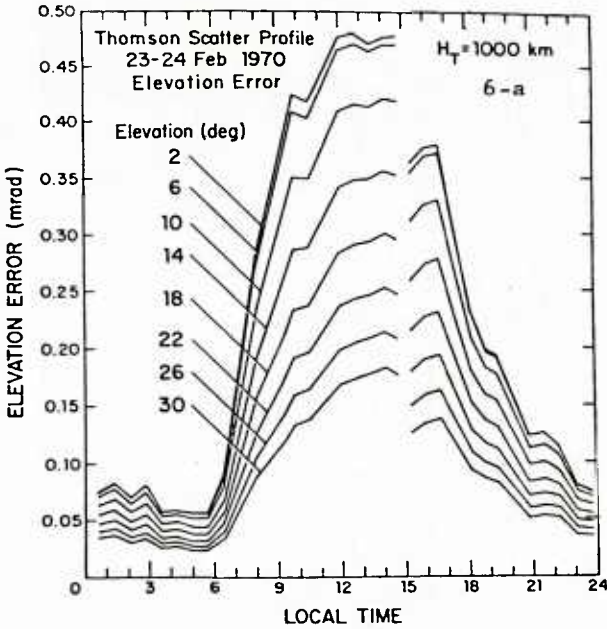


Figure 7. The diurnal variation of the ionospheric component of elevation error at 400 MHz.

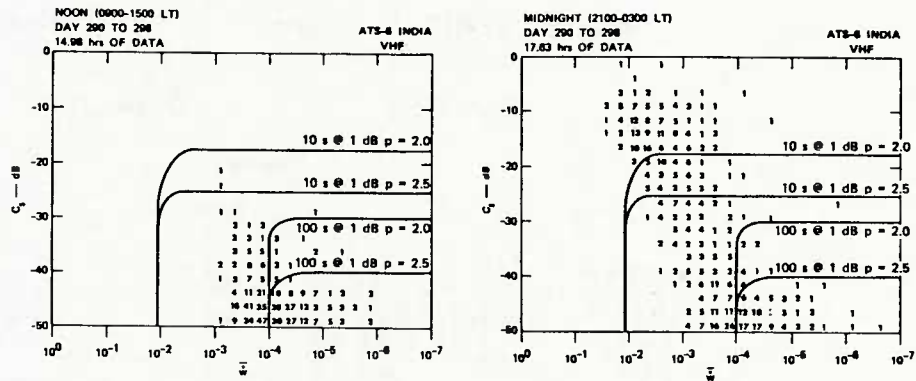


Figure 8. Histograms of C_s (dB) and W for both noon (A) and midnight (B) from a set of S_{ATS-6} differential phase data at 165 MHz obtained at an Indian site. The phase spectrum is assessed to have the form $C_s f^{-p}$ where p is the power law. (After Rino et al., 1978)

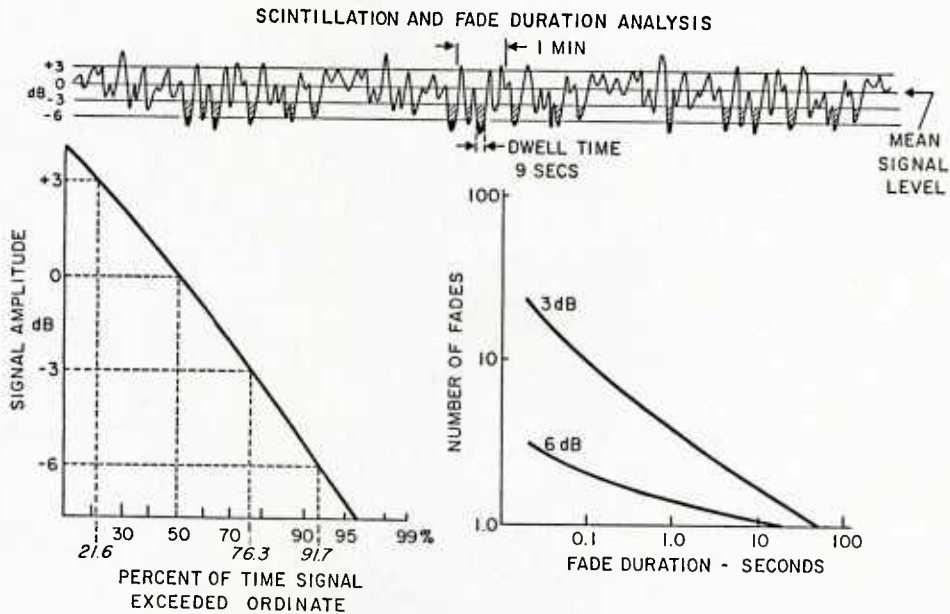


Figure 9. Analysis of ionospheric scintillation for fading characteristics.

ANCON, PERU

LES - 9

249 MHz

 $S_4 = 0.94$

0214 UT

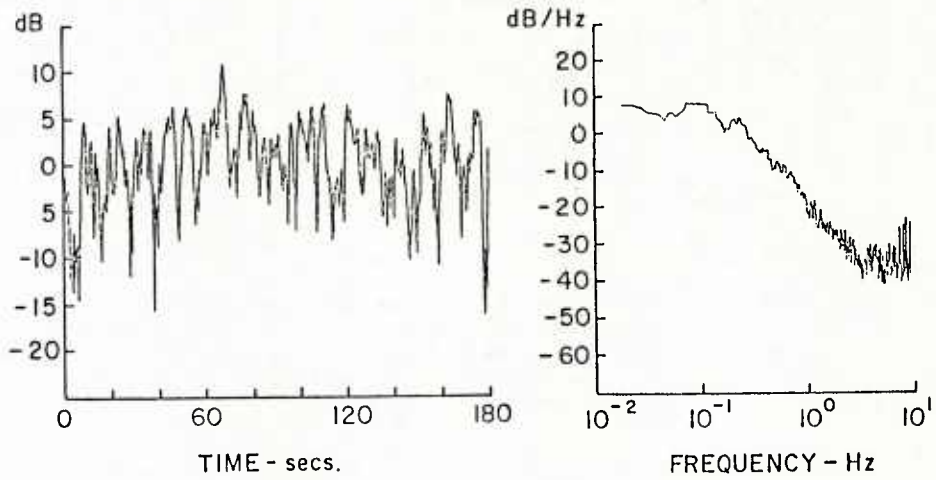


Figure 10. Spectral analysis of equatorial scintillation.

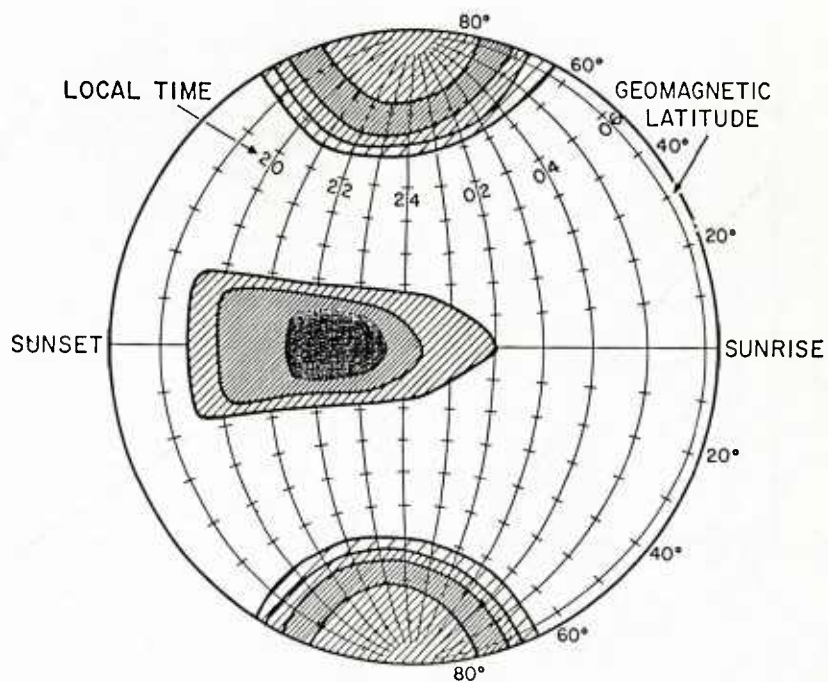


Figure 11. Depth of scintillation fading (proportional to density of crosshatching) for sunset to sunrise period during low and moderate solar activity.

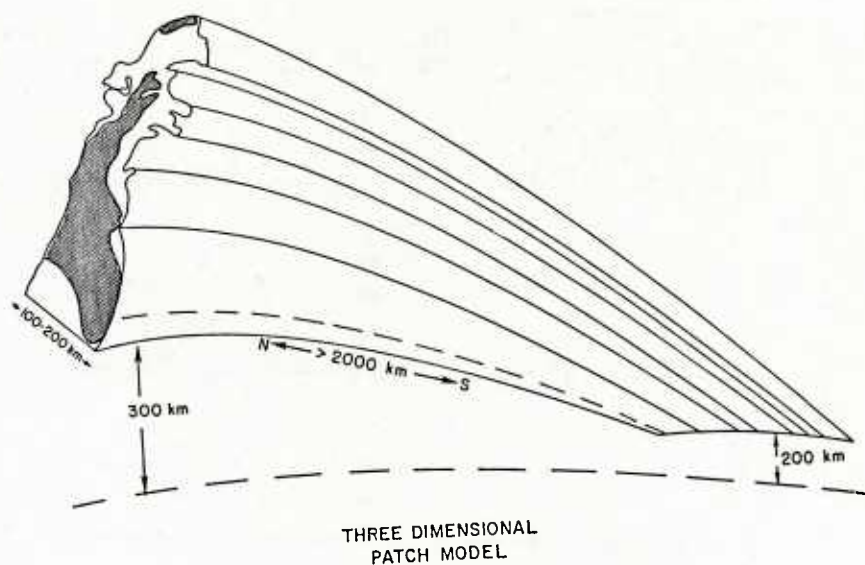


Figure 12. Model of equatorial irregularity patch from the equator to its north or south termination.

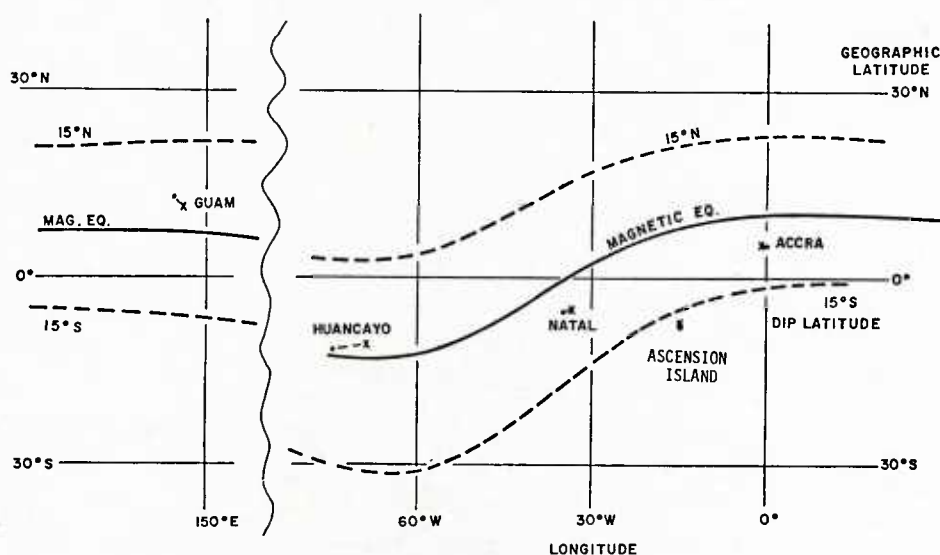


Figure 13. Geographic and geomagnetic positions of observatories taking equatorial data of Figure 14.

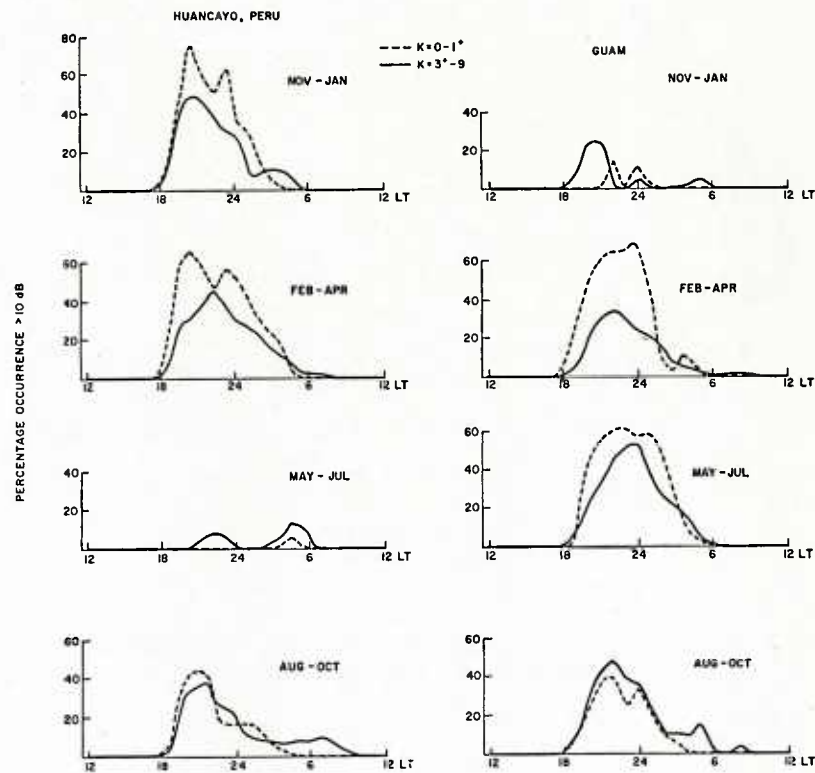


Figure 14. Seasonal patterns of scintillation occurrence for Huancayo, Peru and Guam during a year of moderate solar activity.

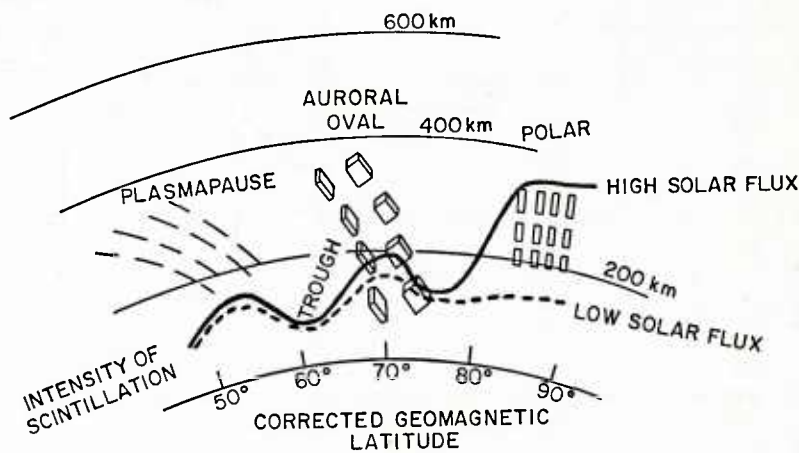


Figure 15. Intensity of scintillation at high latitudes.

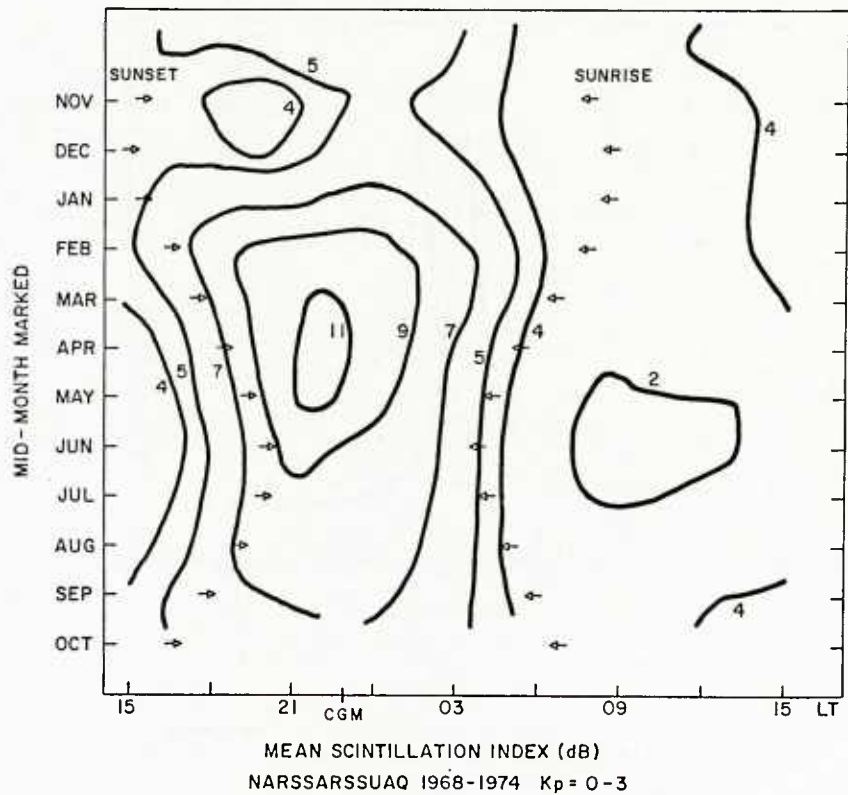


Figure 16. Mean scintillation index (dB) at Narssarssuaq (1968-1974) for low magnetic activity ($K_p = 0-3$).

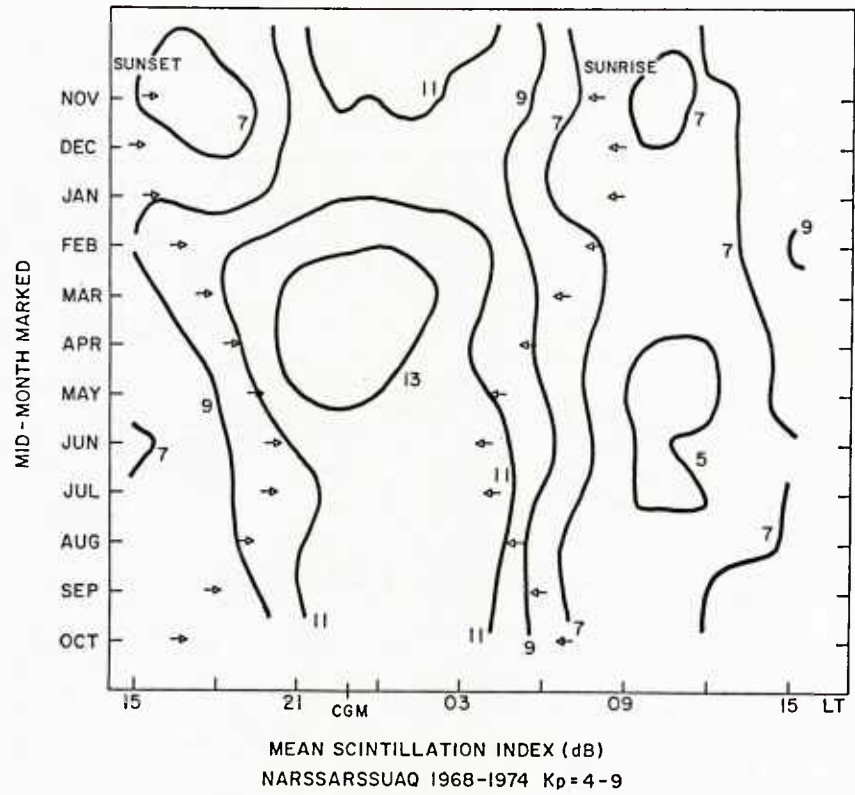


Figure 17. Mean scintillation index (dB) at Narssarssuaq (1968-1974) for high magnetic activity ($K_p = 4-9$).

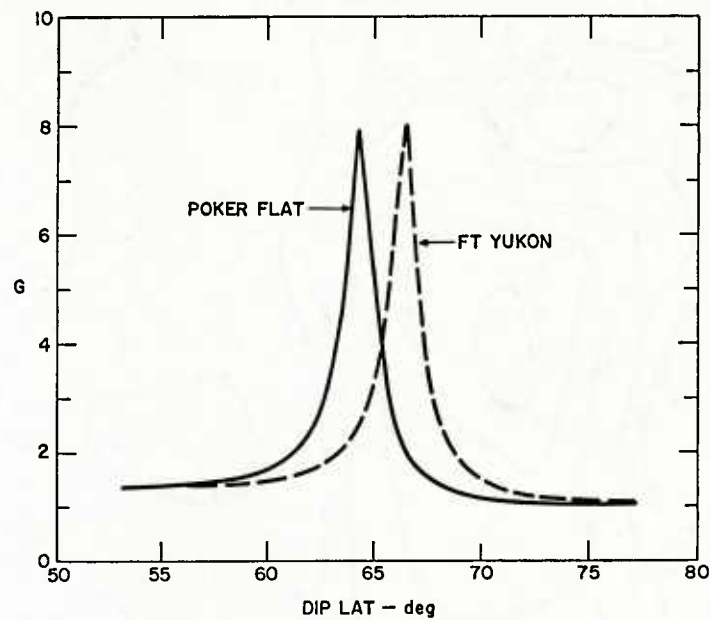


Figure 18. Geometrical enhancement factor for rms phase (8:8:1) in Alaska (Rino and Owen, 1980).

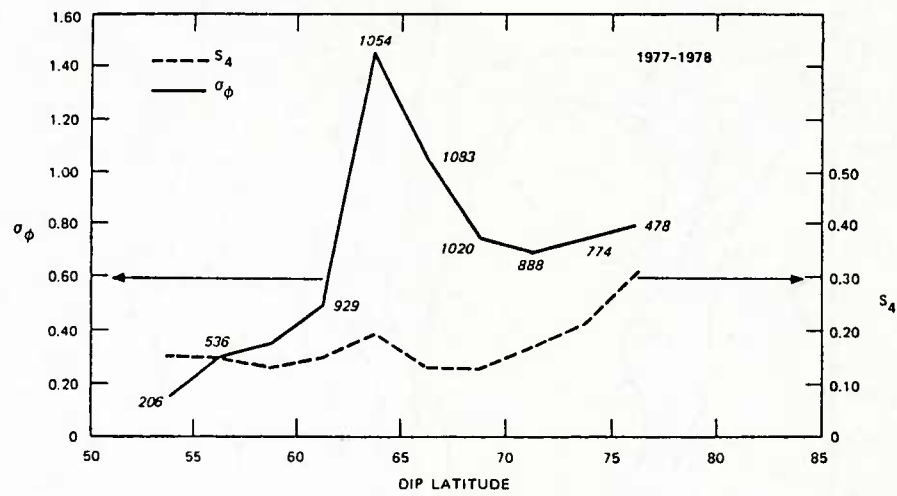


Figure 19. Phase (—) and amplitude (---) scintillation observations in Alaska.

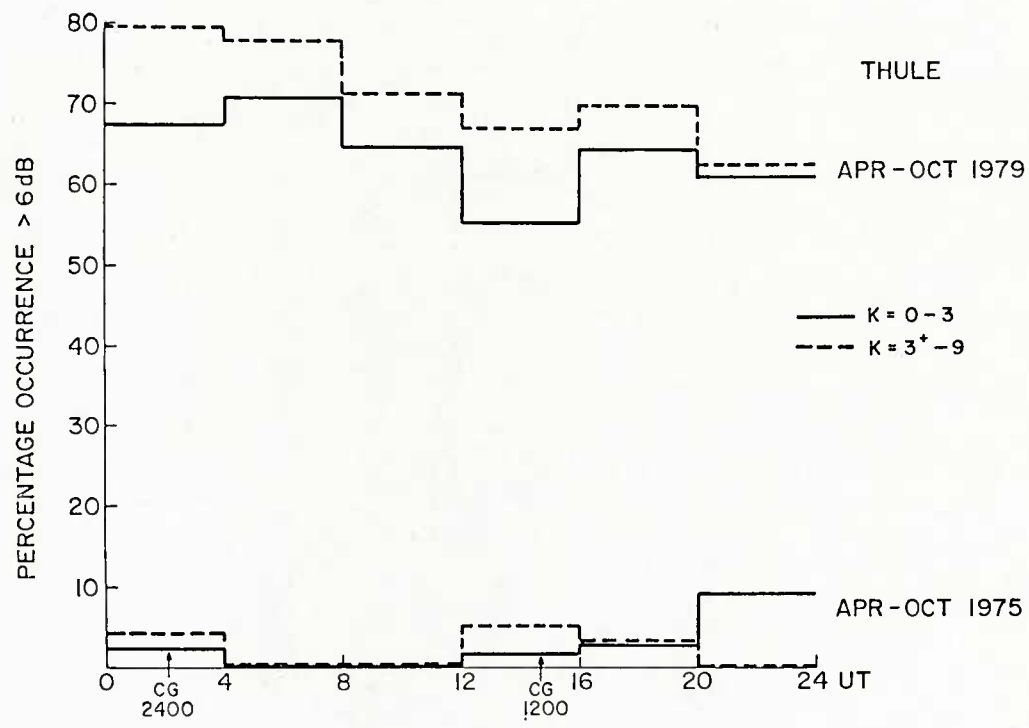


Figure 20. Polar scintillation occurrence during a period of low solar activity (1975) and high solar activity (1979).

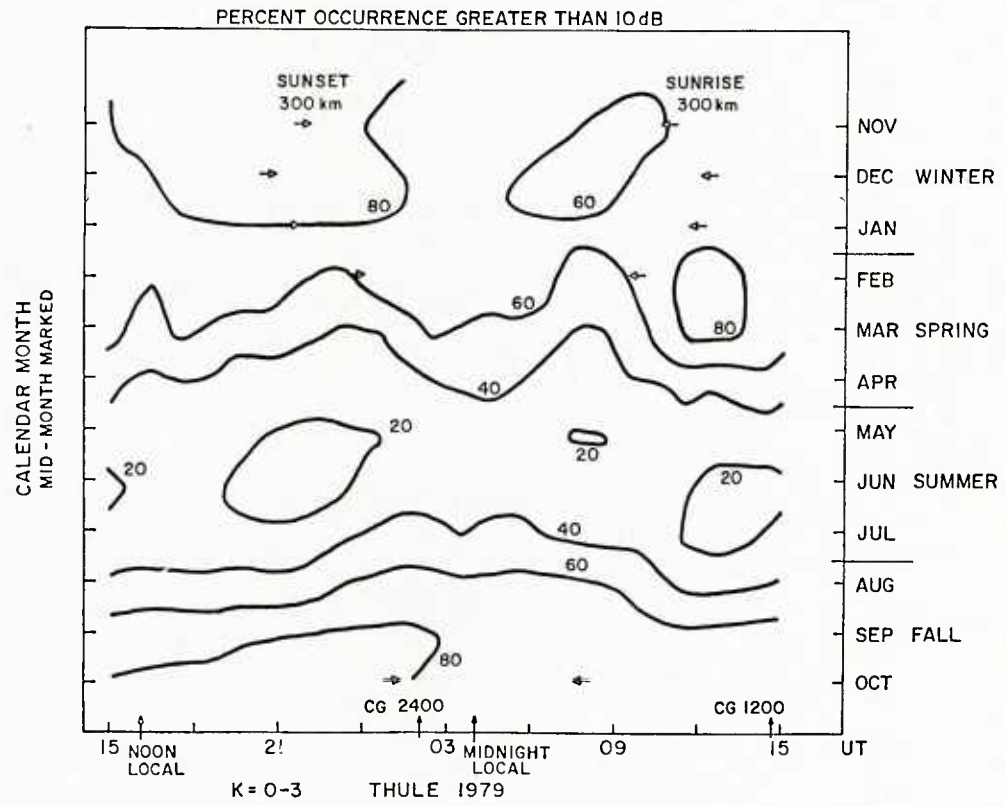


Figure 21. Polar scintillation occurrence patterns for Thule, 1979 with $K_p = 0-3$.

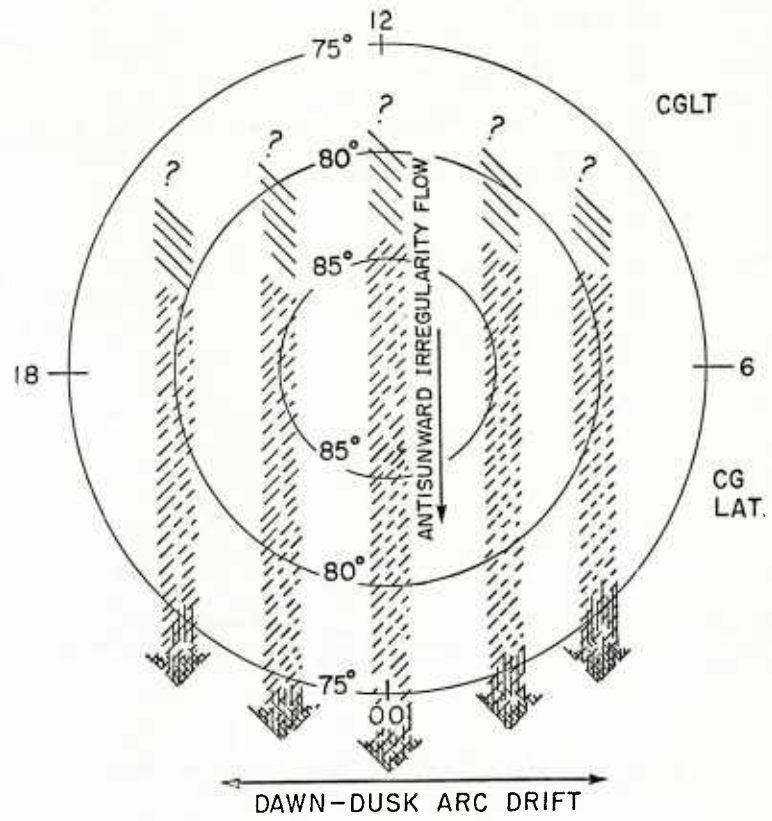


Figure 22. Drift patterns of the polar arcs which produce scintillations.

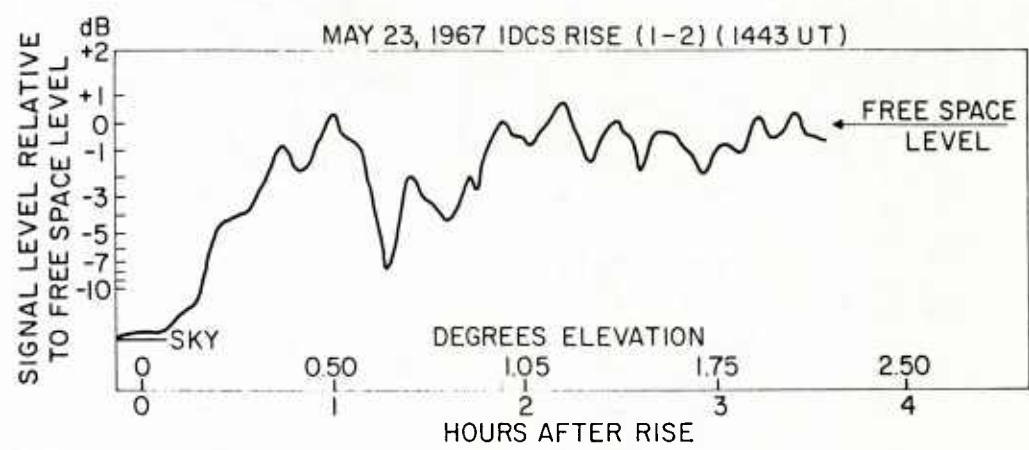


Figure 23. Rise of IDCS synchronous satellite transmitting at 401 MHz. Note long period fluctuations.

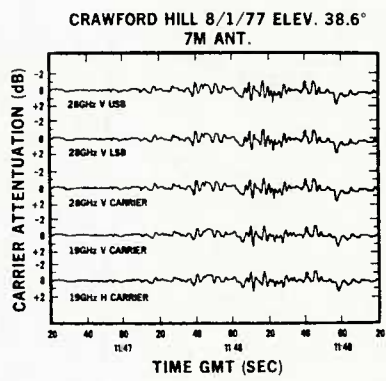


Figure 24a. High angle of elevation scintillation activity. (Cox et al., 1981)

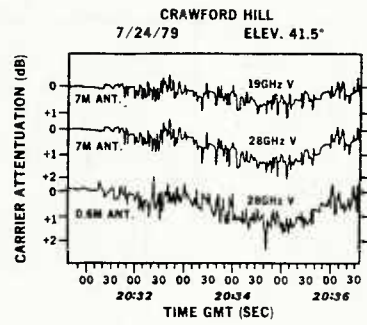


Figure 24b. A wet scintillation event from digital tape records taken using the COMSTAR satellite at 87°W. (Cox et al., 1981)

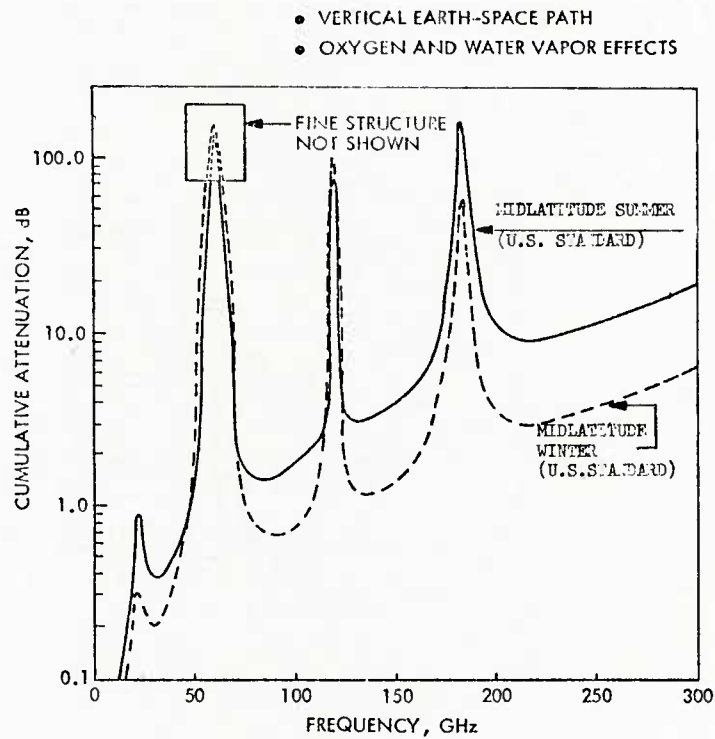


Figure 25a. Seasonal variation of atmospheric attenuation. The curves shown are for a cool, dry mid-latitude winter atmosphere and a warm, moist midlatitude summer atmosphere along a vertical earth to space path.

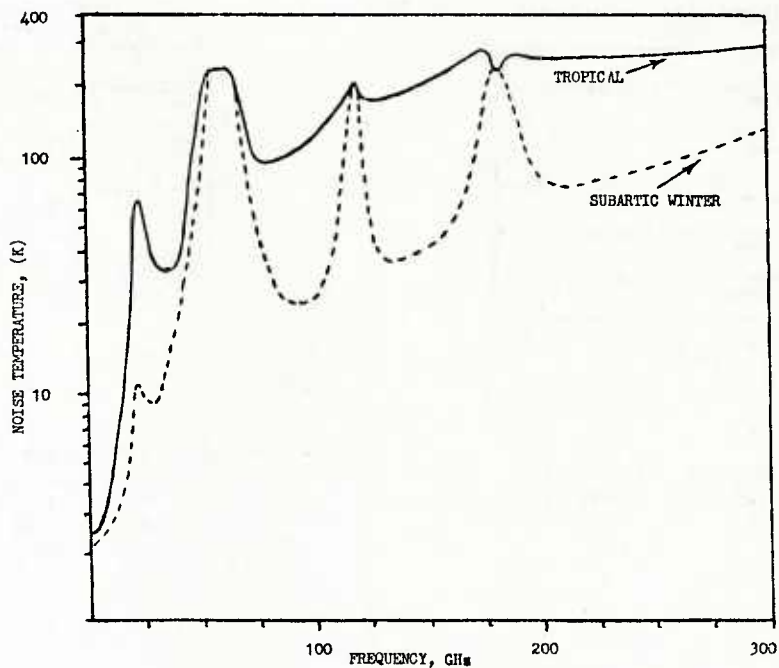


Figure 25b. Atmospheric contribution to noise temperatures for environmental extremes. The two curves give noise temperatures due only to the atmosphere from tropical and sub-arctic atmospheres representing some environmental extreme conditions for a vertical earth to space path.

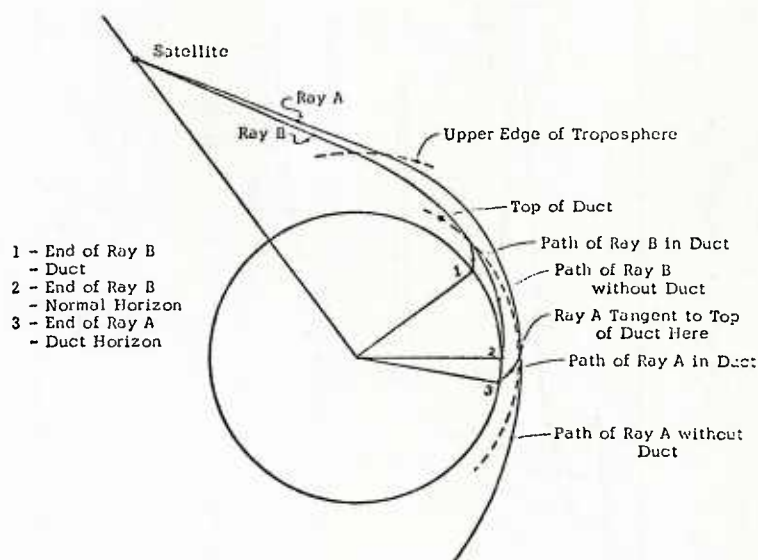


Figure 26. Effect of duct on maximum range.

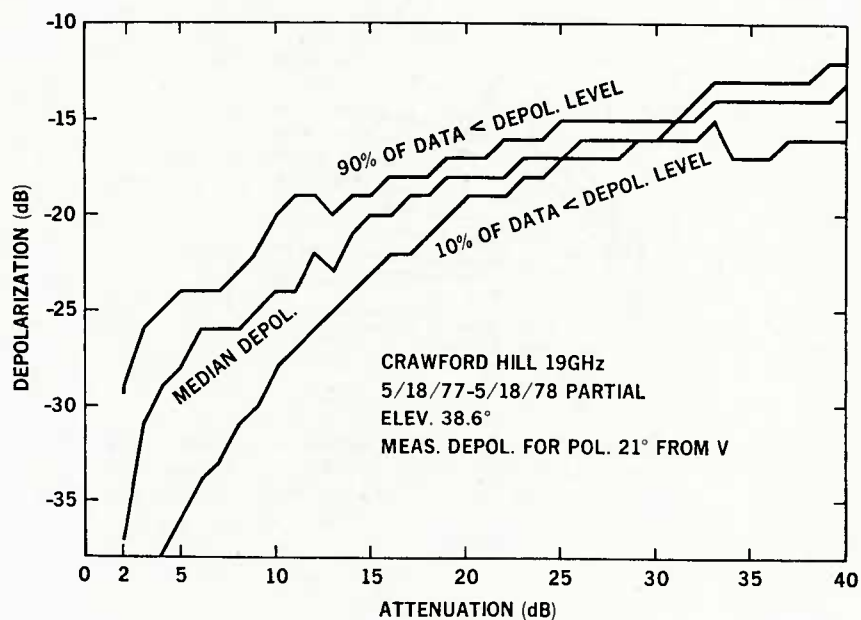


Figure 27. Statistical relationships between copolarized signal attenuation and depolarization at 19 GHz. (Cox et al., 1981).

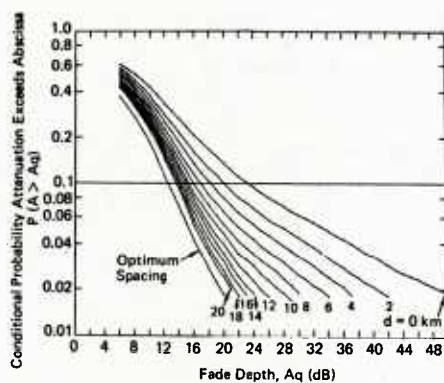


Figure 28. Radar derived conditional probability for Wallops Island, VA, that the attenuations along two paths separated by a distance, d , jointly exceed the abscissa attenuations for $f=100$ GHz and $\theta=45^\circ$. The curve labeled $d=0$ is the single terminal probability (Goldhirsh, 1975).

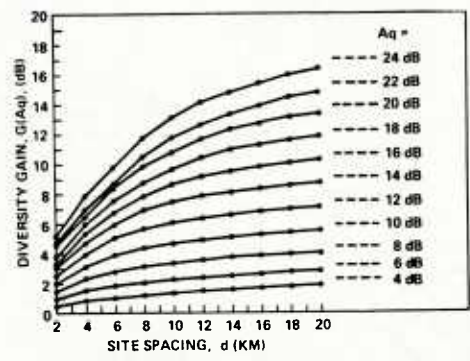


Figure 29. Family of diversity gain curves at 30 GHz. The horizontal dashed lines are the decorrelated case levels at the corresponding single terminal fades (Goldhirsh, 1975).

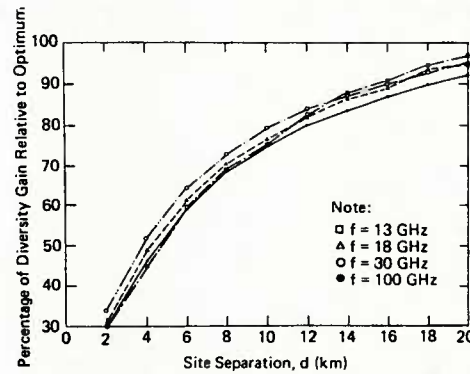


Figure 30. The average percentage of diversity gains relative to the respective decorrelated levels as a function of site separation at the indicated spacings (Goldhirsh, 1975).

LIMITATIONS IN SCATTER PROPAGATION

Ernst Lampert
Siemens Aktiengesellschaft
Hofmannstr. 51
8000 München 70

SUMMARY

A short description of the main scatter propagation mechanisms is presented; troposcatter, meteor burst communication and chaff scatter.

For those propagation modes in particular for troposcatter the important specific limitations are discussed

- link budget and resulting hardware consequences
- Diversity
- mobility
- Information transfer; Intermodulation and intersymbol interference
- frequency range and future extension in frequency range for troposcatter
- compatibility with other services (EMC)

1. INTRODUCTION

Radio waves except ground waves (frequencies up to appr. 10 MHz) propagate in streight direction with the consequence that a communications transmitter and the associate receiver have to be in line of sight (L.O.S.) of each other. This condition seems to be invalid for HF skywave propagation, however there the radiowave is reflected by the ionospheric mirror, hence the wave also propagates along a streight line.

As most of our communication links are set up between terminals on the earth surface (or no more than 1000 m above) the L.O.S. condition is a severe restriction. When not using space borne relay stations, i.e. satellites, electromagnetic (E.M.) wave scattering is the only way to overcome the L.O.S. restriction. Irregularities in the composition of the atmosphere with relevance to E.M. wave parameters produce an energy transfer offset from the streight L.O.S. propagation direction. (This paper will not discuss specular and diffuse reflections from the ground.) Fig. 1 gives an overview over the different scatter machanisms and their application.

In the earth atmosphere such irregularities have been observed in:

- the Troposphere (lowest atmospheric layer up to 10000 m).
Here turbulence is always created by wind shear - wind velocity is smaller at the close proximity to the ground compared to regions further up - and the thermal temperature gradient with height. The changing weather, in particular cold fronts and thunderstorms, produce turbulence. Along with this turbulence irregularities in the dielectric constant are produced and from these areas we get scattered waves. The associated propagation mode is called troposcatter and is used to bridge distances mainly between 100 km and 300 km (up to 700 km) and can be applied with frequencies in the UHF and SHF bands.

From the higher atmospheric layers no scattering has been observed apart from the ionosphere. This layer (composed of several sublayers) is mainly used as a mirror for RF-signals (HF up to 30 MHz). However this mirror becomes transparent for higher frequencies than the MUF (maximum usable frequency) which may vary according to distance, time of day and year between 4 MHz and 34 MHz. However scatter- ing effects have been observed above these frequencies originating from two different mechanisms.

- Ionoscatter is a propagation mode produced by variations in the electron contents of D and lower E-layer. Apart from this effect a very bursty signal with higher power level has been observed which originates from signals scattered at the ionized trails of meteors when passing the ionosphere. This propagation mode is called meteor burst scatter. Of these two modes only the latter is of greater relevance to the communications engineer.
- Man made scattering phenomena might also be exploited in future tactical communications. Chaff, i.e. a multitude of thin conductive foils can be distributed in certain areas of the atmosphere. When operating with the appropriate frequency the dipoles resonate and scatter incoming radio waves. However chaff clouds will fade away within hours. - In the ionosphere irregularities can be produced by heating up certain areas of this layer by emitting high power radio waves with approximately the plasma frequency in vertical direction from the ground. The produced irregularities however are closely related to the geomagnetic field direction in the heated area and scattering will only be effective in directions perpendicular to the magnetic field direction.

In the following chapters the exploitation of these mechanisms will be discussed, whereby one always has to be aware that also a mix in propagation modes can occur, i.e. wave ducting and troposcatter or troposcatter and scatter from aircrafts, meteor burst scatter and sporadic E-layer reflection.

2. GENERAL DESCRIPTION OF THE SCATTERING PROCESS

2.1 Average Path Loss

In scatter propagation the received signal is usually the sum of a multitude of wave components originating from the different areas. It is convenient to think of distinct scattering particles, f.i. blobs of differing dielectric constant although some discussions have to be based on a continuum of scatterers. The wave components are to some extent independent from each other and therefore an incoherent summation of the many component waves takes place at the receiver. As the scatterers are moving, the relative phase of the component waves will, too. The received signal therefore fluctuates and should be described by its characteristic fading parameters: mean power level and statistical moments or actual amplitude distribution.

As it is shown in Fig. 2a, scattered signals are produced at all points in the medium which are illuminated by the incident wave and where inhomogeneities exist. As shown in Fig. 2b we now concentrate on that volume area which is mutually visible by both transmitter and receiver. This so-called common volume or scatter volume is illuminated by the primary flux Φ ,

$$(1) \quad \Phi = \frac{P_1 \cdot G_1}{4\pi \cdot R_1^2}$$

R_1 = distance between transmitter and common volume
 P_1 = transmitter power
 G_1 = transmitter antenna gain

The scattering characteristic of the volume is determined by the average scatter cross section $\sigma(\theta)$ which is dependent on the scatter angle θ . The scatter angle θ is the angle between the direction of the incident ray and that to the receiver. At that location, the power picked up by the antenna has the value

$$(2) \quad P_2 = \frac{\Phi \cdot \sigma(\theta)}{4\pi \cdot R_2^2} \cdot A_2$$

P_2 = received power
 A_2 = effective area of receiver antenna
 G_2 = antenna gain of receiver
 R_2 = distance common volume to receiver

$$(3) \quad P_2 = \frac{G_1 \cdot G_2}{4\pi} \cdot \frac{\sigma(\theta)}{(R_1 \cdot R_2)^2} \cdot \left(\frac{\lambda}{4\pi}\right)^2$$

considering the geometry of Fig. 2b the approximation $R_1 \approx R_2 \approx D/2$ (D = distance transmitter receiver) can be used, so we get

$$(4) \quad \frac{P_2}{P_1} = \frac{G_1 \cdot G_2}{4\pi} \cdot \frac{\sigma(\theta)}{D^4} \cdot \left(\frac{\lambda}{\pi}\right)^2$$

Compared to free space propagation, (4) shows that P_2 at least decreases with the fourth power of the distance instead of the square. Furthermore as $\sigma(\theta)^2$ is decreasing with the scatter angle θ and θ increases with distance, P_2 will decrease at still higher exponent on distance.

The first attempt to figure out the dependence of σ on θ was made by Booker and Gordon [2], who described the irregular composition of the dielectric constant by its spacial correlation function assuming that it is only dependent on the distance between locations but not on their absolute loci. Using an exponentially decaying correlation function they found σ to be dependent on the following parameters (valid only for angles $\theta < 20^\circ$)

$$(5) \quad \sigma(\theta) \approx \frac{(\Delta\epsilon)^2 \cdot \left(\frac{2\pi l}{\lambda}\right)^2}{\lambda \left[1 + \left(\frac{4\pi l}{\lambda} \cdot \sin \frac{\theta}{2}\right)^2\right]^2}$$

$\Delta\epsilon$ = average deviation of relative dielectric constant from its mean (RMS value)
 l = mean diameter of inhomogeneities

If $l \ll \lambda$ we get Rayleigh scattering which produces an almost isotropic radiation (σ is then independent from θ). The important case however is forward scatter with $l \gg \lambda$; for $\theta \neq 0$ we get

$$(6) \quad \sigma \approx \frac{(\Delta\epsilon)^2}{2\pi l} \cdot \frac{1}{\theta^4} = \frac{S_p}{\theta^4}$$

S_p = scattering efficiency

So all scatter links are very sensitive to the actual scatter angle θ which has to be made as small as possible to achieve high values of σ . This general theory cannot be used to set up an actual link budget as several effects have not been addressed or ignored, f.i. $\Delta\epsilon$ cannot be measured; l is usually characterized by the spectrum of its probability distribution and also the dependence of these parameters with respect to height above ground has been ignored. The actually used methods are quite distinct for the different scatter phenomena and will be discussed separately.

2.2 Short Term Amplitude Statistics of the Received Signal

As the received signal adds up from a multitude of independent scattering events it is legitimate to assume and validated by measurements that in case of transmitting a sine wave of fixed amplitude A and frequency ω the received signal will be a narrow band complex gaussian process with a midband frequency ω . The other parameters characterize this signal are its average power P_2 and its bandwidth B_c .

The amplitude distribution $p(A)$ of such a signal is Rayleigh:

$$(7) \quad p(A) = \frac{2A}{\bar{A}^2} \cdot \exp\left(-\frac{A^2}{\bar{A}^2}\right) \quad \begin{array}{l} A = \text{amplitude} \\ \bar{A} = \text{average amplitude} \end{array}$$

While the phase distribution is constant over 0 to 2π . The power density distribution $p(P_2)$ is therefore exponential

$$(8) \quad p(P_2) = \frac{1}{\bar{P}_2} \cdot \exp\left(-\frac{P_2}{\bar{P}_2}\right) \quad \bar{P}_2 = \text{average received power}$$

So there is a considerable probability that the instantly received signal power is very low and might be below system sensitivity. To overcome that drawback diversity methods are used in system design, there are combining methods well covered by Brennan [3] with respect to analogue signal transmission.

Independent from the actual equipment used, the amplitude probability density distribution for small signal amplitudes is modified from

$$(7a) \quad p(A) \propto \frac{A}{\bar{A}^2} \quad \text{for the single Rayleigh fading channel into}$$

$$(9) \quad p(A) \propto \left(\frac{A}{\bar{A}^2}\right)^N$$

whereby N is the order of diversity used.

All diversity systems used to combat statistical fading rely on the fact that the signals used for combining are statistically independent. Real systems require a correlation coefficient between channels

$\rho < 0.6$ in order for the signals to be treated like independent signals. Diversity combining of analogue signals further more requires that the signal RF-bandwidth is smaller than the correlation bandwidth of the channel in order to avoid excessive degradations in the combining procedure.

The actual implementation of the diversity systems (how independent channels are established) will be discussed along with the special scatter mode used.

3. TROPOSCATTER

Troposcatter has now become an established technique in transmitting analogue multichannel voice and TV signals. One of the largest systems operating in Europe is the NATO-ACE-HIGH System, linking together the North of Norway and Turkey, which shows its importance in military communication [4].

3.1 Link Budget

Methods to calculate the average received power have always to rely on empirical data based on actual measurements. The most widely used method has been described in CCIR Rept 238-3 [5] and is based on the data gathered in NBS-Report 101 [6] and has proven to be useful in the past. Nevertheless also this method can still yield values which are up to 10 dB in error.

The loss L (50) not exceeded in 50 % of time may be calculated according to the following equation:

$$(10) \quad L(50)/dB = 30 \cdot \log(f/MHz) - 20 \cdot \log(d/km) + F(\Theta \cdot d / rad \cdot km) - G_p/dB - V(d_e/km)/dB$$

Where by $F(\Theta \cdot d)$ is a function of the product of scatter angle Θ and the actual distance d between transmitter and receiver and is shown in Fig. 3, G_p is the so-called antenna-to-medium coupling loss, which will be discussed separately. The factor $V(d_e)$ is a correction for the various climates.

The parameter $V(d_e)$ has been measured in various locations and it has turned out that it is necessary to distinguish at least between 8 climates in order to describe the troposcatter parameters reasonably correct.

- 1 equatorial (data from Congo and Ivory Coast)
- 2 continental subtropical (Sudan)
- 3 maritime subtropical (West Coast of Africa)
- 4 desert (Sahara)
- 5 Mediterranean
- 6 continental temperate (France, Germany, US)
- 7a maritime temperate over land (UK)
- 7b maritime temperate over sea (UK)
- 8 polar

$V(d_e)$ not only accounts for the different turbulence conditions associated with the different types of climate but also for the frequency of mixed propagation mode conditions.

It has to be noted that $V(d_e)$ is plotted against the so-called effective distance which is calculated from the actual distance d by subtracting the distances d of transmitter and receiver to the actual geometric horizon and in addition a distance d_{se} to account for diffraction. A factor of 130 km is added for convenience in plotting the data

$$(11) \quad d_e = 130 km + d - (d_L + d_{se}) \quad \text{with}$$

$$(11a) \quad d_L = \left(3 \cdot \sqrt{\frac{2h_{te}}{m}} + 3 \sqrt{\frac{2h_{re}}{m}} \right) km$$

d_e = effective distance

h_{te} = transmitter antenna height above average smooth earth

h_{re} = receiver antenna height above average smooth earth

wehrebey equ (11a) is only valid above smooth earth. In general it should be extracted from an actual path profile. $V(d_e)$ varies between +7 dB and -8 dB.

As a link availability of 50 % is not sufficient, but rather values of 95 % to 99,9 % the loss values for these percentages of time have to be calculated using $L(50)$

$$(12) \quad L(q) = L(50) - Y(q)$$

q is that percentage of time during which the loss $L(q)$ is smaller than the calculated value, which implies for $q > 50$ % that $Y(q)$ is negative, usually values between 25 and 35 dB have to be added to $L(50)$ for calculation of path loss when high link availability is required. The mean transmission loss then exceeds free space loss by 55 dB to 75 dB for distances between 100 km and 300 km, see Fig. 1.

The link budget however cannot be established only by knowing medium transmission losses. Because of the fading nature of the received signal a fading margin has to be added to the medium transmission loss, which can be calculated from the probability density formulas under the condition that the outage probability $1-q$ is below a certain value (in general q between 90 % and 99,99 %). This reasoning would require a fading margin of the order of another 30 dB if only a single transmission path would be used. In order to get physically realizable equipment (power amplifiers and antenna dishes) diversity has to be used to reduce the fading margin to values below 10 dB at the expense of more complex equipment and usually at least two antennas at each site.

To illustrate the situation the characteristic values for an experimental troposcatter link in southern Germany have been calculated:

distance between terminals A, B	115 km
antenna elevation A	0 °
antenna elevation B	0,6 °
min. scatter angle	22 mrad = 1,3 °
transmission frequency (C-band)	4,5 GHz
effective distance d_e	203 km
correction factor for central europa	4 dB
medium transmission loss $L(50)$	213 dB
free space loss for 115 km	146,7 dB

Margin with respect to higher availability

availability	90 %	95 %	99 %	99,9 %
Y/dB	10	14	18	25

additional fading margin

availability	90 %	95 %	99 %	99,9 %
single channel	8,2	11,4	18,4	28,4
Quadruple space diversity	- 5	- 3	- 1	+ 2

(it has to be borne in mind, that the diversity figures refer to maximum ratio combining and as space diversity is used an other 6 dB of antenna gain is available when using 4 dishes.)

When using a 3 m dish, 250 W transmitter power along with a 5 dB noise figure receiver front end, the following value of signal to noise density ratio is available in a single channel, when short and long term variations are considered

time %	90	95	99	99,9
C/No/dB Hz	62	55	44	28

These data illustrate that in particular for high values of link availability diversity is mandatory, especially when it is taken into account that this prediction may be uncertain by about 10 dB.

3.2 Antenna-to-medium Coupling Loss

The example of a link budget shows that it is necessary to use high power amplifiers and big antennas in order to achieve receive power levels which are high enough to transmit multichannel voice signals. It has been found however that an increase in antenna size only results in a very small increase in receiver power level when the antennas are already large. Because of the antenna-to-medium coupling loss increase in antenna size will not result in the same increase in receiver power compared to L.O.S. [77].

As equ. (10) is essentially based on measurements with low gain antennas the receiving antenna can collect the energy of all the wave components scattered from the various irregularities at different location. When changing over to high gain antennas the system loses this capability (the effect is naturally a

combined one of receiver and transmitter antennas). Therefore the coupling loss G_p in Equ. (10) is tabulated in CCIR Rept. 238-3 [5] with respect to the product of the antenna gain values of both transmitter and receiver antennas.

The loss becomes noticeable for gain values of the individual antenna beyond 30 dB and compensates almost all additional gain when the value approaches 50 dB. Antennas with larger L.O.S. gain values are only of interest, as with them the correlation bandwidth can be increased while the fading frequency decreases. The complete mechanism of antenna-to-medium coupling loss is not fully understood yet, in particular its dependence on distance.

3.3 Correlation Bandwidth B_c and Fading Frequency f_s

When simultaneous by transmitting more than one frequency over a troposcatter link they do not fade coherently when their frequency separation becomes appreciable. A measure of the bandwidth within fading can be considered to occur coherently for all frequency components is the correlation bandwidth B_c . Its approximate value is calculated by using the maximum delay time difference between the paths of all wave components contributing essentially to the received signal. Usually the 3 dB-beamwidth of the antennas is used, see Fig. 2b:

(13)

$$B_c = \frac{2 \cdot c \cdot r_E}{\varphi \cdot D^2} = \frac{22 \text{ MHz}}{\frac{\varphi}{\text{degree}} \cdot \left(\frac{D}{\text{km}}\right)^2}$$

φ Antenna beamwidth

c Velocity of light

r_E equivalent earth radius

D link length

Usually the correlation bandwidth is wider than the value given by (13) because the scatter efficiency at the higher end of the common volume is smaller than at the lower edge. This effect becomes particularly noticeable for antennas with beamwidth ($\varphi > 1,5^\circ$).

The maximum fading frequency f_s can be calculated using similar thoughts [8] and leads to the following relation (which is only valid for small antenna elevation angles):

(14)

$$\frac{f_s}{\text{Hz}} = \frac{2\varphi/\text{rad}}{300} \cdot \frac{f}{\text{MHz}} \cdot \frac{v}{\text{m/s}}$$

f RF frequency

v average vertical velocity of turbulence

The fading velocity increases with RF frequency, imposing greater dynamic problems on the equipment.

Actual measurements however show that the highest fading frequencies associated with very deep fades occur when aircrafts fly through the common volume in this case fading frequencies up to 50 Hz along with 30 dB fades can be measured, especially in tactical scenarios this effect may not be neglected.

3.4 Diversity

Diversity paths can be established either by using independent receiver locations (space diversity), which can easily be obtained when placing the antennas side by side or by using transmissions of the same information on different frequencies usually at least 50 MHz apart (minimum about 5 times B_c). This frequency diversity scheme however needs two transmitter at each site for establishing a duplex link and a frequency assignment for 4 different values, spaced in a way that no receiver overload occurs from both transmitters at the own location.

So space and frequency diversity need bulky equipment. The amount of antennas can be reduced when using orthogonal polarizations for transmission at each site, Fig. 4, as the cross-polarization attenuation of the medium, although fluctuating, is usually above 20 dB. With only two antennas, one transmitter feeding both, and a single frequency for each direction, four diversity paths can be set up. The fading on these paths however is only independent when the two crossing paths, Fig. 4, do not use the same common volume. This restriction is violated when the link profile shows almost plain earth conditions and the antenna spacing is identical on both ends of the link. The remedies have been discussed in detail by R. Larsen [9].

A further method to reduce the amount of equipment is the application of angle diversity. Along with the discussion of the antenna-to-medium coupling loss it has been pointed out that energy reaches the receiving station from different directions. Using sophisticated feed systems for the antenna more than one beam in elevation can be formed. This diversity method is less effective than space or frequency diversity because of the higher loss in the elevated beams as those paths cannot use the smallest possible scatter angle and the difference in elevation has to be of the order of the beamwidth in order to provide a sufficient degree of decorrelation on both paths. This limits the application of angle diversity to systems with high directivity (beamwidth $< 0,7^\circ$).

3.5 Intermodulation

As the troposcatter channel shows a high degree of delay dispersion the transmitted signal will be distorted. Because of the fading characteristics, only constant envelope modulation methods are used. Analogue multi-channel voice transmission therefore uses FM-FDM with a modulation index below 2, the maximum number of channels used varies between 60 and 120. In small systems (low power, small antenna) the number is limited because of the receiver sensitivity. In large systems however because of the varying group delay distortion intermodulation limits the channel performance. There is no simple way of calculation of that noise. Usually the shaded area in Fig. 2b is divided into 2 to 3 paths and the possible intermodulation is calculated using conventional methods and assuming fixed signal amplitude in each path. For a 60 channel link the signal-to-intermodulation ratio can become as small as 48 dB (path length 400 km).

With analogue signal transmission care has to be taken not to approach the correlation bandwidth not only because of intermodulation but also because of the diversity combiner as that system can only weight the individual signals by fixed, frequency independent parameters.

3.6 Digital Signal Transmission

When transmitting digital signals over a troposcatter channel common means of characterizing such a link f.i. by bit error rate become meaningless. Usually only errors occur when there is a deep fading, for signal levels more than 4 to 5 dB above this threshold level no errors will occur. As the errors occur in bursts the channel has to be characterized by its outage rate with respect to a given error rate threshold, see Osterholz [10].

The channel correlation bandwidth and the group delay distortion however not necessarily impose the same stringent limit on the signal bandwidth (data rate) as in analogue systems. Because of the exact knowledge of the transmitted signal - having received it correctly -, distortion, in particular intersymbol interference can be compensated to a certain degree. When using decision feedback systems [11], the limit of an ineducible error rate associated with normal equalizer systems [12] will not necessarily exist. Digital Data Transmission via troposcatter is still not a standard procedure and presently available candidate systems are still under evaluation [13]. Long term planning of NATO assumes to upgrade its systems to data transmission with rates up to 8 Mbit/s, which will be about the upper limit attainable.

3.7 Frequency Band Selection

Presently, operational systems use frequency region around 900 MHz, 2 GHz and 4.4 to 5 GHz, also experimental systems have been built using 8 GHz. Planning data rely on measurements performed below 10 GHz, so prediction for frequencies above 10 GHz is very uncertain.

Equ. (10) shows that the pathloss grows with the third power of frequency. When maintaining fixed antenna areas at both terminals, enhancement of the received signal should result when rising the frequency. This gain however is offset by antenna-to-medium coupling loss and the additional difficulties in transmitting the same amount of power out of the antenna at a higher frequency. Higher frequencies are only favourable when cold weather fronts cross the common volume, the decrease in power level, because of the increase in the lower scale of turbulence, is smaller at higher frequencies.

Electromagnetic Compatibility (EMC) problems request troposcatter systems to leave the 900 MHz. As the 2 GHz and 4.5 to 5 GHz bands are already very crowded (at least in Europe) it becomes difficult to establish new links in this band. In particular, as it has been shown in para. 3.1, the link uses almost excessive power levels for a high percentage of time, therefore interference with other systems is likely, a situation which can be improved by transmitter power control [14].

3.8 Mobility

Troposcatter can be used to continuously transmit wideband signals over distances up to 500 km. The necessary equipment uses antennas of 3 m to 10 m diameter and beyond, transmitter power values of 1 to 10 kW as well as sophisticated multichannel receivers. As the pathloss is very sensitive to the scatter angle (6), antenna alignment has to be done very carefully and because of the varying refraction index averages over a certain period of time is necessary. Mobile usage is therefore impossible, except excessive link margin is available. Transportable systems have to be built with a still high link margin compared to para. 3.1, as it is unlikely that under actual deployment conditions always the most favourable link condition can be attained. This measure will however increase the risk of having EMC problems with other services sharing the same band.

4. METEOR BURST COMMUNICATION

4.1 Principal Characteristics

Meteor bursts can be used to bridge distances between 800 km and 1500 km using frequencies in the VHF band between 30 MHz and 100 MHz [15, 16, 17]. Billions of ionized meteor trails are produced daily by meteors with a mass range of 10^{-7} to more than 10 grams in a height between 80 to 120 km. The interaction between radiowave and ionized trail is either a scatter mechanism where each electron individually scatters the radio wave. In this case the trail is called "underdense". A specular reflection of the radiowave can occur when the electron density inside the trail is high, the trail is then called "overdense". The dividing line between both is at an electron density of about 2×10^{14} electrons/m, which is produced by a meteor with a mass of about 1 milligram. As the average number of meteors observed per day is almost inversely proportional to its weight, one would expect the number of underdense events being much greater than that of overdense. However the multitude of these events provide such a small scatter cross section that they cannot be observed. In practice therefore only 70 % are from underdense events [16].

Although with underdense trails a scattering process is involved, geometric reflection conditions have to be established between the trail, a rod of ionization, and transmitter A and receiver B. The meteor trail therefore has to be tangent to a prolate spheroid with A, B being foci. In contrast to troposcatter the ray projection onto the earth surface is essentially not restricted to the great circle. In general reflections occur not along that path, because of the inevitable tilt of the trail with respect earth surface. Usually the multitude of reflections occur at so called hot spots which are located about 5° to 10° of the great circle [15].

The ionized trails of a meteor are generated in a height of about 80 km. After having been generated the electrons will diffuse into the neighborhood thereby reducing the electron density in the trail. A meteor trail has therefore only a restricted lifetime, which is shorter for higher frequencies as here higher electron densities are required to cause an appreciable effect. The lifetime depends also on its actual location with respect to path in particular angle of reflection and distance between transmitter and trail.

Although the earth is exposed continuously to a multitude of very small meteors, a continuously available link cannot be established using meteor trail reflection, as only in a small percentage of time a suitably oriented meteor of adequate characteristics will be present. The channel is therefore to be probed continuously and when a trail is present the prestored information can be transmitted with as high a speed as possible, whereby the message length should not exceed the lifetime of the trail (about 0.5 s).

4.2 Link Budget

For calculating the link budget the bistatic radar reflection equation (3) in conjunction with analytical expressions on the scatter cross section is used [16]. The results of these calculations are shown in Fig. 5. These values indicate that such calculations can only be used as a rule of thumb whether transmitter power and antenna gain values are sufficient to produce at least for some burst events received signal power levels which are above threshold of the particular system. In the STC comet system [15] over a distance of 1000 km 200 W transmitters have been used to transmit data in bursts with a rate of 2000 baud (FSK). The system used an ARQ modem (based on 7 bit characters) and attained an average throughput over a 24 h interval of about 150 baud, i.e. a duty cycle of 7.5 % [16].

With meteor scatter, too, antenna gain and transmitter power are not interchangeable numbers as the beam-width of the antennas has to be wide enough to illuminate the whole area where suitably oriented trails are likely to occur. For a 1000 km link this value is about 50° [15].

Recent publications suggest that the intervals between usable meteor trails are distributed in a poisson process [17].

$$(15) \quad P_n(t) = \frac{(t/t_{iA})^n}{n!} \exp(-t/t_{iA})$$

where $P_n(t)$ is the probability that exactly n bursts occur during time interval t and t_{iA} is the average time interval between bursts. t_{iA} can be calculated using measured data of a reference system along with the following scaling equation [17]:

$$(16) \quad t_{iA} = t_{iAR} \left\{ \frac{G_T}{G_{TR}} \cdot \frac{G_R}{G_{RR}} \cdot \frac{R_R}{R} \cdot \frac{P_T}{P_{TR}} \right\}^{-0.6} \left(\frac{f}{f_R} \right)^{2.4}$$

$G_{T,R}$ antenna gain of transmitter/receiver
 R range
 P_T transmitter power
 f RF-frequency

Index R denotes the parameters of the reference system, for the COMET-System these would be; $G_R = G_T = 10$ dB, $P_T = 200$ W, $R = 2$ kbit/s, $f = 37.5$ MHz, $t_{iA} = 4$ s, whereby t_{iAR} has to be corrected when the range is different from the reference system [17].

Although the data rate within a burst is limited because of dispersion, this restriction has not yet become visible as the power level in the system still limits the transmitted bitrate and not the distortion (neglecting the tailends of underdense trails).

4.3 Real-time Data Transmission

From the measured data it can be seen that considerable delay times can be involved in the transmission of a certain message, in particular when its length approaches the order of several hundred bits. In military C³ systems this fact calls for additional processing in the terminal to update the message.

4.4 Electromagnetic compatibility

Meteor burst communication systems are restricted to the lower VHF-frequency band, whereby the region below 100 MHz is crowded with mobile services using transmitter power levels of the order of 10 W. Because of the impossibility to use highly directional antennas and the necessity to probe the channel continuously, a sharing of a particular frequency is not possible and the problems are about the same as with TV-transmitter in band I. It is therefore very unlikely that a great number of meteor burst links can be established simultaneously in the European region, although digital signal processing in the equipment is no more the essential problem.

5. CHAFF PRODUCED SCATTER PROPAGATION

Chaff is used since World War II to produce large reflecting areas for radio waves. So in a certain angle region the normal range radars were saturated and the own combat aircraft could be masked by this chaff cloud. - Chaff consists of clouds of thin aluminum foil or metallized glass strips of approximately half wave length. The applicable frequency range is therefore upper UHF and lower SHF band. Packages of these dipoles - at least several hundred thousand - are released from aircrafts or rockets producing large dipole clouds floating slowly downward. With chaff communication channels especially for over the horizon links can be established. The equipment and link set up is rather identical to that used for troposcatter. The scatter mechanism is however more efficient [18]. For short haul links (100 km to 150 km) a decrease in transmission loss of 10 to 20 dB can be expected. So the disposal of chaff into the common volume of a troposcatter link could be used to overcome link outage periods in case of power amplifier failure. If the over-the-horizon link is only needed for a short time (1 hour) common radio relay equipment together with a chaff cloud could be used to bridge distances up to 150 km, whereby the adjustment of the antennas for optimum scatter angle is uncritical.

6. CONCLUSION

An attempt was made to review the relevant propagation characteristics of scatter links and to show the limitations with respect to system application. Presently scatter propagation is restricted to static links. Although there exist transportable equipments for troposcatter, setup is still time consuming and frequency coordination in a mix of L.O.S. and over-the-horizon links is difficult and almost impossible in a rapidly changing scenario because of the likelihood of scatterlinks to interface with other users.

All scatter links are restricted in the admissible signal bandwidth because of the characteristics of the medium. This aspect is presently not relevant in meteor burst communication as with state of the art equipment the limit can hardly be approached. In digital troposcatter, developments in diversity combining will in future allow to transmit signals with a wider band compared to the conclusion bandwidth.

Planning of scatter links is still a problem and any prediction will have considerable uncertainties involved which makes it difficult to guarantee EMC.

LITERATURE

1. Ince, A. N.: Aspects of Electromagnetic Wave Scattering in Radio Communications, AGARD-CP244, 1977
2. Booker, H. G. and Gordon W. E.: A Theory of Radio Scattering in the Troposphere, Proc. I.R.E., April 1950
3. Brennan, D. G.: Linear Diversity Combining Techniques. Proc IRE, Vol. 47, June 1959.
4. Ince, A. N. and Vogt, I. M.: Propagation Measurements on the ACE-High Troposcatter System
5. CCIR-Rept. 238-3 Vol. V Propagation in Non-ionized Media Para XIV Plenary Assembly Kyoto 1978
6. NBS-Report 101B Transmission Loss Predictions for Tropospheric Communication Circuits, National Bureau of Standards, 1967
7. Lewin, L.: Troposcatter Aperture-Medium Coupling Loss AGARD-CP 244, Aspects of Electromagnetic Wave Scattering etc., 1977, paper 4
8. Grosskopf, J.: Wellenausbreitung, B-I-Hochschultaschenbuch Bd. 141/141a, 1970
9. Larsen, R.: Space-Polarization Diversity in Troposcatter Systems Paper 7 in Proc of AFCEA Conf on "Digital Tropospheric Scatter Systems" 26 March 1980 Brussels
10. Osterholz, J. L.: Design Considerations for Digital Troposcatter Communications Systems, AGARD-CP244, 1977, paper 22
11. Mouser, P.: Digital Transmission Performance on Fading Dispersion Channels, IEEE Trans COM, Jan 1973, pp 33 - 39
12. Di Toro, M. J.: Communication in Time-Frequency Spread Media using Adaptive Equalization Proc. IEEE, Bd. 56, pp. 1653 - 1679, Oct. 1968
13. Vral et al.: Technical Aspects of Digital Transmission in the ACE High System. Proc of AFCEA Conf. on Digital Tropospheric Scatter Systems, 1980, Brussels
14. Braine, M. R.: Interference Reduction due to Transmit Power Level Control on Tropospheric Links, ibid. paper 6
15. Ince, A. N.: Interception of Signals Transmitted via Meteor Trails, AGARD-CP 244, paper 19
16. Brown, D. W. and Williams, H. P.: The Performance of Meteor-Burst-Communications at Different Frequencies, AGARD-CP 244, paper 24
17. Oetting, J. D.: An Analysis of Meteor Burst Communications for Military Application, IEEE COM-28, Sept. 1980, pp 1591 - 1601
18. Lampert, E.: Review on Communication Aspects of Chaff-Produced Scatter Propagation, AGARD Conf. Proc. 192 on Artificial Modification of Propagation Media, Brussels 1976

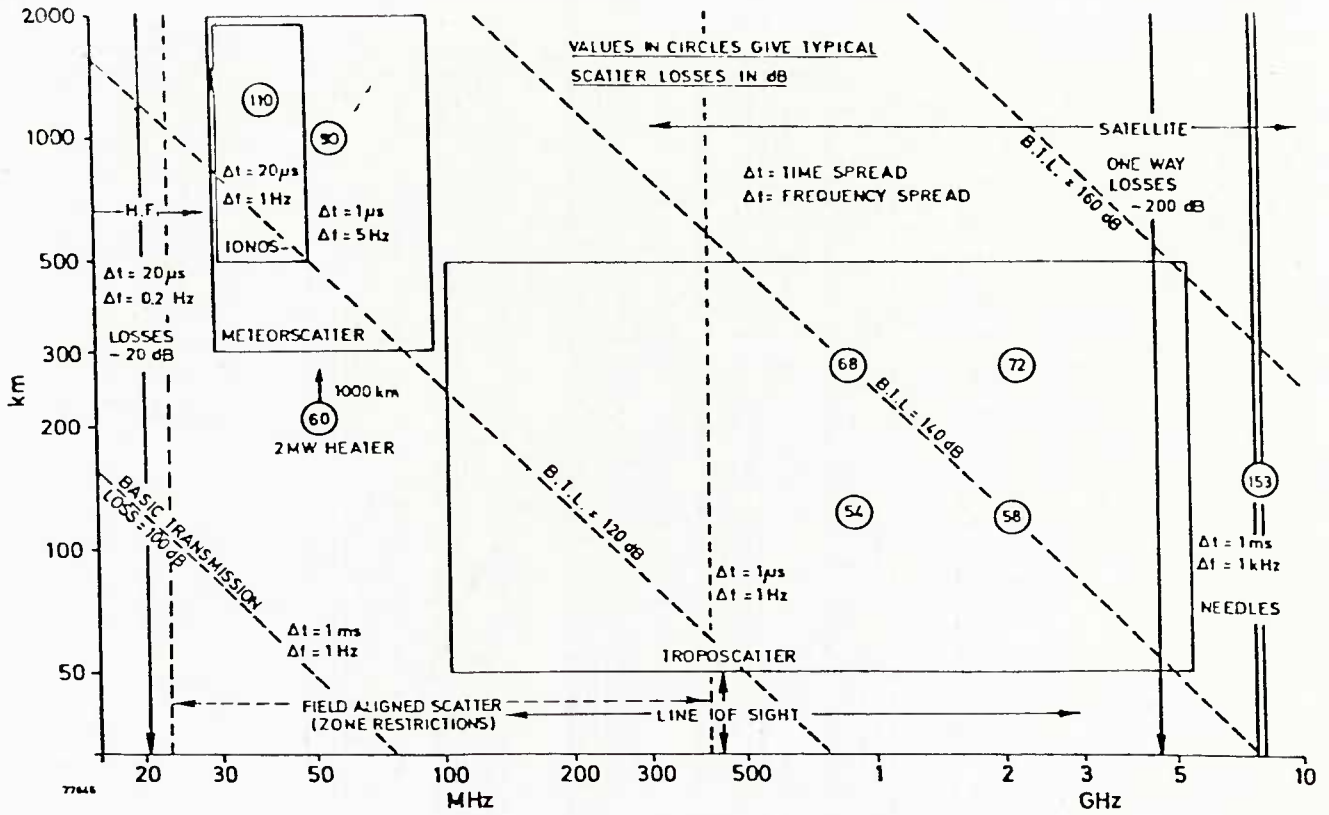


Fig.1 Typical frequencies and ranges of scatter communication systems, after Ince [1]

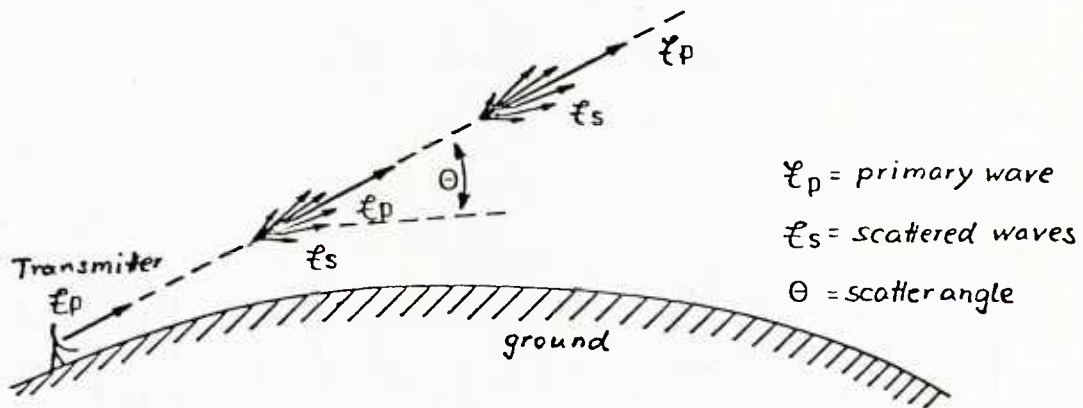


Fig.2(a) Scattered wave from a plane wave travelling through the troposphere

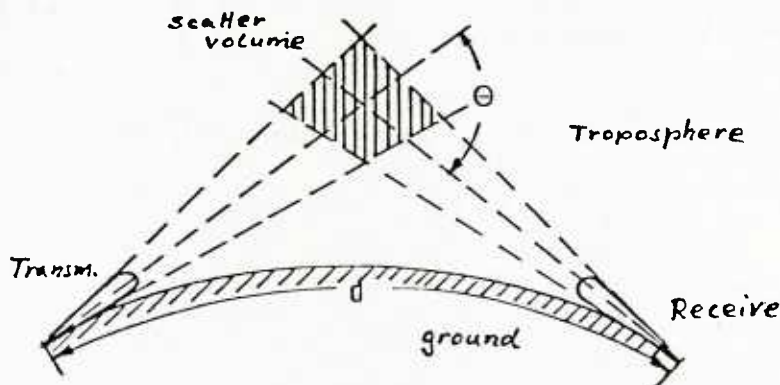


Fig.2(b) Geometry of a scatter link

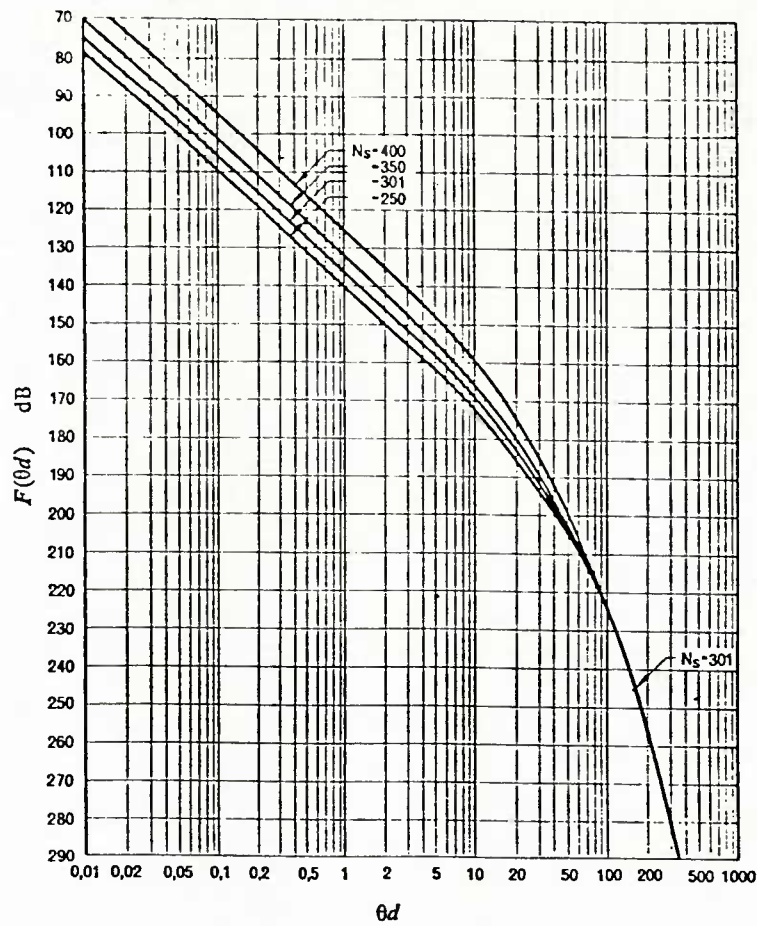


Fig.3 Attenuation function $F(\theta d)$, after CCIR-Rept 238-3

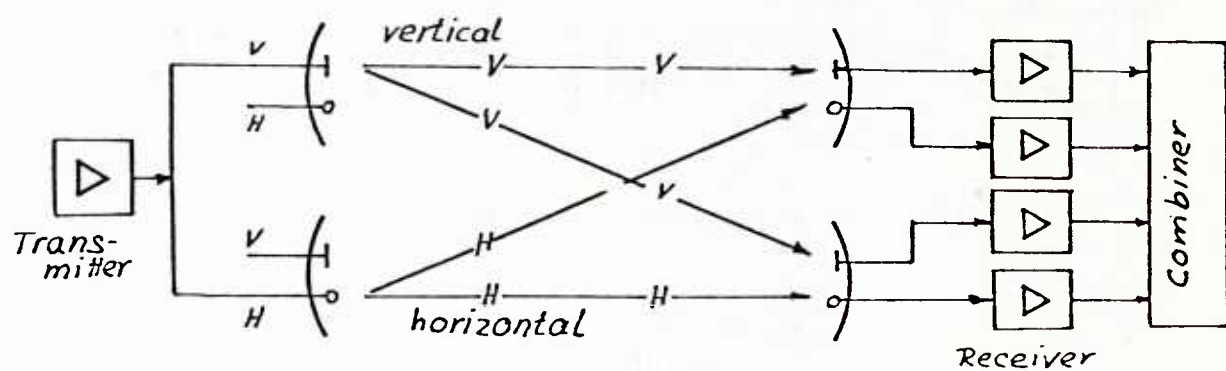


Fig.4 Quadruple diversity using orthogonal polarization

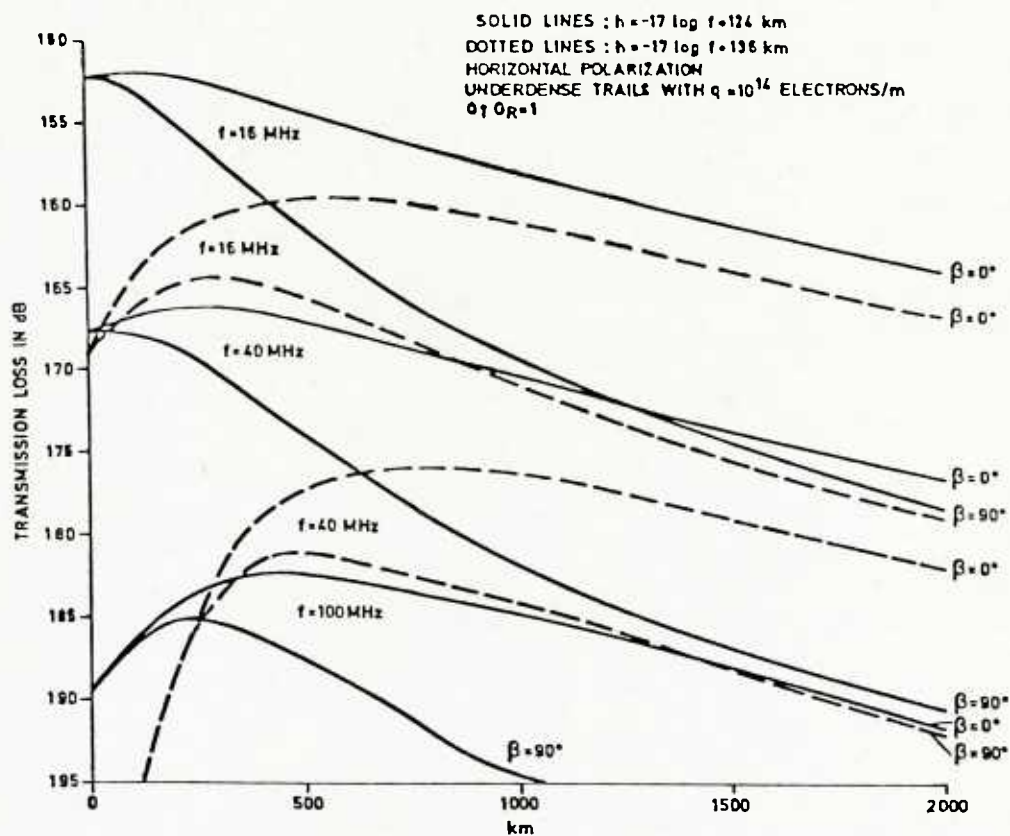


Fig.5 Transmission loss for meteor burst communication after Brown and Williams[16]

Introduction to Propagation Effects on Typical Systems

by

H.J. Albrecht

Summary.

Depending on the actual application of a propagation path between two points, or within an area, a system may display particular behaviour. In other words, its characteristics may be affected by certain propagation conditions. This paper aims at a general introduction to such effects.

Particular attention is paid to examples which allow to illustrate certain problems and possible remedies, and represent a suitable supplement to a more detailed discussion of propagation effects on typical systems.

1. INTRODUCTION

As has been mentioned in the introductory review at the beginning of this Lecture Series, application areas of electromagnetic wave propagation may comprise systems utilized for communication, surveillance including radar, and navigation, of which the first category concerns the largest variety of possible link types. It is thus the logical one to use to introduce the subject of propagation effects on typical systems. Reference is again made to a summarizing chart (fig. 1) showing representative features of various link types; it has been used for the introductory lecture to the tutorial part of this Lecture Series (Albrecht, 1982).

In general, an operational system may only employ one of the kinds of propagation paths shown in the figure, although a back-up link may frequently be established with some other path. On the other hand, the user is well advised to consider all possible types of paths for an operating system, its frequency range and the locations involved; such alertness is essential to be aware of possible intentional or unintentional interference. Similarly, it allows to optimize the performance of one's own links by the proper application of terrain shielding, power adaptation, etc..

Whenever scientific propagation results are to be applied to systems, appropriate planning requires models which describe the general behaviour of medium characteristics for average conditions. Reference is herewith made to a recent AGARD-Lecture Series on the subject of modelling such features in the entire spectrum of electromagnetic wave propagation (Soicher, 1979).

This short paper is intended to serve as a brief introduction to the more detailed lectures referring to typical system examples. The following comments are subdivided into the two main groups of tactical applications, systems using stationary and transportable terminals only and those employing mobile ones in addition. The first-mentioned group is normally represented by terminal characteristics which either require higher levels of radiated transmitting power or more precise antenna adjustment, or both. On the other hand, the second group, in addition, contains all other types of terminals, including those required to operate while in motion.

2. Typical Systems with Stationary and Transportable Terminals

2.1 Fixed Communication Nets

In this area, all five columns of fig. 1 may be considered relevant. Terrestrial cable links of both, more orthodox wire construction and more modern design using fibre-optics, may be utilized alone or in combination with any medium-dependent links. PTT and PTT-related nets employing cable links may be supplemented by those using field cables. Predominant features are shown in the left-hand column of the chart. More details are contained in Proceedings of AGARD-Symposia conducted in recent years (Hodara 1977, Halley 1981).

With regard to the use of optical (and infrared) systems in tropospheric environment, characteristics of the medium have to be taken into account. As had been mentioned in the introductory lecture to the tutorial portion of this Series, there are frequency bands displaying adequate transparency for communication and surveillance systems. However, a need of adaptation to actual tropospheric conditions exists for any system in the tactical environment. For some more general information on system effects, reference is made to a lecture in an AGARD Lecture Series a few years ago (Höhn, 1978); the present state of the art and R & D trend have been dealt with more recently (Halley, 1981).

Radio-relay links are an area of widely spread and popular application. They are in principle characterized by line-of-sight VHF, UHF and SHF propagation with the

features indicated. The following lecture in this series will deal with this important field in detail (Fitzsimons, 1982). With regard to a possible influence of another propagation mechanism, attention is drawn to scatter paths from third locations; they may cause unintentional or intentional interference to receiving terminals in radio-relay systems.

For distances larger than those usual for radio-relay links, scatter propagation may be utilized on VHF, UHF and SHF. The appropriate column illustrates relevant characteristics. More details were contained in the appropriate tutorial lecture (Lampert, 1982a).

Yet larger distances and similarly wide bandwidths are features of satellite communication, which is, in fact, the use of radio-relay concepts with a relay terminal in space and therefore line-of-sight paths throughout. The right-hand column in fig. 1 summarizes their performance. Special criteria have been dealt with in the appropriate tutorial lecture (Aarons, 1982). It remains to be pointed out again that satellite communication terminals are, in principle, susceptible to interference via scatter or line-of-sight paths.

If smaller bandwidths are sufficient for the use envisaged but large distances are also required, the employment of HF-links is possible. Depending on the actual distance range, ground-wave propagation or paths with ionospheric reflections are to be considered. A summary is given in the chart. Details were again contained in the tutorial part of this Lecture Series (Rush, 1982).

2.2 Fixed Surveillance Applications

The information contained in fig. 1 may easily be adapted to the characteristics of surveillance or radar systems. The area of tactical radar normally comprises propagation features given by line-of-sight paths. Details will be given by one of the following lectures (Prew, 1982).

For completeness' sake, attention is drawn to the surveillance in a specified target area by means of long-distance surveillance, typically using HF-radar facilities with ionospheric reflections or passive surveillance from space. For such cases, the two right-hand columns fig. 1 illustrate relevant propagation criteria.

3. Typical Systems including Mobile Terminals

This group of systems represents undoubtedly the most important one for typical applications. Mobility is a predominant requirement for any system used in such environment, for purposes of communication, surveillance, navigation, and others.

As a general remark, high mobility in equipment normally renders difficult a precise adjustment of antennas within an acceptable fraction of time. Such limitation leads to scatter links being somewhat impracticable, and reduces the amount of radiated power available with mobile terminals in HF-links and line-of-sight applications on higher frequencies.

3.1 Combat Net Radio (CNR)

Combat-Net-Radio links may usually include any mobile and transportable terminals equipped with single-channel access and of almost any size, even manpack equipment, depending on the level and service of communication required. Any combination of terrestrial cable, line-of-sight, and HF ground-wave links may be used, as long as bandwidths requirements can be satisfied.

Propagation characteristics should be considered highly variable, depending on variable surroundings of terminals. The susceptibility to interference can be minimized by ad hoc adjustment and adaptation to local condition; this calls for appropriate know-how and experience. On the other hand, near-field conditions around antennas may detrimentally affect the performances of both, receivers and transmitters. For some more details, reference is made to the tutorial lecture on ground wave propagation (Palmer, 1982).

3.2 Air/Ground/Air and Air/Air Communications

If tasks of terrestrial support of air warfare are considered similar to fixed communications in general, items mentioned in section 2.1 are relevant. The remainder, and certainly the larger and more difficult portion, of air/ground/air and air/air communications is of highly mobile nature. An additional restriction is presented

by the usual limitation of electric power aboard aircraft and the problem of antenna design.

In principle, columns in fig. 1 dealing with line-of-sight and HF-paths indicate criteria encountered in this field of applications. Under certain operating conditions, the use of satellite communications offers distinct advantages inasmuch as phased-array-antennas aboard an aircraft may be programmed to radiate towards a fixed point in space, if navigational data are used as additional input data. With geo-stationary satellites, an efficient communication system may thus be possible.

Details on the important field of propagation problems associated with aircraft communications systems are contained in one of the following lectures on the subject (Burgess, 1982).

3.3 Navigation Systems

Systems to determine one's own location represent an important attribute in any military environment, in particular with mobile operations, and these belong to fundamental requirements in tactical applications. In principle, there are two different categories of feasible systems as far as propagation problems are concerned, viz., those operating in the lower part of the HF-region and below down to 10 KHz, and satellite systems in the UHF range. Typical examples are the OMEGA system around 10 KHz and the Global Positioning System GPS (NAVSTAR) around 2 GHz. The behaviour of relevant propagation media has been described in the review lecture, paper no. 1, of this Series. Obviously, the main criteria for any system of location determination is the accuracy achievable. With satellite systems, sources of error due to variable atmospheric transparency may be corrected by frequency diversity methods. On the other hand, an adequate level of accuracy with OMEGA-applications requires optimum identification and adaptation to variable characteristics of waveguide-like propagation within the belt between ionospheric D-layer and Earth's surface. The present state of the art and current trend in research and development had been topics of a very recent AGARD-Symposium (Belrose, 1982).

3.4 Multifunction Information Distribution Systems (MIDS)

Advanced future systems for the tactical environment include facilities for communication, navigation, and identification; they are thus multifunctional by definition and are consequently designated as such. As a particular requirement, communications necessary for command and control are also to be offered by such systems.

Inherent wide bandwidth and mobile operation of at least considerable portions of such systems point towards line-of-sight propagation links, with some chance of using satellite links under conditions indicated previously. The appropriate columns in fig. 1 are relevant. As far as details can be made available, the lecture on systems for multifunction information distribution and command, control, and communications (C³) will deal with relevant aspects (Lampert, 1982b).

4. Conclusions

An attempt has been made to introduce the lectures addressing propagation problems with reference to typical systems. It is to be remembered that any information given in this Lecture Series can only contain details up to a certain degree. Nevertheless, it is anticipated that some of the more important problem areas can be indicated and dealt with. It is to be hoped that these system-oriented lectures, together with the tutorial ones presented as the initial part of this Series, assist the user in identifying and applying methods of improving the performance of current and future system configurations.

References

- Aarons, J. (1982) Propagation characteristics of satellite links, Paper No. 4 in AGARD Lecture Series No. 120, May 1982
- Albrecht, H.J. (1982) General review of EM spectrum characteristics in tactical applications, Paper No. 1 in AGARD Lecture Series No. 120, May 1982
- Belrose, J. (1982) (ed.) Medium, long and very long waves propagation (at frequencies less than 3000 kHz), Proceedings, AGARD-EPP-Symposium, September 1981, Brussels, Belgium

- Burgess, B. (1982) Propagation problems associated with aircraft communication systems, Paper No. 8 in AGARD Lecture Series No. 120, May 1982
- Fitzsimons, T.K. (1982) E.M. Propagation problems for tactical radio-relay links, Paper No. 7 in AGARD Lecture Series No. 120, May 1982
- Halley, P. (1981) (ed.) Special topics in optical propagation, Proceedings AGARD-CP-300, AGARD-EPP-Symposium, April 1981, Monterey, U.S.A.
- Hodara, H. (1977) (ed.) Optical fibres, integrated optics, and their military applications, Proceedings AGARD-CP-219, AGARD-EPP-Symposium, May 1977, London, United Kingdom
- Höhn, D.H. (1978) Introduction to optical problems of systems, Paper No. 1 in AGARD Lecture Series No. 93, May 1978
- Lampert, E. (1982a) Limitations in scatter propagation, Paper No. 5 in AGARD Lecture Series No. 120, May 1982
- Lampert, E. (1982b) Systems of multifunction information distribution and for command, control, and communications - C³, Paper No. 9 in AGARD Lecture Series No. 120, May 1982
- Palmer, F.H. (1982) Ground-wave propagation characteristics of interest to the tactical communicator, Paper No. 2 in AGARD Lecture Series No. 120, May 1982
- Prew, B.A. (1982) Propagation effects in tactical radars, Paper No. 10 in AGARD Lecture Series No. 120, May 1982
- Rush, C.M. (1982) Propagation aspects of ionospheric links over short and medium distances, Paper No. 3 in AGARD Lecture Series No. 120, May 1982
- Soicher, H. (1979) Aerospace propagation media modelling and prediction schemes for modern communications, navigation, and surveillance systems, AGARD Lecture Series No. 99, June 1979

H.J.A. '81
AGARD-LS-120

COMMUNICATION LINKS IN MILITARY APPLICATIONS

NATO UNCLASSIFIED

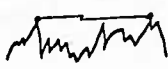
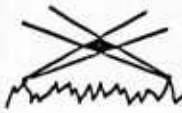


LINK	TERRESTRIAL CABLE		LINE-OF-SIGHT & DIFFRACTION PATHS	SCATTER PATHS TROPOSCATTER IONOSCATTER	HF-GROUND WAVE & REFLECTIONS AT IONOSPHERE	SATELLITE LINKS LINE-OF-SIGHT SPACEBORNE RELAY
	WIRE	FIBRE OPTICS				
OPERATING FREQUENCY	AUDIO	>100 THZ	ABOVE 30 MHZ VHF UHF SHF EHF/ OPTICS	100 MHZ - 15 GHZ VHF UHF SHF	3 - 30 MHZ HF	ABOVE 100 MHZ VHF UHF SHF
TYPICAL SYSTEM APPLICATIONS	PTT AND PTT-RELATED		CNR MIDS (R&D)	(R&D) ACE HIGH		SEVERAL SATCOM SYSTEMS
PATH CRITERIA	CONSTRUCTIONAL CONDITIONS		LINE-OF-SIGHT AND/OR DIFFRACTION	IONO-SCATTER TROPO-SCATTER DEPENDENT ON MEDIUM	IONOSPHERIC CONDITIONS & THEIR VARIATIONS REQUIRE ADAPTATION	LINE-OF-SIGHT CONDITIONS, BUT ATMOSPHERIC EFFECTS
BANDWIDTHS	~4.0 KHZ	>100 MHZ	WIDE BANDWIDTHS POSSIBLE (UP TO 10% OF OPERATING FREQUENCY)	WIDE BANDWIDTHS, PRECAUTIONS WITH DATA TRANSMISSION	SMALL BANDWIDTHS, SMALL NO. OF CHANNELS	WIDE BANDWIDTHS POSSIBLE
DISTANCES	NET-DEPENDENT		SHORT DISTANCES	MEDIUM DISTANCES	LARGE DISTANCES	LARGE DISTANCES
MOBILITY	STATIONARY, BUT GENERAL NET ACCESS		STATIONARY, MOBILE OR TRANSPORTABLE	STATIONARY OR TRANSPORTABLE ONLY	STATIONARY, MOBILE OR TRANSPORTABLE	STATIONARY, MOBILE OR TRANSPORTABLE
PHYSICAL LIMITATIONS	CONSTRUCTIONAL FEASIBILITY		MULTIPATH ENVIRONMENT, TROPOSPHERIC CONDITIONS	EFFECTS OF SCATTER MEDIUM	IONOSPHERIC CONDITIONS	CONSTANCY OF ATMOSPHERIC TRANSPARENCY
EW HAZARDS	EMP	(EMP IF ABOVE SURFACE)	EMP: INTERCEPT & ECM: SIDELOBES, DECREASING WITH FREQUENCY	EMP: INTERCEPT AND ECM: SIDELOBES AND SIDE SCATTER	EMP: INTERCEPT AND ECM, EVEN GLOBAL	EMP: INTERCEPT AND ECM WITHIN GROUND COVERAGE

Fig. 1 General Criteria of Typical Paths and Links

E.M. PROPAGATION PROBLEMS FOR TACTICAL RADIO RELAY SYSTEMS

BY

T.K. FITZSIMONS

ALLIED RADIO FREQUENCY AGENCY,
IMS. NATO HQ, BRUSSELS

SUMMARY

The designer or user of a tactical radio relay system is faced with a set of technical and operational problems that, for the most part, are not encountered by the designer of a fixed or non-tactical radio relay system. Although the EM propagation mechanisms for tactical and fixed systems are the same, since they both use the radio frequency spectrum from roughly 100 MHz up to tens of GHz, the problems of EM propagation manifest themselves in different ways and the considerations leading to equipment or system optimisation are different. This paper gives a description of a tactical radio relay deployment and discusses problems of siting the terminals. Propagation mechanisms such as refraction, reflection, diffraction and fading are discussed and an assessment given of attenuation caused by rain. Statistical data, based on field observation of a large tactical system is presented. Distributions of signal margin and link lengths are presented together with data on availability of line-of-sight paths. Different approaches to the prediction of performance are discussed and the paper assesses likely trends in the use of higher frequency bands and the role of the computer.

1. INTRODUCTION TO TACTICAL RADIO RELAY SYSTEMS

1.1 The propagation problems associated with tactical radio relay systems are problems of path loss prediction. In general the problem is solved by shrewd application of first-hand field experience and by incorporating into the system and equipment design sufficient performance margin to set against the normal range of propagation uncertainties. To understand the problem and the form of solution it is necessary to first examine a typical tactical radio relay system. So-called "area communication systems" are just now being introduced into the battlefield. These are systems which do not reveal any hierarchical structure and which present the same access possibilities and the same communications facilities to the user wherever he is in the area being served (figure 1).

1.2 The radio relay system provides the multi-channel connecting links between the switching centres and also from the switching centres to the access nodes which are the points of entry to the system for groups of either static or mobile subscribers. Figure 2 shows all of these connections being made by radio relay but the access node to switching centre connection may sometimes be made by cable. In a tactical environment the location of a switching centre may be changed a number of times a day; the access nodes will also change their positions several times a day sometimes independently of any change in the switching centre positions. Even while portions of the system are being repositioned, it is a requirement to have alternative points of entry for the subscriber groups and to have alternative paths through the system to the destination.

1.3 The configuration shown in figures 1 and 2 represents a snapshot of the system at a particular time. A typical performance requirement in the specification would be for set-up and tear-down times of the radio relay terminals to be of the order of 1/2 to 1 hour. Under battlefield conditions the lifetimes of the links might be only a few hours. Figure 3 shows that under the calmer conditions of tactical exercises, the lifetimes can be measured in days, with a median lifetime of 1.5 days in the divisional area of the system and 3 days in the more rearward Corps area. Even these durations are very short when compared with non-tactical radio links. In addition to uncertainty of the link duration at the time of planning and setting-up, there are a number of other constraints. First, although the location of the radio relay terminal itself will be chosen to give some height advantage, it must also afford physical and radio shielding from the enemy. Second, the siting within the location area may be hindered by difficult approaches and by the presence of other equipments and vehicles. Third the terminal vehicle may not reach the nominated location for a number of reasons such as impassable roads, human error involving map reading and navigating. The siting, and hence antenna pointing uncertainties apply at both ends of the link. A typical siting for a tactical radio relay terminal then might be on a hill but not at the summit; on a slope on the far side from the enemy if possible and among trees just less than the maximum height of the antenna mast. The following summarises some of the important features or consequences of siting of tactical radio relay terminals that are not normally encountered in the non-tactical environment:

the siting will be a compromise between having the least obstruction on the radio path, and concealment from the enemy, compatible with speed of changing the system connectivity

there will be an uncertainty in the positions of both the near and distant terminals

the E.M. environment will be to some extent unpredictable and will probably change during operation of the link

in a highly dynamic battlefield situation little or no surveying of the radio path or the terminal areas may be possible

the maximum possible received signal level may not be achievable because of need for antenna concealment or the need to steer the antenna to maximise the signal to interference ratio.

1.4 Final background aspects of these tactical military systems concern the nature of the communications, antennas and the frequency spectrum. The number of users served by an access node and their requirements for circuit availability are such that tactical radio links are typically 15 or 30 multiplexed voice channels; exceptionally the links may have capacities of about 60 and 120 channels. The systems being phased out of service are mostly analogue voice, frequency division multiplexed; the area systems are supported by digitally coded (Delta or PCM), time division multiplexed radio relay. This is the main difference between the old and new radio relay and the propagation related problems remain fundamentally the same. One can only refer to typical transmitter occupied bandwidths, since there are as yet no standards other than those that may have been established for interoperability and the imposition of rastered channels does not of itself imply a specific transmitter spectrum distribution. A rough guide is that the 15 channel links have about 500 kHz occupied bandwidth and the 30 channels links just less than 1 MHz.

1.5 Provision has been made in a number of different radio frequency bands for the operation of radio relay systems. In NATO Europe, with minor variations, allocations to radio relay are confined within the following bands:

225-400	MHz
790-960	MHz
1350-1850	MHz
4.4-5.0	GHz
and 14.5-15.35	GHz

1.6 Although the total spectral allocation to radio relay in any one band may be small, for example 30 MHz in the lowest band, the transmitters and receivers are required to be tunable over the whole of the range. The antennas used must therefore be fairly broad-band especially in the lower bands. Consideration of prime power generation with a mobile installation dictates that the antenna should be physically large to obtain gain while problems associated with man-handling, concealment, robustness, broad-banding and, in the higher bands beamwidth, all place limitations on size and hence gain. Typical gain values for the first three bands are 8-11 dBi, 13-18 dBi, and 18-24 dBi respectively. There is not much experience available yet on the deployment of tactical equipments in the two highest bands but an analysis of the problem of antenna steering for signal acquisition suggests that in both cases beamwidth rather than physical size would be a limiting factor. In both cases it is suggested that the antenna beamwidth should not be less than 90 m radians (or 5.1 degrees) giving a maximum gain of just under 30 dB.

1.7 This conclusion is based on a computation of the loss of potential antenna gain when the two antenna beams are misaligned, together with a field study to establish the type and range of alignment error. It was found that errors in elevation were small and could be ignored. The distribution in azimuth alignment error was assumed to be Gaussian with positive and negative errors equally likely. The probability of decoupling loss was calculated by combining the probabilities of various angular offsets for the pair of antennas. The results showed that the ratio of (beamwidth/rms alignment error) could be used as a parameter to express the probability. If the antenna beams are de-coupled during attempts to establish the link, there needs to be a signal margin in hand over a certain detectable level. The results of the analysis are shown in this form in figure 4. It can be seen that, to have a high probability of not exceeding a stated threshold margin, or conversely to keep the required threshold margin within reasonable limits, the ratio of beamwidth/rms error needs to be greater than 2.0. Indeed it appears that a factor of 3.0 represents a good compromise; below this value the threshold margin required rises rapidly while above 3.0 the threshold margin required does not reduce substantially while system performance, in the form of potential antenna gain, is sacrificed. Field trials, using an antenna mast fitted with an azimuth ring calibrated in degrees and with a boresight, produced an error distribution with a rms value of 1.7 degrees. Using the factor of 3, obtained from figure 4 indicates a lower limit of about 5.1 degrees (90 m radians) for the beamwidth. Even with this limitation the results show that it is necessary to have up to about 15-30 dB signal margin in hand during the attempt to set up the link in order to have a 95 to 99% chance of successful reception.

2. PROPAGATION MODELS

2.1 In the introduction it was stated that the propagation problems associated with radio relay are simply problems of path loss prediction. Certainly, with the possible exception of rain attenuation, the mechanisms are well understood. In the frequency bands up to about 1 GHz, it is possible to achieve communication between tactical radio relay terminals on obstructed paths with the signal being diffracted over one or more obstructions. In all of the radio relay bands there will be refraction and the possibility of reflections. In only the highest band allocated for military radio relay use (14.5-15.35 GHz) does there need to be an allowance for rain attenuation, and in the two highest bands some allowance will be necessary for fading.

2.2 REFRACTION

The decrease of the atmosphere's refractive index with height bends the path of the E.M. wave at VHF frequencies and above. The effect of this bending is such that in order to represent E.M. rays by straight lines, the earth's radius a , is replaced by one equal to $4/3$ rd a . Using this relationship to construct a grid on which to plot path profiles, one finds that

$$h = D^2/2 \quad (1)$$

where h = height in feet above mean sea level (msl)

D = distance to the horizon in miles

a condition being that $h \ll D$.

In metric units, $h = D^2/17$ with h in metres, (2)
and D in kilometres.

Using either of these relationships, a grid, or in more familiar terms, a path profile graph can be prepared on which a sectioned geographic contour can be drawn. E.M. ray constructions can then indicate whether the path is obstructed, or whether there is sufficient clearance to constitute radio line-of-sight. A line of sight path is usually defined as one for which not only can a ray be drawn between the antennas without cutting an obstacle but there is also First Fresnel Zone clearance. The cross section of the First Fresnel Zone is an ellipse as shown in figure 5 and for radio line of sight there should be no obstacle intrusion into the ellipse. The radius, and hence the clearance required at any point along the axis between the antennas, is given by:

$$\left\{ \lambda d(1 - 4\alpha^2)/4 \right\}^{1/2} \quad (3)$$

where d is the path length,
 λ the operating wavelength in
the same units as the radius
and α the distance from mid-path
expressed as a fraction of d .

The ellipse of the First Fresnel Zone is such that a reflection occurring on the perimeter would arrive at the receiver antenna having travelled one half-wavelength further than the direct ray. Meeting the clearance condition gives confidence that the available power at the receiver antenna approaches that which it would be in free space and in the event of a reflection occurring on the path, the interference effect will not be great.

2.3 REFLECTIONS

A full treatment just covering the geometry of reflections from the ground would be very lengthy. For a tactical radio relay system the effort is hardly justifiable since the necessary detail of the terrain and the conditions in the reflecting region are not normally available. Figure 6 shows the geometry of an unobstructed link above a smooth earth. A direct and a reflected wave are shown arriving at the receiver antenna. The received field strength is the vector sum of these two rays. For the conditions

$$r \gg h'_1, h'_2$$

and

$$d \gg (h'_1 + h'_2),$$

the path length difference between the two rays, Δd , is approximately given by

$$\Delta d = 2h'_1 h'_2 / d. \quad (4)$$

If the magnitude of the direct wave field strength at the receiver is unity and that of the reflected wave is R , then the vector addition will be

$$\left\{ 1 + R^2 - 2R \cos(2\pi \Delta d / \lambda) \right\}^{1/2} \quad (5)$$

for cases of small grazing angles where a phase change of 180 degrees occurs on reflection for both vertical and horizontal polarisations. The attenuation, A , relative to the direct ray is:

$$A = 10 \log_{10} \left\{ 1 + R^2 - 2R \cos(4\pi h'_1 h'_2 / \lambda d) \right\} \quad (6)$$

For the case of $R = 1$ and substituting for the Cosine term the attenuation is

$$A = 10 \log_{10} \{ (-4 \cdot \sin^2 (2\pi h'_1 h'_2 / \lambda d)) \} \text{ dB} \quad (7)$$

$$A = -6 \text{ dB} - 20 \log_{10} \sin (2\pi h'_1 h'_2 / \lambda d) \text{ dB} \quad (8)$$

At short ranges there is therefore a variation of attenuation with change in antenna height (figure 7). At VHF and lower UHF frequencies, height/gain tests are carried out when setting up a link to obtain the maximum signal.

2.4 In practice, the ranges are such that there will probably be no observable variation of signal with height; at the lower frequency ranges there may be a coherent reflection which produces a reflection loss but in the higher frequency bands the antenna directivity together with the need to ensure line of sight conditions makes this unlikely. Few paths occur, such that a single coherent reflection can be assumed. The terrain in the reflection region is likely to be rough and for this condition an equivalent reflection surface has been proposed (figure 8). The amount of terrain detail necessary for this type of approximation is not normally available when engineering tactical links. In addition, the effective antenna height is not easily determined in rough terrain and a reflection may in any case occur from an obstacle or terrain feature which is off-line and does not appear on the path profile chart. For these reasons, even though considerable amounts of digitised terrain data are now stored and available at short notice, it is still not worthwhile to attempt to calculate with any expected degree of precision, the contribution of reflection losses in a tactical environment.

2.5 DIFFRACTION

When the First Fresnel Zone includes obstacles, diffraction may occur particularly in the lower frequency bands, where the longer wavelength effectively makes the top of an obstacle appear sharper. For an obstructed path such as the one shown in figure 9 there are several models for calculation of the path loss. The methods of Bullington (ref 1) Epstein and Peterson (ref 2) and Deygout (ref 3) are most often used by radio relay planners and frequency assigners. Diffraction can occur with the tip of the obstacle either above or below the line joining the two antennas. The Fresnel Kirchoff diffraction formula defines a dimensionless parameter

$$v = \pm \sqrt{\Delta a / \lambda} \quad (9) \text{ where } \Delta a = r_1 + r_2 - d \quad (10)$$

the positive sign applies when the knife edge is above the line of centres and the negative sign when the knife edge is below. The diffraction loss, which is the ratio of the free space field and the diffracted field, is a function of this parameter which in turn is a function of

$$d_1, d_2, \text{ and } h_0$$

Extension of the classical approach to more than one knife edge is very complex and even for the approximations used by various authors, there are limitations to using an analytical approach in the field. The Bullington method attacks the problem of multiple knife edges, by geometrically reducing them to a single 'equivalent' knife edge positioned at the intersection of the transmitter and receiver horizon rays (figure 10). In some cases, this method can lead to very large errors in the estimation of the diffraction loss. The Epstein-Peterson method adds the diffraction factors of each of the obstacles. The loss for the edge nearest the transmitter is derived assuming a receiver at the second edge. The loss for the second edge is then obtained by assuming a transmitter at the first knife edge (figure 11).

$$\text{The attenuation } A = f(a, b, h_{01}) + f(b, c, h_{02}) \quad (11)$$

The Deygout method evaluates the Fresnel-Kirchoff parameter for each of the obstacles in the absence of the other. The knife edge with the higher Fresnel-Kirchoff value is defined as the main edge and the loss due to that edge is calculated. The loss for the other edge is then computed assuming a transmitter placed on the main edge (figure 12).

$$\text{The attenuation } A = f(a, (b + c), h_1) + f(b, c, h_{02}) \quad (12)$$

These methods can be used for three or more knife edges. Deygout claims close agreement to experimental results for three or more knife edges at frequencies of 160 MHz, 1800 MHz and 2.45 GHz. Of the three methods, that of Epstein and Peterson is considered easier to apply than that of Deygout while giving more accurate results than the Bullington method.

2.6 Unfortunately, many paths on which obstructions occur also have reflections and the most rigorous treatments taking into account reflection and diffraction tend to underestimate the path loss by up to about 10 dB. It is possible to attribute some of this error to a so-called "clutter loss" caused by the local terminal environment having trees, buildings and other small obstructions and reflecting surfaces. The need to be able to assess quickly the likelihood of successful operation of a link without the complications of the rigorous methods has led to the use of empirical formulae which give a statistical estimate of the path loss. The equations relate path loss simply to frequency, path length and antenna height and have a stated standard deviation. One

well known equation is due to Egli (ref 4). From measurements on links in the ranges 50 to 250 MHz and 288 to 910 MHz Egli derived the following equations:

$$L_{50} = 88.0 + 20 \log_{10} f + 40 \log_{10} d - 20 \log_{10} h_t - 20 \log_{10} h_r \quad (13)$$

for $h_r \geq 9\text{m.}$

$$\text{and } L_{50} = 78.4 + 20 \log_{10} f + 40 \log_{10} d - 20 \log_{10} h_t - 10 \log_{10} h_r \quad (14)$$

for $h_r < 9\text{m.}$

where L_{50} is the median predicted path loss

f = frequency in MHz

d = path length in km

h_t = transmitter antenna effective height in metres

h_r = receiver antenna effective height in metres.

The standard deviation for both equations:

$$\sigma = 5 \log_{10} f - 2 \text{ dB.} \quad (15)$$

For example, at 300 MHz the standard deviation is 12 dB.

There are a number of such equations in use. Certain ones are preferred for paths having optical line of sight, others are used in the cases of one or two obstacles. Typical deviations are in the range 7-10 dB. When further data from field deployments are examined in Part 3 of this paper, it will be seen why the empirical equations can be useful in assessment and frequency assignment for radio relay systems.

2.7 FADING, AND ATTENUATION DUE TO PRECIPITATION

The formal and empirical equations for obstructed paths are normally applied to radio links operating on radio frequencies up to about 1 GHz. Beyond 1 GHz it is normally necessary to have at least optical line of sight and preferably First Fresnel Zone clearance. Consideration though must be given to fading and attenuation due to precipitation in this range.

2.8 Although precipitation of any type can cause attenuation of the radio signal, rain is the most likely cause in the regions where radio relay systems are most often deployed. Although attenuation due to rain can be detected at frequencies above about 2 GHz, the extent is not appreciable until about 8 GHz and it then increases rapidly with frequency. There are several theories to describe the effects. The attenuation predicted by Ryde and Ryde (ref 5) is shown in figure 4. The attenuation mechanisms are generally well agreed and variations in predicted effects are due mainly to differences in assumptions of rain patterns and the drop-size distribution of the rain drops. Many experiments have been carried out to confirm the theory but the results have been in most cases disappointing. One of the problems is caused by the need to monitor the rainfall at frequent intervals of distance along the radio path. Heavy rain is required to produce noticeable attenuation at frequencies up to about 10 GHz and such rain tends to originate from cells embedded in the general area of rain. CCIR Report 563-1 gives the size of the average rain cell as a function of rainfall rate. The values reproduced below were based on direct or indirect measurement in three different climatic zones. Estimated values of rain cell size based on meteorological observation in the UK (ref 6) are given for comparison.

Rainfall Rate	Diameter of Cell	
	CCIR Best-fit Curve	UK estimate
75 mm/hour	2.4 km (average)	1.5 km
50 mm/hour	2.8 " "	2.0
25 mm/hour	3.5 " "	3.0
10 mm/hour	4.8 " "	5.0

Generally the attenuation experienced is greater than the predicted value and tends to the maximum possible values permitted by the theories. The attenuation experienced, both in extent and frequency of occurrence will obviously depend on the location. Figure 15 shows rainfall rates for two locations, one in North West Europe and one in

Singapore. There is very little difference in incidence of low rainfall rates between these two very different climates but in the range of 10mm/hour (heavy rain) to 50mm/hour (downpour) the incidence is roughly five times less for N.W. Europe. These rainfall rate distributions have been used together with predicted attenuation at 15 GHz to produce the predicted annual distribution of rain attenuation in figure 16. At the 0.1% incidence level the predicted attenuation is 0.6 dB/km for NW Europe and just over 2 dB/km for Singapore. For comparison, the equivalent values when operating at 8 GHz would be approximately 0.1 dB/km and 0.3dB/km respectively. The results show that even though predictions tend to be on the low side by a factor of about 2, when considering operation in Europe and using the allocated radio relay frequency bands, it is only at 15 GHz that allowance needs to be made for rain attenuation either when designing the equipment or subsequently deploying it in the field. Snow will also cause attenuation but there is no adequate theory to account for this type of precipitation attenuation. In the light of the difficulties associated with rain attenuation and bearing in mind the variable quality of snow the problem of relating snowfall rate observations to attenuation may remain for some long time.

2.9 Fading caused by changes in the atmosphere's refractive index when the atmosphere is not well mixed, is generally observed only on radio links above about 1 GHz. The phenomenon is usually restricted also to fairly long links of the order of 50 km or more. Given these conditions, fades as great as 40 dB may be encountered. The deepest, most rapid fades probably involve multipaths and should therefore be frequency dependent. The depth of fades for a given percentage of time should also increase with frequency and with distance. The results of experiments available at the time the author was carrying out a survey in support of defining a future radio relay system, did not bear this out. The results are shown in table 1.

TABLE 1: MEASUREMENTS OF FADING ON MICROWAVE, LINE OF SIGHT, OVERLAND LINKS

Author (Reference)	Path Length (km) Location	Frequency GHz	Duration of Test	Fading(dB)		Time of Year
				1% of time	0.1% of time	
Carrassa (7)	189 Italy	1.0	1 month	-	27	Worst month
Matwich, Nuttall (8)	32 USA	1.0	4 months	9	20	Summer
"	"	2.0	"	9	25	"
Miller, Byam (9)	68 USA	2.0	Jan-Mar Jun-Oct	4 8	6 17	
Miller, Byam	"	4.0	Jan-Mar Jun-Oct	6 11	10 18	
Durkee (10)	64 USA	4.6	7 months	17	22	
Crawford, Jakes (11)	27 USA	4.2	4 months	7	18	Summer
"	"	4.2	"	-	7	Winter

The experiments of Miller and Byam (ref 9) were carried out simultaneously at 2.0 and 4.0 GHz. The results are not significantly different at either the 1% or 0.1% occurrence levels. One expectancy that is borne out is that deep fades occur more often during summer months when the atmosphere will be less well mixed. The results, though inconclusive, are sufficient to indicate that at SHF frequencies the design of a tactical radio relay system should include an in-built signal margin of 20-30 dB. This margin will, under normal circumstances, provide an adequate buffer against both fading and rain attenuation since heavy extensive rain and still, layered-air conditions are unlikely to exist at the same time.

Observations of fading on tactical radio relay links operating in the UHF range do not show a high incidence of deep fading. For example, data obtained from 45 links which were monitored during 23 hour periods failed to reveal any evidence of deep fading. The median value of fluctuation observed was only 1.2 dB with only one instance of fade exceeding 3 dB during the period of observation. The transmission frequency was around 800 MHz and the tests were spread over one year. It is possible that the method

and means of recording failed to detect short deep fades but it is more likely that the results truly reflect an absence of deep fades on short UHF links. Pallant (refs 12 and 13) reported similar results for measurements on a 40 km link at 775 and 850 MHz.

3. PRACTICAL ASPECTS OF TACTICAL RADIO RELAY

3.1 There exists considerable experience on the deployment of radio relay links using the frequency bands below 1 GHz. Although a greater physical clearance is required to establish an unobstructed First Fresnel Zone, the longer the wavelength the greater will be the possibility of receiving an adequate signal on an obstructed path. There is little field experience so far using the frequency bands above 1 GHz where diffraction is much less likely to provide an acceptable signal. It will be necessary for operation in the SHF bands to establish line of sight conditions and to make some allowance, in the form of a signal margin, for fading and attenuation due to rain. The effect of the fading could alternatively be overcome by using a diversity system, either space or frequency, but, while this is a practical consideration for fixed systems, it is not likely to find application in the tactical environment.

3.2 In the forward area of the battlefield, there will be less time to set up radio relay links and to optimise performance. The need to be particularly prudent in physically shielding and camouflaging the terminal from the enemy would appear to make the VHF and UHF bands, the most favoured for use in the forward area and to use the frequency bands above 1 GHz in the rearward areas where time to set up, duration of the link and distance from the enemy are all more favourable.

3.3 When the network concept for tactical radio relay was developed the VHF band was predominantly used. The need to use the frequency bands below 150 MHz for other systems, particularly those which require to operate while moving, forced the move to the use of the 225-400 MHz band then also the 790-960 MHz band as requirements increased. A new transition to the higher bands is in progress, partly because of the imminent fielding of the new area systems and partly because, once again, of competition for spectrum space below 1 GHz. It is possible that some virtues will be found in this necessity and, as experience is gained, it may prove possible or even advantageous to use SHF links even in forward areas. Data gathered from field exercises certainly indicate that without changing deployment strategy to any great extent it should be possible to make full use of the bands 1350-1850 MHz and 4.4-5.0 GHz. Within certain tactical limitations it should also be possible to make good use of the 14.5-15.35 GHz band and a number of nations are considering specific radio relay uses such as Down-the-Hill and Local Distribution Access in this band. The data which supports these expectations is of link lengths, signal margins and incidence of line-of-sight paths. The data was obtained from observations of a national tactical radio relay system operating in the Federal Republic of Germany. To the extent that the tactical and strategic considerations which cause a particular deployment approach to be adopted are basically the same for most forces in the Central Region of Europe, and because the parameters of the radio relay equipments are similar, the data presented here is probably typical for most other national deployments.

3.4 Figure 17 shows the distribution of link lengths for a total of 312 links. The observations were made on a number of different deployments over a period of one year. The links all operated in either the 225-400 MHz band or the 790-960 MHz band. There was no systematic pre-selection of the links to be reported so the data is representative of a full Corps deployment. The median value of 17 km seems rather low when one considers that the equipments have a path loss capability typically in the range 145-150 dB. The distribution however shows a reasonable incidence of links above 40 km and a few links which begin to exploit the equipment's capability.

3.5 The same deployments were monitored for received signal level. The results are shown in the form of a distribution of signal level margins, in figure 18 for the 225-400 MHz band and figure 19 for the 790-960 MHz band. The signal level margin is defined as that in excess of the signal that is just necessary to produce an acceptable transmission quality in the presence of normal receiver and antenna noise. This was judged to occur at a bit error rate of 1 in 10^5 . The number of paths for which data was available was 290 in the 225-400 MHz band and 275 in the 790-960 MHz band. In both cases the distributions are nearly Gaussian. For the lower of the two bands the median value of signal margin was 22 dB and 5% had a margin approaching 40 dB or more. In the other band the median margin was lower at 17 dB but again 5% had margins well in excess of 30 dB.

3.6 To put these distributions of signal margin into perspective, it is necessary to reiterate one or two aspects of operational needs and path loss calculation difficulties. Operationally there must be a high probability that the link will work at the first attempt and that it is not necessary to devote a long time to optimising a marginal link. Although frequency assigners and system planners have a choice of path loss equations for diffraction paths operating on frequencies below 1 GHz and some design aids such as nomograms or slide rules based on the equations exist, the accuracy achieved and, most of all, the time required has often precluded their use in the field. In addition to developing a path profile between transmitter and receiver and carrying out the calculations, it is necessary, in order for that exercise to be worthwhile, to at least examine the path profiles of perhaps two or three paths between other transmitters and the receiver. In practice therefore, the user has fallen back on experience and used sites and paths that have given good results in the past.

3.7 It must be remembered that the results although taken from field exercises were from an unusually benign environment. As far as could be ascertained the operating condition was determined by receiver noise. In a battlefield environment the performance of many receivers will be determined by noise plus interference. The interference may be unfriendly, that is to say jamming or it could be friendly in the sense that it is not intentional. In time of crisis the "friendly" interference may arise from lack of frequency allocations within a particular Corp area, the need to operate in adjacent Corps areas or the need to make decisions regarding assignment of frequencies without having all the possible data required about the electro-magnetic environment in a dynamically fluid situation. In these circumstances the antenna bearing for maximum received signal strength may not be the bearing for maximum signal to noise plus interference. Assessed against this potential background the signal margins do not appear excessive.

3.8 Whether the paths whose signal margins are shown in figures 18 and 19 could be operated at frequencies in the SHF range will depend in part on whether line of sight conditions could be established. From the same basic data, it was possible to plot profiles for 310 links and test them for First Fresnel Zone clearance using equation(3). The results are tabulated below for spot frequencies within the different radio relay bands:

Table 2: Availability of Line of Sight Paths

	Number	Percentage of Total
Having LOS at 15 GHz and above	219	71
5 GHz and above	189	61
1.6 GHz and above	168	59
800 MHz and above	144	47
300 MHz and above	89	29
Total	310	

The results are shown graphically in figure 20. The percentage having optical line of sight was 78% and it is the added requirement of having FFZ clearance that reduces the number of links qualifying. The results suggest that the main problems of propagation and its prediction on these links would have been due to reflections as opposed to diffraction. Assuming that the paths are representative of future deployment intentions, it appears that not only will it be possible to operate a high percentage of links in the SHF band but, by avoidance of reflecting surfaces, the uncertainty in path loss calculation and hence link performance will be reduced.

4. FUTURE POSSIBILITIES

4.1 The performance characteristics of most tactical radio relay equipment are likely to be basically unchanged for the next twenty years or more. Most NATO nations are in the process of fielding new equipments for the area systems and the only changes that might occur therefore are in the areas of deployment strategy, antenna design and, when the system planner is in the position to choose, to use the higher or highest frequency band for a particular link. The use of both vertically and horizontally polarised antennas may also be adopted as an aid to frequency assignment.

4.2 In the treatment of propagation problems and specifically the calculation of path loss, the use of computers in the field has commenced. Although many nations have stored in computer, digitised terrain data, initial attempts to use computer assisted methods of path loss calculation in the field do not use terrain data. Terrain height values have been extracted from contour maps, usually by manual processes. The area under consideration is treated as a large grid and spot heights are noted at regular intervals and recorded against the appropriate coordinates. Typically, intervals of 500 metres may be used for gently rolling terrain, 250 metres for hilly terrain and 125 metres for rugged, closely contoured terrain. The computer is programmed to interpolate between adjacent spot values when producing a path profile between a pair of geographic coordinates. To map a Corps area could require nearly half a million spot values and for application in the battlefield, data concerning a much larger area needs to be stored or available on short notice if flexibility of deployment is to be maintained. This prevents for the moment the use of rigorous methods of calculation and forces the use of statistical methods such as those represented by Egli. This limitation will probably be removed when computers of larger storage capacity, and of specification suitable for military, battlefield use, become available and also when progress has been made in the ability to exchange terrain data. This would present the possibility of making knife edge diffraction and reflection calculations.

4.3 The main benefit to be obtained from the introduction of computer assisted methods in the field will be the greater ability to make in a very short time meaningful signal to interference calculations even if statistical equations have to be used. In spite of an apparently generous allocation of frequencies for tactical radio relay, constraints imposed by multiple installations at a co-site, dense deployments placing other co-sites within interference range, and the need for autonomous operation of other radio relay systems in adjacent Corps areas, all combine to create significant problems in making efficient network-wide frequency assignments. This problem would exist even if the error in path loss prediction could be reduced to zero and as long as either the assignment

algorithm can take some account of the propagation prediction errors or alternative solutions to the frequency assignment problem can be generated then the first benefit of the computer will be to meet the need for speed in making the necessary co-site and intersite calculations. Improvement in the accuracy of predicting signal to interference will probably then follow partly out of necessity but also out of the enhanced opportunity to compare computer prediction with results.

REFERENCES

1. Bullington, K. "Radio Propagation at Frequencies above 30 Megacycles" Proc. I.R.E., Oct 1947.
2. Epstein, J., Peterson, D.W., "An experimental study of wave propagation at 850 Mc/s" Trans. I.R.E. Antennas and Propagation, April 1955.
3. Deygout, J. "Multiple Knife Edge Diffraction of Microwaves". IEEE Trans. Vol. AP-14, July 1966.
4. Egli, J.J. "Radio Propagation above 40 Mc/s over Irregular Terrain" Proc. I.R.E., October 1957
5. Ryde, J.W., Ryde, D. "Attenuation of centimetre waves by Rain, Hail and Clouds" Rept. 8516. General Electric Co. Research Labs. Wembley, England. May 1945.
6. Briggs, J. (Met. Office, Bracknell, UK) Private Communication, 1970.
7. Carassa, F. "Prove di Propagazione con le Frequenze di 250, 500, 1000 MHz". Alta Frequenza 25, 1956
8. Matwich, H.R., Nuttall, E.D., "Propagation test on 955.5 MHz, 1965 MHz and 6730 MHz". J. American Inst. Elec. Eng. 1957.
9. Miller, J.E., Byam, L.A. "A Microwave Propagation Test". Proc. I.R.E. 38. No. 6. June 1950.
10. Durkee, A.L., "Results of Microwave Propagation Tests on a 40 mile Overland Path". Proc. I.R.E. 36 No. 2, Set 1948.
11. Crawford, A.B., Jakes, W.C. "Selective Fading of Microwaves". Bell Systems Telephone Journal No. 31. 1952.
12. Pallant, K.R., "Propagation Measurements over Short Non-Optical Paths at UHF". GEC Report No. 14150C. April 1962.
13. Pallant, K.R. "Further Propagation Measurements over Short Non-Optical Paths at UHF". GEC Report No. 14256C. October 1962.

Acknowledgement

The field data on tactical radio relay systems quoted in this paper is due to the U.K. Ministry of Defence. Mr. A.M.J. Mitchell of the Royal Signals and Radar Establishment, Malvern initiated the efforts to collect the data and was also responsible with the author for the data processing and original presentation.

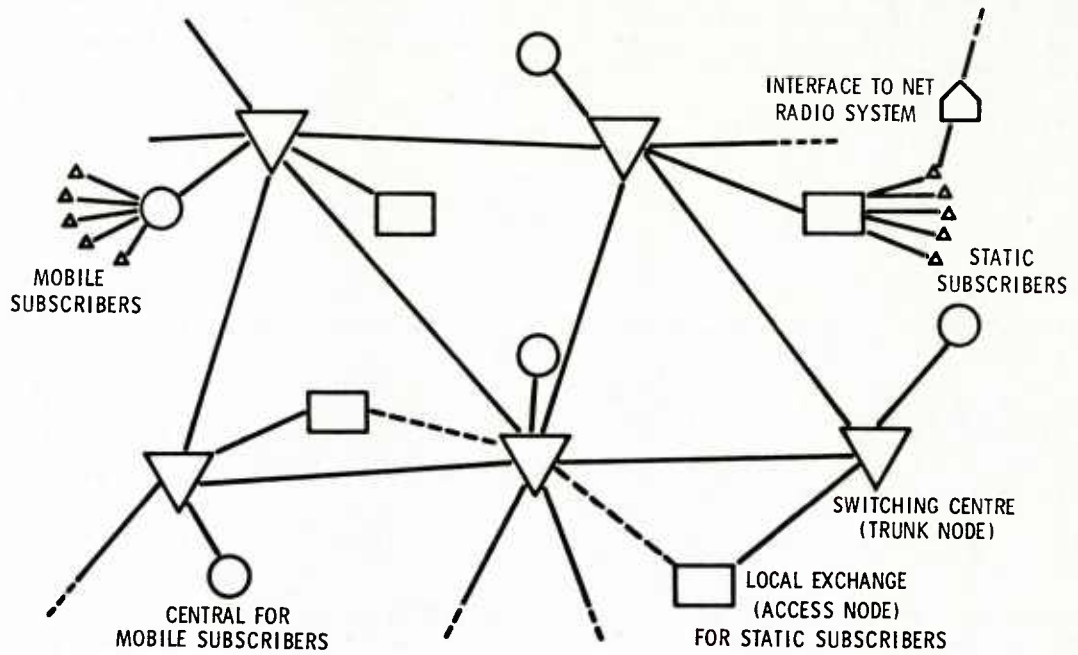


Figure 1. PORTION OF AN AREA TRUNK COMMUNICATION SYSTEM

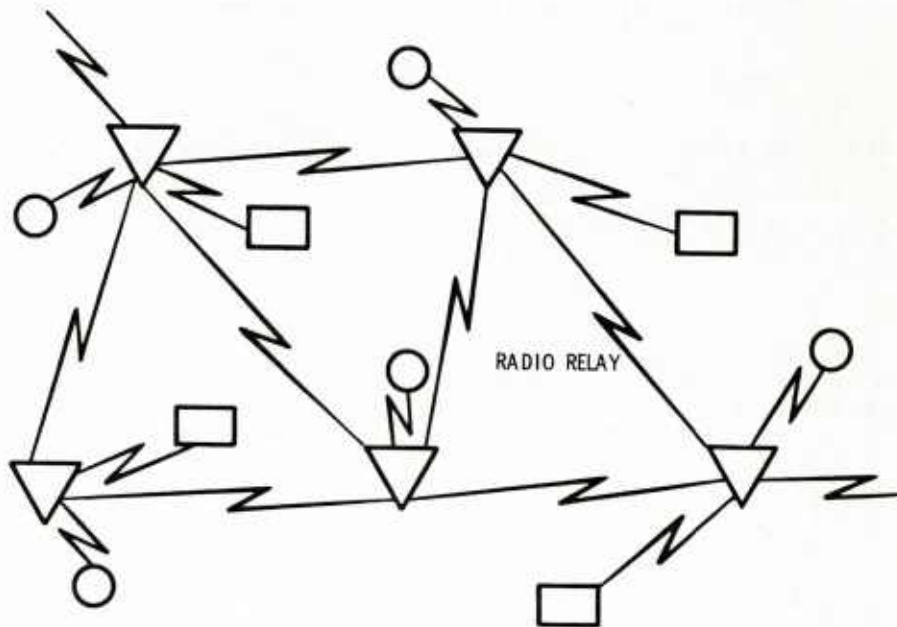


Figure 2. TACTICAL RADIO RELAY LINKS IN THE AREA COMMUNICATIONS SYSTEM

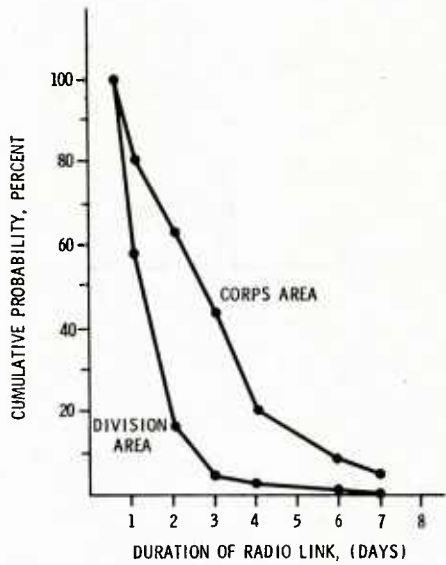


Figure 3. DISTRIBUTION OF LINK DURATION

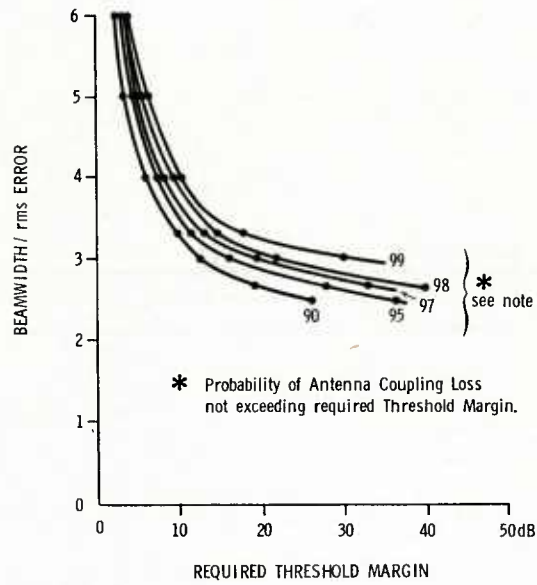


Figure 4. DEPENDENCE OF REQUIRED THRESHOLD MARGIN ON BEAMWIDTH / RMS ERROR

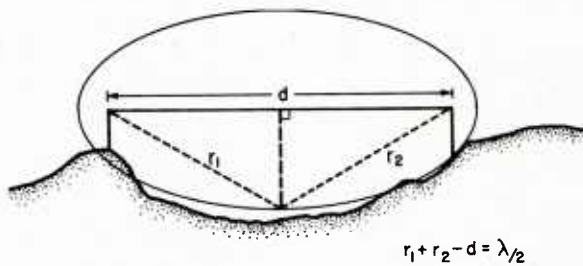


Figure 5. FIRST FRESNEL ZONE ELLIPSE

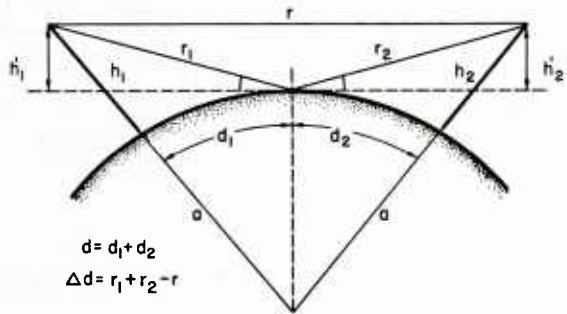


Figure 6. REFLECTING PATH OVER SMOOTH SPHERICAL EARTH

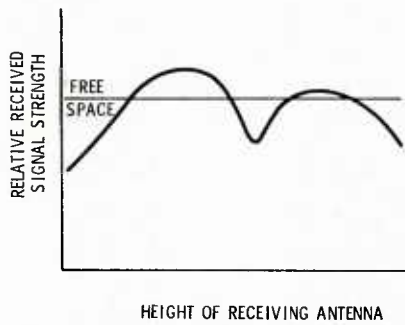


Figure 7. VARIATION OF SIGNAL STRENGTH WITH HEIGHT IN THE REFLECTING REGION

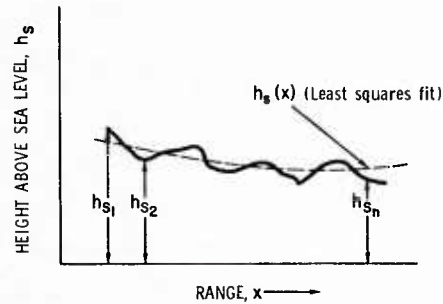


Figure 8. CURVE FIT TO ROUGH TERRAIN TO OBTAIN EQUIVALENT REFLECTING SURFACE

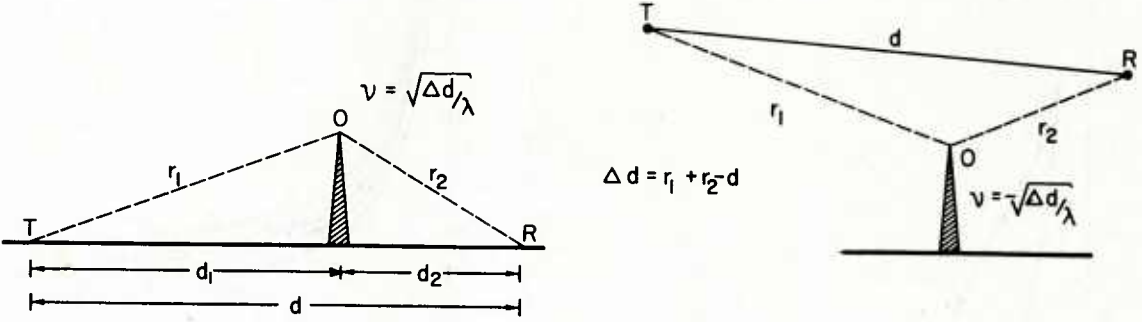


Figure 9. KNIFE-EDGE DIFFRACTION

MULTIPLE KNIFE EDGES

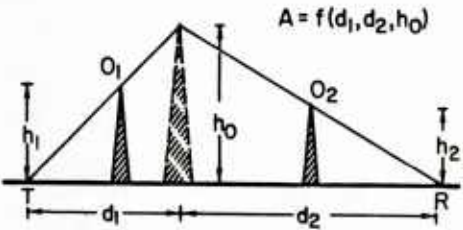


Figure 10. BULLINGTON METHOD

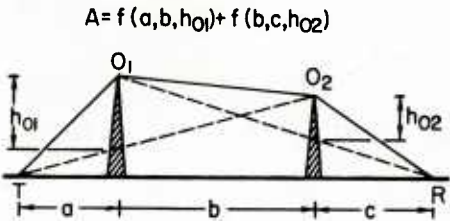


Figure 11. EPSTEIN-PETERSON METHOD

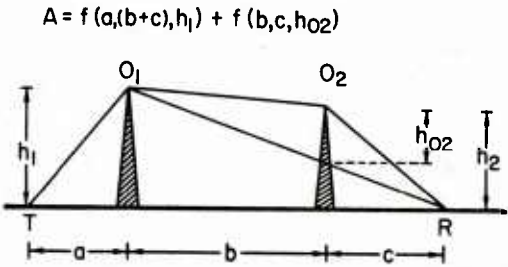


Figure 12. DEYGOUT METHOD

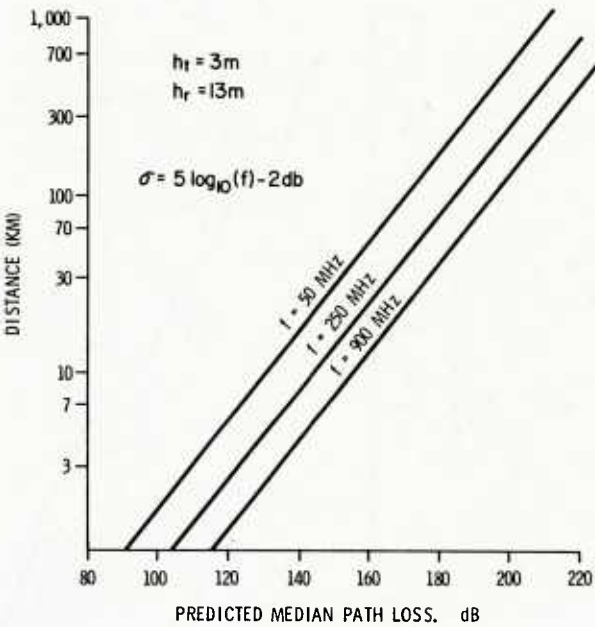


Figure 13.
EGLI STATISTICAL PATH LOSS PREDICTION

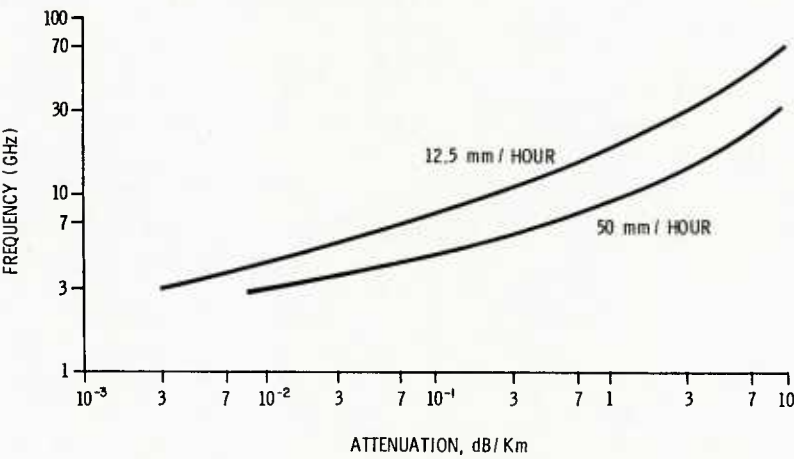


Figure 14.
RAIN ATTENUATION AS A FUNCTION
OF FREQUENCY. (RYDE THEORY)

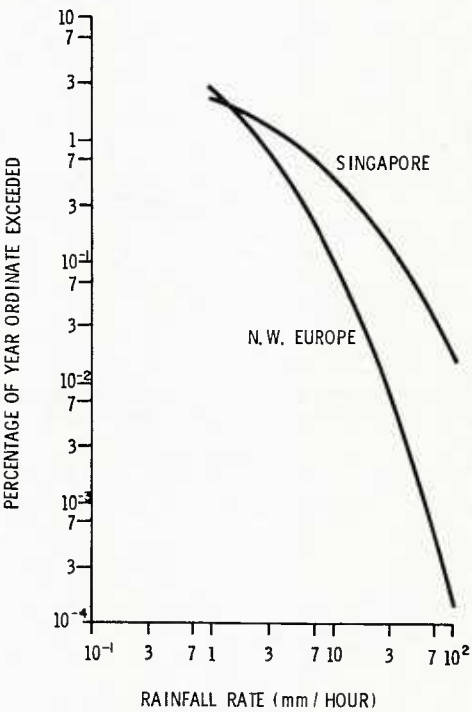


Figure 15.
RAINFALL RATE DISTRIBUTIONS

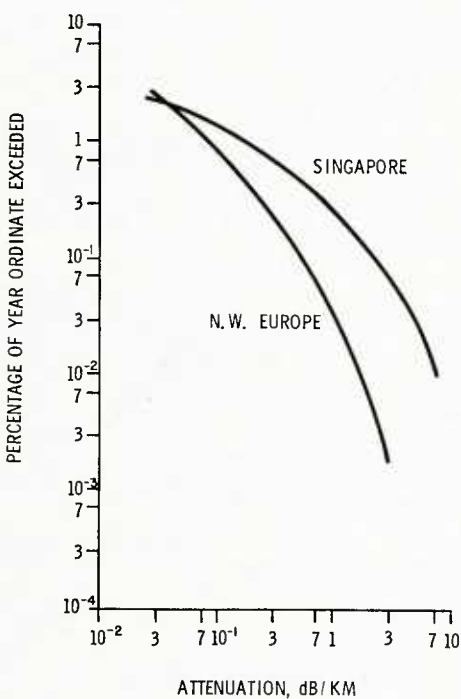


Figure 16.
PREDICTED RAIN ATTENUATION
DISTRIBUTION AT 15 GHz

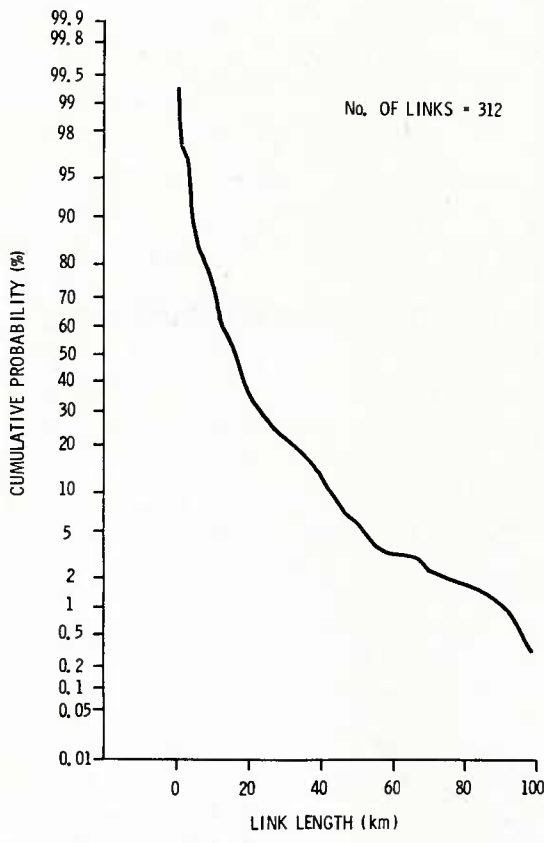


Figure 17. DISTRIBUTION OF LINK LENGTHS

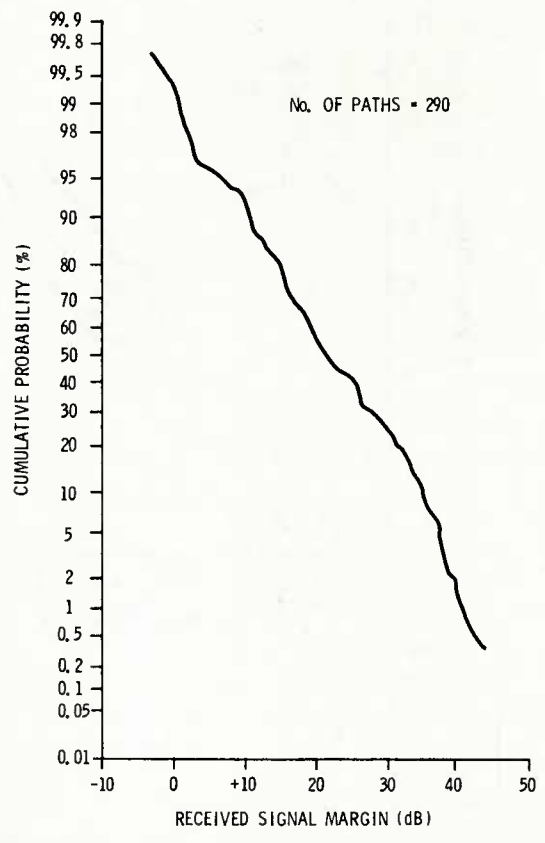


Figure 18. DISTRIBUTION OF SIGNAL MARGIN, 225-400 MHZ BAND

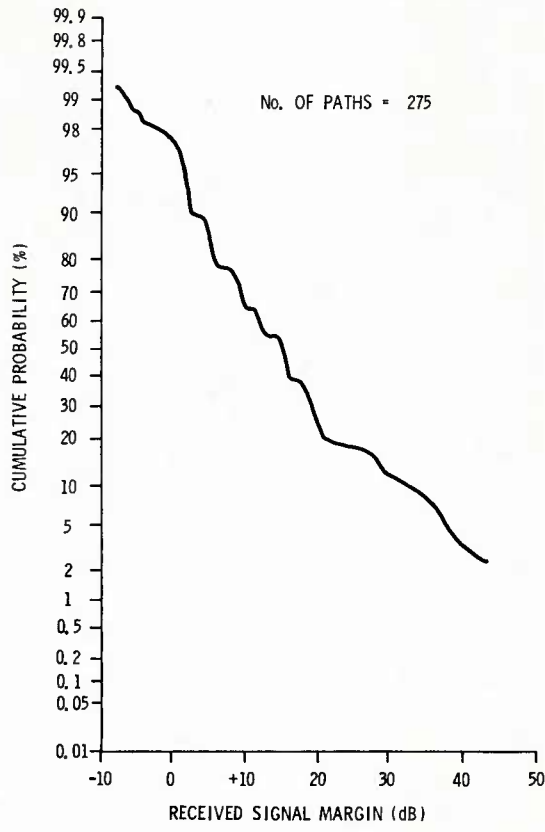


Figure 19. DISTRIBUTION OF RECEIVED SIGNAL MARGIN, 790-960 MHz BAND

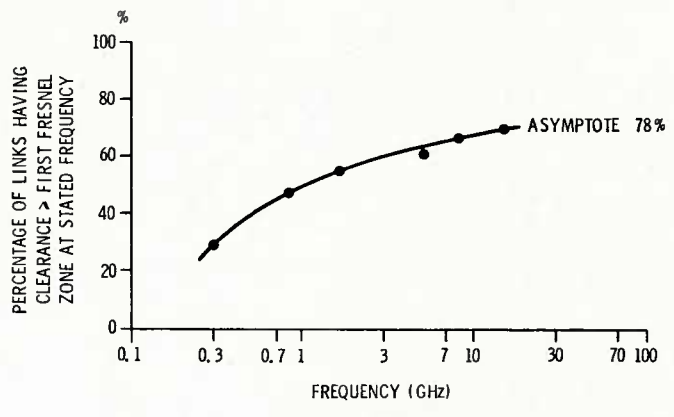


Figure 20. INCIDENCE OF LINE OF SIGHT LINKS

PROPAGATION PROBLEMS ASSOCIATED WITH AIRCRAFT COMMUNICATIONS SYSTEMS

by

Dr B Burgess
 Royal Aircraft Establishment
 Farnborough
 Hants
 GU14 6TD
 UK

SUMMARY

Communications with mobiles is assuming increasing importance in a military context, with the advances in technology enabling not only greater amounts of information to be transferred, but also fostering a much harsher electromagnetic environment. The trend towards digital communications systems coupled with the possible demand for wider bandwidths means that the propagation medium characteristics that influence the performance of these links are somewhat different from those that need to be addressed for narrowband analogue modulation transmissions. The paper will review the various types of communications systems that are used with aeromobile platforms and will then discuss the various propagation problems that arise in achieving systems with good overall performance. The links are conveniently divided into two types, viz beyond-line-of-sight and line-of-sight systems, and span the frequency range from LF through to microwaves.

1 INTRODUCTION TO AIRBORNE COMMUNICATIONS

In discussing propagation influences on aeromobile communications it is worthwhile to have some perspective of the developments of the subject, which will help to give a better appreciation of the problems that the transmission medium imposes on the systems that have been and are being developed.

Aircraft communications goes back to almost the start of flying. Wireless had been tried out in airships and aircraft for some time before the First World War; in the UK Marconi and the Royal Engineers had mounted an experimental wireless set under an airship at the Royal Aircraft Establishment (then the Royal Aircraft Factory) in 1911. The transmissions were in the frequency band somewhat below the current HF band (3-30 MHz) at frequencies we would not refer to as MF (300 kHz - 3 MHz). During the First World War wireless sets were operated at these frequencies and used long wire antennas that trailed from the aircraft (Ref 1); this form of communication was used more extensively in aircraft than on the ground in the forward areas of the Western Front. Prior to World War II, communications with aircraft was almost entirely by HF, and commonly employed hand-operated morse. However it is of interest to note that as early as 1928 the first trials of voice air-ground communications were being made in the USA and in that country there was no transition from morse to voice in airborne communications (Ref 2).

World War II saw the development and introduction of VHF (~100 MHz) for airborne communications (Ref 3). This was employed for the control of fighter aircraft during the Battle of Britain, and the end of the war saw VHF in general use in military air fleets with longer term plans to go the 225-400 MHz band. Just after the end of World War II, before VHF Air Traffic Control communications were fully implemented, air-to-ground communications were conducted using frequencies between 3 and 6 MHz and ground-to-air communications at about 300 kHz. Using these frequencies comments such as "why can we hear the broadcast bands loud and clear but ATC communications is terrible?" were common; and where air-to-ground communications were often found to be poor whereas the same ground station could receive distant broadcast stations (> 1000 km) loud and clear. These type of problems will be returned to later in the paper.

As of today the VHF (AM) band, 118-136 MHz, is used for Civil Air Traffic Control communications and the 225-400 MHz UHF band for military air-ground communications. These frequencies are of course constrained by line-of-sight (los) propagation and any communication link between the ground and aircraft at ranges beyond line-of-sight (blos) require the use of HF frequencies or some form of relay mode.

In the early 1960s with the emergence of satellite communications, the possibility of high quality communications for blos ranges was with us. While air-ground communications via satellites has been demonstrated (Ref 4), with superior quality to HF, it is still not, even today, evident in aircraft use, except in a few special applications. One of the main reasons for this state is the cost of satellite communications, including its airborne installation. While UHF frequencies can be used for aircraft-ground communications using satellites, SHF frequencies, or the EHF band, are more likely to be used in the longer term.

The above remarks have been concerned with communications to fixed wing aircraft. Over the last twenty years rotary wing aircraft (helicopters) have come into widespread use, and in some Air Forces are used in comparable numbers to fixed wing aircraft. Where control is by civil or military Air Traffic Control Authorities they will use VHF or UHF frequencies as mentioned above. However since the Army uses this form of air transport there is a need to use communications compatible with that of the Army; this is usually in the VHF (FM) band, 30-88 MHz. For ranges which are beyond line-of-sight, and for helicopters these can be relatively short, recourse to HF communications may have to be made.

In summary, for aircraft communications the frequency bands currently used range from LF (ground-to-air only) and HF for long range operations, through the VHF (FM) and VHF (AM) bands to UHF for short range line-of-sight use. There are a few special links which use VLF (10-30 kHz) and satellite communications, the former being highly unlikely to find general use while the latter form of communications may become

more widely used by aircraft when costs are reduced significantly in the longer term. There is still one type of communications system to be mentioned which will come into use in the near term future. This system is a relatively high capacity data link for tactical aircraft use (Ref 5). The data link will operate in the 960-1216 MHz band and will share the band with aeronautical navigational users. Unlike other air communications systems very advanced modulation schemes will be employed mainly to protect the transfer of information from deliberate interference, ie frequency hopping and direct sequence spread spectrum over the whole 960-1216 MHz band. By contrast modulation techniques used, at LF and HF are (1) for slow speed data, frequency shift keying (FSK), say 85 Hz for LF and 850 Hz for HF frequency shifts, and (2) single sideband (SSB) for voice transmissions at HF within a 3 kHz band. At VHF and UHF voice transmissions are contained in basebands of some 25 to 100 kHz, using either AM or FM modulation. Table I summarises the above facts.

TABLE I

Band	Frequency	Service	Modulation
LF	< 300 kHz	Low Speed Data	FSK
HF	2- 30 MHz	Voice Radio Teletype	SSB FSK
VHF (1)	30- 88 MHz	Voice	FM
VHF (2)	118- 136 MHz	Voice	DSB AM
UHF (1)	225- 400 MHz	Voice	DSB AM
UHF (2)	960-1215 MHz	Data	MSK/Spread Spectrum

Modulation and services in common use in aircraft communications systems

2 FACTORS INFLUENCING SYSTEM PERFORMANCE

Before considering in detail propagation problems associated with the above-mentioned aircraft communications systems, discussion will be made of some of the constraints that are imposed on the communications system performance because the system is an aeromobile one. The interaction of these system constraints with propagation constraints will follow naturally in the later sections of the paper.

Consider Figure 1 which gives in block form the components of a communications system. At the outset it is important to appreciate the difference between a mobile air-ground circuit and a point-to-point or broadcast circuit. On a point-to-point circuit advantage can be taken of the fixed transmission path in order to use directive antennas at both ends of the link in order to give high gain or directivity. This is not generally possible with aeromobiles, especially in the military context, where low gain antennas are employed on the ground in order to give wide geographic cover, while on the aircraft, due both to its size compared to wavelength of transmission or reception, and also its mobility, the antenna must essentially be characterised by omnidirectional coverage. Thus on antenna considerations alone the link budget can suffer some tens of dB degradation compared with fixed links.

Turning to the transmitting characteristics, the aircraft transmitter is usually some 10 to 20 dB lower in output power than those available for ground use; this is mainly due to limitations in aircraft power supplies. This is not too serious at VHF and UHF frequencies, though in the HF band ground transmitters can often be used with powers in excess of 10 kW and usually in the hundreds of kW range compared to an aircraft's use of 40-400 W transceivers. With both the variability in ionospheric propagation and also the noise and interference in the HF band, coupled with low gain antennas and low power transmitters, it is not surprising that early users queried why their communications were so poor compared with the broadcast bands.

Maslin (Ref 6) has considered these factors in detail when dealing with the assessment of HF broadcast airborne communications reliability. Figure 2 gives an example of a power budget for a HF long range sky wave propagation at night. The vertical axes are scaled in power and the horizontal axis has an arbitrary scale representing progression from the transmitter power output through to the receiver input. Note the dominating contribution of the propagation path loss. In this particular case where power budget links at 4 and 9 MHz have been shown, whereas the propagation loss at both frequencies are similar, the overall signal-to-noise ratio is some 25 dB at 9 MHz, which would be totally satisfactory, but at 4 MHz a totally unacceptable value is obtained. The reason for this major discrepancy is the very poor radiation efficiency of the aircraft antenna at 4 MHz.

The mobility of the airborne terminal can also constrain some of the communications transceiver's characteristics. The movement of an aircraft away or towards a ground transmitter can result in a Doppler shift of the transmitted carrier by 1 Hz/MHz/Mach Number, approximately. Thus a carrier radiating on 100 MHz being received by an aircraft travelling at Mach 2.0 would suffer a Doppler shift of approximately 200 Hz. Thus any modulation scheme used for data or voice must be designed to cope with these carrier frequency shifts; so must all the various filters designed in the receiving systems.

Lastly a factor which affects aeromobile systems significantly as all frequencies which are of much less importance for ground users is that of multipath. For line-of-sight systems, ie those using frequencies appropriate to the VHF, UHF and 1 GHz bands, where one end of the link, or both are elevated, an indirect path via reflections from the ground can have very marked effects on the performance of communications systems. In the next section cases will be discussed which consider low flying aircraft information and aircraft/ground links over sea paths where these problems are discussed. In a similar way, beyond line-of-sight links also suffer from multipath but in these cases the ionosphere is the main cause for concern. The limitations that this phenomena puts on modulation schemes will be discussed. While analogue modulation schemes can be relatively tolerant of this effect, digital links, which are becoming increasingly

important, can be highly susceptible to multipath unless certain ameliorating steps are taken.

3 PROPAGATION EFFECTS ON SYSTEMS

In order to discuss propagation effects in aircraft communications, applications in each of the frequency bands will be taken, ranging from LF for broadcast uses, through HF and how problems associated with the ionosphere can be overcome to the effects of multipath in line-of-sight systems causing degradation of voice circuits and data links. In all these cases an understanding of the propagation considerations leads to means of improving or alleviating the problems.

3.1 Air-Ground LF Communications

Williams and Ince (Ref 7) discusses the factors that influence the reliability of low data rate LF radio communication links. While the approach taken will give a statistical estimate of link reliability the propagation model upon which the system study is based is limited due to the lack of sufficient observational data. Low frequencies (LF) propagate well over sea water, but with significantly higher attenuation over land paths. The effects of the ionosphere on LF propagation has been well reviewed by Belrose (Ref 8), but a reliable means of predicting LF coverage out to ranges of the order of 3000 km is still awaited. Figures 3 and 4 show a plot of signal strength against distance of transmissions from two transmitters in UK on frequencies of 45 and 60 kHz under daytime conditions. These were taken onboard an aircraft flying in a Northerly direction from the transmitter. The dominant characteristic of the received signal is its very stable amplitude, ie no fading of any appreciable magnitude. However a very deep minimum in signal level is associated with the 60 kHz measurements at a range of some 1300 km from the transmitter, while at 45 kHz, no such minimum is observed. It is generally accepted that this type of result can be explained by the combination of ground wave and one-hop skywave transmissions at these frequencies; propagation conditions remaining very stable with time and thus one observes either constructive or destructive interference between the multipath transmissions which must change extremely slowly with time. At night-time, with different skywave propagation conditions, a significantly different signal strength against distance plot is obtained. Figure 5 shows such a plot for the 60 kHz transmissions from MSF, Rugby, England. Strong skywave interference occurs from some 200 km outwards with interference minima of some 20-30 dB magnitude.

These measured signal strength plots have been generally accounted for (Ref 9) by using Waveguide mode and Wave-hop theory (Ref 10) with appropriate models of the lower ionosphere. These type of measurements however are not predictable from any recognised prediction model as yet, though the major researches necessary for this have already been undertaken (Ref 11).

3.2 HF Communications to Small Aircraft (Ref 12)

It is often necessary to communicate with aircraft or helicopters at ranges that are relatively short (50-500 km), yet because of their flight profiles they are beyond line-of-sight. For small airborne platforms difficulties in communications arise from a number of factors in these situations.

- (a) For small aircraft the antenna efficiencies are poor at the low end of the HF band, and this coupled with the limited power onboard an aircraft means that the effective radiated power at these frequencies can be only of the order of a watt or less.
- (b) At these ranges of 50-500 km, when using skywave modes, frequencies at the lower end of the HF band must be used (see (a) above).
- (c) Interference in the 2-6 MHz band at night is normally high, since low MUF's tend to crowd users into this part of the HF band.
- (d) The rapid variation in optimum working frequency with range for the short distance considered here, imposes an almost unacceptably high workload for the aircrew.
- (e) Ground station antennas often do not have adequate high angle performance; also the need to cover a wide range of azimuths means that directive antennas cannot be used on the ground.
- (f) Propagation paths in auroral regions can be subject to severe attenuation which tends to vary as the inverse square of the frequency.

Maslin (Ref 12) has attempted to quantify this problem and suggest appropriate solutions to obtain the best available performance for such a link. He looked at four propagation paths appropriate to ranges between aircraft and ground station of 250, 1200, and 2500 km. For the 2500 km range he took two paths that were well separated in latitude. For each path the predicted median signal to noise ratio was calculated and the results are shown in Figures 6, 7 and 8. In these figures, the short range station is designated W, while the medium and two long distance stations are designated X, Y and Z respectively. Further shaded blocks correspond to those frequencies that can sustain a signal to noise density ratio in excess of 45 dB in steps of 5 dB. Since the signal to noise density corresponds to median values, the achievement of a given criterion gives a communications reliability of about 50%. Thus cross hatched squares in the figures indicate signal to noise density values between 55 and 60 dB, indicating that a 50% reliability or greater would be produced for a SSB voice link working in a 3 kHz bandwidth channel with a signal to noise density equal to 55 dB.

Examining Figure 6, which is for a 250 km link, shows that satisfactory communication only occurs for a few hours a day throughout the year, and in the summer in particular, a link would most likely be not available.

Figures 7 and 8 show the results for longer path links, viz 1200 and 2500 km respectively. It is evident that better coverage in the length of time of day that can support satisfactory communications can be achieved, though no individual link can give a full coverage over the whole day. Of interest also is

that the longest range (2500 km) whilst giving the longest cover in the 24-hour period, does not in general have as high a signal/noise density as the 1200 km link.

Figure 9 illustrates the maximum signal to noise density obtainable for any frequency for a given hour of a day by a small aircraft transmitting in both high and low sunspot number years; a combination of all path lengths (250, 1200 and 2500 km) has been taken. It is evident that a 55 dB signal to noise density criterion can be achieved for a large percentage of the day by using the longer path circuits.

A particular valuable feature of using more than one remote station is that a reasonably constant signal to noise density can be achieved throughout a 24-hour period provided that different ground stations are used at different times of day. If these remote stations are at various ranges and on different bearings from the aircraft, planning could probably eliminate the need for any frequency change. This would be of great advantage for the crew of small aircraft. These advantages and others are given by Maslin and are shown in Table 2.

TABLE 2

Factors connected with using remote ground receiving stations

Requirements for remote station working		Consequences of using remote stations	
A	Only frequencies above ~ 7 MHz are required	1	Poor aircraft antenna efficiencies are avoided
		2	Interference is reduced at night since lower frequencies are employed by other users
		3	Ground antenna size is reduced
B	Antennas required only narrow azimuthal beamwidth and low angle coverage	1	Good directivity should be obtainable; thus noise and interference can be discriminated against
		2	Antenna steering techniques are not necessary
C	Aircraft should be at least 1000 km from remote stations	1	Frequency changing with time of day is not necessary as often as for shorter range links
		2	Changes in aircraft position will not necessitate frequency changing
		3	For aircraft in Northern waters reflection of signals in auroral regions can be avoided
D	Two or three remote stations ideally required with adequate geographical separation	1	Whole 24-hour period can be covered by using ranges of ~ 1200 km by day, ~ 2500 km by night
		2	Frequency changing can be effectively eliminated by careful choice of ground station operation
		3	Pilot workload is reduced by using a single frequency

The above example has shown how a propagation problem associated with a difficult communication link has by treating it as part of a wider system concept, allowed a solution to the problem through an insight into the propagational behaviour of these links.

In assessing these HF skywave links heavy reliance has been made on prediction programmes that have been developed over the years, in particular by Bradley and co-workers at the Rutherford and Appleton Laboratories in England. An excellent review paper on prediction of HF skywave signal strengths has been given by Bradley (Ref 13) in a recent AGARD Lecture Series.

3.3 Multipath Propagation at UHF

Propagation at VHF/UHF is not normally regarded as a problem as far as air-ground communications are concerned. Provided antenna sitings on both the aircraft and on the ground are addressed adequately propagation effects only play a major role in link performance through the free space loss parameter and terrain influences. Various organisations, such as broadcasting/television authorities have, in the past, undertaken considerable measurement programmes to arrive at coverage maps for their transmissions in these frequency bands. Based upon such information prediction programmes such as those of Gierhart and Johnson (Ref 14) have been produced. The propagation model that they use is applicable between 100 MHz and 2 GHz. Conceptually the model is similar to that developed by Longley and Rice (Ref 15) for propagation over irregular terrain, particularly in that path loss (attenuation) calculated for (a) line-of-sight, (b) diffraction and (c) scatter regions are adjusted to give continuous values through the transition regions. The model includes allowances for (a) average raybending, (b) horizon effects, (c) long-term fading, (d) ground antenna patterns, (e) surface reflection multipath, (f) tropospheric multipath and (g) atmospheric absorption. Other effects such as ducting, rain attenuation, rain scatter, ionospheric scintillation are less common and are not included. However an update version of the programme does now include allowances for some of these effects. In this frequency range, time and space variations are treated on a statistical basis, the statistical variations becoming important at ranges greater than about the radio horizon.

A particularly important feature of the Gierhart and Johnson model is that aircraft altitude is

considered and thus the lobing structure of the antennas is considered and show deep spatial fading patterns.

A comprehensive review of propagation effects of the troposphere on radio communications has been made by Hall (Ref 16) and is recommended for further study of this topic.

3.3.1 UHF voice communications

Air-to-air communications in essence is free of ground effects for most operations; however there is one scenario in particular where ground effects can be very important. If one takes two tactical aircraft flying in formation at low level, they could be at altitudes of several hundred metres and separated up to distances of 1 km. Under these conditions voice communications using amplitude modulation; double sideband (AM-DSB) can be severely degraded (Ref 17). A basic mechanism of this communications degradation is believed to be multipath, ie a direct path between aircraft plus multiple indirect waves which are reflected and/or scattered from the terrain below. An analyses of this effect can be put in perspective by quoting from Stratton (Ref 18, p507) on the subject of reflection from a plane lossy dielectric, ".... the complexity of what appeared to be the simplest of problems - the reflection of a plane wave from a plane absorbing surface - is truly amazing". Following on from this it will be appreciated that real terrains exhibit topographical features whose scale vary from small to large in comparison with the wavelength employed (in the region of 1 metre) and its complex dielectric constant may vary considerably with location and with water content. Aircraft antenna radiation patterns are usually highly structured, so that ground illumination is complex and both direct and indirect signals may be affected significantly by aircraft attitudes. The aircraft traverses the terrain at high speeds (say 200 to 300 metres/second) so that correspondingly rapid phase and amplitude fluctuations of the indirect signal are to be expected; there is often appreciable aircraft vertical motion which adds further to the effects.

Pavey (Ref 19) has made a detailed study of this effect and following Beckman and Spizzichino (Ref 20) the indirect wave reflected from a rough earth is treated as a combination of specular reflection and diffuse scattering. These two components are distinguished by their phase coherence, the specularly reflected waves combining with the direct wave to give regularly spaced interference fringes, while the diffuse scattering imposes random spatial variations on the reflected wave. Now depending on the characteristics of the ground roughness, which can be measured in terms of a spatial auto-correlation distance (Ref 20, p81), viz a measure of the distance between peaks and troughs, the reflecting surface can act either as a glistening surface or as a corrugated surface. For the corrugated surface case, the first Fresnel zone is less than the spatial auto-correlation distance, while for the glistening surface the first Fresnel zone is larger than the correlation distance. In this latter case the reflection comes predominantly from an elongated region between the two aircraft and may be regarded as an ensemble of scattering patches.

Of importance to the communication link is the fact that the scattered signals exhibit a Doppler frequency shift associated with all the scattering regions. The received reflected signal from the ground thus has imposed upon it a spread of frequencies, whose rms bandwidth can be written in the form

$$2 \alpha v (\sin \gamma_0) / \lambda$$

where α is the rms value of the slope of the ground scattering areas, v is the velocity of the aircraft over the terrain, γ_0 is the grazing angle of the incident wave and λ the wavelength of the transmissions. Putting typical values of the parameters into the above expression shows that noise like signal components will be generated with frequencies of the order of hundreds of Hz at UHF. The frequency bandwidth of this extraneous signal is proportional to the carrier frequency and also velocity of the aircraft. The main terrain characteristic which governs this phenomena is its rms slope α .

Depending upon antenna siting upon the aircraft the received reflected wave can be of equal magnitude or greater than the direct wave. This could easily arise if the antennas were mounted on the bottom of aircraft, and there was appreciable pitch and roll which is quite feasible in low level flights.

Another insight into the effects of the phenomena is to consider the AM-DSB signal which carries the voice information. In the frequency domain, the signal is made up of a carrier and two sidebands, the sidebands carrying the audio voice frequency components. The carrier will contain at least half the power that is transmitted, depending upon the modulation index. Thus due to multipath effect significant power from the carrier can be translated into the audio bands containing the speech information, where the speech energy is already spread over the whole audio frequency band. Similarly the sideband frequencies themselves will also generate other frequency components and thus exacerbate the degradation in performance.

Having understood the basic propagation phenomena, it is now feasible to implement remedies to overcome the effects, but that is outside the scope of this paper, except to say that the remedies studied have given the expected improvement in speech intelligibility.

3.3.2 UHF data link (Ref 21)

As a concluding example of communications system performance dependant on propagation characteristics, the transmission of digital signals will be considered between a helicopter and a ground station (or ship) or between two helicopters over the surface of the sea. The frequencies of interest will be 225-400 MHz (military UHF band) or around 1000 MHz. The geometry of the communication links will generally be such that the height of the helicopters will be small in comparison with the distance between helicopters or helicopter and ground station so that the grazing angle of the sea reflected waves will lie between 0 and a few degrees, ie for vertical polarization waves, at and below the Brewster angle. Thus at the longer ranges one can expect to have contributions from the reflected signals approaching the value of the direct wave and hence interference fringes will appear in the signal against distance plot.

Referring to Figure 10 this interference region is shown as the space above the radio horizon plane and signal amplitude can be calculated from free space propagation theory together with the Fresnel reflection coefficients calculated for sea water. Alternatively one can use Gierhart and Johnson's

(Ref 14) computer programmes, but a physical model will be used here for illustrative purposes. These can be obtained from most standard texts on electromagnetic theory. If the sea is not flat and perfectly smooth but has a roughness factor then recourse to scattering theory has to be made (vide Ref 20 and Ref 22). However at long ranges where the grazing angle will be small, say $< 1^\circ$, and the reflection coefficient large, the roughness factor of a scattering surface indicates that wave heights have to be in excess of 10 metres for a frequency of 300 MHz in order for the sea surface not to be treated as an effective smooth surface. At the plane of the radio horizon the direct and reflected wave are of equal amplitude, have exactly the same path length, but are 180° out of phase, for both vertical and horizontal polarization, and thus the total field is zero or close to zero. In practice the two received signals would not be of exactly equal amplitude.

Beyond the radio horizon (Fig 10) one enters the diffraction region. An extensive treatment of UHF propagation in this region is given in Reed and Russell (Ref 22). In summary, the signal level in this region is smallest at the surface of the earth and gradually increases in strength with height as the radio horizon is approached. Superimposed on this vertical profile is a general decrease in radio field strength with increasing distance from the transmitter. A single height gain function converts ground wave field strengths to elevated field strengths, for any particular terrain, frequency and polarization provided the receiver is below the radio horizon.

A factor which will cause signal levels to depart from free space theoretical values is the influence of atmospheric refractivity. Most actual atmospheric vertical refractivity profiles are not significant to UHF propagation; the radio horizon may vary a little about the value determined for a 'standard' atmosphere, and is normally taken as $\sqrt{(1.5h)}$ n miles, where h is expressed in feet. Certain meteorological conditions, such as temperature inversions, can give rise to an effect known as super-refraction. At these latitudes of Northern Europe this effect is sufficiently uncommon that it can be treated as a special effect. Thus one would expect the theory given above to give reasonable agreement with measured results, but variations from these predictions will be expected due to rough sea effects and atmospheric refractivity changes, especially at the longer ranges.

Figures 11 and 13 give a theoretical plot of signal strength against distance for air-air transmissions over a sea-path with helicopters at 1000 ft and 4000 ft altitude respectively and with transmission frequencies of 237 and 386 MHz. Note the 10-15 dB sinusoidal variations in signal level with distance right out to ranges of some 150 n miles. Figures 12 and 14 give experimental measurements of signal strength at 386 MHz at these same altitudes for air-air propagation paths up to some 150 n miles. The agreement between theory and experiment is quite good. The depths of the nulls vary between 10 and 20 dB and the periodicity of the spatial fading compares favourably with the theoretical predictions.

Of importance to the communications link performance when data is being passed over the link is the bit error rate (ber). In the experiments which recorded signal level against distance and mentioned above, 16 kb/s data was also transmitted and the ber of these transmissions were also measured (Ref 21). It was found that the strongly fading signal, which is characteristic of air-to-air UHF propagation over the sea, was often correlated with periods of alternate high and low ber, the high ber occurring at minima of signal levels. This was very evident in the fading patterns that occurred in the first 30 n mile from the transmitter for the 1000 foot altitude flights. Beyond about 30 n miles the signal strength fades become much slower and the correlation of high ber with low signal level became somewhat displaced, suggesting that a decreasing signal level with time caused more errors than an increasing signal even though the signals were of the same magnitude. This phenomenon is believed to be due to a.g.c. delay in the radio receiver.

While it is evident that better ber performance could be obtained by increasing the transmitted power by the requisite amount, this may or may not be a practical solution in an aircraft. Alternatively it will be noted from the propagation studies that the minimum in signal levels are caused by interference effects that are frequency dependent. With judicious choice of a range of frequencies and using spread spectrum techniques with an error correction code, an adequate signal to noise criteria should be possible in order to give the required ber performance.

4 REFERENCES

- 1 DICKSON, D.A., 1979, "Wireless in World War I Aircraft", Journal of the Royal Signals Institution, XIV, 42.
- 2 WHITE, F.C., 1973, "Air-Ground Communications: History and Expectations", IEEE Trans Comm 21, 398-407.
- 3 GATES, B.G., 1947, "Aeronautical Communications", Journal IEE, 94, Pt III A, 11, 78-80.
- 4 BARNES, G.W., HIRST, D., JAMES, D.J., 1971, "Chirp Modulation Systems in Aeronautical Satellites", AGARD Conference Proceedings No 87, Paper 30.
- 5 BURGESS, B., 1981, "Trends in Future Airborne Communications Systems", Jour. IEE Electronics and Power, 27 No 9, 608-610.
- 6 MASLIN, N.M., 1978, "Assessing the circuit reliability of an HF skywave air-ground link", The Radio and Electronic Engineer, 48, 493-503.
- 7 WILLIAMS, H.P., INCE, A.N., 1967, "Range of LF transmissions using digital modulation", Proc. IEE, 114, 1391-98.
- 8 BELROSE, J.S., 1981, "LF Propagation - an Overview", AGARD Conference Proceedings No 305, "Medium, Long and Very Long Wave Propagation", Paper 20.

- 9 CAMPBELL, P.H.M., 1979, "The Influence of the Ionosphere on Low Frequency Radiowave Propagation", Unpublished Ph. D. Thesis, University of Leicester.
- 10 JONES, T.B., MOWFORTH, K., 1981, "A Review of the Analytical Techniques for Determining the Phase and Amplitude of a VLF Radiowave Propagating in the Earth-Ionosphere Waveguide". AGARD Conference Proceedings No 305, "Medium, Long and Very Long Wave Propagation", Paper 16.
- 11 BURGESS, B., JONES, T.B., 1975, "The Propagation of LF and VLF Radiowaves with Reference to some System Applications", The Radio and Electronic Engineer, 45, 47-61.
- 12 MASLIN, N.M., 1979, "HF Communications to Small Low Flying Aircraft", AGARD Conference Proceedings No 263, "Special Topics in HF Propagation", Paper 3.
- 13 BRADLEY, P.J., 1979, "Propagation at Medium and High Frequencies", AGARD Lecture Series No 99. "Aerospace Propagation Media Modelling and Prediction Schemes for Modern Communications, Navigation and Surveillance Systems", Papers 3 and 9.
- 14 GIERHART, G.D., JOHNSON, M.E., 1973, "Computer Programs for Air/Ground Propagation and Interference Analysis 0.1 to 20 GHz", DoT Report No FAA-RD-73-103.
- 15 LONGLEY, A.G., RICE, P.L., 1968, "Prediction of Tropospheric Radio Transmission Loss over Irregular Terrain, a Computer Method". ESSA Tech. Report. ERL 79-ITS 67.
- 16 HALL, M.P.M., 1979, "Effects of the Troposphere on Radio Communications". Peter Peregrinus Ltd/Institution of Electrical Engineers (London).
- 17 HARRIS, R.M., 1981, "Characterisation of the Dynamical Response of Receivers to Fading". Proc. of I.E.R.E. Conference on Radio Receivers and Associated Systems", pp325-334.
- 18 STRATTON, J.A., 1941, "Electromagnetic Theory". (McGraw Hill)
- 19 PAVEY, N.A.D., 1978, Unpublished MOD Report.
- 20 SPIZZICHINO, A., BECKMAN, P., 1963, "The Scattering of Electromagnetic Waves from Rough Surfaces". (Pergamon.)
- 21 HARRIS, R.M., 1978, "Performance Predictions and Trials of a Helicopter UHF Data Link". AGARD Conference Proceedings No 239 "Digital Communications in Avionics" Paper 20.
- 22 REED, H.R., RUSSELL, C.M., (1966) Ultra-High Frequency Propagation". (Chapman and Hall)
- 5 ACKNOWLEDGEMENTS

Much of the material presented in this lecture was formulated from work undertaken at the Royal Aircraft Establishment, Farnborough over the past five to ten years and I wish to acknowledge the contribution made by my colleagues to this work. A number of them are named in the list of references.

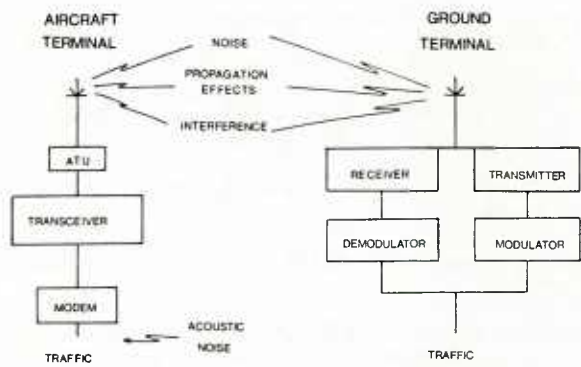


Fig 1 Air-ground communications link

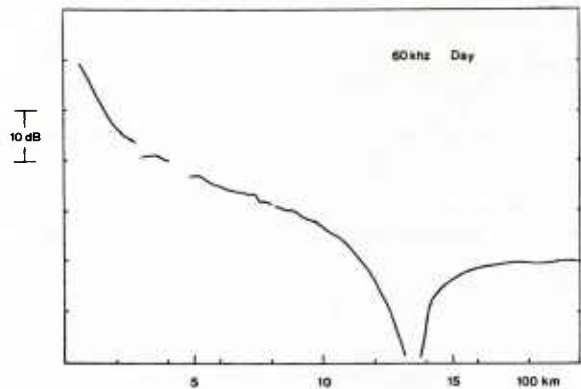


Fig 3 Signal strength variation with distance for transmissions from MSF (Rugby), 60 kHz, daytime conditions

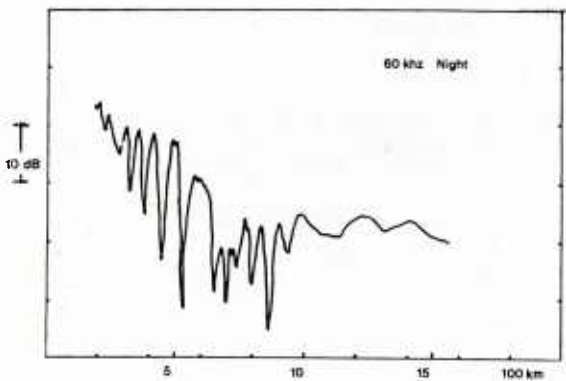


Fig 5 Signal strength variation with distance for transmissions from MSF (Rugby), 60 kHz, nighttime conditions

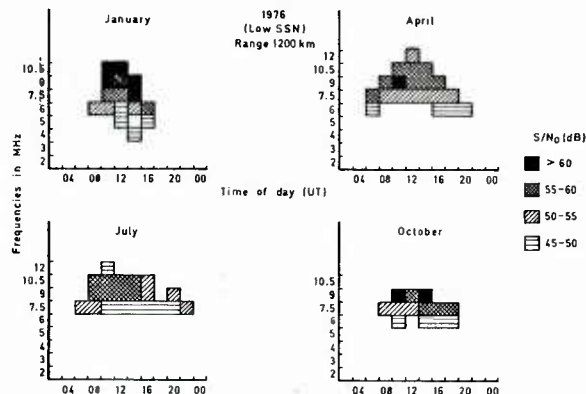


Fig 7 Medium range communications (aircraft to station X)

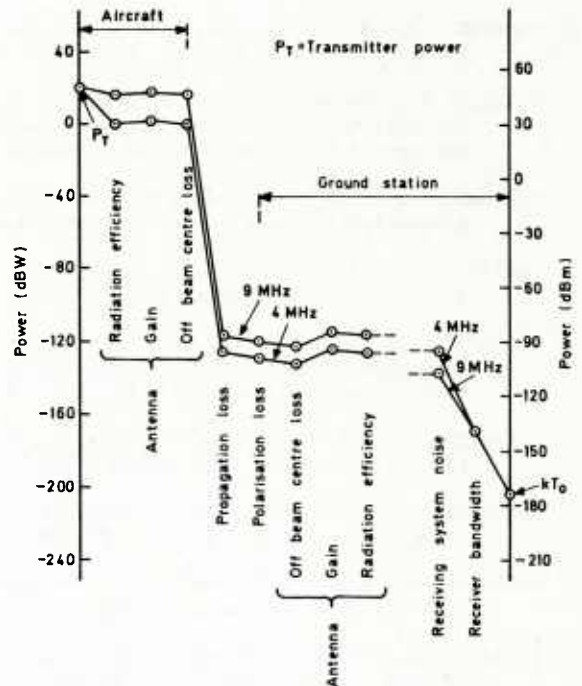


Fig 2 Power level diagram for air-ground link, range 2000 km, low sunspot number, winter midnight (Ref 6)

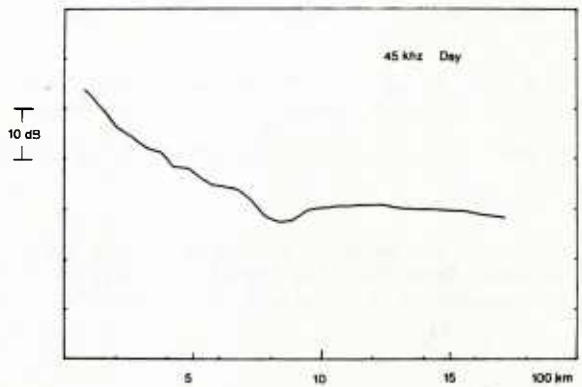


Fig 4 Signal strength variation with distance for transmissions from GBY (Inskip), 44.95 kHz, daytime conditions

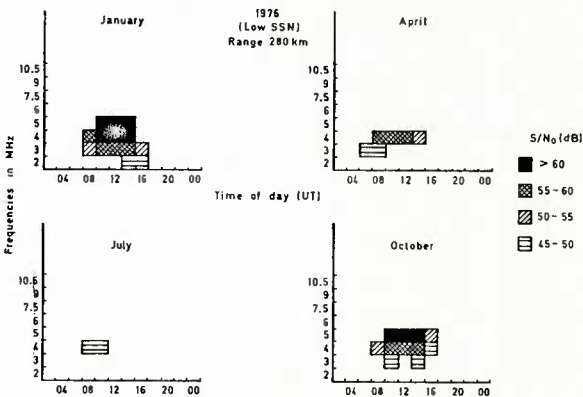


Fig 6 Short range communications (aircraft to station W)

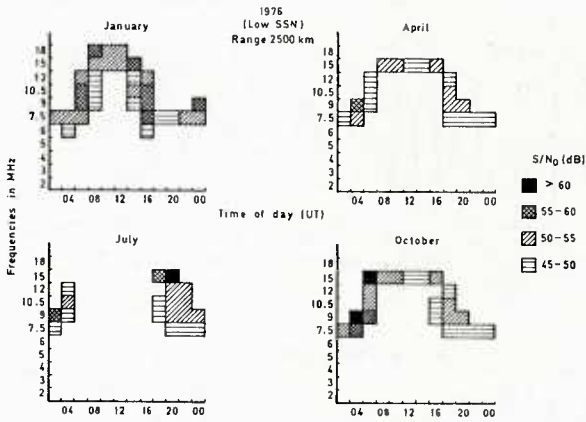


Fig 8 Long range communications (aircraft to station Y)

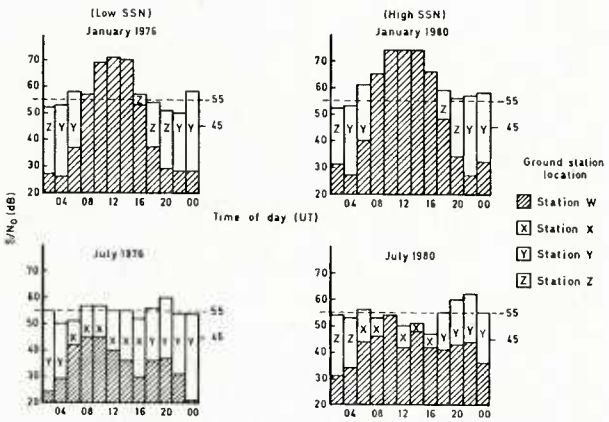


Fig 9 Communications from aircraft to various ground stations. Optimum frequencies are used

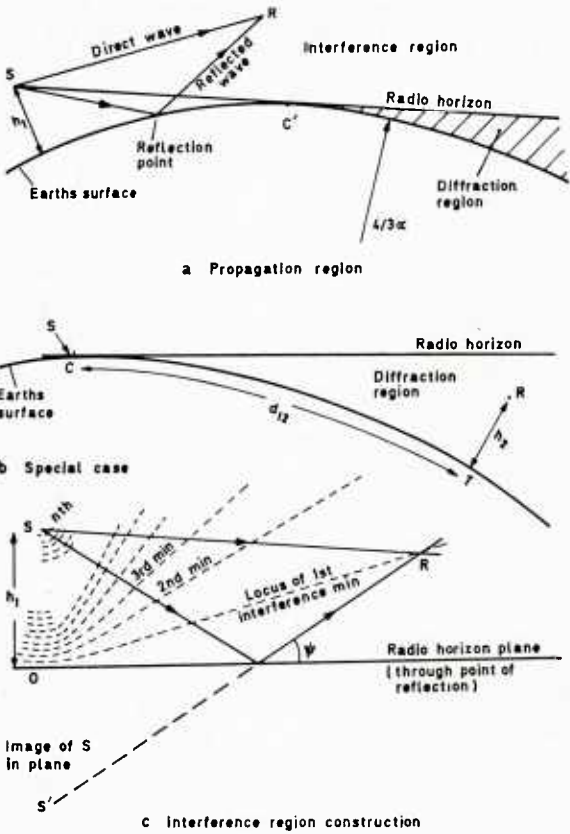


Fig 10 Interference and diffraction regions

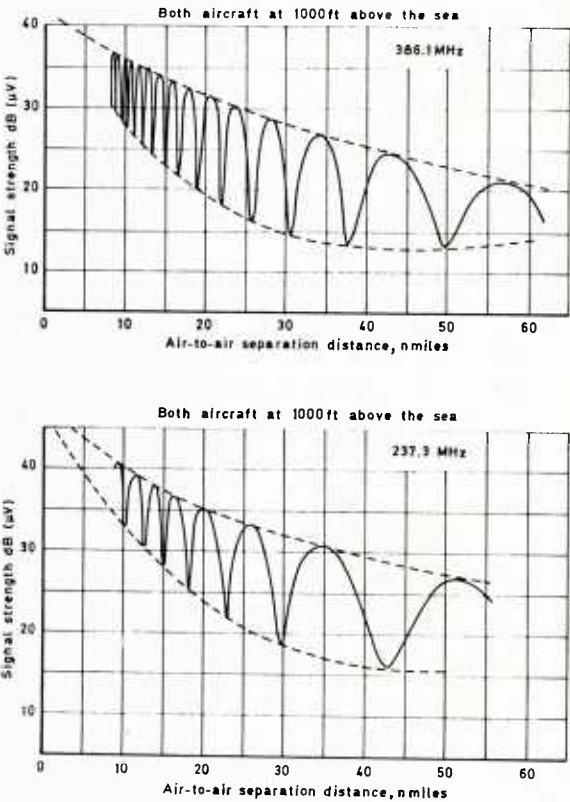


Fig 11 Theoretical air-air propagation profiles, helicopters at 1000 ft: 237 and 386 MHz

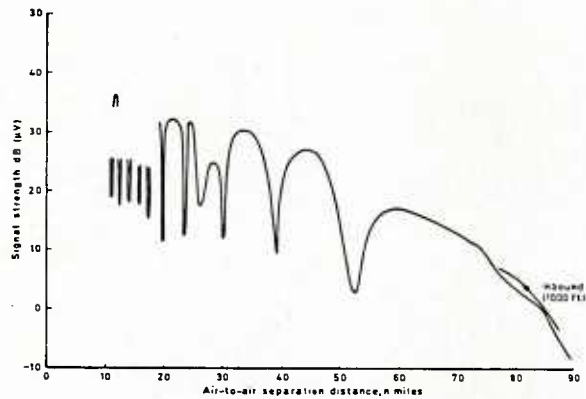


Fig 12 Experimental air-air propagation profiles, helicopters at 1000 ft: 386 MHz

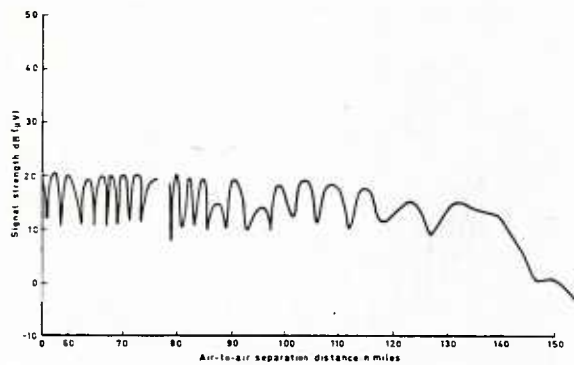


Fig 14 Experimental air-air propagation profiles, helicopters at 4000 ft: 386 MHz

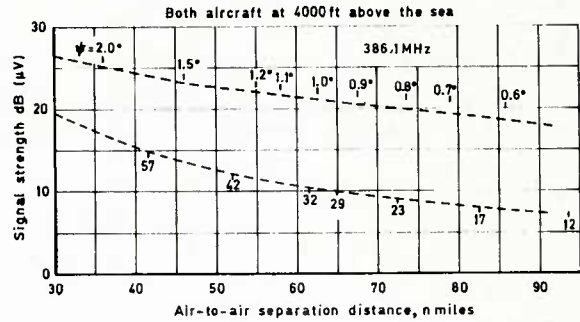
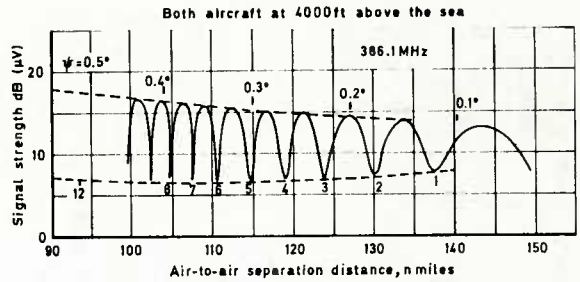


Fig 13 Theoretical air-air propagation profiles, helicopters at 4000 ft: 386 MHz

SYSTEMS OF MULTIFUNCTION INFORMATION DISTRIBUTION
AND FOR COMMAND, CONTROL AND COMMUNICATIONS-C³
BY

E.W. Lampert
Siemens AG
Hofmannstrasse 27
8000 München 70
West Germany

Summary

The areas where communication systems in support of C³ are used will be indicated along with the fundamental characteristics of those systems.

Presently, C³-systems heavily rely on voice transmission whereas in future the data processing environment will request highly sophisticated digital C³-systems.

In this area the Multifunction Information Distribution System (MIDS) is the best developed system concept. Therefore a description of the different features a MIDS can offer to the user is given. These are

- Information transmission
- Navigation
- Identification.

These features impose certain requirements upon the propagation path which result in limitations in frequency range, signal and equipment design of the system.

The "Joint Tactical Information Distribution System (JTIDS)" with both variants TDMA and DTDMA and also the "Systeme Integre d'identification, de Navigation, de Trafic control, d'Anticollision, de communication (SINTAC)" is described as representative examples of a MIDS. In particular the following points are emphasized

- Link protocols and
- Hardware implementation.

The capabilities of these systems are checked against the mentioned user requirements and the limits within which these general requirements can be fulfilled are shown.

1. Introduction

Command, control and communication, C³, encompass an overall system of which equipment, software and personnel are components which are required to provide a Control Center with extensive data to make decisions, which may be supported by the C³ software. The resulting commands then have to be reliably disseminated to the forces under control.

When C³ is understood in that way, it comprises the following elements: sensors (active and passive), data processing, displays, communications, and associated software. The most difficult problem is however to build up a complete, interoperable system with these components. Therefore, improvements in the C³ structure are not achieved by merely adding new technology and equipment to the present system, its careful integration is the decisive factor.

In the present context, the communications component of the C³ problem in the tactical arena will be emphasized, whereas the other parts will only be touched upon to the extent to which there is obvious interaction.

2. State-of-the-Art Systems and resulting Requirements

Presently voice communication is predominant in tactical C³ system. In the area of the FEBA (forward edge of the battle area) this situation will never change totally with respect to the army. Its voice transmission uses the VHF-Band (30MHz-80MHz), applies analogue FM using preassigned channels and therefore does not provide adequate break-in capability nor jamming resistance.

Air-to-air communication and air-to-ground, ground-to-air communication also rely on analogue voice and use AM₃ in the UHF-Band (225-400MHz). Much of the air-ground, ground-air communication is thereby embedded in a C³ loop, set up between manned aircraft and intercept/recovery controller whereby the latter has access to the data base and computer of a Control and Reporting Center (CRC).

Besides voice, Navy C³ structures rely very much on LINK 11, a digital data transmission system used for exchange of radar track data and their management (1). So it is mainly used by the Control Center to collect sensor data from different platforms. LINK 11 has a net structure in which the Control Center interrogates a specific platform which then broadcasts all available sensor information. This information can be received not only by the Control Center but also by all other platforms participating in the same LINK 11 net. The network has an architecture providing a many-to-many connectivity. LINK 11 uses a specific message protocol (M-series) permitting only a specific set of formatted messages. As the link is used in a maritime environment HF ground wave has to be used instead of higher frequencies which would only provide L.O.S capabilities. This restricts the throughput of such a type of digital link to data rates below 2kbit/s even if multiple subcarrier modulation methods are used. The network protocol (roll-call broadcast) and the limited throughput prevent direct information distribution among a large number of platforms (>10).

Radar track data are also transmitted via LINK 1, a point-to-point link between CRC-S. As communication takes place via low-data-rate PTT-wirelines, this type of link will not be discussed any further.

The Navy (in particular US) uses LINK 4 to execute fighter control and therefore uses UHF-frequencies. Like LINK 11, it uses a TDMA-structure: the commands to the separate aircraft are transmitted sequentially, reports from the individual fighters are only transmitted after interrogation from the control center.

LINK 4 using C-series messages, LINK-1 using S-series messages and LINK 11 are not interoperable in base-band because of different network protocol and different message catalogue. It needs a specific software package resident in a communication computer to set up a so-called "LINK-baffer".

Presently available LINK-systems for mobile use have very limited capacities and voice is used in many cases where a direct digital interface between sensor/weapon system and C³-system would be appropriate. In cases of stress an unnecessary burden is therefore imposed upon personnel.

In conclusion, voice is extensively used in all forces to perform C³ functions and it is not foreseen that voice will become superfluous in future. There will always be a mix of voice and data in future LINK-systems. This calls for a standardized voice digitization in order to feed voice through different transmission media

and to multiplex both voice and data. The data themselves are a mix of C^2 data and sensor information. Both need to be transmitted without uncontrolled delay and because of its importance a certain degree of jamming resistance should be provided, together with cryptographic secure encyphering capabilities.

Present C^3 -systems have nodal structure which is very vulnerable. Any change over to distributed C^3 -structures and databases require that the available information has to be distributed to any place where it might be necessary. This requirement calls for a nodeless architecture with a many-to-many connectivity.

As in a rapidly changing scenario with mobile subscribers the location of each network participant cannot be known in advance the net subscriber has to have the capability to receive messages from any direction. Its antenna should have an omnidirectional coverage. As a wide area coverage is required, too (up to 300 n mls) the frequency band to be used should not exceed the UHF-band. Nevertheless reliable data transmission is required in such a scenario where severe multipath effects will always be present.

The multitude of data to be handled by a C^3 -system are sensor data which refer to geographical information. It is therefore necessary to use a common geographical grid, preferably geographical longitude-latitude-coordinates. For any consumer of those data it is necessary to know either the time of its origin or the system has to process the data in a way that this knowledge is unnecessary. The first proposal would either require a common synchronized time-reference-system or the transmission of the delay time between generation and transmission of that particular set of data. Both may impose additional burden on the communication system, especially when jamming resistance is required. It has therefore become common practice to extrapolate those real time data, when besides position also a velocity vector is available.

3. Concept of the Multifunction Information Distribution System (MIDS)

The lack of a consistent C^3 concept in tactical scenarios along with the introduction Joint Tactical Information Distribution System (JTIDS) together with the NATO-AWACS-system triggered in NATO the development of the MIDS-concept. It is therefore not very surprising that NATO-MIDS and US-JTIDS are almost synonymous. As JTIDS can also provide navigation data and within limits support identification, such a system is considered being multifunctional with the emphasis on communication.

In the NATO-Airborne Early Warning and Control System (AWACS) the link between airborne platform and ground sites is formed by an ERCS (ECM-Resistant-Communication-System) which actually uses presently available JTIDS equipment making only use of the communication function. The first potential application of a MIDS would be the Airborne Command and Control System (ACCS). -NATO reviewed the principal possibilities of a JTIDS-system and from these inputs developed a draft strawman for a MIDS being aware of the fact that the JTIDS-system design has not yet stabilized. It will be shown later that it is still an open issue whether it will remain an orthodox TDMA-structure or change into a more flexible, but more complex DTDMA (Distributed TDMA)-system.

It is self-understood that a system to be designed for present and future needs has to have a sufficient Anti-Jamming (A/J)-Margin, must be cryptographically secure, provide interoperability with present systems and sufficient growth capability in capacity. Dedicated net masters which could diminish the system survivability should be avoided.

MIDS clearly asks for a data distribution system between fixed/mobile ground and airborne platforms with the following features:

- Data exchange has to take place in a way that a masterless many-to-many connectivity is attained. In particular a completely receiver-oriented information distribution is to be attained, which implies common encryption procedures, a common and unique reference grid for position, status and identification reports.
- formatted data transmission in particular real time position and sensor data, and also command and control messages, the message catalogue to be used has to have sufficient power to support C^3 in tactical scenarios like air defense, it must provide growth capability, too.
- voice transmission capability
- free text message transmission, i.e. continuous data transmission with rates 2^N . 75 bps ($N=1 \div 8$).
- in order to provide a limited over-the-horizon data transmission capability a terminal must be capable of transmitting messages from a participant which is not visible to the majority of the net participants. This capability should not need a complete dedicated set of equipment.

The inclusion of a navigation and identification components in the MIDS originate from the fact that in a TDMA structure time synchronism of the terminals is necessary which therefore has to be supported by hardware. This fact can be used to calculate the delay time between the terminals, furthermore the organizational structure of the net requires that each terminal has a own reference number specifically assigned that piece of equipment and transmits periodically messages in which identity, position and status are shown.

The identification function originally was restricted to the use of position messages in the correlation process with primary sensor data, which is a report only identification. -A question-and-answer mode would be highly desirable, whereby the problem of response delay time and object designation is of significant importance.

4. JTIDS-Characteristics as MIDS candidate

4.1 JTIDS fundamental waveform

In order to provide a sufficient A/J margin for such a system a spread spectrum modulation scheme with a band width of the order of 100 to 200 MHz is required. On the other hand a radio frequency below 2GHz is to be used. As there exists no unoccupied band or one assigned for spread spectrum systems the waveform has to be designed so that no appreciable interference occurs between the new user and the already established services. The only band where such conditions can be established is the LX-Band 960 to 1215MHz, excluding the IFF-notches at 1030MHz and 1090MHz. The primary users in the LX-band are the TACAN and DME-systems, both of them use a pulsed waveform and analysis shows that it is essential for a new system also to use a pulsed waveform with a pulse length of the same order of time. As the presently used TACAN-X-mode signal uses double pulses spaced $12\mu s$ apart, care should be taken that not both pulses are affected by the new waveform. JTIDS therefore uses the following principle pulse, Fig. 1 :

- Carrier frequency range 969 to 1206 MHz excluding the IFF-Bands at 1030 MHz and 1090 MHz
- Pulse length $6,4\mu s$
- Pulse repetition rate $13\mu s$
- double pulse-3B-Waveform-with a minimum frequency spacing of appr. 20 MHz between the carrier frequencies of each pulse
- Modulation in each pulse: 32 chips of Minimum-Shift-Keying (MSK)

Frequency hopping (FH) normally occurs from pulse to pulse with a distance between channels of 3MHz which corresponds to the bandwidth of the modulated pulse. -To achieve additional processing gain besides the FH

only 5 bit of information are transmitted in each pulse. The spread spectrum encoding is done by means of assigning a specific 32-element code word to 5 bit information. The complete orthogonal alphabet is constructed by cyclic shifting a single code vector through all possible stages. Complete randomness of the transmitted chips is achieved by simply adding an encyphering bit stream.

At a receiver for detection and demodulation of the pulse, time synchronism has to be built up to a fraction of the 200ns basic element. This feature provides a time delay resolution up to 20ns which results in a distance resolution of less than 6m. So in trilateration measurements accuracies better than 20m should be achievable. - As the waveform has a single peak correlation property it is suitable to resolve multipath, as long as its time delay difference is beyond 200ns (60m). Shorter delays can cause severe pulse distortion. In order to avoid this, information is transmitted twice (in the so-called 3B-waveform) on different frequencies and one then can make use of frequency diversity combining methods.

The FH modulation however has a further aspect with respect to propagation. On large airborne platforms like E-3A it is not possible to attain omnidirectional antenna patterns with a single antenna. When using two antennas one in the forward radome and a second in the tail cone, interferometer lobing will occur (2). This antenna characteristic would be detrimental to omnidirectional signal transmission. As FH is used in conjunction with frequency diversity and further algebraic error correction encoding of information it is admissible for system design to operate with an equivalent antenna diagram which does not show these deep interferometer nulls, Fig.2.

The FEC (Forward-Error-Correction coding) uses a 5 bit (31,15) Reed-Solomon (R-S) Code for algebraic encoding. Of the 31 5 bit-characters in each word 15 are used for information transmission, i.e. 75 bit, whereas 16 characters are used to transmit check information. An Error detection code (EDC) which extends over 3 R-S-words (225 bit) provides additional 12 check bits to prevent undetected false decoding in the R-S-decoder. If FEC is used information is always transmitted in multiples of 75 bit frames, shorter words can be inserted (header) using shortened R-S-Codes.

4.2 JTIDS-TDMA-Architecture

The JTIDS-Phase I system has a TDMA structure. In contrast to satellite TDMA, burst synchronisation is not maintained with respect to a specific point in space-the satellite transponder-but with respect to the start of the time slot at each terminal. In such a net all participating units (PU) use a common system time to which they keep their individual clock synchronized. So each PU can exchange information with any other PU only by transmitting information into the Radio-TDMA-bus. In order to avoid overlap of signals originating from different sources, in such a system intervals have to be inserted between transmissions. In JTIDS these delay time intervals have a length of about 2ms which is sufficient for a net coverage of about 300 nm1s.

In order to manage the TDMA system the time is divided in Timeslots (TS) of a length of 2^{-7} s during which a message burst from a specific terminal is transmitted (109 3A-waveform symbols). A continuous numbering of these TS is only sensible over a certain time period, which is $3 \times 2^{15} = 98\,304$ TS \approx 12,8 minutes. This periodicity interval is called epoch. According to the individual PU need to transmit information, TS within this epoch are assigned to each PU, in the minimum 1 TS per epoch where the position (P-) message is transmitted. In air defense scenarios it is more appropriate to use periodicity intervals which are of the same order of magnitude as the revolution of the surveillance radar, therefore the epoch is divided into 64 cycles. So we arrive at the following timing structure, Fig. 3:

1 day = 112,5 epochs; 1 epoch = 64 cycles = 12,8 min.

1 cycle = 1536 TS = 12s; 1 TS = 2^{-7} s = 7,812 ms

As the transmission of information is only possible in the TS-s assigned to that particular PU, considerable delay time intervals in the terminal are inevitable. Real time data therefore have to be extrapolated.

Between the beginning of the TS and the actual transmission a jitter determined by the crypto unit has been introduced in order to avoid an easy jamming of the start of the message. -The message data transmission has to be preceded by a preamble consisting of 32 - 3B- symbols in order to safely detect a message start from background noise and clutter.

To receive a message the crypto unit of the terminal calculates the following parameters for each TS: -jitter, -the 8 frequencies of the 32 preamble symbols, - cyphertext for each pulse within the preamble, -FH values and cyphertext for message data.

The terminal has a built-in multifrequency matched filter which is 8 frequencies wide. This assembly is now set to the precalculated preamble values. After successful detection of the preamble, further message detection can be done with a single channel system using synchronous frequency dehoppping succeeded by the m-ary demodulation of the 32 character alphabet. In the following R-S-demodulator FEC decoding is done. The validity of the demodulated/decoded message is then checked by means of the 12 check bits in the EDC-decoder.

This rather complex modulation/demodulation scheme provides an almost optimum A/J performance, although a pulsed signal with specific restrictions has to be used because of compatibility with existing services.

When a terminal has received a message it is only in coarse synchronism because it does not know yet the message propagation delay. This delay can now either be computed by receiving P- messages from different terminals along with measuring the differential time delay or by just interrogate a synchronised PU with a Round-Trip-Timing (RTT) request message. This time update is required from time to time in a synchronized net. It has turned out that a stringent hierarchy is necessary to prevent oscillations, hence a time master is required. The net however can survive for some hours without its master.

The navigation function in JTIDS-TDMA needs also a hierarchical structure. A baseline of the position grid has to be established by means of two position reference master stations. The own position is then established by means of propagation delay time measurements and triangulation, moving PU-s have also to use dead-reckoning algorithms (3). Only those PU-s may be used for interrogation which have better position and timing accuracy. General data about the accuracy of the navigation function out in the field are not yet available. One should be aware that with all triangulation systems there exist geometrical constellations, which will result in a high position error.

TDMA systems not only need an exact time synchronization but also a "net management". A unique assignment of TS-s to each PU for its transmissions is necessary. Multiple assignment of the same TS to more than one PU has to be avoided. When a net is fully used, i.e. all available TS-s are assigned to PU-s, a change in capacity distribution because of changes in the tactical scenario becomes difficult.

This problem could be overcome by just adding a further net by assigning a further distinct FH-spread-spectrum pattern to the same user community. Now more than one transmission can take place in a single TS. These overlapping signals can nevertheless be discriminated because of the different codes used in the signals. One has however to be aware of the propagation oriented "near-far" effect. -The set-up of the second and further nets imposes restrictions on the many-to-many architecture, although the whole user community is still synchronized to the same clock. While participating in one net, one cannot listen to the information exchanged in

the second.

A fixed TDMA-structure with fixed assigned TS does not meet all requirements of C³ as there occur infrequent messages which must not suffer a long delay time in the terminal. The specific JTIDS signal design allows to use some of the TS of a single net in a contention mode, i.e. simultaneous use of the same TS at a time. There is then a certain likelihood that the call does not get through, because the one with the smallest propagation delay time will be decoded. If traffic in these TS-s is of low duty factor this effect is bearable.

Relaying in a JTIDS-TDMA net is straightforward. The message received in a TS is retransmitted by the PU assigned to be relay on a specific TS. So relay messages load the net with twice its information flow. The relay procedure can also be used to act as a gateway between nets in multinet operation.

The use of multinet and contention mode imply that more than one signal is present at a time. This situation may have bad influence on existing systems like TACAN. Present frequency allocation plans for peace time therefore do not permit general use of these modes in a JTIDS-net.

The identification function in a JTIDS-net relies on two aspects: one is the accuracy of the navigation function while the other is the availability of sufficient net capacity for that function. These TS-s should be used in the contention mode in order to avoid long delay times. A further problem which needs still further discussion in the scientific community is the Question & Answer mode in IFF, in particular the problem of designating the target. In a communication system with a many-to-many connectivity this cannot be done just by calling anybody to report its status and position. The multitude of the then arriving responses will not be resolvable. - Asking for the identity of a target at a certain position would require that the interrogated platform also has accurate position data available and is equipped with a JTIDS-terminal. - So presently the identification function is still restricted to the use of the P- message in the track correlation processing. Interoperability of JTIDS with present and future IFF equipment in a Q & A mode is not possible.

4.3 JTIDS-Class I Terminal

In the course of the phase I JTIDS implementation, the first step was to develop a terminal for major ground and airborne platforms. This is the JTIDS-class I terminal often only called HIT (Hughes Improved Terminal). A class II - fighter terminal is presently under Full-Scale-Development (FSD) contract with the USAF. - As major platforms need a wider coverage compared to fighter C³ the class I terminals are equipped with 1KW - transmitters, while the class II will only use 200W transmitter power.

The class I - terminal uses the already described basic pulse (3B-waveform). The encoding of a total message consists of 20 bit header and 225 bit of message data as shown in Fig. 3. Fig. 4 shows the present hardware implementation of a class I terminal. The heart of the equipment is the Transceiver-Processing-Unit (TPU). This unit is responsible for data processing, signal processing and transmit /receive. It houses a full size 166bit mini computer which is loaded with an operational computer program of about 40K-Words. The signal processor - a hard wired digital card assembly is responsible for timing, R-S-processing, EDC-processing and signal generation and detection. The transmitter/receiver function includes 8 synthesizers, detection, modulation and frequency conversion. The TPU-output signal is successively amplified to 150W in the Low-Power-Amplifier (LPA) and to 1KW in the High-Power-Amplifier. Unfortunately in all cases it is not possible to build antenna and equipment closely together. Cables (with considerable loss) are required to connect them. To avoid excessive noise figures of the system transmit/receive path separation is done immediately behind the antenna together with the preamplification of the received signal. The Antenna-Coupler-Unit controls the output signals, harmonics and possible spurious in the IFF-bands are suppressed by filtering. Further detection circuits control the restrictions imposed on the JTIDS-RF emission by the frequency allocation authority.

As the class I terminal fills up a full 2m 19" rack it is not suitable to be used in a fighter aircraft. The major effort in developing a class II-terminal is therefore directed toward miniaturisation, furthermore more computer power is required.

4.4 JTIDS-DTDM-Architecture

While the JTIDS-TDMA system with the class I terminal is already in production, this is not the case with DTDM-terminals. There only exist a few Advanced Development Models (ADM) and Full-Scale Development (FSD) is only under contract by the USN since Jan. 82. So little is known about the actual design and changes in the system resulting from hardware experience and field trials. The presentation of DTDM has therefore to rely completely on the description forwarded in AGARDograph No. 245 (4), where details can be found.

DTDM uses the same basic single pulse but now makes use of the fact that even in a fully loaded single net TDMA configuration the pulse duty cycle does not exceed 18 %. In such a situation, random access could be achieved by using time-hopping (5) in addition to direct sequence spectrum spreading and FH instead of the controlled access within a TDMA system. DTDM therefore just interleaves the pulses of the successive messages which would be transmitted in a TDMA-system message after message wise, Fig. 5. The message transmission in a DTDM system is then distributed over a period of 80 to 300ms. The time interval between pulses is derived from the crypto unit. The terminal therefore has an advance knowledge to which message the just received pulse has to belong to.

The major problem areas are synchronisation, simultaneous reception of several signals belonging to different messages and transmit-receive conflicts. In contrast to TDMA where one only has to measure the arrival time of a single message and then demodulate/decode it, in DTDM one has to keep track of the arrival time of all the different messages which are quasi simultaneously received. Because of the difference in arrival time, there is a high probability that different pulses (with different frequencies and cryptotext) arrive simultaneously. Calculations have shown that at least 2, better 4 receiver channels have to be built into a terminal down to the demodulator output level in order to prevent noticeable message loss.

Whereas the synchronisation problem can be solved with appropriate equipment and insertion of specific messages, conflicts in transmitting and the simultaneous need of reception of pulses cannot. It is obvious that reception of signals with level values of -90 to -100dBm is not possible when simultaneously transmitting +60dB in the same equipment (mostly on a different frequency but in the same band). A terminal which has a high traffic load to transmit cannot have a high receive capability. This limits the many-to-many architecture.

In general one may say that TDMA provides a more transparent architecture as long as the required capacity does not call for multiple nets, whereas DTDM does not call for a stringent TS management. The increase of the transmission rate of one terminal in a DTDM net without giving notice to other participants will only slightly degrade the message error rate in the net.

In a DTDM net there is a high probability of overlap of pulses in certain geographic locations. From an EMC point of view we then have a situation which is compatible with the TDMA contention mode. So a full

electromagnet compability test program has to be run before that system could be turned into an operational mode.

Even if DTDMA should become operational the system will always include a TDMA interoperable mode.

4.5 Message catalogues

Present JTIDS-TDMA terminals operate with the IJMS (Interim JTIDS Message System) using standard 245 bit messages. Future TDMA systems will probably use TADIL-J, which uses a multitude of different message formats relying on a combination of up to 8 75 bit-R-S-words. Present issues of the TADIL-J catalogue signify a close interrelation with a TDMA architecture. IJMS and TADIL-J are US activities.

NATO is presently drafting a STANAG on LINK 16 which tries to standardize the communication function of a JTIDS-TDMA system. It presently only uses a subset of TADIL-J. On the other hand there also exists a draft STANAG 4175 on a MIDS which tries to leave it open, whether a TDMA or a DTDMA structure will be appropriate.

All these link standardization efforts have one great problem in common. They only try to assure interoperability in the radio frequency layer. The standardization in the data-interface layer which is necessary when talking about LINK-interoperability has not yet been comprehensive by addressed.

5. Systeme Integre d'Identification, de Control de Trafic, d'Anticollision, et de Communication (SINTAC-2)

The SINTAC system has undergone several changes and is still in the process of continuous evolution. Presently SINTAC uses the same basic waveform as JTIDS does and also the alike TDMA-structure. SINTAC however does not only address military air defense tasks but is to yield a comprehensive concept to substitute present civil aircraft communication, navigation and identification equipment with a single CNI-System. While the military version SINTAC-2 will use FH, the civil system SINTAC-C2 does not.

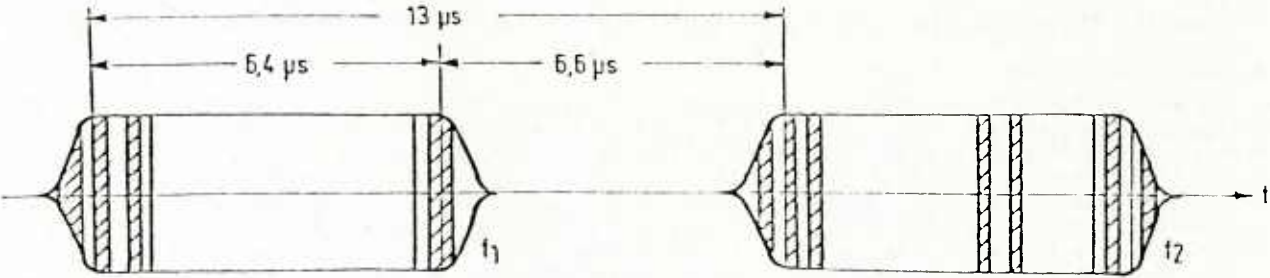
As the plans have the aim to substitute all TACAN and DME systems in a transition period by the SINTAC-CNI-System EMC is not considered being such an imminent problem. The activities however had to address the problem of direct identification by Question and Answer. Here SINTAC presents a unique approach using TS-s, subdivided in time. Signal exchange takes place in time subslots designating the distance to the target to be interrogated. Practical experiments and extensive computer simulations are still outstanding.

6. Conclusions

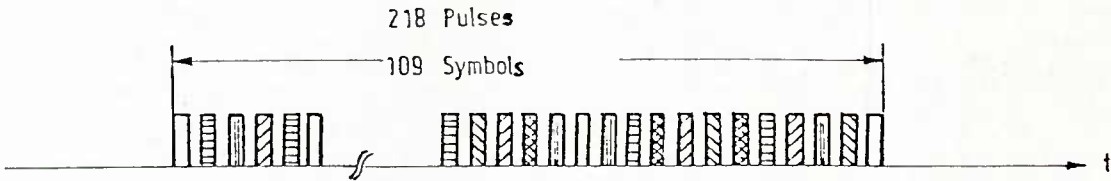
MIDS-Systems are presently designed emphasizing the communications aspects. The radio wave propagation problems are overcome to a great extent by combined use of spread spectrum modulation techniques (direct sequence and frequency hopping), frequency diversity and algebraic encoding of the messages. Because of fundamental differences in architectural requirements and the resulting effects on the layout of the radio wave propagation path the multifunctional components presently only support the still necessary stand alone systems for navigation and IFF. As the present MIDS-concept is the only one which could be of general applicability, its restrictions have been analyzed in greater depth than other systems. Evolution is still possible, more comprehensive solutions may come about in the next few years. The fundamental problem is however to establish general electromagnetic wave compability with existing services in the LX-band.

Literature

1. Bolen, N.E.: The Implications of Modern TDMA Communications Techniques for C³ System Architecture, Proc of Defense Research Group Seminar on "New Trends in the Area of Communication," Bruz, France, June 1977 p. 485 ff.
2. Taylor, J.G.: A JTIDS Performance Model for the E-3A, Modelling and Simulation of Avionic Systems and Command, Control and Communications System, paper 12, AGARD-CP 268
3. Fried, W.: Principles and Simulation of JTIDS Relative Navigation
IEEE Trans, AES, Jan. 1978.
4. Leondes, C, T. editor.: Principles and Operational Aspects of Precision Position Determination System
AGARDograph 245, 1979
5. Rubin, J.: Distributed TDMA-An Approach to JTIDS Phase II
ibid. paper 37.



1 Symbol of a 3B-basic Waveform



Frequency Hopping in a Message

Fig.1 Principle JTIDS-TDMA waveform

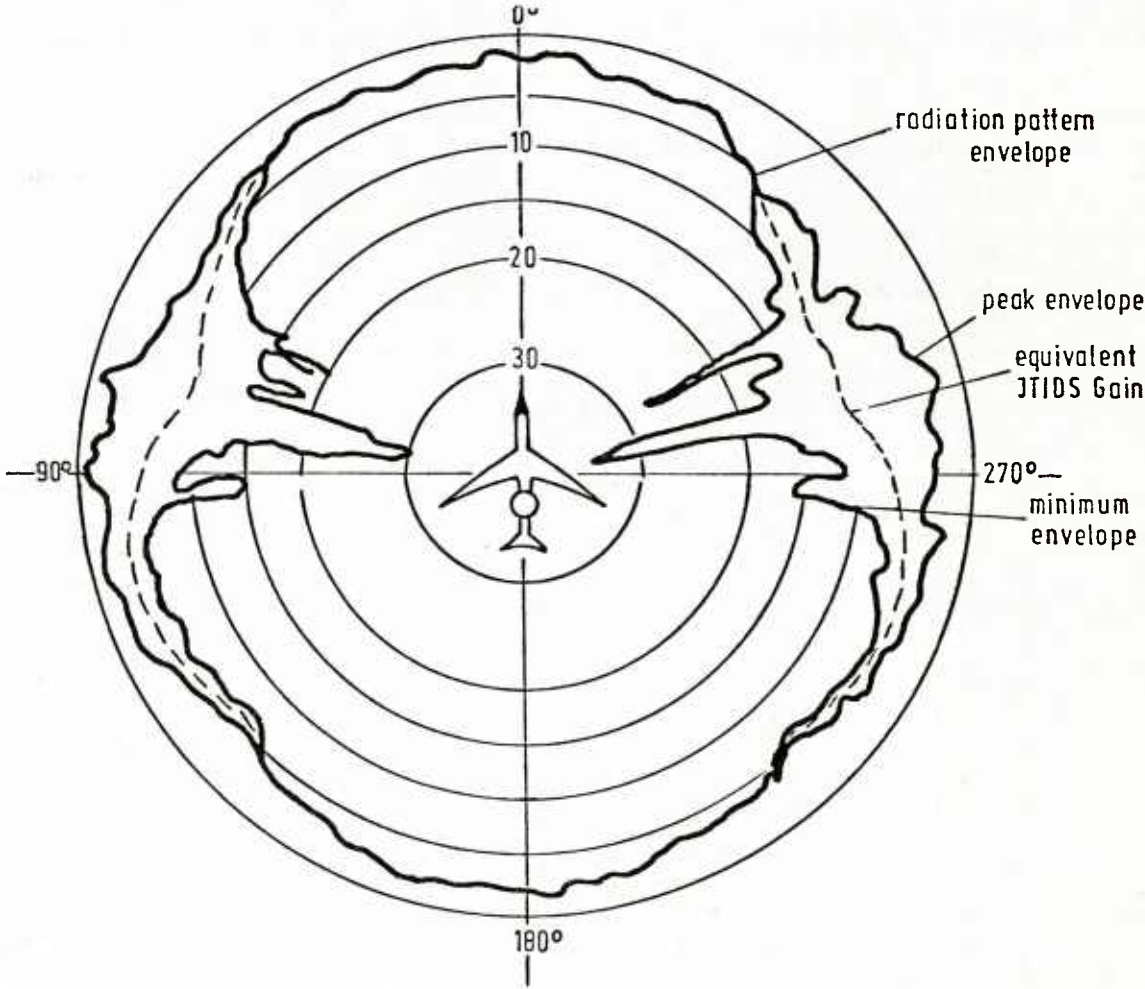


Fig.2 E-3A JTIDS dual antenna radiation pattern after Taylor [2]

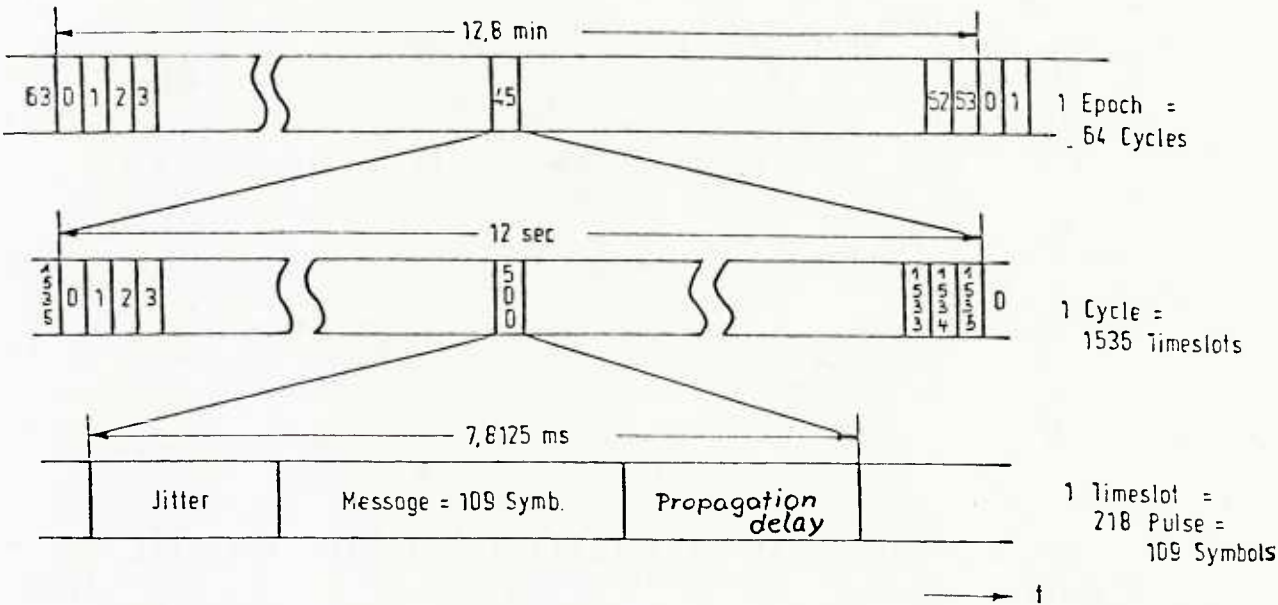


Fig.3 Timing structure for TDMA-JTIDS

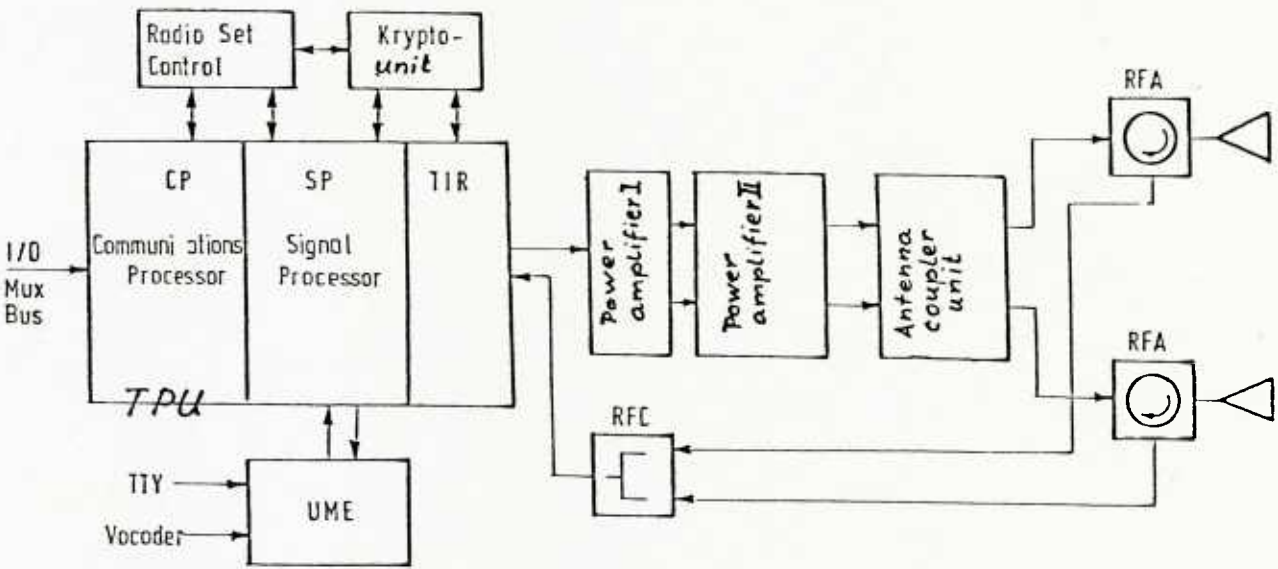


Fig.4 JTIDS-class I terminal (HIT) block diagram

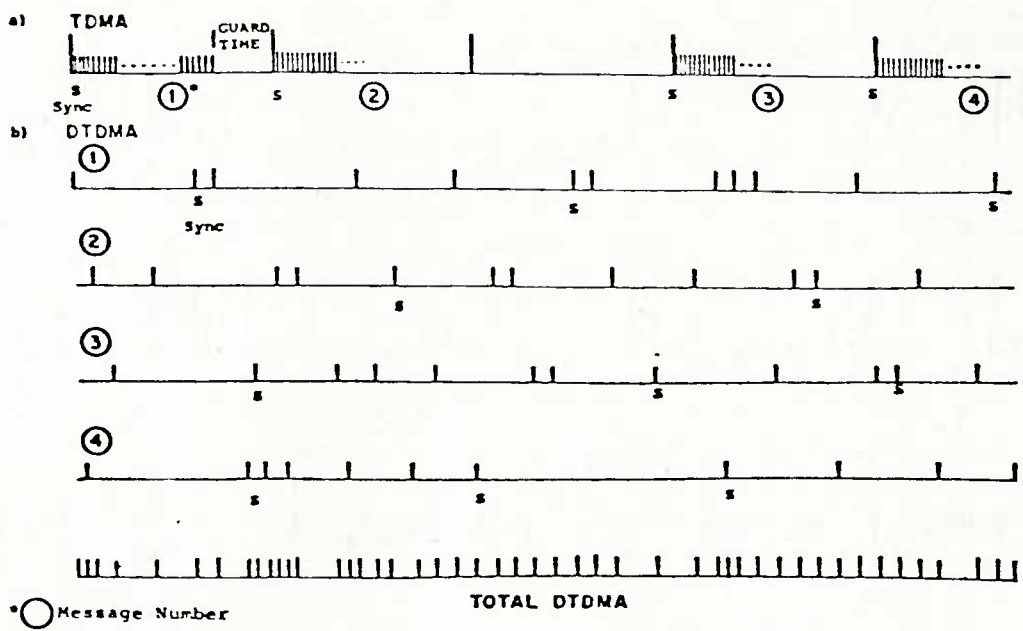


Fig.5 Principle of DTDMA-pulse timing after Rubin (5)

PROPAGATION EFFECTS IN TACTICAL RADARS

Dr B A Prew
Principal Scientific Officer
Royal Signals and Radar Establishment
Great Malvern
Worcestershire
UK

Summary

Tactical battlefield radars are employed in surveillance and target acquisition roles at ranges of approximately 1-20 km; their main targets being enemy ground vehicles and personnel. As with all types of radar the operating environment has a significant effect on the design and performance of these systems and propagation considerations are an important factor.

The three major propagation factors which limit the performance of tactical radars are (i) the availability of line of sight (ii) ground clutter and (iii) effects of the weather. The ways in which propagation factors affect the choice of such radar parameters as frequency, polarisation and RF waveform will be discussed, and the ways in which propagation constraints can be minimised by the design of the signal processing system will be considered.

In an EW environment an important operational requirement is to minimise the probability of the location of the radars position by the enemy, and propagation effects such as multipath and diffraction will be considered in broad terms in this context.

Introduction

This paper deals specifically with ground-based battlefield surveillance and target acquisition radars which have as their main targets enemy ground vehicles and personnel at ranges up to a maximum of 20 km. It will be apparent, however, that some of the aspects discussed are of more general applicability to other types of tactical radar. We shall first address the question of what the general performance requirements are for radars of this type.

Performance Requirements

(i) Surveillance

The radar has to be able to survey a designated sector and to detect, locate, recognise and identify all targets within it, with a high probability of success and a low false alarm rate, both by day and night and under all weather and battlefield atmosphere conditions.

(ii) Target Acquisition

Having located any targets within the sector, then in order for them to be engaged by suitable weapon systems, they have to be acquired. This would be done by either communicating the surveillance information to weapon systems which have their own acquisition and tracking sensors, or in the case of artillery batteries, for example, the surveillance radar employed by the artillery observation post (OP) may have an acquisition mode to enable it to control artillery fire directly.

Propagation Factors Affecting Radar Performance

(1) Availability of line-of-sight

The availability of line-of-sight (LOS) between the radar and the ground area to be surveyed is, of course, fundamental to the operation of the radar. For a ground based tactical system it would be an important part of the setting-up procedure for the operator to choose both the location of the radar, and the elevation of the antenna, in order to optimise the radar coverage of the designated surveillance sector. A useful aid in this setting up stage is the availability within the radar of a clutter-mapping facility which enables the operator to monitor, and hence minimise, the "dead-ground" element in his observation area.

However, it must be borne in mind that in optimising his location for best surveillance coverage, the radar operator may also be increasing his vulnerability to enemy countermeasures; this point will be discussed in a later section.

(2) Clutter

Clutter may be defined as any unwanted radar echo. The two main sources of clutter as far as battlefield surveillance radars are concerned are the ground itself and returns from precipitation, and we shall deal with these separately.

(i) Ground Clutter

Ground clutter can be either extended or of isolated form. Returns from objects such as pylons, windmills and isolated buildings are known as point clutter. Extended clutter consists of many individual scatterers distributed throughout the radar resolution cell.

In order to gain some feel for the effect of clutter it will be instructive to calculate the magnitude of the clutter return from the ground assuming parameters typical of a battlefield surveillance radar.

The area of ground illuminated by the radar is given by $\frac{C\tau R \theta_B \sec \phi}{2}$ where C is the velocity of propagation, τ the pulse duration, R the range, θ_B the antenna azimuth beamwidth, and ϕ the angle of depression of the antenna beam as measured from the horizontal. In describing the echo signal from extended clutter it is usual to consider the radar cross-section per unit area illuminated and this is given the symbol σ^0 . Depending upon the type of terrain, and also upon the grazing angle, σ^0 can take values ranging from 10^{-4} to 10^{-1} . The corresponding range of echo areas, at a range of 5 km, for a radar with a pulse length of 1 μ sec, and an azimuth beamwidth of 6° at a depression angle corresponding to a radar height of 2 metres (~ 0.4 mil) is 7.5 to 7.5×10^3 m^2 . Under typical conditions, then, the clutter echo area is of the order of a few hundred square metres. To put this into perspective the mean echo area of a typical ground vehicle target, such as a tank, is an order of magnitude smaller.

Evidently, in order to detect a target the radar must be able to discriminate against the clutter returns and a powerful technique for achieving this is provided by the doppler effect. Doppler radars are, of course limited to detecting moving targets and a problem arises from the fact that natural extended clutter, such as vegetation, will not in general be stationary but will exhibit a wind generated oscillatory motion. In order to make use of the doppler effect to discriminate against clutter, then, we have to do more than simply eliminate "DC" returns. In the simplest type of signal processing it would also be necessary to filter out a sufficient part of the low frequency end of the doppler band to ensure that under most conditions signals from wind-blown clutter would be eliminated. The disadvantage of such a simple approach is that the radar would not be capable of detecting slow moving targets with velocities within the filtered out part of the doppler band.

Slow moving objects which may be personnel or vehicles travelling at an aspect such as to have a small radial velocity component, could be important targets to the operator of a battlefield radar, and more sophisticated signal processing techniques are required to extract them. An improvement over the simple filtering approach can be achieved by employing an adaptive low frequency cut-off for the doppler filter which would then ensure that the doppler bandwidth reduction was no greater than necessary to cope with the prevailing clutter conditions, hence increasing the probability of detecting any slow moving targets. Another approach makes use of a "balanced" processor i.e. one which is able to distinguish between advancing and retreating targets. In principle, given sufficient integration time, such a processor should cancel the signals from oscillating vegetation while passing signals due to the unidirectional motion of real targets. In practice the non-symmetrical motion of wind-blown vegetation and the limited integration time available (limited by the requirement for the radar to scan the whole sector in a time of order 10 seconds) reduce the performance of balanced processors in this application.

Since the magnitude of the ground clutter signal is directly dependent on the size of the radar resolution cell, an alternative approach to the doppler effect for discrimination of targets from clutter is to make the resolution cell smaller. By reducing the pulse length and/or azimuth beamwidth of the radar it is possible to decrease the clutter signal to a level of the same order as or, ideally, to less than the magnitude of the target return. Such a high resolution radar could detect stationary as well as moving targets but if it was required to cover the full surveillance sector, much faster signal processing would be required to deal with the increased number of resolution cells. In addition, the achievement of the required very small antenna beamwidth and very short pulse length is not trivial. The former could only be obtained by increasing the operating frequency of the radar since for obvious practical reasons a tactical radar could not employ a large aperture antenna, while the high degree of range resolution required would probably have to be obtained through the extra complexity of pulse-compression techniques. The factors affecting the choice of operating frequency for battlefield radars will be discussed in a later section.

(ii) Point Clutter

We noted earlier that in addition to extended ground clutter, unwanted returns were also obtained from isolated point objects. These returns are usually less of a problem than those from extended natural clutter since they originate mainly from man-made objects which are not generally wind-blown and can therefore be filtered out quite easily. However, man-made structures can have very large echo areas (up to 10^4 m^2) compared with wanted targets and can lead to a reduction in the sensitivity of the radar by raising the noise level. This occurs because the radar microwave oscillators are never perfectly stable in phase or frequency. Thus, during the round-trip delay time between transmitting and receiving a pulse the local oscillator will have changed phase slightly and the down conversion of the signal from a stationary object will result in the generation of a train of video pulses with randomly varying amplitudes giving rise to noise within the doppler band. It is important, therefore, for the oscillator stability to be such that the radar performance can be maintained under the point clutter conditions likely to be encountered in practice. For a battlefield radar a practical example of this problem would be that of detecting personnel moving in the vicinity of a large target, such as a barn.

(iii) Multipath Reflections

The final topic on the subject of ground reflections is concerned with the effects of interference between the signal directly transmitted from the radar to the target and the signal reflected from the earth's surface. The basic effect is best illustrated by considering the highly idealised case of the radar and target being situated on a plane reflecting surface (fig 1).

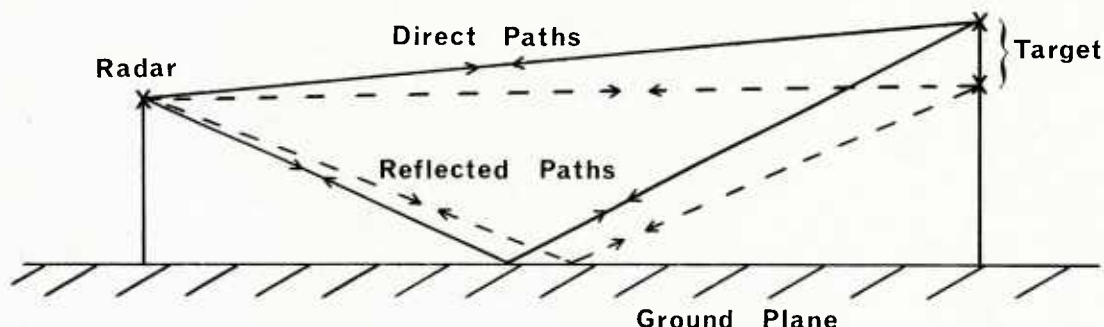


Fig.1 Ground Plane Reflections

The direct and reflected waves will generate an interference pattern resulting in a vertical lobing effect in the elevation coverage of the antenna. In the idealised case of the direct and reflected path lengths being almost equal so that the signal amplitudes are approximately the same, provided there is no reflection loss, the effect is to cause the radar range to vary from zero to twice the free-space range as the height of the radar is varied. For a more realistic situation where the ground is not flat and the reflection coefficient is less than unity, the maxima and minima of the interference pattern are less pronounced but the radar range performance is still dependent on radar height. It is particularly important for the radar operator to appreciate that if he attempts to minimise the radar's physical profile by operating it as close to the ground as possible he may well reduce its range performance.

(3) Precipitation

The presence of precipitation has two distinct effects on the propagation of radar signals (i) it gives clutter echoes, and (ii) it attenuates the signals. We shall deal first with the clutter aspect.

(i) Rain clutter

The volume, V , occupied by a radar beam with horizontal beamwidth θ and vertical beamwidth ϕ with a pulse duration τ , at a range R is given approximately by

$$V = \frac{\pi R^2}{4} \theta \phi \frac{C\tau}{2} \quad \text{where } C \text{ is the velocity of propagation}$$

If this volume is completely filled with rain falling at a rate of pmm hr^{-1} and the radar wavelength is λ cm then the echo area is given by

$$\sigma_R = 6 \times 10^{-6} \rho^{1.6} \lambda^{-4} V$$

For $p = 4 \text{ mm hr}^{-1}$, $\lambda = 3 \text{ cm}$ (i.e. a frequency of 10 GHz), $\theta = 5^\circ$, $\phi = 10^\circ$, $\tau = 1 \text{ us}$ and $R = 5 \text{ km}$, σ_R has a value of approximately 30 m^2 , which is comparable to the echo area of a typical target.

In most cases rain is wind-driven and to a first order the corresponding velocity spectrum can be described by the function

$$G(V) = G_0 \exp \left[\frac{-(v - \bar{v})^2}{2 \sigma_v^2} \right]$$

where v is the wind velocity and σ_v is a parameter dictating the spectral width and has a typical value of $1 - 2 \text{ m sec}^{-1}$. It will be observed that the spectrum is centred on the wind velocity. Denniss⁽¹⁾ quotes the following probability density function for windspeed during periods of rainfall for temperate regions of the world:-

$$p(\bar{v}) = \frac{\bar{v}}{28.2} \exp \left[\frac{-\bar{v}^2}{56.4} \right]$$

where \bar{v} is measured in $\text{m} \cdot \text{sec}^{-1}$ Fig (2) shows the probability of exceeding a particular value of windspeed.

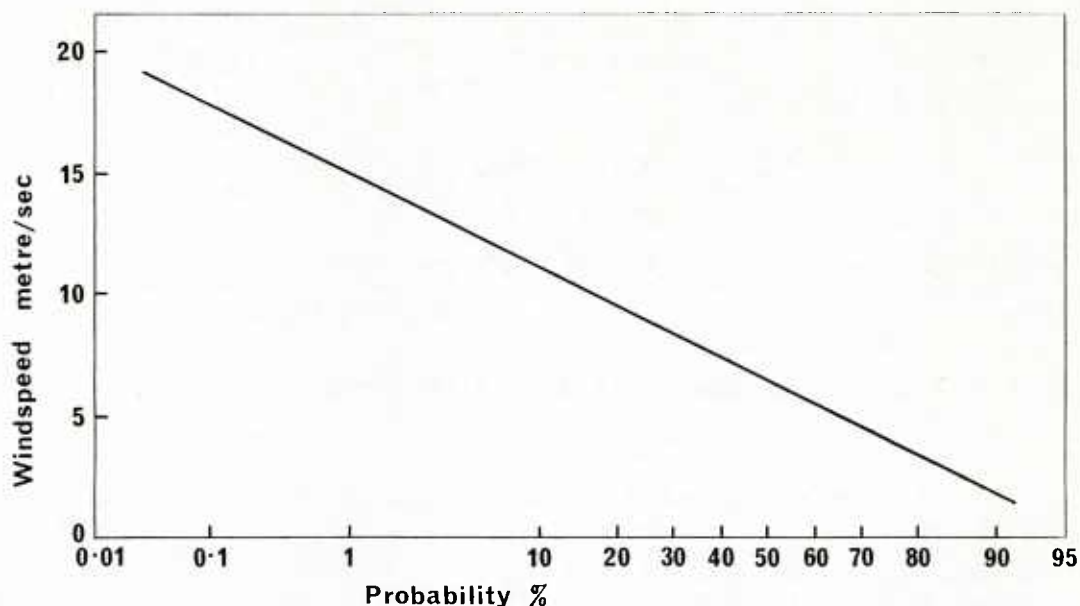


Fig. 2 Probability of Exceeding Any Windspeed During Rainfall

Clearly the rain spectrum will be centred on velocities in the same range as that of many targets and it would require highly sophisticated signal processing techniques to eliminate the rain clutter echoes. A much simpler solution is to employ circularly polarised signals. This will typically reduce the returns from rain clutter by 15 - 20 dB while reducing wanted target returns by 4 - 6 dB. The loss experienced by target signals is of course a disadvantage, particularly if the circular polarisation is a permanent feature of the radar. However, although optimum radar performance would be obtained by employment of a linearly polarised antenna to which a circular polariser could be fitted during periods of rain, and removed in the dry, this may not be practicable for a tactical equipment.

(ii) Rain attenuation

In the absence of precipitation the attenuation of radar signals is due primarily to oxygen and water vapour. The incident microwave energy causes the molecules to make transitions to higher rotational energy levels resulting in absorption of some of the power, which is then lost.

The attenuation of a radar signal due to the atmosphere may be expressed by an exponential law. The two-way attenuation is equal to $\exp(-0.46\alpha R)$ where α , the attenuation coefficient, is measured in dB per unit range. The attenuation of radar signals as a function of frequency in a clear atmosphere is shown in fig (3). It can be seen that resonant absorption peaks for water vapour occur at 22 and 180 GHz whilst there are oxygen resonances at 60 and 120 GHz. There is also a general tendency for the attenuation to increase with increasing frequency over the microwave and millimetre wavebands.

In the presence of precipitation the signal attenuation can increase substantially. Fig (4) gives the attenuation as a function of frequency for different rainfall rates. In making use of this data it is important also to consider the probability with which the various rainfall rates occur. Two statistics of particular significance are that the rainfall rate is greater than 4mm/hour for 1% of the average year and greater than 1mm/hour for 4% of the average year.

In selecting a frequency for a tactical radar, the performance under adverse weather conditions is an important consideration. The factors affecting the choice of frequency form the subject of the next section.

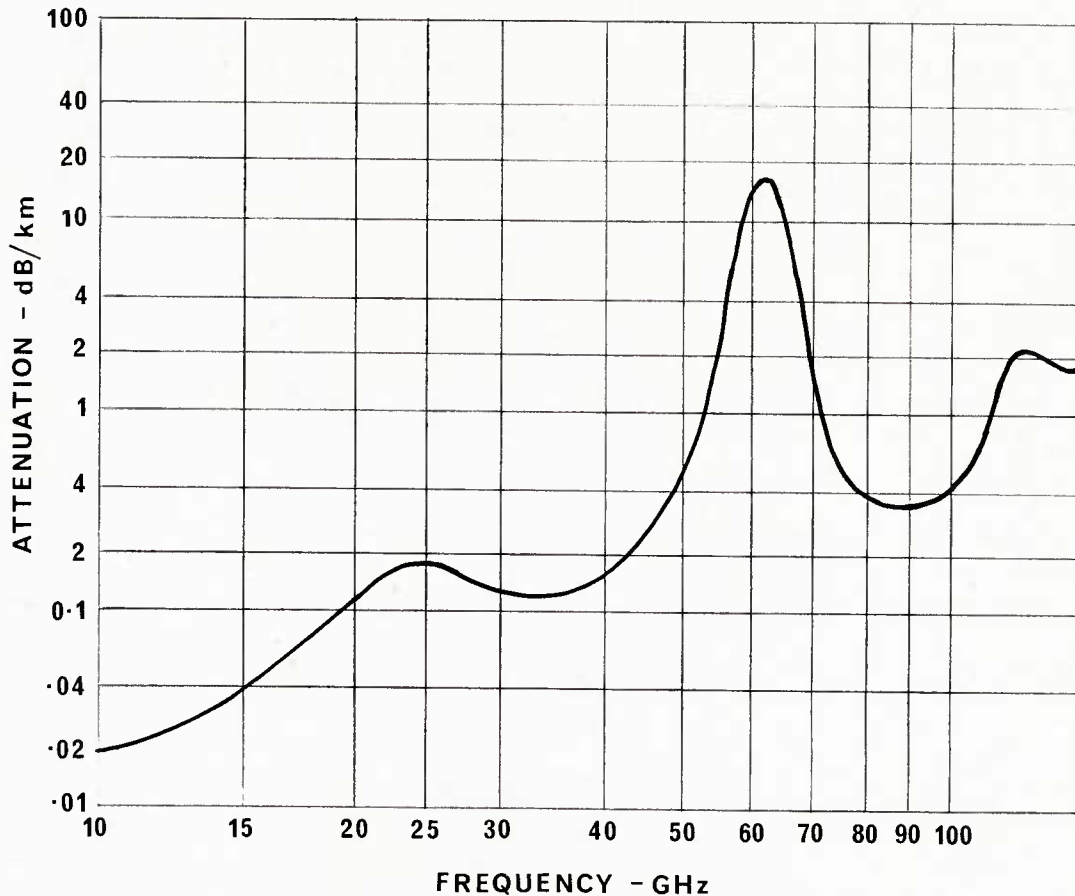


Fig.3 Average Atmospheric Absorption of EM Waves at Sea Level

Frequency of Tactical Radars

The factors involved in the selection of the transmitter frequency for a battlefield radar include:

- (i) The limitation on antenna size coupled with the angular resolution and accuracy requirements.
- (ii) The requirement for "all-weather" performance.
- (iii) The frequency dependence of both target and clutter echo areas.
- (iv) The availability of components with the required performance.
- (v) The enemy's, ESM and ECM capabilities.
- (vi) Electromagnetic compatibility with other operational equipments.

Only the first four items will be discussed in this paper.

- (i) Antenna size and resolution

In fig 5 is shown the relationship between azimuth resolution and frequency with antenna aperture as parameter. It is apparent that in order to achieve a sensible value of resolution, say 400m at 10 km, coupled with an antenna of acceptable size the frequency has to be at least 10 GHz.

- (ii) We have already discussed the question of back scattering from and attenuation by precipitation and have established that the radar performance degrades with increasing frequency. We have seen that the employment of circular polarisation can reduce substantially the backscatter from rain but for a fixed volume of rain the backscatter increases with increasing frequency up to frequencies of 100 GHz at least, whereas the echo area of typical targets is relatively insensitive to frequency within this range.

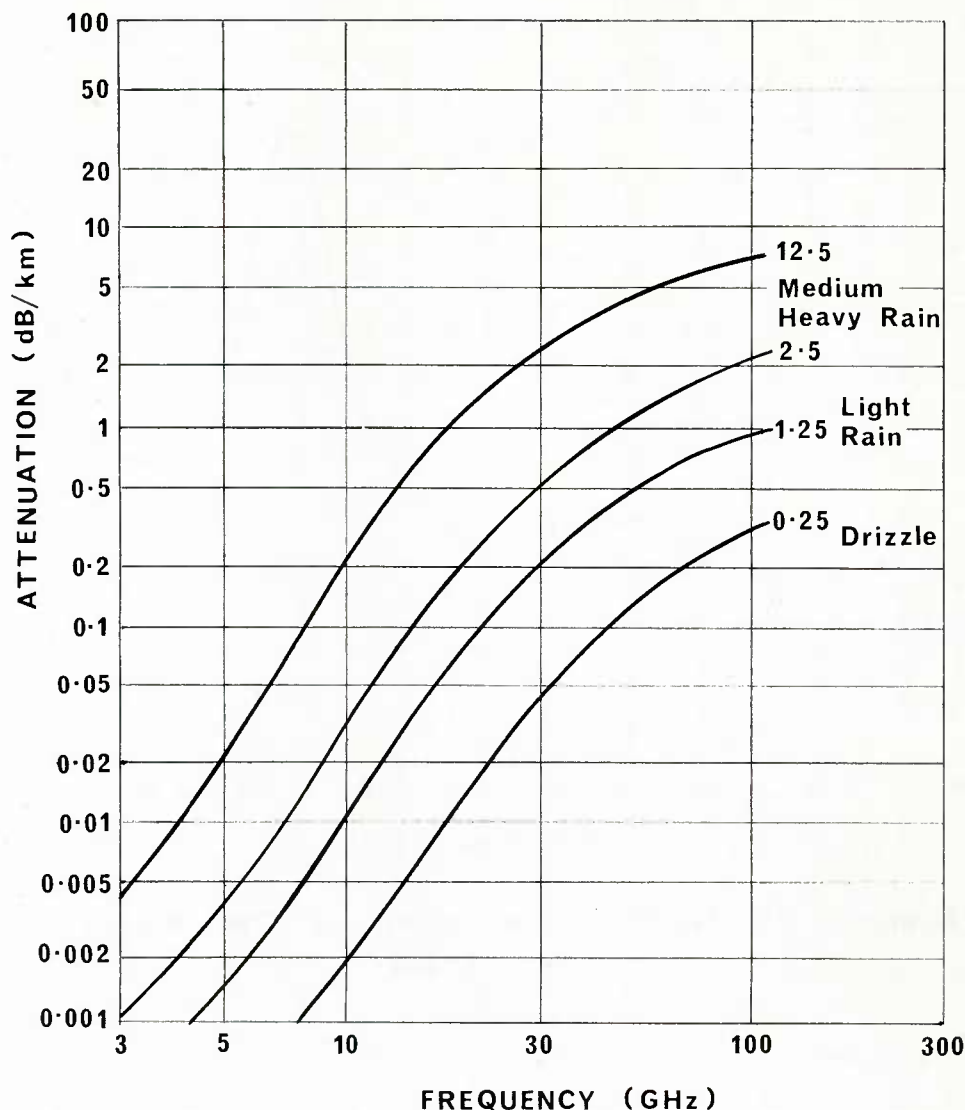


Fig.4 Attenuation Due to Rainfall

Although some reduction in rain clutter can be achieved at the higher frequencies by reducing the antenna beamwidths, and hence the volume of rain illuminated, this approach cannot be taken too far in the case of a surveillance radar which has to scan a large sector. Thus, if the elevation beamwidth is made too small it will be necessary to scan the antenna in elevation as well as azimuth in order to provide complete coverage of undulating terrain.

- (iii) Extensive measurements have been made of the backscatter from different types of ground clutter and inevitably there are considerable differences between the results of different workers. There is, however, a trend towards greater clutter returns as the frequency is increased for natural ground clutter.

Measurements of the mean echo-areas of typical ground vehicles show little evidence of frequency dependence within the range 10-100 GHz although the returns from some specific aspects of a target may vary with frequency depending upon the shape of the dominant reflector. From the point of view of target detectability, then, there is no advantage in going to the higher frequencies but there may be some advantage to be gained in target classification capability. Thus moving parts on vehicles which may only give a small echo at say X-band ($\lambda = 3$ cm) because of their small size will give a much larger echo at F-band ($\lambda = 0.3$ cm) so that the target doppler spectrum contains more information for characterisation of the target.

- (iv) In general the availability of components reduces as the frequency is increased. A related point is that the mechanical tolerances required to achieve particular performance levels with components scales with wavelength so that the difficulty, and hence cost, of making high frequency components tends to increase.

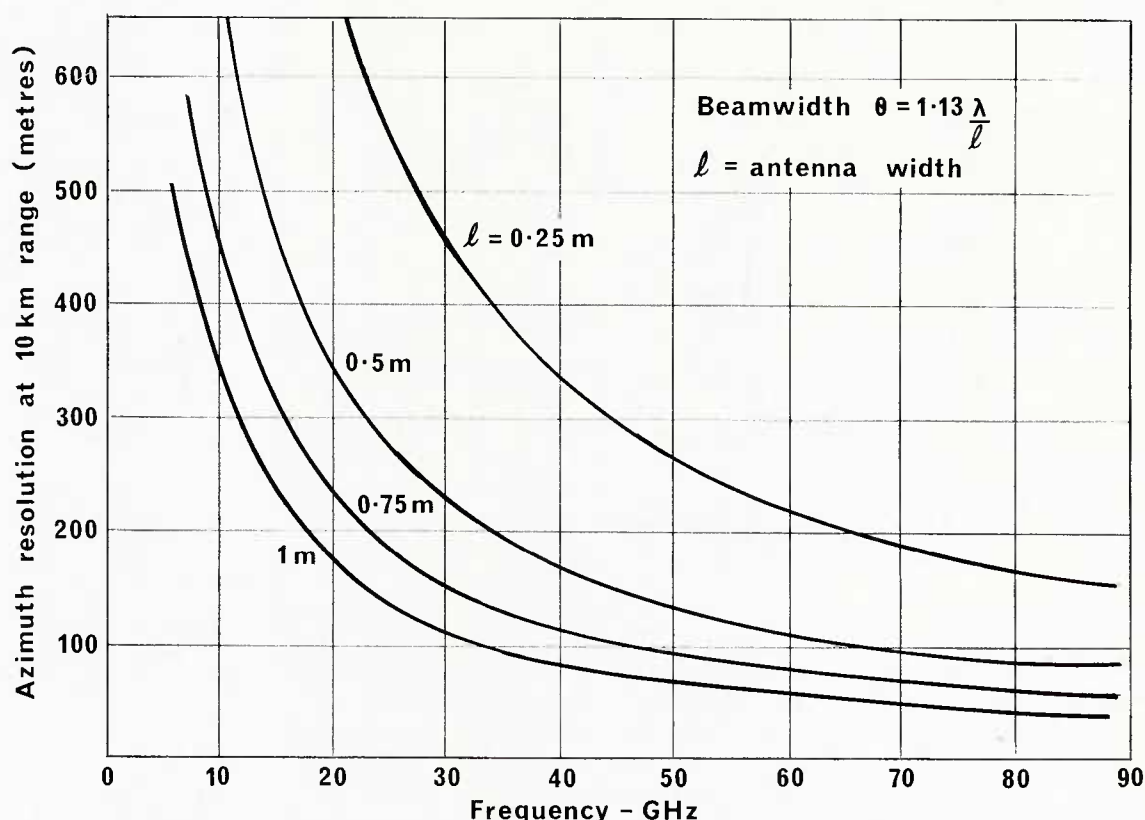


Fig.5 The Relationship Between Azimuth Resolution and Frequency

To conclude the discussion of choice of frequency (1) we have established a lower limit at X-band ($\lambda = 3$ cm) in order to achieve sensible values of angular resolution and accuracy with an antenna size acceptable for a portable equipment (2). Increasing the frequency allows the possibility of reducing antenna size (and hence perhaps overall equipment size) whilst retaining good angular resolution and accuracy. However, if the frequency is increased too much there may be unacceptable losses of performance in adverse weather (3).

At millimetre wave frequencies, the components, particularly the antenna, can be made very small and increased spectral information may be obtained. Although the penalty in terms of reduction of range performance in poor weather would be unacceptable for a long range surveillance system such high frequencies would be suitable for short range systems such as required by TGSMs. Indeed such systems are driven to the millimetre wavebands by the requirement that the antenna size has to be very small.

Choice of RF waveform

There are two major factors which have to be considered in selecting the transmitter waveform for a tactical radar. The first is the ability of the waveform to discriminate against clutter and the second is the desirability of minimising the probability of the radar being detected. We have already seen that a conventional pulse-doppler radar system provides a satisfactory system for use on the battlefield since it allows the use of both range-gating and doppler processing to discriminate against ground clutter. However, simple pulsed systems require the transmission of high peak power compared with CW systems and are thus easier for an enemy to detect and locate.

CW systems

Pure CW systems of course have no range discrimination capability and are of no use in a cluttered environment. A large number of modulation systems for CW radars has been proposed including FMCW, noise modulation, and pseudo-random modulations of various types. Of these the pseudo-random modulations appear to be most promising for the particular type of radar under consideration.

For application as modulating waveforms pseudo random signals have two important properties: (1) they have many of the characteristics of noise and (2) they can be defined explicitly (as opposed to statistically) as a function of time. The signals most often employed are binary digital sequences with maximum length sequences having the particular practical advantages for this application of being easy to generate and delay. One of the most attractive means of employing these codes is to biphase modulate the carrier using 0 and 180° as the two levels. The resulting transmitted spectrum is shown in fig 6.

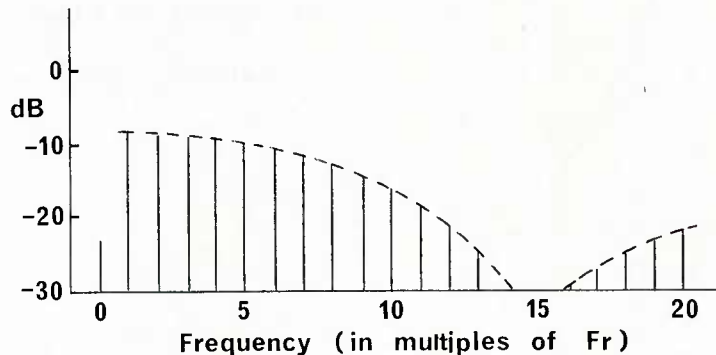


Fig.6 A PRC Spectrum

By suitable choice of code length and bit rate a waveform with satisfactory processing gain against clutter can be generated which will also have a power level approximately 20 dB less than the peak power of a typical pulsed radar of the same performance. In addition the signal is noise-like to a certain extent thus making it more difficult for the signal to be detected.

Pulse Compression Systems

Pulse Compression waveforms represent an intermediate situation between simple pulsed and modulated CW systems. The process of pulse compression in its simplest form requires that the transmitted radar pulse is frequency modulated with a linear frequency sweep. The received pulse is applied to a dispersive filter matched to the transmitted pulse with the result that the energy contained within the original long pulse of duration T , say, is compressed into a shorter pulse of duration approximately $(f_2 - f_1)^{-1}$ where $f_2 - f_1$ is the frequency range over which the transmitted pulse is swept. Thus pulse compression systems have the detection performance associated with the energy in the long duration low power pulse but retain the range resolution capability of the compressed pulse duration. Such systems thus have the desirable property of reducing the peak power transmitted.

In principle, then, both suitably modulated CW and pulse compression waveforms have potential ECCM advantages over simple pulsed systems. These advantages, however, are obtained at the expense of increased radar complexity, and also, in the case of pulse compression, at the expense of increasing the minimum radar range. Both these waveform types have been implemented in radars and of course the current pace of advances in technology, particularly in signal processing techniques, will ensure that the extra complexity is of decreasing significance.

Propagation factors affecting detection and location of battlefield radars.

In a tactical situation an important operational requirement is to minimise the probability of a radar being detected and if it is detected, to minimise the enemy's ability to locate the radar with sufficient accuracy to take effective counter-measures. The nature of typical battlefield terrain and the effect that it has on the propagation of radar signals is of considerable significance in determining the vulnerability of the radar to enemy ESM.

The performance of an ESM receiver is fundamentally limited by the magnitude of the signal it receives from an emitter and in a DF mode the location accuracy will be limited by the apparent direction of arrival of the signal. A parameter of considerable importance in determining the vulnerability of a radar to enemy detection and location is the range between the radar and ESM sites. For typical rolling and slightly hilly countryside the probability of obtaining line of sight (LOS) between two points decreases rapidly with increasing range. The author is grateful to M P Warden ref (2) of RSRE for supplying some terrain data derived from a contour map of typical Western European terrain and this is shown in table (1). The table shows the probability of line of sight, one crest, or two crests for four typical intercept sites and a random selection of radar sites.

Number of Crests	PROBABILITY			
	Site 1	Site 2	Site 3	Site 4
	11-20 km	11-20 km	11-20 km	11-20 km
LOS	0.14	0.22	0.17	0.41
1 Crest	0.44	0.48	0.50	0.35
2 Crests	0.24	0.21	0.23	0.17
>2 Crests	0.175	0.10	0.11	0.075

TABLE 1.

It is apparent that the data for site 4 is significantly different from the other sites in giving a much higher probability of line-of-sight. If the data from this site is disregarded then the average probability figures for the 11-20 km range bracket are as follows:

Probability of LOS	0.18
Probability of 1 crest	0.47
Probability of 2 crests	0.23
Probability of > 2 crests	0.12

It should be emphasised that these path profile figures neglect topographical features such as trees and buildings since these were not included on the contour map used to derive the statistics. Clearly they could raise the effective ground level by about 10m and influence LOS probabilities significantly.

In order to locate a radar, at least two intercept stations are involved in plotting a fix. If the paths between each site and the radar position can be regarded as uncorrelated in terms of their topographical features then the probability of LOS to both sites will be 0.18^2 i.e. 0.03. There is, then a quite low probability, in this range bracket, of LOS to two intercept stations simultaneously and in many cases ESM equipment will be operating on signals arriving over diffracted paths or by reflection.

In cases where line-of-sight does not exist between transmitter and receiver the received signal power can only be described statistically unless details of the path profile are known, and even then relatively small topographical features, such as trees, for example, can have a significant effect on propagation loss if they are close to a terminal. To give some indication of the magnitude of the signal attenuation due to diffraction the single crest geometry shown in fig (7) is assumed.

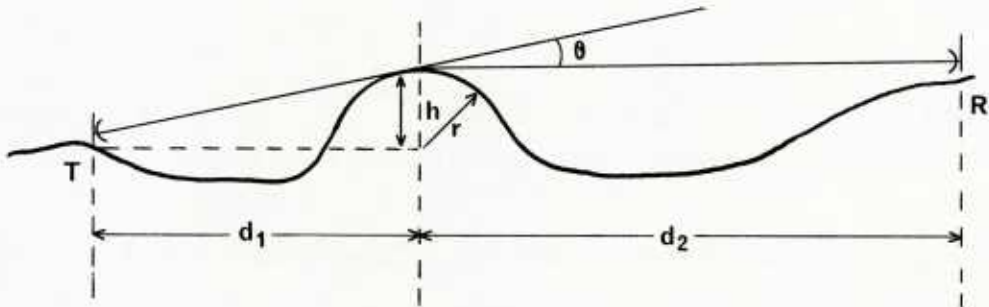


Fig.7 Diffraction Geometry for Single Crest

Here, the intercept receiver is assumed to be in a favourable position on top of a crest such that the major contribution to the diffraction angle θ is provided by the angle subtended by the transmitter at the crest.

i.e. $\theta = \tan^{-1} h/d_1$ or $\theta = h/d_1$ for $\theta \leq 10^\circ$

The attenuation obtained for a crest height of 30m for crests of different radii of curvature is shown in fig (8) as a function of the distance d_1 between the radar and the crest centre.

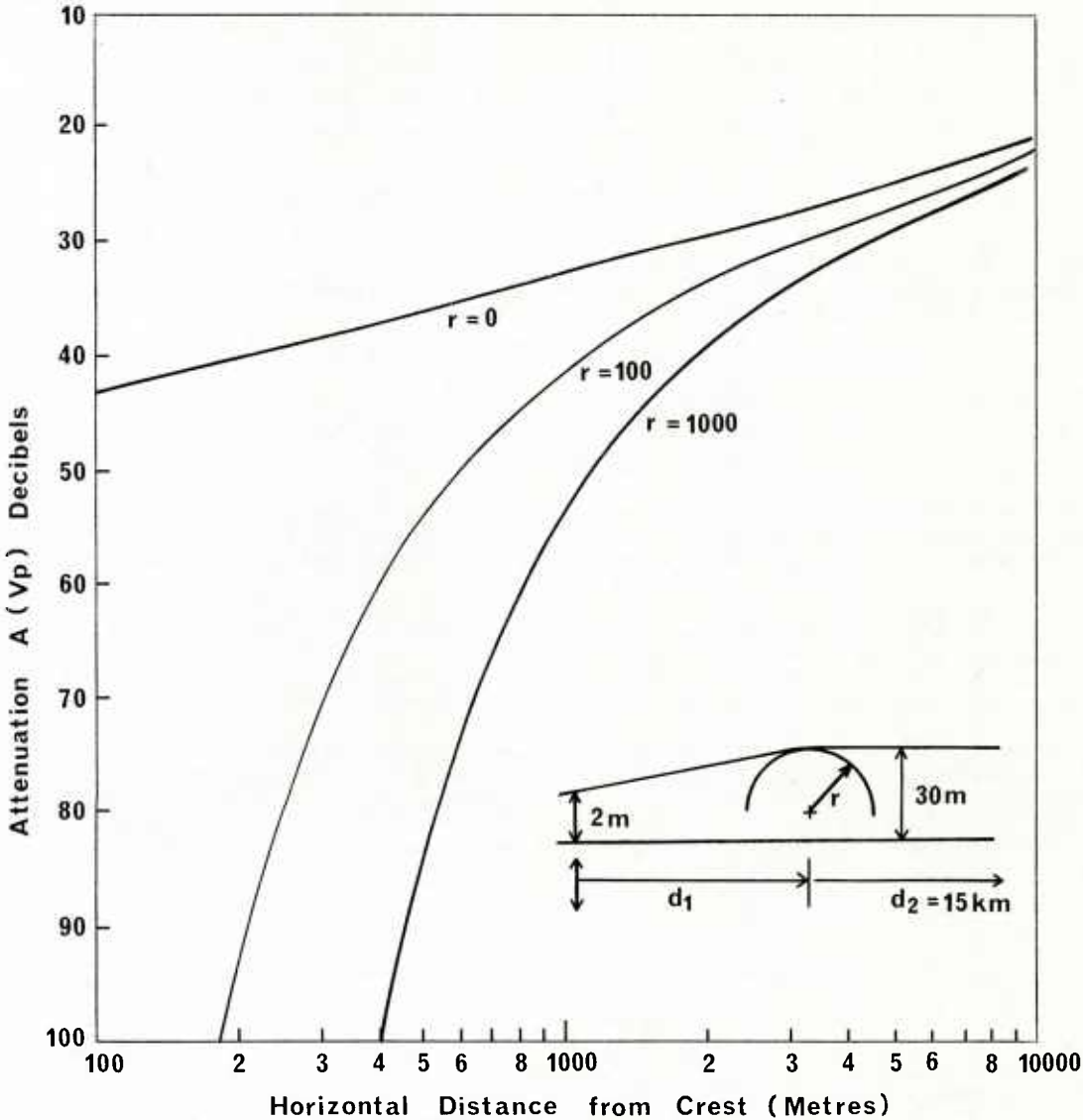


Fig.8 Crest Attenuation for 30m Ridge Height

It is apparent that the presence of a crest between radar and intercept receiver can give significant attenuation and this attenuation increases as the transmitter to crest distance decreases, as would be expected.

The theoretical attenuation provided by crests may be reduced by the forward scattering effect produced by the presence of discrete objects such as single trees or buildings etc. on top of the crest. Such objects may scatter forward significant power even when the diffracted field is very low. However, although this will tend to increase the probability of the radar being detected it is likely to reduce the accuracy with which the intercept station can determine the bearing of the radar. Given that in a practical situation it is unlikely that a radar would remain undetected even though the terrain attenuation is large, then the presence of discrete forward scatterers on a crest is likely to be a positive advantage to the radar in disguising its true position.

Apart from forward scattering and diffraction, multipath propagation is the only other phenomenon of significance in determining the accuracy with which an intercept receiver can determine emitter bearings. Such propagation can arise from reflection or forward scattering from hillsides or in general from any suitably inclined ground. Multipath effects can occur of course even when there is line-of-sight between radar and receiver and can lead to significant bearing errors. These errors arise because of the problem which the ESM equipment has in identifying the direct path to the radar which may not be the direction of maximum signal power since the antenna main-lobe may not actually be sweeping past the ESM site. However, given that the sector swept by the radar does include the receiver site, the directly received signal will arrive before any reflected signals and hence for a pulsed signal this time relationship could be used to identify the correct bearing.

In a more complex scenario where multipath propagation is present in addition to the absence of line-of-sight between transmitter and receiver this will obviously further reduce the probability of the intercept station achieving an accurate bearing measurement.

To summarise on the subject of propagation effects in an EW environment, if there is line-of-sight between radar and ESM sites then the probabilities of the radar being both detected and located accurately are high. Equally, of course, the radar has a high probability of detecting the presence of the intercept station. In order to reduce the radar's vulnerability, the operator must site the equipment to take advantage of the propagation effects which we have outlined.

In overall conclusion we have seen that propagation related factors have a significant effect on the selection of many of the radar system parameters and are also of considerable importance in selecting an operational site for the equipment.

Copyright (C) Controller HMSO, London, 1982.

References:

- 1 Dennis, P MOD(PE) unpublished work
- 2 Warden, M P MOD(PE) unpublished work

SELECTIVE BIBLIOGRAPHY

This bibliography has been prepared to support AGARD Lecture Series No. 120. It is intended to supplement references given for each of the Lectures. The material has mainly been provided by the Fachinformationszentrum Energie, Physik, Mathematik GmbH, Karlsruhe, F.R.G.; other relevant references have been added.

Contents

1. AGARD-Conference Proceedings
2. General Propagation and System Aspects
3. Terrestrial Cable Systems
4. Terrestrial VHF/UHF Propagation
5. Terrestrial SHF/EHF Propagation
6. Propagation on HF and below
7. Terrain and Surface Effects
8. Space/Earth and Space/Space Propagation
9. Optical Propagation
10. Miscellaneous

The first section, AGARD Conference Proceedings, contains details on AGARD Documentation referred to in the following sections, and useful as general sources of information.

1. AGARD Conference Proceedings

- AG 42 The Upper Atmosphere above F2 Maximum,
H. Poeverlein (Editor), 1959,
Meeting of Ionospheric Research Committee of Avionics Panel
Paris, France, May 1959

- AG 74 Propagation of Radio Waves at Frequencies below 300 kc/s
W.T. Blackband (Editor), 1964,
Meeting of Ionospheric Research Committee of Avionics Panel
Munich, Germany, September 1962

- CP 3 Propagation Factors in Space Communications
W.T. Blackband (Editor), 1967,
Meeting of Ionospheric Research Committee of Avionics Panel
Rome, Italy, September 1965

- CP 49 Ionospheric Forecasting
V. Agy (Editor), 1970,
Meeting of Electromagnetic Wave Propagation Committee of Avionics Panel
Grey Rocks, Canada, September 1969

- CP 70 Tropospheric Radio Wave Propagation
H.J. Albrecht (Editor), 1971,
Electromagnetic Wave Propagation Panel Meeting
Düsseldorf, Germany, September 1970

- CP 103 Aerospace Telecommunication Systems
F.I. Diamond (Editor), 1972,
Avionics Panel Meeting
London, United Kingdom, May 1972

- CP 159 Electromagnetic Noise Interference and Compatibility
T.J. Sueta, P. Halley (Editors), 1975,
Joint Meeting of Avionics and Electromagnetic Wave Propagation Panels
Paris, France, October 1974

- CP 192 Artificial Modification of Propagation Media
H.J. Albrecht (Editor), 1977,
Electromagnetic Wave Propagation Meeting
Brussels, Belgium, April 1976

- CP 208 EM Propagation Characteristics of Surface Materials and Interface Aspects
H.J. Albrecht (Editor), 1977,
Electromagnetic Wave Propagation Panel Meeting
Istanbul, Turkey, October 1976

- CP 209 Propagation Limitations of Navigation and Positioning Systems
J. Aarons, H. Soicher (Editors), 1977,
Electromagnetic Wave Propagation Panel Meeting
Istanbul, Turkey, October 1976

- CP 238 Operational Modelling of the Aerospace Propagation Environment
H. Soicher (Editor), 1978,
Electromagnetic Wave Propagation Panel Meeting
Ottawa, Canada, April 1978

- CP 245 Millimeter and Submillimeter Wave Propagation and Circuits
E. Spitz (Editor), 1979,
Electromagnetic Wave Propagation Panel Meeting
Munich, Germany, September 1978

- CP 263 Special topics in HF propagation
W.J. Coyne (Editor), 1979,
Electromagnetic Wave Propagation Panel Meeting
Lisbon, Portugal, May/June 1979

- CP 269 Terrain Profiles and Contours in Electromagnetic Wave Propagation
A.W. Biggs (Editor), 1979,
Electromagnetic Wave Propagation Panel Meeting
Spatind, Norway, September 1979
- CP 284 Propagation Effects in Space/Earth Paths
H.J. Albrecht (Editor), 1980,
Electromagnetic Wave Propagation Panel Meeting
London, United Kingdom, May 1980
- CP 295 The Physical Basis of the Ionosphere in the Solar-Terrestrial System
E. Schmerling (Editor), 1981,
Electromagnetic Wave Propagation Panel Meeting
Naples, Italy, October 1980

2. General Propagation and System Aspects

Aarons, J.; Whitney, H.E.; Allen, R.S.

Global morphology of ionospheric scintillations
Proc. IEEE, Vol. 59, pp. 159-172, 1971

Bean, B.R.; Dutton, E.J.

Radio Meteorology
National Bureau of Standards,
US-Dept. of Commerce, 1966

Birch, J.N.

Overview of DOD spread spectrum communications.
Signal (USA).
Vol. 34, No. 10, 49, 51-4. Aug. 1980.

Cook, C.E.

Optimum deployment of communications relays in an interference environment.
IEEE Trans. Commun. (USA).
Vol. COM. 28, No. 9, PT. 1, 1608-15. Sept. 1980.

Cook, W.J.; Weatherford, J.E.

The world administrative radio conference 1979 results and impact on defense
and national security.
ICC' 80. 1980 International Conference on Communications.
PT. I, XXVII+444P., 7.5/1-4. New York, USA. IEEE. 1980.

Fitts, R.E.

The strategy of electromagnetic conflict
Peninsula Publishing
Los Altos, California, U.S.A.

Holt, E.H.

Atmospheric data requirements for Battlefield obscuration applications.
Final Report
AD-A100398, ERADCOM/ASL-TR-0061 800600 85 p. Jpn.
2661 HC A05/MF A01.

Huebner, R.E.

Communications for marine corps tactical command and control systems, some
considerations.
IEEE Southeastcon 1981 conference proceedings.
913 P., 682-5. New York, USA. IEEE. 1981.

Katzenstein, W.E.; Moore, R.P.

Preferred frequency bands for radiolocation service between 40 and 300 GHz.
Final Report
AD-A080658, NWC-TP-6134 800100 11 p. Jpn. 1565 HC A02/MF A01.

Lampert, E.

Review on communication aspects of chaff-produced scatter propagation,
AGARD CP 192, pp. 3-1 to 3-10, 1976.

Manning, L.A.

Bibliography of the Ionosphere,
Stanford University Press, Stanford, Calif., 1962.

Marcus, M.J.

Analysis of tactical communications jamming problems
IEEE Transactions on Communications, Sept. 1980.
Vol. COM-28, pt. 1, p. 1625-1630.

Mooradian, G.C.

Atmospheric, space and underwater optical communications for naval applications.
Proceedings of the Society of Photo-Optical Instrumentation Engineers,
Vol. 150. Laser and Fibre Optics Communications. 83-91. 1978.

Mulhearn, P.J.

On surface-based advective radar ducts.
AD-A071454, RANRL-TN-5/78 78 1200 29p. Jpn. 180 HC A03/MF A01.

Probert, D.E.

Aspects of evolving systems in telecommunications modelling.
Proceedings of the International Conference on Cybernetics and Society.
1140 P., 452-8. New York, USA. IEEE. 1980.

Winkler, G.M.R.

Path delay, its variations, and some implications for the field use of precise frequency standards
Proc. IEEE, Vol. 60, No. 5, pp. 522-529, 1972.

3. Terrestrial Cable Systems

Fiber Optics in tactical systems.
Mil. Electron./Countermeas. (USA).
Vol. 6, No. 6, 36-7, 40-1. June 1980.

Barnoski, M.K.

Fiber systems for the military environment.
Proc. IEEE (USA).
Vol. 68, No. 10, 1315-20.

Mondrick, A.R.; Steensma, P.D.

Tactical fiber optic communication applications for the army.
1978 Wescon Technical Papers.
1116 P., 5.3/1-14. North Hollywood, CA, USA.
Western Periodicals Co.. 1978.

Schmidt, W.; Zwick, U.

Fabrication and test of optical fibre cables for military and PTT applications.
Proceedings of the 29th International wire and cable Symposium.
XV+456 P., 306-11. Fort Monmouth, NJ, USA. US Army
Commun. Res. Dev. Command. 1980.

Steensma, P.D.; Mondrick, A.

Battlefield fiber network.
Laser Focus (USA).
Vol. 15, No. 7, 52, 54, 56. July 1979.

4. Terrestrial VHF/UHF Propagation

Allen, J.P.; Funnell, G.

Triffid-The British Army's new tactical UHF radio relay equipment.
Commun. and Broadcast. (GB).
Vol. 4, No. 3, 30-6. Summer 1978.

Bogusch, R.L.; Guigliano, F.W.; Knepp, D.L.; Michelet, A.H.

Frequency selective propagation effects on spread-spectrum receiver tracking.
Proc. IEEE (USA), Vol. 69, p. 787-796, July 1981.

Chisholm, J.H.; Morrow, W.E.; Nichols, B.E.; Roche, J.F.; Teachman, A.F.

Properties of 400 Mc/s
Long distance tropospheric circuits,
Proc. I.R.E. 50, 2464-2482, 1962

Davis, J.R.; Hobbis, C.E.; Royce, R.K.

A new wide-band system architecture for mobile high frequency communication networks.
IEEE Trans. Commun. (USA).
Vol. COM. 28, No. 9, PT 1, 1580-90. Sept. 1980.

Dow, R.I.

The truffid tactical radio-relay equipment.
Electron. and power (GB).
Vol. 27, No. 7-8, 5303. July-Aug. 1981.

Fehlhaber, L.; Giloi, H.G.

Effects of nocturnal ground-based temperature inversion layers on line-of-sight radio links, in AGARD CP 208, pp. 9-1 to 9-15, 1976.

Freret, P.; Eschenbach, R.; Crawford, D.; Braisted, P.

Applications of spread-spectrum radio to wireless terminal communications.
NTC' 80. IEEE 1980 National Telecommunications Conference.
Vol. 4, (480+528+522+272) P.; 69.7/1-4. New York,
USA. IEEE. 1980

Minkhoff, J.; Weissman, I.

A review of VHF/UHF scattering from a heated ionospheric volume, in
AGARD CP 192, pp. 8-1 to 8-21, 1976.

Rogers, J.D.; Stears, M.

Compact digital tropospheric scatter equipment for military applications.
Conference on Communications Equipment and Systems.
XVI+272 P.; 228-33. London, England. IEE. 1980.

Unkauf, M.G.; Tagliaferri, O.A.

Tactical digital troposcatter systems.
NTC 78. Conference record of the IEEE 1978 national telecommunications conference.
PT II, XX+354 P., 17.4/1-5. New York, USA. IEEE. 1978.

C.C.I.R. Rec. 310

Definitions of terms relating to propagation in the troposphere.

C.C.I.R. Rec. 370

VHF and UHF propagation curves for the frequency range from 30 MHz to 1000 MHz.

5. Terrestrial SHF/EHF Propagation

Corcoran, V.J.

Electronically scanned phased arrays for near millimeter wave imaging in a dynamic tactical environment.
Proc. Soc. Photo-Opt. Instrum. Eng. (USA).
Vol. 259, 107-14. 1980.

Cram, L.A.; Woolcock, S.S.

Review of two decades of experience between 30 GHz and 900 GHz in the development of model radar systems, in AGARD CP 245,
pp. 6-1 to 6-15, 1978.

Currie, N.C.; Dyer, F.B.; Hayes, R.D.

Some properties of radar returns from rain at 9.375, 35, 70, and 95 GHz,
IEEE International Radar Conf., Arlington, Va., April 1975, pp. 215-220.

Falcone, V.J., jr.; Abreu, L.W.

Atmospheric attenuation of millimeter and submillimeter waves.
EASCON' 79. IEEE Electronics and Aerospace Systems Conference.
PT I, XIX+96 P.; 36-41. New York, USA. IEEE. 1979.

Flood, W.A.

Overview of near millimeter wave propagation.
Proc. Soc. Photo-Opt. Instrum. Eng. (USA).
Vol. 259, 52-7. 1980.

Foote, F.B.; Reber, E.E.; Hodges, D.T.

Active/passive near-millimeter wave imaging for tactical applications.
Proc. Soc. Photo-Opt. Instrum. Eng. (USA).
Vol. 259, 131-6. 1980.

Gallagher, J.J.; McMillan, R.W.; Shackelford, R.G.

Military systems applications at near-millimeter wavelengths.
Modern utilization of infrared technology V; Proceedings of the Fifth Annual Seminar, San Diego, Calif., Aug. 29, 30, 1979. (A80-39101 16-35)
Bellingham, Wash., Society of Photo-Optical Instrumentation Engineers,
p. 170-190, 1979.

Goldhirsch, J.

The use of radar at non-attenuating wavelengths as a tool for the estimation of rain attenuation at frequencies above 10 GHz.
EASCON' 79. IEEE Electronics and Aerospace Systems Conference.
PT. I; XIX+96 P.; 48-55. New York, USA. IEEE. 1979.

Hayes, D.T.; Lammers, U.H.W.; Marr, R.A.; McNally, J.J.

Millimeter wave propagation measurements over snow.
EASCON' 79. IEEE Electronics and Aerospace Systems Conference.
PT. II; XIX+335 P.; 362-8. New York, USA. IEEE. 1979.

Keeping, K.J.; Rogers, D.S.; Sureau, J.-C.

A scanning switch matrix for a cylindrical array (C-band tactical radar).
1981 IEEE MIT-S international microwave symposium digest.
XXVII+543 P.; 419-21. New York, USA. IEEE. 1981.

Kleinjung, E.

Non-ionised propagation media with artificially modified precipitation characteristics, in AGARD CP 192, pp. 1-1 to 1-10, 1976.

Knox, J.E.

Millimeter wave propagation in smoke.
EASCON' 79. IEEE Electronics and Aerospace Systems Conference.
PT. II; XIX+335 P.; 357-61. New York, USA. IEEE. 1979.

Liebe, H.J.; Hopponen, J.D.

Variability of EHF air refractivity with respect to temperature, pressure, and frequency, IEEE Trans. on Antennas and Propagation, Vol. AP-25, No. 3, pp. 336-345, 1977.

Liebe, H.J.

Atmospheric oxygen microwave spectrum-experiment versus theory
IEEE Trans. on Antennas and Propagation,
Vol. AP-25, No. 3, pp. 327-335, 1977.

McMillan, R.W.; Shackelford, J.C.; Snider, D.E.

Millimeter-wave beamrider and radar systems.
Proc. Soc. Photo-Opt. Instrum. Eng. (USA).
Vol. 259; 166-71. 1980.

McMillan, R.W.; Wiltse, J.C.; Snider, D.E.

Atmospheric turbulence effects on millimeter wave propagation.
EASCON' 79. IEEE Electronics and Aerospace Systems Conference.
PT. I; XIX+96 P.; 42-7. New York, USA. IEEE. 1979.

Rider, G.C.; Clarke, J.

A long range propagation experiment to investigate the incidence of anomalous propagation in the NW Atlantic.
Second international conference on antennas and propagation.
Vol. 2, (XXX+538+XXIX+301) P.; 2/168-72 Part.2. London, England, 1981.

Seashore, C.R.

Millimeter optics: A system application overview.
Proc. Soc. Photo-Opt. Instrum. Eng. (USA).
Vol. 259; 144-51. 1980.

Sollfrey, W.

Nomograms for the calculation of propagation effects on tactical millimeter wave radio links.
Interim Report, 1 Jan.- 1 Jul. 1979
AD-A073900; CORADCOM-77-0142-1 790800 DAAB07-77-C-0142
36 p. Jpn. 728 HC AO3/MF AO1.

C.C.I.R. Report 719

Attenuation by atmospheric gases

C.C.I.R. Report 721

Attenuation and scattering by precipitation and other atmospheric particles

C.C.I.R. Report 723

Worst-month statistics

C.C.I.R. Report 724

Propagation data for the evaluation of co-ordination distance in the frequency range 1 to 40 GHz.

6. Propagation on HF and below

Albrecht, H.J.

Further studies on the chordal-hop theory of ionospheric long-range propagation, Archiv, Met. Geoph., Biokl., Ser. A, 11, pp. 383-391, 1959.

Albrecht, H.J.

Monitoring multi-frequency mode delay over long distances for ionospheric frequency selection, in AGARD CP 49, pp. 21-1 to 21-10, 1969.

Bernhardt, P.A.; Da Rosa, A.V.; Park, C.G.

Chemical depletion of the ionosphere, in AGARD CP 192, pp. 15-1 to 15-16, 1976.

Bradley, P.A.; Lockwood, M.

Ionospheric predictions for HF radio systems: the future, in AGARD CP 295, pp. 32-1 to 32-13, 1980.

Damboldt, Th.

Comparison of measured and predicted MUFs at a remote location, in AGARD CP 263, pp. 7-1 to 7-6, 1979.

Davies, K.

Ionospheric Radio Propagation
Nat. Bureau of Standards Monogr. 80, 1965.

Fejer, J.A.; Leer, E.

Excitation of parametric instabilities by radio waves in the ionosphere
Radio Science, Vol. 7, pp. 481-491, 1972.

Haerendel, G.

Modification of ionized media by chemical substances - a review of physical processes, in AGARD CP 192, pp. 13-1 to 13-15, 1976.

Hsu, F.M.; Giordano, A.A.; De Pedro, H.E.; Proakis, J.G.

Adaptive equalization techniques for high-speed transmission on fading dispersive HF channels.

NTC' 80. IEEE 1980 National Telecommunications Conference.

Vol. 4, (480+528+522+272) P.; 58.1/1-7. New York, USA. IEEE. 1980.

Jones, T.B.; Spracklen, C.T.

Some effects of a high altitude barium release on the propagation characteristics of HF radio waves, in AGARD CP 192, pp. 16-1 to 16-7, 1976.

Mendillo, M.; Forbes, J.

Spatial-temporal development of molecular releases capable of creating large-scale F-region holes, in AGARD CP 192, pp. 14-1 to 14-8, 1976.

Perkins, F.W.; Oberman, C.; Valeo, E.J.

Parametric instabilities and ionospheric modification
Journ. Geoph. Res., Vol. 79, pp. 1478-1496, 1974.

Utlaut, W.F.

Ionospheric modification induced by higher-power HF-transmitter - potential for communication and plasma physics research, in AGARD CP 192, pp. 6-1 to 6-4, 1976.

C.C.I.R. Rec. 373

Definitions of maximum transmission frequencies

C.C.I.R. Report 250

Long-distance ionospheric propagation without intermediate ground reflection

C.C.I.R. Report 255

Long-term ionospheric propagation predictions

C.C.I.R. Report 262

ELF, VLF and LF propagation in and through the ionosphere

C.C.I.R. Report 266

Ionospheric propagation characteristics pertinent to terrestrial radio-communication systems design

C.C.I.R. Report 725

Ionospheric properties

C.C.I.R. Report 726

Ground and ionospheric side - and back-scatter

C.C.I.R. Report 727

Short-term predictions of operational parameters for ionospheric radio-communications

C.C.I.R. Report 728

Ionospheric modification by high-power HF transmissions

7. Terrain and Surface Effects

Felsen, L.B.; Green, A.

Ground-wave propagation in the presence of smooth hills and depressions, in AGARD CP 208, pp. 7-1 to 7-13, 1976.

Grzenda, C.; Cybrowski, W.; NG, P.

Digital troposcatter radio performance over simulated path profiles.
NTC' 78. Conference record of the IEEE 1978 national telecommunications conference.
PT II; XX+354 P.; 17.5/1-4. New York, USA. IEEE. 1978.

Hagn, G.H.

VHF Radio system performance model for predicting communications operational ranges in irregular terrain.
IEEE Trans. Commun. (USA).
Vol. COM. 28, No. 9, PT. 1; 1637-44. Sept. 1980.

Hill, M.L.; Whyte, T.R.; Weiss, R.O.; Rubio, R.; Isquierdo, M.

Use of atmospheric electric fields for vertical stabilization and terrain avoidance. Guidance and Control Conference, Albuquerque, NM August 19-21, 1981, Collection of Technical Papers. (A81-44076 21-12) New York, American Institute of Aeronautics and Astronautics, Inc. p. 401-410, 1981.

Küsters, E.R.

Biological and geophysical factors of electromagnetic wave propagation and their use in digital data banks, in AGARD-CP-269, 1979.

Mooradian, G.C.

Surface and subsurface optical communications in the marine environment.
Opt. Eng. (USA).
Vol. 20, No. 1; 071-5. Jan.-Feb. 1981.

Noma, A.A.; Misulia, M.G.

Programming topographic maps for automatic terrain model construction
Surveying and Mapping, Vol. 19, p. 3, 1976.

Palmer, F.H.

The CRC VHF-UHF propagation prediction program: description and comparison with field measurements, in AGARD CP 238, pp. 49-1 to 49-15, 1978.

C.C.I.R. Rec. 527

Electrical characteristics of the surface
of the Earth

C.C.I.R. Report 236

Influence of terrain irregularities and
vegetation on tropospheric propagation

8. Space/Earth and Space/Space Propagation

Aarons, J.

Equatorial scintillations: a review IEEE Trans. on scintillations
Antennas and Propagation, AP-25, No. 5, pp. 729-736, 1977.

Albrecht, H.J.

Using ionospheric prediction charts to tentatively forecast VLF signal
intensity in satellite communications, in AGARD-CP-3, pp. 175-179, 1965.

Albrecht, H.J.; Makaruschka, R.; Menzel, R.

Propagation criteria with tactical satellite communications, in AGARD CP 103,
pp. 14-1 to 14-12, 1972.

Allen, R.S.; DuLong, D.D.; Grossi, M.D.; Katz, A.H.

Ionospheric range error correction in precision radar systems by adaptive
probing of the propagation medium, in AGARD CP 209, pp. 6-1 to 6-16, 1976.

Basu, S.

Correlated measurements of scintillations and in-situ F-region irregularities
from OGO-6 Geoph. Res. Lett.,
Vol. 3, No. 11, pp. 681-684, 1976.

Booker, H.G.

The use of radio stars to study irregular refraction of radio waves in the
ionosphere, Proc. IRE,
Vol. 43, pp. 1437-1449, 1965.

Bucher, E.A.; White, D.P.

Time diversity modulation for UHF satellite communication during scintilla-
tion
Nat. Telecom. Conference PT. III, Dallas, Tex., pp. 43.4-1 to 43.4-5, 1976.

Collins, L.D.

EHF satellite communications for mobile terminals.
AAS Paper 80-205 801000 American Astronautical Society and American Institute
of Aeronautics and Astronautics, Annual Meeting on Space Enhancing Technologi-
cal Leadership, Boston, Mass., Oct. 20-23, 1980.

Costa, E.; Kelley, M.C.

Calculations of equatorial scintillations at VHF and gigahertz frequencies
based on a new model of the disturbed equatorial ionosphere
Geoph. Res. Lett., Vol. 3, No. 11, pp. 677-680, 1976.

Crane, R.K.

Ionospheric scintillations
Proc. IEEE, Vol. 65, No. 2, pp. 180-199, 1977.

Crane, R.K.

Prediction of the effects of rain on satellite communication systems
Proc. IEEE, Vol. 65, No. 3, pp. 456-474, 1977.

Cummings, W.C.; Richardi, L.J.; Jain, P.C.

Fundamental performance characteristics that influence EHF MILSATCOM Systems.
IEEE Trans. Commun. (USA). Co: IECMBT.
Vol. COM-27, No. 10, P. 1; 1423-35, Oct. 1979.

Davies, K.

Recent progress in satellite radio beacon studies with particular emphasis
on the ATS-6 radio beacon experiment
Space Science Reviews, Vol. 25, pp. 357-430, 1980.

Denaro, R.P.

NAVSTAR: The all-purpose satellite.
IEEE spectrum (USA).
Vol. 18, No. 5; 35-40. May 1981.

McElroy, D.R.; Eaves, R.E.

EHF systems for mobile users --- for satellite communication.
Communications Satellite Systems Conference, 8th, Orlando, Fla.,
April 20-24, 1980, Technical Papers.
(A80-29526 11-32) New York, American Institute of Aeronautics and
Astronautics, Inc., p. 509-515, 1980.

Evans, A.G.; Hermann, B.R.; Feil, P.J.

Global positioning system sensitivity experiments
Final Report
AD-A097851; NSWC/TR-81-4 810100 Strategic Systems
Dept. 27 p. Jpn. 2007 HC A03/MF A01.

Fante, R.L.

Effect of source bandwidth and receiver response time on the scintillation
index in random media,
Radio Science, Vol. 12, No. 2, pp. 223-229, 1977.

Frediani, D.J.

Technology assessment for future MILSATCOM systems:
The EHF bands.
DCA-5; ESD-TR-79-43 790412 F19628-78-C-0002 294 p. Jpn. 180 HC A13/MF A01.

Fremouw, E.J.; Bates, H.F.

World-wide behaviour of average VHF-UHF scintillations
Radio Science, Vol. 6, No. 10, 1971.

Fritz, R.B.; Pope, J.H.

Artificial ionospheric modification and scintillations of VHF satellite
signals in R. Leitinger (ed), "Proceedings of the Symposium on the Future
Applications of Satellite Beacon Measurements",
Universität Graz, p. 222, Juni 1972.

Hodge, D.B.

Frequency scaling of rain attenuation, IEEE Trans. on Antennas and Propaga-
tion, Vol. AP-25, No. 3, pp. 446, 1977.

Hortenbach, K.J.

Multiple ground reflection effects on fading behaviour of VHF/UHF satellite
transmissions, IEEE Trans. on Antennas and Propagation, AP-18, No. 6,
pp. 836-838, November 1970.

Hunt, W.T.

The effect of the propagation medium on high data rate transmissions at low
elevation angles, in AGARD CP 70, pp. 14-1 to 14-8, 1970.

Jain, P.C.

Use of EHF frequency bands in future military satellite applications.
ICC' 79; International Conference on Communications, Boston, Mass.,
June 10-14, 1979, Conference Record.
Vol. 2, (A80-25901 09-32) Piscataway, N.J., Institute of Electrical
and Electronics Engineers, Inc., p. 33.4.1-33.4.4., 1979.

Jayasuriya, D.A.R.; Medeiros Filho, F.C.; Cole, R.S.

Scintillation fading in an absorption region. Second international conference
on antennas and propagation.
Vol. 2, (XXX-538+XXIX+301) P.; 2/221-4 Part 2, London, England. IEEE. 1981.

Leiphard, J.P.; Zeek, R.W.; Bearce, L.S.; Toth, E.

Penetration of the ionosphere by very-low-frequency radio signals - interim results of the LOFTI I experiment, Proc. I.R.E., 50, 6-17, 1962.

Lindal, G.F.; Hotz, H.B.; Sweetnam, D.N.; Shippony, Z.; Brenkle, J.P.; Hartsell, G.V.; Spear, R.T.; Michael, W.H. jr.

Viking radio occultation measurements of the atmosphere and topography of Mars: Data acquired during 1 martian year of tracking.

J. Geophysical Res. (USA).

Vol. 84, No. B14; 8443-56, 30 Dec. 1979.

Parkinson, B.W.; Lassiter, E.M.; Cretcher, C.K.

Ionospheric effects in NAVSTAR GPS, in AGARD CP 209, pp. 1-1 to 1-12, 1976.

Poeeverlein, H.

Transparency of the ionosphere and possible noise signals from high altitudes at extremely low frequencies, in AGARD AG 42, pp. 344-3, 1959.

Rorden, L.H.; Smith, R.L.; Helliwell, R.A.

An interpretation of LOFTI I: VLF observations, in AGARD AG 74, pp. 75-81, 1964.

Soicher, H.

Ionospheric and plasmaspheric effects in satellite navigation systems, IEEE Trans. on Antennas and Propagation Vol. AP-25, No. 5, pp. 705-708, 1977.

Soicher, H.

Plasmaspheric signal time-delay effects in satellite ranging systems, in AGARD CP 209, pp. 2-1 to 1-10, 1976.

Szuszcwicz, E.P.; Holmes, J.C.; Tsunoda, R.T.; Narcisi, R.

Coincident radar and rocket observations of equatorial spread-F.

Geophysical Research Letters,

Vol. 7, p. 537-540, July 1980.

Taur, R.R.

Simultaneous 1.5 and 4 GHz ionospheric scintillation measurement Radio Science, Vol. 11, No. 12, pp. 1029-1036, 1976.

Tuck, J.S.

Military satellite communications systems architecture, EASCON' 79;

Electronics and Aerospace Systems Conference Arlington, Va., October 9-11, 1979, Conference Record, Vol. 3, (A80-26776 09-32) New York,

Institute of Electrical and Electronics Engineers, Inc., p. 612-61, 1979.

Umeki, R.; Liu, C.H.; Yeh, K.C.

Multifrequency spectra of ionospheric amplitude scintillations Journ. Geoph. Res., Vol. 82, No. 19, pp. 2752-2760, 1977.

Walson, G.R.; Green, D.W.; Royden, H.N.

Use of Sirio faraday rotation data in navigation of the Voyager 1 and 2 spacecraft.

Alta Freq. (ITALY). Vol. 49, No. 5; 372-80, Sept.-Oct. 1980.

Whitney, H.E.; Basu, S.

The effect of ionospheric scintillation on VHF/UHF satellite communications Radio Science, Vol. 12, No. 1, pp. 123-133, 1977.

Whitney, H.E.; Malik, C.

A proposed index for measuring ionospheric scintillations Planetary and Space Science,
Vol. 17, 1069, 1969.

Wittwer, L.A.

A trans-ionospheric signal specification for satellite C³ applications.
Technical Report, 1 Jan. - 31 Dec. 1980.
AD-A101377; DNA-5662D 801231 Atmospheric Effects Div.
60 p. Jpn. 2757 HC A04/MF A01.

C.C.I.R. Report 426

Methods for predicting radio noise and the attenuation and refraction
of radio waves in relation to space telecommunication systems

C.C.I.R. Report 564

Propagation data required for space telecommunication systems

9. Optical Propagation

Blackman, G.R.; Marvin, J.W.

Automatic temporal analysis of smoke/dust clouds.
Proc. Soc. Photo-Opt. Instrum. Eng. (USA).
Vol. 205; 180-4. 1979.

Forrester, P.A.; Hulme, K.F.

Laser rangefinders. Review.
Opt. and quantum electron. (GB).
Vol. 13, No. 4; 259-93. July 1981.

Hänel, G.

Discussion on artificial fog modification, in AGARD CP 192, pp. 4-1 to 4-3, 1976.

Kaminski, W.R.

Range calculations for IR rangefinder and designators.
Proc. Soc. Photo-Opt. Instrum. Eng. (USA).
Vol. 227; 65-79, 1980.

Mason, R.S.

Laser communications via an atmospheric link.
NTC' 80. IEEE 1980 National Telecommunications Conference.
Vol. 4, (480+528+522+272) P.; 27.1/1.-9. New York, USA. IEEE. 1980.

Rye, B.J.

Refractive-turbulence contribution to incoherent backscatter heterodyne lidar returns.
J. Op. Soc. AM. (USA).
Vol. 71, No. 6; 687-91. June 1981.

Wiener, T.F.

Strategic laser communications.
Signal (USA).
Vol. 35, No. 1; 43-8. Sept. 1980.

Wiener, T.F.

Strategic laser communications
NTC' 80. IEEE 1980 National Telecommunications Conference.
Vol. 4, (480+528+522+272) P.; 27.4/1-5. New York, USA. IEEE. 1980.

10. Miscellaneous

Baltzer, G.

Digital voice cipher system for defence applications.
Philips telecommun. Rev. (Netherlands).
Vol. 39, No. 1; 33-40. March 1981.

Barton, P.; Waddoup, W.D.

Reduction of tracking errors induced by multipath at low elevation angles.
NTC' 80. IEEE 1980 National Telecommunications Conference.
Vol. 4, (480+528+522+272) P.; 11.2/1-7. New York, USA. IEEE. 1980.

Broad, W.J.

Nuclear pulse. I - Awakening to the chaos factor. Science,
Vol. 212, May 29, p. 10.09-10.12, 1981.

Cook, C.E.

Relay-augmented data links in an interference environment.
NTC' 80. IEEE 1980 National Telecommunications Conference.
Vol. 4, (480+528+522+272) P.; 63.6/1-5. New York, USA. IEEE. 1980.

Finkel, L.; Greeley, D.M.; Papasso, F.P.

Role of phased array radars in the future TACS.
Eascon' 80 record. IEEE Electronics and aerospace systems conventions.
196-203. New York, USA. IEEE. 1980.

Johnson, T.A.; Graf, E.R.

Geometric considerations in the modelling of environmental clutter.
IEEE Southeastcon 1981 conference proceedings.
913 P.; 643-5. New York, USA. IEEE. 1981.

Levanon, N.; Yalin-mor, E.

Doppler radar tracking of hostile fire.
IEEE Trans. Aerosp. and electron. syst. (USA).
Vol. AES-17, No. 3; 469-71, May 1981.

De Martino, A.; Penazzi, C.A.

Electronic Systems for Remote Sensing and Ranging.
27th International Electronics Scientific Congress.
133-42. Rome, Italy. Rassegna Internazionale Elettronica Nucleare ed
Aerospaziale. 1980 .

Pinson, L.J.; Viguet, G.S.

Automatic testing of performance of an electro-optical imaging system
under obscured atmospheric conditions.
Proc. Soc. Photo-Opt. Instrum. Eng. (USA).
Vol. 255; 64-8. 1980.

<p>AGARD Lecture Series No.120 Advisory Group for Aerospace Research and Development, NATO ELECTROMAGNETIC PROPAGATION PROBLEMS IN THE TACTICAL ENVIRONMENT Published April 1982 160 pages</p> <p>Modern battlefield activities require an increasing employment of electronic equipment. The large variety of applications extends from communications to surveillance, from reconnaissance to command and control. With regard to efficiency and limitations, many systems depend on the characteristics of the propagation medium and on operational adaptation to the propagation environment.</p> <p>P.T.O.</p>	<p>AGARD-LS-120</p> <p>Electromagnetic wave transmission Tactical command and control Combat zones</p>	<p>AGARD Lecture Series No.120 Advisory Group for Aerospace Research and Development, NATO ELECTROMAGNETIC PROPAGATION PROBLEMS IN THE TACTICAL ENVIRONMENT Published April 1982 160 pages</p> <p>Modern battlefield activities require an increasing employment of electronic equipment. The large variety of applications extends from communications to surveillance, from reconnaissance to command and control. With regard to efficiency and limitations, many systems depend on the characteristics of the propagation medium and on operational adaptation to the propagation environment.</p> <p>P.T.O.</p>	<p>AGARD-LS-120</p> <p>Electromagnetic wave transmission Tactical command and control Combat zones</p>
<p>AGARD Lecture Series No.120 Advisory Group for Aerospace Research and Development, NATO ELECTROMAGNETIC PROPAGATION PROBLEMS IN THE TACTICAL ENVIRONMENT Published April 1982 160 pages</p> <p>Modern battlefield activities require an increasing employment of electronic equipment. The large variety of applications extends from communications to surveillance, from reconnaissance to command and control. With regard to efficiency and limitations, many systems depend on the characteristics of the propagation medium and on operational adaptation to the propagation environment.</p> <p>P.T.O.</p>	<p>AGARD-LS-120</p> <p>Electromagnetic wave transmission Tactical command and control Combat zones</p>	<p>AGARD Lecture Series No.120 Advisory Group for Aerospace Research and Development, NATO ELECTROMAGNETIC PROPAGATION PROBLEMS IN THE TACTICAL ENVIRONMENT Published April 1982 160 pages</p> <p>Modern battlefield activities require an increasing employment of electronic equipment. The large variety of applications extends from communications to surveillance, from reconnaissance to command and control. With regard to efficiency and limitations, many systems depend on the characteristics of the propagation medium and on operational adaptation to the propagation environment.</p> <p>P.T.O.</p>	<p>AGARD-LS-120</p> <p>Electromagnetic wave transmission Tactical command and control Combat zones</p>

<p>In order to optimize system performance, operational personnel should possess adequate knowledge of system-relevant propagation criteria, and in addition, a training level which permits an efficient reaction under changeable battlefield conditions. This Lecture Series on Electromagnetic Propagation Problems in the Tactical Environment should be of interest to qualified technical officers and teaching staff, as well as to other personnel qualified in engineering science or natural sciences and connected with tactical electronics of any kind.</p> <p>The material in this publication was assembled to support a Lecture Series under the sponsorship of the Electromagnetic Wave Propagation Panel and the Consultant and Exchange Programme of AGARD presented on 3–4 May 1982 in Munich, Germany and on 6–7 May 1982 in Paris, France.</p> <p>ISBN 92-835-1419-X</p>	<p>In order to optimize system performance, operational personnel should possess adequate knowledge of system-relevant propagation criteria, and in addition, a training level which permits an efficient reaction under changeable battlefield conditions. This Lecture Series on Electromagnetic Propagation Problems in the Tactical Environment should be of interest to qualified technical officers and teaching staff, as well as to other personnel qualified in engineering science or natural sciences and connected with tactical electronics of any kind.</p> <p>The material in this publication was assembled to support a Lecture Series under the sponsorship of the Electromagnetic Wave Propagation Panel and the Consultant and Exchange Programme of AGARD presented on 3–4 May 1982 in Munich, Germany and on 6–7 May 1982 in Paris, France.</p> <p>ISBN 92-835-1419-X</p>
<p>In order to optimize system performance, operational personnel should possess adequate knowledge of system-relevant propagation criteria, and in addition, a training level which permits an efficient reaction under changeable battlefield conditions. This Lecture Series on Electromagnetic Propagation Problems in the Tactical Environment should be of interest to qualified technical officers and teaching staff, as well as to other personnel qualified in engineering science or natural sciences and connected with tactical electronics of any kind.</p> <p>The material in this publication was assembled to support a Lecture Series under the sponsorship of the Electromagnetic Wave Propagation Panel and the Consultant and Exchange Programme of AGARD presented on 3–4 May 1982 in Munich, Germany and on 6–7 May 1982 in Paris, France.</p> <p>ISBN 92-835-1419-X</p>	<p>In order to optimize system performance, operational personnel should possess adequate knowledge of system-relevant propagation criteria, and in addition, a training level which permits an efficient reaction under changeable battlefield conditions. This Lecture Series on Electromagnetic Propagation Problems in the Tactical Environment should be of interest to qualified technical officers and teaching staff, as well as to other personnel qualified in engineering science or natural sciences and connected with tactical electronics of any kind.</p> <p>The material in this publication was assembled to support a Lecture Series under the sponsorship of the Electromagnetic Wave Propagation Panel and the Consultant and Exchange Programme of AGARD presented on 3–4 May 1982 in Munich, Germany and on 6–7 May 1982 in Paris, France.</p> <p>ISBN 92-835-1419-X</p>

AGARD

NATO  OTAN7 RUE ANCELLE · 92200 NEUILLY-SUR-SEINE
FRANCE

Telephone 745.08.10 · Telex 610176

DISTRIBUTION OF UNCLASSIFIED
AGARD PUBLICATIONS

AGARD does NOT hold stocks of AGARD publications at the above address for general distribution. Initial distribution of AGARD publications is made to AGARD Member Nations through the following National Distribution Centres. Further copies are sometimes available from these Centres, but if not may be purchased in Microfiche or Photocopy form from the Purchase Agencies listed below.

NATIONAL DISTRIBUTION CENTRES

BELGIUM

Coordonnateur AGARD – VSL
Etat-Major de la Force Aérienne
Quartier Reine Elisabeth
Rue d'Evere, 1140 Bruxelles

ITALY

Aeronautica Militare
Ufficio del Delegato Nazionale all'AGARD

CANADA

Defence
Department
Ottawa



National Aeronautics and
Space Administration

Washington, D.C.
20546

SPECIAL FOURTH CLASS MAIL
BOOK

Postage and Fees Paid
National Aeronautics and
Space Administration
NASA-451

Official Business
Penalty for Private Use \$300



DENMARK

Danish
Østerbrogade
Copenhagen

FRANCE

O.N.E.R.A.
29 Avenue
92320 Châtillon

GERMANY

Fachinfo.
Physik, Mathematik
Kernforschungszentrum
D-7514 Eggenstein

GREECE

Hellenic Air Force
Research and Development
Holography, etc.

ICELAND

Director of Aviation
c/o Flugrad
Reykjavik

UNITED KINGDOM

Defence Research Information Centre
Station Square House
St. Mary Cray
Orpington, Kent BR5 3RE

UNITED STATES

National Aeronautics and Space Administration (NASA)
Langley Field, Virginia 23365
Attn: Report Distribution and Storage Unit

THE UNITED STATES NATIONAL DISTRIBUTION CENTRE (NASA) DOES NOT HOLD STOCKS OF AGARD PUBLICATIONS, AND APPLICATIONS FOR COPIES SHOULD BE MADE DIRECT TO THE NATIONAL TECHNICAL INFORMATION SERVICE (NTIS) AT THE ADDRESS BELOW.

PURCHASE AGENCIES*Microfiche or Photocopy*

National Technical
Information Service (NTIS)
5285 Port Royal Road
Springfield
Virginia 22161, USA

Microfiche

Space Documentation Service
European Space Agency
10, rue Mario Nikis
75015 Paris, France

Microfiche or Photocopy

British Library Lending
Division
Boston Spa, Wetherby
West Yorkshire LS23 7BQ
England

Requests for microfiche or photocopies of AGARD documents should include the AGARD serial number, title, author or editor, and publication date. Requests to NTIS should include the NASA accession report number. Full bibliographical references and abstracts of AGARD publications are given in the following journals:

Scientific and Technical Aerospace Reports (STAR)
published by NASA Scientific and Technical
Information Facility
Post Office Box 8757
Baltimore/Washington International Airport
Maryland 21240, USA

Government Reports Announcements (GRA)
published by the National Technical
Information Services, Springfield
Virginia 22161, USA



Printed by Technical Editing and Reproduction Ltd
Harford House, 7-9 Charlotte St, London W1P 1HD

ISBN 92-835-1419-X